

Transport processes in the production of organic acids from lignocellulosic feedstocks by *Aspergillus niger*

Da Fonte Lameiras, Francisca

DOI

[10.4233/uuid:38c1fd73-bff2-4660-aa40-48a4c28e16f7](https://doi.org/10.4233/uuid:38c1fd73-bff2-4660-aa40-48a4c28e16f7)

Publication date

2018

Document Version

Final published version

Citation (APA)

Da Fonte Lameiras, F. (2018). *Transport processes in the production of organic acids from lignocellulosic feedstocks by Aspergillus niger*. [Dissertation (TU Delft), Delft University of Technology]. <https://doi.org/10.4233/uuid:38c1fd73-bff2-4660-aa40-48a4c28e16f7>

Important note

To cite this publication, please use the final published version (if applicable).
Please check the document version above.

Copyright

Other than for strictly personal use, it is not permitted to download, forward or distribute the text or part of it, without the consent of the author(s) and/or copyright holder(s), unless the work is under an open content license such as Creative Commons.

Takedown policy

Please contact us and provide details if you believe this document breaches copyrights.
We will remove access to the work immediately and investigate your claim.

**Transport processes in the production of organic acids
from lignocellulosic feedstocks
by *Aspergillus niger***

Dissertation

for the purpose of obtaining the degree of doctor
at Delft University of Technology,
by the authority of the Rector Magnificus Prof.dr.ir. T.H.J.J. van der Hagen,
chair of the Board for Doctorates
to be defended publicly on
Monday 9 April 2018 at 10:00 o'clock

by

Francisca DA FONTE LAMEIRAS

Master of Science in Biological Engineering, Minho University, Portugal
born in Guimarães, Portugal

This dissertation has been approved by the

Promotor: Prof. dr. ir. J.J. Heijnen

Copromotor: Dr. W.M. van Gulik

Composition of the doctoral committee:

Rector Magnificus,	chairperson
Prof. dr. ir. J.J. Heijnen,	promotor
Dr. W.M. van Gulik,	copromotor

Independent members:

Prof. dr. J. Teixeira	Minho University, Portugal
Prof. dr. M. de Mey	Ghent University, Belgium
Prof. dr. J. Teixeira de Mattos	University of Amsterdam, The Netherlands
Dr. ir. S. Hartmans	DSM
Prof. dr. H.J. Noorman	TNW, TU Delft

Reserve member:

Prof. dr. W.R. Hagen	TNW, TU Delft
----------------------	---------------

The research presented in this thesis was performed at the Cell Systems Engineering section, Department of Biotechnology, Faculty of Applied Sciences, Delft University of Technology (The Netherlands).

This project was carried out within the research programme of BE-BASIC Foundation.

ISBN: 978-94-6299-902-2

Copyright © 2018 by Francisca Lameiras

Cover illustration designed by Igor Mekhtiev

Printing: Ridderprint, the Netherlands

**Transport processes in the production of organic acids
from lignocellulosic feedstocks
by *Aspergillus niger***



Table of contents



List of abbreviations	vii
Summary/Samenvatting	ix
Chapter 1 General Introduction	1
Chapter 2 Tools for quantitative metabolomics of <i>Aspergillus niger</i> chemostat cultures	25
Chapter 3 Stoichiometry and kinetics of single and mixed substrate uptake in <i>Aspergillus niger</i>	51
Chapter 4 Metabolic network analysis and transport mechanisms of lignocellulosic substrates in <i>Aspergillus niger</i>	79
Chapter 5 Transport insights on citric and itaconic acid in <i>Aspergillus</i> <i>niger</i>	105
Chapter 6 A metabolomics study in <i>Aspergillus niger</i> reveals a putative amino acid transporter	141
Chapter 7 Concluding Remarks and Outlook	163
Supplementary material	171
References	219
Acknowledgements	235
<i>Curriculum vitae</i>	239
List of Publications	241

List of abbreviations

aa Amino acid

Ala Alanine

Asn Asparagine

Asp Aspartic acid

Btu British thermal unit

Cit Citric acid

C_x Biomass concentration inside the reactor

C_{x,out} Biomass concentration outside the reactor

Cys Cysteine

D Dilution rate (h^{-1})

E_{pmf} proton motive force

F Faraday constant (96.5 kJ/v e⁻mol)

G Gibbs free energy

g_{dw} Grams of dry cell weight

Gln Glutamine

Glu Glutamic acid

Gly Glycine

Glyc Glycolytic metabolites

H⁺ Proton

His Histidine

Ile Iso-Leucine

Ita Itaconic acid

Leu Leucine

Lys Lysine

MeOH Methanol

Met Methionine

Mtoe Million tonnes of oil equivalent

Phe Phenylalanine

pH_{in} Intracellular pH

pH_{out} Extracellular pH

pka Acid dissociation constant

PPP Pentose phosphate pathway

Pro Proline

q_i Biomass specific conversion rate of compound
i ($\text{mol/h}/\text{Cmol}_x$)

R Gas constant ($8.314 \times 10^{-3} \text{ kJ/molK}$)

R_i Rate of compound i (Cmol/h)

T Temperature (in K or °C)

TCA Tricarboxylic acid cycle

Thr Threonine

TOC total organic carbon

Trp Tryptophan

Tyr Tyrosine

Val Valine

Z Charge of transported molecule

μ Growth rate (h^{-1})

X_i Degree of reduction of compound i

ψ Membrane potential (V)

Summary

Filamentous fungi, especially from the genus *Aspergillus*, are well known for the production of organic acids in fermentation industry. Nonetheless, in present time the competing chemical conversion routes are still more profitable, leaving space for further investigations and improvement on the biological routes.

In view of the known high citric acid production capacity of *Aspergillus niger*, this fungus should be well suited as a cell factory for the production of other industrially relevant acids as succinic, fumaric, itaconic and malic. In addition, it is known that *A. niger* grows on decaying fruits and plant material thereby enzymatically degrading lignocellulosic constituents into a mixture of mono- and oligosaccharides. Therefore *A. niger* is well suited to be cultivated on plant waste material. However, so far little is known about the mechanisms of sugar import and organic acid export in *A. niger*. Thus more knowledge on substrate uptake and organic acid export mechanisms and their kinetics, will contribute to exploit *A. niger* as a cell factory for organic acid production from lignocellulosic feedstocks.

As a tool for the fundamental studies of substrate uptake and product excretion, we have first defined a continuous cultivation protocol, and a rapid sampling platform for intracellular metabolite quantification (**chapter 2**). Quantitative metabolomics is an important *omics* tool in a synthetic biology approach to develop *A. niger* for the production of the mentioned acids. Such studies require well defined and tightly controlled cultivation conditions and proper rapid sampling, sample processing and analysis methods. In **chapter 2** we present the development of a chemostat for homogeneous steady state cultivation of *A. niger*, equipped with a new dedicated rapid sampling device. In addition, a quenching method for quantitative metabolomics in *A. niger* based on cold methanol was evaluated and optimized with the aim of avoiding metabolite leakage during sample processing. The optimization was based on measurements of the intermediates of the glycolysis, TCA and PPP pathways and amino acids, using a material balancing approach. Leakage was found to be absent at -

20° C for a 40% (v/v) methanol concentration in water. Under these conditions the average metabolite recovery was close to 100%.

Once the cultivation setup and metabolic platform were settled, we focused at the import mechanisms and kinetics of substrate uptake (**chapters 3 and 4**) and product transport (**chapters 5 and 6**).

To investigate the kinetics and stoichiometry of growth of this fungus on lignocellulosic sugars, in **chapter 3** we carried out batch cultivations on six representative monosaccharides (glucose, xylose, mannose, rhamnose, arabinose and galacturonic acid) and a mixture of these. Growth on these individual substrates was characterized in terms of biomass yields, oxygen/biomass ratios and specific conversion rates. Interestingly, in mixtures, some of the carbon sources were consumed simultaneously and some sequentially. With a sequential chemostat cultivation experiment performed on a feed mixture of the six substrates, we found that the uptake of glucose, xylose and mannose could be described with Michaelis-Menten type kinetics. However, these carbon sources seem to be competing for the same transport systems, while the uptake of arabinose, galacturonic acid and rhamnose appeared to be repressed by the presence of other substrates.

As a follow up of previous stoichiometric and kinetic studies, in **chapter 4** we open the black box model of the previous chapter. We have measured intracellular and extracellular concentrations of the six selected substrates which allowed the assessment of the most probable import mechanism for these substrates. For glucose, xylose, arabinose, mannose and rhamnose it was found that proton symporter was the most plausible transporter, while galacturonic acid was assumed to enter the cells through passive diffusion at a cultivation pH of 2.5. In addition, the results from eleven carbon-limited chemostat steady states of *A. niger* on a mixture of six substrates at different growth rates were used as input for a flux analysis from which we obtained estimations of ATP costs and NADPH requirements for biomass growth on these

lignocellulosic sugars. The energetics of growth of *A. niger* were based on well-known pathways for some substrates and most plausible pathways for others.

Regarding the product related study, in **chapter 5** we focused on the transport of two organic acids: citric acid, essential for the food and beverage industries; and itaconic acid, used in the chemical and polymer industries. *A. niger* as a cell factory is capable of producing citric acid in high quantities, but can also produce itaconic acid when metabolically engineered. The objective of this work was to study the membrane transport of these acids in *A. niger* and focus on two important aspects at industrial scale: high product concentrations (close to the solubility limit) and a low cultivation pH, which is beneficial for the downstream processing (facilitating acid recovery and avoiding the use of titrants and production of waste materials). We performed steady state chemostat experiments at low (2.5) and high (5.5) cultivation pH, using xylose as the substrate whereby either citric acid or itaconic acid was added to the feed medium. We observed that citric acid uptake at pH=2.5 was much higher than at pH=5.5. Interestingly, the calculated permeability coefficient for the undissociated citric acid appeared far below expectation, which indicates the presence of a transport protein. From intra- and extracellular acid levels, the most plausible uptake mechanism appeared to be proton antiport. Itaconic acid uptake, however, was very low at both conditions, and inhibited xylose uptake. Furthermore, we investigated at pH = 2.5 the transport and metabolism of itaconic acid in itaconic acid producing and non-producing strains at high concentrations of this acid. From measurements of intra- and extracellular itaconic acid levels we found that export of the produced itaconic acid in the producing strain is most likely through a proton antiport mechanism.

In addition to previous findings, in **chapter 6**, we applied quantitative metabolomics tools in dynamic chemostat experiments to disclose the function of a putative fumaric acid transporter (*fumT*) isolated from *Rhizopus delemar*, which was overexpressed in *A. niger*. It was found that under aerobic xylose limited continuous cultivation, amino acids were imported into the cellular space in the mutant strains which carry *fumT*. From the metabolomics analysis and an amino acid pulse experiment, it appeared that

this transporter might be a high affinity general amino acid permease using a proton symport system as the transport mechanism.

Samenvatting

Filamenteuze schimmels, vooral van het geslacht *Aspergillus*, zijn bekend om de productie van organische zuren, met name citroenzuur, in de fermentatie-industrie. Gezien de grote citroenzuur productiecapaciteit van *Aspergillus niger*, zou deze schimmel goed geschikt moeten zijn voor de productie van andere industrieel relevante zuren zoals barnsteenzuur, fumaarzuur, itaconzuur en appelzuur. Op dit moment zijn de concurrerende chemische productieroutes van deze zuren echter nog winstgevender, waardoor er noodzaak is voor verder onderzoek ter verbetering van de biologische routes.

Verder is het bekend dat *A. niger* groeit op rottend fruit en ander plantenmateriaal, door enzymatische afbraak van lignocellulosische bestanddelen tot een mengsel van mono- en oligosacchariden, die vervolgens worden opgenomen. Daarom is *A. niger* van nature geschikt om op plantenafvalmateriaal te worden gekweekt. Er is echter tot nu toe weinig bekend over de mechanismen voor import van mono- en oligosacchariden en de export van organische zuren in *A. niger*. Meer kennis over substraat import- en product exportmechanismen en hun kinetiek zal daarom bijdragen aan het exploiteren van *A. niger* als industrieel micro-organisme voor de productie van organische zuren uit plantenafval.

Om goed gedefinieerde studies van substraatopname en productuitscheiding te kunnen uitvoeren werden allereerst een chemostaat protocol, een snelle bemonsteringsmethode en een analytisch platform voor kwantitatieve metaboolanalyse ontwikkeld. Kwantitatieve metaboolanalyse is een belangrijk stuk gereedschap binnen een synthetische biologie-benadering gericht op het ontwikkelen van *A. niger* stammen voor efficiënte productie van genoemde zuren. Dergelijke studies vereisen goed gedefinieerde en streng gecontroleerde kweekomstandigheden en snelle bemonstering, monsterverwerking en analysemethoden. In **hoofdstuk 2** wordt de ontwikkeling van een aangepast chemostaat systeem voor de homogene steady-state kweek van *A. niger*, uitgerust met een nieuw ontwikkeld snel

bemonsteringsapparaat, beschreven. Daarnaast werd een fixatiemethode voor onmiddellijke stopzetting van alle metabole activiteit in *A. niger* op basis van een koud methanol/water mengsel ontwikkeld. Deze methode werd geoptimaliseerd om metabolietlekage tijdens de fixatie en monsterverwerking te minimaliseren. Deze optimalisatie was gebaseerd op metingen van metabolieten van de glycolyse-, TCA- en PPP-routes en aminozuren in het totale monster, het cel pellet en het filtraat en het opstellen van massabalansen voor de verschillende metabolieten. Leckage bleek afwezig te zijn bij fixatie van de monsters in 40% (v/v) methanol/water bij een temperatuur van -20°C. Onder deze omstandigheden bleek de gemiddelde metaboliet recovery bijna 100%.

Vervolgend werd, gebruik makend van de ontwikkelde methoden, onderzoek gedaan naar substraat opname (**hoofdstuk 3 en 4**) en product transport (**hoofdstuk 5 en 6**).

Om de kinetiek en stoichiometrie van de groei van deze schimmel op diverse substraten te onderzoeken werden batch fermentaties uitgevoerd op zes representatieve monosacchariden (glucose, xylose, mannose, rhamnose, arabinose en galacturonzuur) en een mengsel hiervan (**hoofdstuk 3**). Groei op deze substraten werd gekarakteriseerd in termen van biomassaopbrengst, zuurstof consumptie/biomassa productie verhoudingen en biomassa specifieke omzettingssnelheden. Interessant is dat, in combinatie, sommige van de koolstofbronnen tegelijkertijd en enkele sequentieel werden geconsumeerd. Door het uitvoeren van een koolstof gelimiteerd, stapsgewijs uitgevoerd chemostaat experiment op een mengsel van de zes substraten bij elf verschillende groeisnelheden, vonden we dat de opname van glucose, xylose en mannose beschreven kon worden met Michaelis-Menten-type kinetiek. Uit de resultaten bleek dat deze substraten lijken te concurreren voor dezelfde transportsystemen, terwijl de opname van arabinose, galacturonzuur en rhamnose geremd leek te zijn door de aanwezigheid van andere substraten.

Als een vervolg op vorige stoichiometrische en kinetische studies, openen we in **hoofdstuk 4** het Black Box-model van het vorige hoofdstuk. Metingen van de

intracellulaire en extracellulaire concentraties van de zes geselecteerde substraten werden uitgevoerd om, in combinatie met thermodynamische analyse, tot een uitspraak te komen welke importmechanisme voor deze substraten de meest voor de hand liggende zijn. Voor glucose, xylose, arabinose, mannose en rhamnose bleek dit proton symport te zijn terwijl werd aangenomen dat bij een cultivatie pH van 2.5 galacturonzuur wordt geïmporteerd via passieve diffusie van het ongedissocieerde zuur. Daarnaast werden de resultaten van het stapsgewijs uitgevoerde chemostaat experiment gebruikt als input voor een metabole fluxanalyse waaruit we schattingen van ATP- en NADPH- behoeften voor groei op de zes verschillende plantensuikers konden verkrijgen. In het gebruikte stoichiometrische model voor de groei van *A. niger* werden in een aantal gevallen bekende metabole routes voor het metabolisme van de substraten geïncorporeerd, terwijl in sommige gevallen aannames moesten worden gedaan.

Met betrekking tot het product gerelateerde onderzoek hebben we ons in **hoofdstuk 5** gericht op het transport van twee organische zuren, namelijk citroenzuur, essentieel voor de voedings- en drankenindustrie; en itaconzuur, gebruikt in de chemische en polymeerindustrie. Zoals gezegd is *A. niger* in staat om grote hoeveelheden citroenzuur te produceren, maar kan, na genetische modificatie, ook itaconzuur produceren. Het doel van het onderzoek was om het membraantransport van deze zuren in *A. niger* te bestuderen en ons daarbij te concentreren op twee belangrijke aspecten op industriële schaal: hoge productconcentraties (dichtbij de oplosbaarheidslimiet) en een lage cultivatie-pH, wat gunstig is voor de product opwerkingsstap (vermijden van het gebruik van titranten en daardoor vermijden van productie van afvalmaterialen). Daartoe werden steady state chemostaat experimenten uitgevoerd bij lage (2.5) en hoge (5.5) cultivatie-pH, met gebruik van xylose als het substraat waarbij citroenzuur of itaconzuur aan het voedingsmedium werden toegevoegd. Hierbij werd waargenomen dat de opname van citroenzuur door de cellen bij pH = 2.5 veel hoger was dan bij pH = 5.5. Interessant was dat de berekende permeabiliteitscoëfficiënt voor het niet-gedissocieerde citroenzuur veel lager was dan verwacht, wat zou kunnen duiden op de aanwezigheid van een

transporteiwit voor de import van citroenzuur. Uit gemeten intra- en extracellulaire zuurniveaus bleek het meest plausibele opnamemechanisme proton antiport te zijn. De opname van itaconzuur was echter onder beide condities erg laag terwijl de xylose-opname geremd werd door de aanwezigheid van dit zuur. Verder hebben we bij pH = 2.5 het transport en metabolisme van itaconzuur in itaconzuur producerende en niet-producerende stammen bij hoge concentraties van dit zuur onderzocht. Uit metingen van intra- en extracellulaire itaconzuur niveaus bleek dat export van het geproduceerde itaconzuur in de producerende stam waarschijnlijk gebeurt via een proton antiport mechanisme.

Gebruik makend van metabooloom metingen tijdens steady state en dynamische chemostaat experimenten werd de functie van een vermeende fumaarzuur transporter (*fumT*), geïsoleerd uit *Rhizopus delemar*, die tot overexpressie werd gebracht in *A. niger*, onthuld (**hoofdstuk 6**). Hierbij werd gebruik gemaakt van kwantitatieve metabooloom analyses in combinatie met dynamische chemostaat experimenten. Er werd gevonden dat in aërobe xylose gelimiteerde chemostaat experimenten aminozuren werden geïmporteerd door de *fumT* bevattende mutanten. Uit de resultaten van metabooloom analyses uitgevoerd tijdens steady state cultivaties en een aminozuurpuls experiment bleek dat deze transporter waarschijnlijk een aminozuur permease is met hoge affiniteit, welke een groot aantal verschillende aminozuren importeert met behulp van proton symport als transportmechanisme.

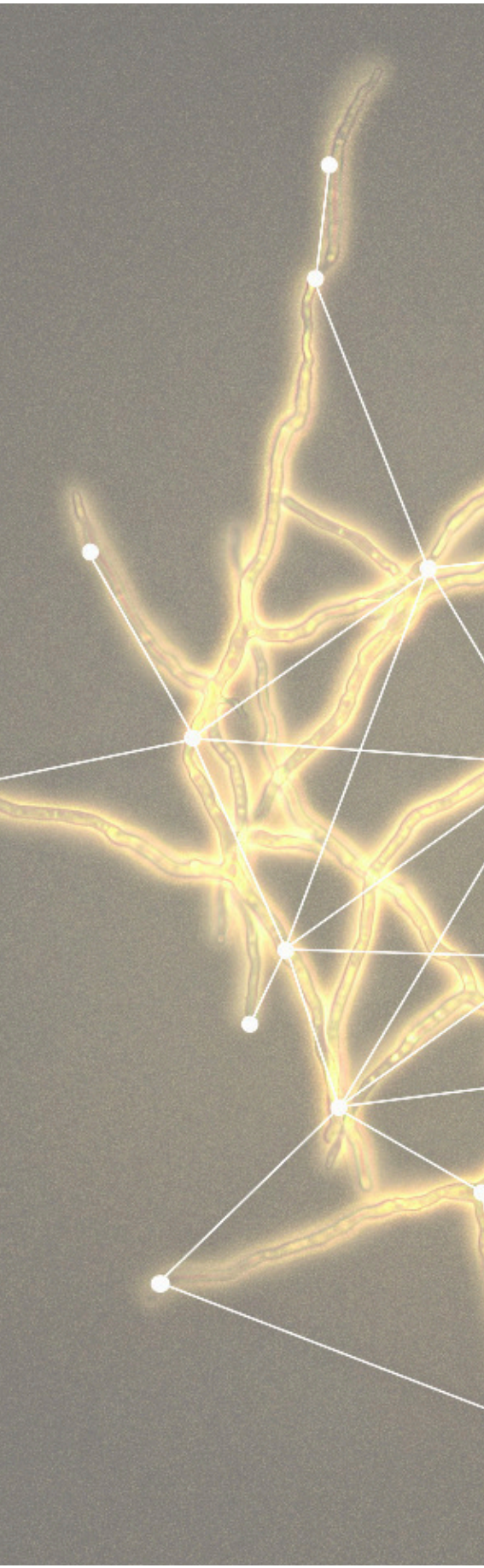


To my family
& Julien

The role of the infinitely small in nature is infinitely large



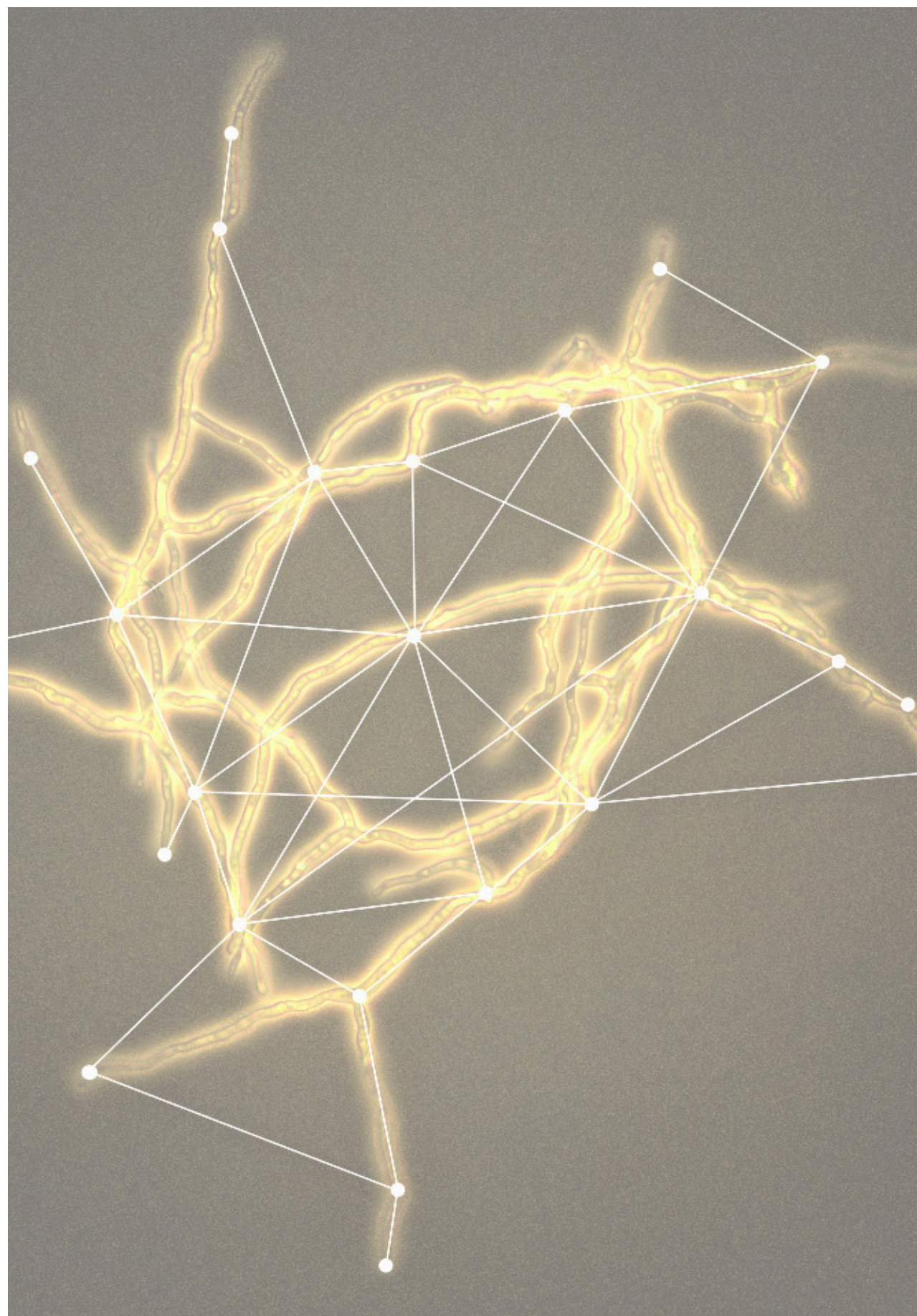
-Louis Pasteur



In this chapter, an overview of the state of the art of fungal biotechnology can be found, as well as basic concepts of cellular transport mechanisms. In the end, the scope and overview of the thesis are presented.

Chapter 1

General introduction



1.1. Bio-based production of fuels and chemicals

Our planet still relies largely on coal, natural gas and petroleum, extracted from the earth's crust, for production of energy, fuels and chemicals. These three fossil sources have covered more than 80% of the energy demand of the US in the last 100 years (EIA, 2016) - Fig. 1.1.

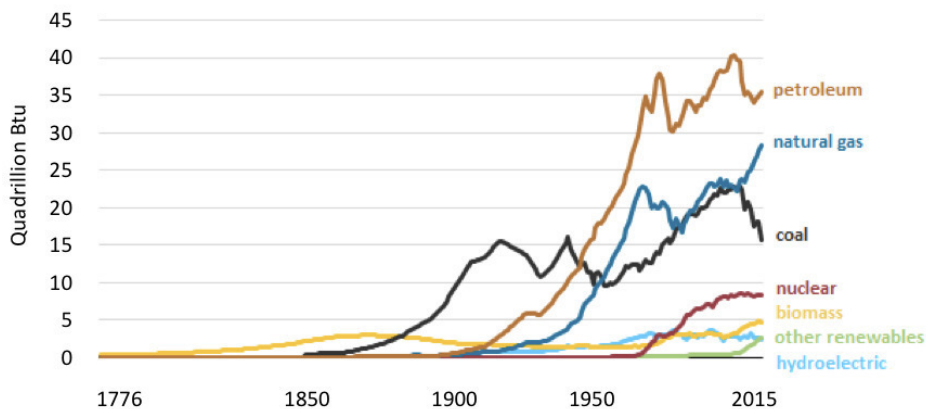


Fig. 1.1. Energy consumption (Btu: British thermal unit) in the United States between 1776 and 2015 (Source: EIA, 2016).

With respect to the total worldwide energy demand, the situation is very similar. Currently only a small part of the total energy consumption is covered by sustainable sources such as wind, solar, biofuels and biomass (IEA, 2015) - Fig. 1.2.

The combustion of fossil fuels results in carbon and hydrogen oxidation leading to the production of carbon dioxide, water and heat. Invariably and virtually inevitably the process results in the production of sulphur oxides and due to incomplete combustion. The emission of these compounds (mainly carbon dioxide and methane) results in a steady supply of greenhouse gases to the atmosphere (Sengupta, 2010) leading to climate changes. Thus, this problem needs to be addressed.

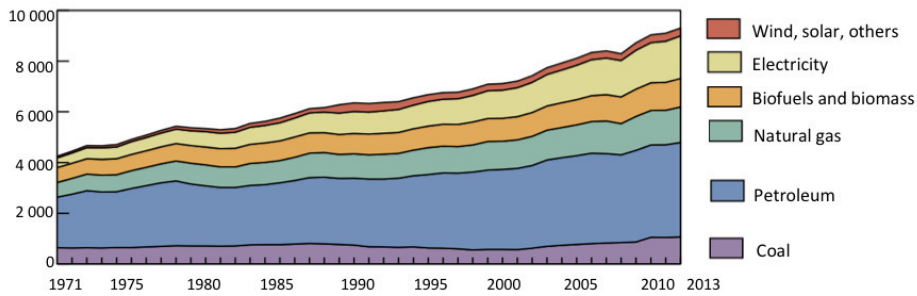


Fig. 1.2. World total energy coverage from 1971 to 2013 by fuel in Mtoe (Million Tonnes of Oil Equivalent)
(Source: IEA, 2015).

Organizations and world leaders are encouraged to come up with alternative resources for production of energy, fuels and chemicals. Biomass emerged in the 1970's as an alternative resource which can be used for the same purposes with some modifications to the existing processes.

Biomass is classified as “all organic matter on the earth's surface derived from recent biological material” (Sengupta, 2010), being mainly plant waste streams including vegetation, agricultural crops and algae, organic waste and animal manure.

One way of valorization of plant waste streams is their use as a substrate for microorganisms (fermentation) for the production of biofuels, which are subsequently combusted to carbon dioxide and water, yielding useful energy, similarly as discussed above, with the advantage that carbon is recycled at a much faster pace (photosynthesis) when compared to fossil fuels.

The use of microorganisms, such as bacteria, yeast or filamentous fungi for the production of goods is a very ancient practice, emerging from the Neolithic ages where fermented beverages were produced. Nevertheless, the discovery of microorganisms occurred only in 1674 by Antonie van Leeuwenhoek in Delft, upon the invention of the microscope. Since then, microorganisms and their products have been broadly applied in Biotechnology to realize a bio-based and sustainable production of fuels and chemicals.

Bio-based production uses biomass as a substrate in a biochemical conversion process, and includes fermentative conversion routes. Whereas in chemical production each conversion implies a different industrial process, in fermentation based biochemical production each conversion might involve a different enzymatic step within the same microbial cell (Straathof, 2014).

In addition, production by biological (i.e. enzymatic conversions) yields very (stereo)specific compounds. Although organic acids represent only a small part of the potential products' scope of microorganisms, they have countless applications and a significant impact on our daily lives, as discussed in the following section. Organic acids such as malic acid, fumaric acid, itaconic acid and succinic acid are currently produced on an industrial scale by chemical synthesis. Malic acid is obtained by double hydration of maleic anhydride; fumaric acid is produced by isomerization of maleic acid; succinic acid is obtained from partial hydrogenation of maleic acid, oxidation of 1,4-butanediol and carbonylation of ethylene glycol; and itaconic acid is produced by the distillation of citric acid.

This work addresses a bio-based alternative for production of organic acids from sustainable feedstocks by a fermentative route in filamentous fungi.

1.2. Production of organic acids by filamentous fungi

Filamentous fungi, especially from the genus *Aspergillus*, are well-known for the production of organic acids, which can be classified in two groups: TCA cycle derived acids (citric, itaconic, malic, fumaric, succinic and oxalic acid) and glucose derived acids (gluconic and kojic acid) – Fig. 1.3.

For most of the organic acids, excretion from the cells requires a plasma membrane transporter, except for gluconic acid which is oxidized extracellularly by glucose oxidase.

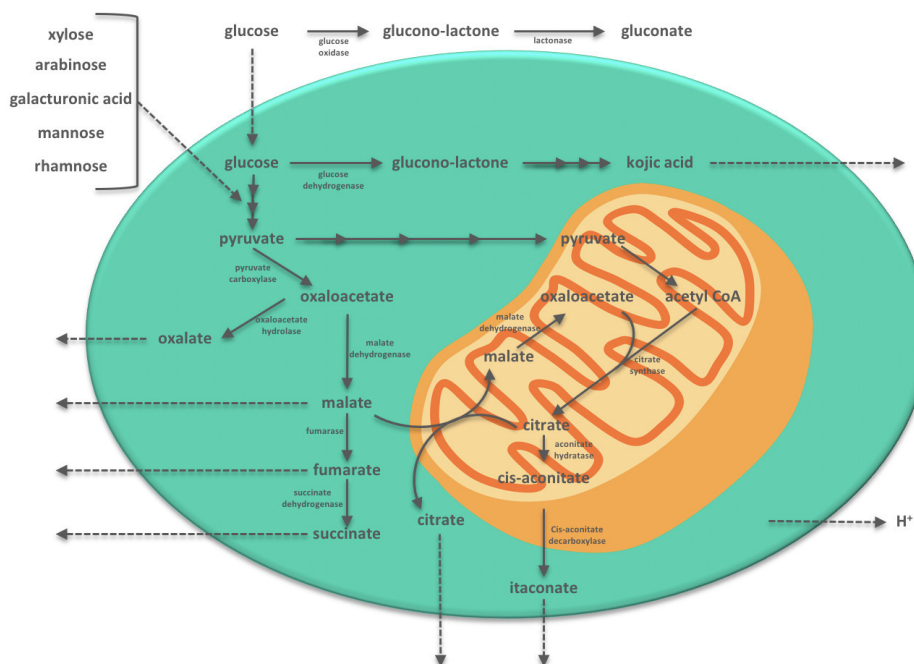


Fig. 1.3. Organic acids production in the genus *Aspergillus*
(adapted from Witteveen, 1993).

For efficient production of the TCA cycle related acids there are four important aspects to consider: a high substrate import rate; a high flux through the glycolysis and TCA cycle; the ATP, redox cofactors and electrical charge should be balanced intracellularly; and the acids and corresponding protons must be transported through the plasma membrane to the extracellular environment (Witteveen, 1993).

A list of the most common filamentous fungi used for production of organic acids can be found in Table 1.1.

As listed, the genus *Aspergillus* contains the workhorses of the fungal fermentation industry for production of organic acids. Nonetheless, to date the competing chemical conversion routes are still more cost-effective.

Table 1.1. Organic acid production by filamentous fungi
(Goldberg *et al.*, 2006; Kubicek *et al.*, 2010; Liaud *et al.*, 2014).

Organic acid	Filamentous fungi	Applications
Citric acid	<i>Aspergillus niger</i> <i>Yarrowia lipolytica</i>	Preservative, pH adjustment in food, beverage, pharmaceutical and cosmetic industries
Gluconic acid	<i>Aspergillus niger</i> <i>Penicillium spp.</i>	Food additive Glass and metal cleaning
Itaconic acid	<i>Aspergillus terreus</i> <i>Aspergillus itaconicus</i> <i>Ustilago maydis</i>	Co-polymer and detergents
Oxalic acid	<i>Aspergillus niger</i>	Cleaning and bleaching
Kojic acid	<i>Aspergillus oryzae</i> <i>Aspergillus flavus</i>	Precursor for food additives and cosmetic industry
Succinic acid	<i>Aspergillus flavipes</i>	Food additive Precursor of polymers, resins and solvents
Malic acid	<i>Aspergillus spp.</i>	Food additive Synthesis of polymers
Fumaric acid	<i>Aspergillus niger</i> <i>Rhizopus delemar</i>	Food additive Synthesis of polymers

Organic acids, when compared to the antibiotics penicillin or β -lactam from *Penicillium spp.*, seem to have a lower impact on human well-being and are considered as “high volume-low value” products, but they are the most interesting from a production point of view: their production is the most efficient in terms of yield and productivity: the efficiency of glucose converted to citric acid is higher than 80% (Magnuson and Lasure, 2004).

The species *Aspergillus niger*, subject of study in this project, is a common filamentous fungus which grows aerobically on decaying plant organic matter in soil and litter, and is usually recognized by its dark coloured spores, and hence often known as the “black mold”. This microorganism (Fig. 1.4.) is able to grow within broad ranges of temperature (6 - 47°C) and pH (1.4 - 9.8) (Schuster *et al.*, 2002).

A. niger became famous in industrial Biotechnology for the production of citric acid, since the early 1900s. This organic acid is the main acidulant used in food industry and the process has obtained a GRAS (Generally Regarded As Safe) status (Schuster *et al.*, 2002).

A. niger is able to convert glucose to citric acid with more than 80% efficiency and can reach a titer of up to 300 g/l. A cause for the high production of citric acid is believed to be the fact that *A. niger* did not evolve tight regulatory mechanisms to control acid production, as the natural environment of this organism includes low substrate concentrations (Magnuson and Lasure, 2004). Thus, in artificial high sugar concentrations, the acid production is reckless. This acid production ability, the chelation capacity of citric acid, as well as the high solubility of metals in it, may allow *A. niger* to grow in environments where metals are limited, conferring a competitive advantage for this filamentous fungus (Karaffa and Kubicek, 2003).

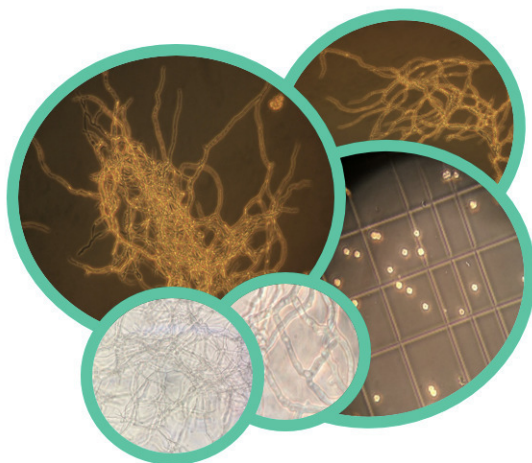


Fig. 1.4. *Aspergillus niger* microscopic image collection.

Apart from citric acid, *A. niger* has been used in industry for production of other organic acids such as gluconic and oxalic acid, although the market sizes are considerably smaller for the latter. Other species of *Aspergillus* (such as *A. terreus*) are able to produce itaconic acid up to 80 g/l in large scale bioprocesses (Okabe *et al.*, 2009; Willke and Vorlop, 2001). *A. niger*, although not a natural producer of itaconic acid, has also been shown to produce this acid (with a titer of 7.1 g/l) when engineered to express heterologous cis-aconitate decarboxylase (van der Straat *et al.*, 2014, 2013). Several other non-producing host microorganisms have been metabolically engineered

for the production of itaconic acid with titers ranging from 14.5 mg/l to 7.8 g/l (van der Straat and de Graaff, 2016). Their efforts, however, did not result in an organism which can compete with the natural producer *A. terreus*, with respect to TRY (titer, rate and yield).

There are numerous studies addressing the production process of organic acids, but a real understanding as to how *A. niger* is able to produce citric acid at such high concentrations is still lacking.

The study of the uptake mechanisms of different substrates (see section 1.3.), as well as the identification of the transporters of substrates and organic acids (see section 1.4.) are important approaches towards process improvement, which will be addressed in this study. Such understanding will allow exploitation of this fungus for the production of other organic acids. In this project, glucose, xylose, arabinose, galacturonic acid, mannose and rhamnose were the studied substrates and citric and itaconic acid were the studied organic acids.

1.3. Substrate uptake versatility of *A. niger*

For a process to be successful at large scale, a high titer, rate and yield in itself are not sufficient. The costs of the used substrate and the downstream processing are also important parameters for the overall economic feasibility of the process. A high substrate cost and an expensive purification of the product can easily absorb the advantage of a high productivity obtained (Sauer *et al.*, 2008).

Therefore, cheaper substrates like second generation feedstocks, have been addressed. However, the change of white/industrial biotechnology from expensive artificial highly refined carbohydrate substrates to more sustainable and cheaper second generation feedstocks, such as lignocellulosic hydrolysates, represents a challenge in the transition from single-sugar to mixed-substrate utilization (van Maris *et al.*, 2006).

Second generation feedstocks do not compete with food supplies and are cheaper, but are much more complex with respect to biochemistry and microbiology than first generation ones. They consist of different fermentable sugars from plant biomass of agricultural crops waste, which are currently insufficiently used. Of the global 200×10^9 tons per year of plant biomass produced, over 90% is lignocellulose. About $8\text{--}20 \times 10^9$ tonnes of this plant biomass is potentially accessible but remains unexploited (Lin and Tanaka, 2006).

Lignocellulose is composed of three structural heteropolysaccharides: cellulose (40% to 50%), hemicellulose (25% to 35%) and lignin (15% to 20%) (de Souza *et al.*, 2011). Besides glucose, sugar monomers in hemicellulose can include xylose, mannose, rhamnose, arabinose, and small amounts of galacturonic acid. Pectins on the other hand are rich in galacturonic acid.

Fortunately, using *A. niger* as a cell factory has benefits in the use of mixed-substrates from plant cell wall debris as feedstock, due to its good fermentation capabilities of both C5 and C6 sugars and secretion of high levels of enzymes. Specifically, the extensive variety of excreted enzymes which allow degradation of plant cell wall polysaccharides plays an important role on the dynamic uptake of different carbon sources (Gouka *et al.*, 1997; de Vries *et al.*, 2001).

Rumbold *et al.*, 2009 tested the performance of six common industrially relevant microorganisms by submitting them to growth conditions that they encounter in a second generation production process (mixture of sugars, inhibitors, extreme pH, etc.). The generated data were used to rank the organisms by relative performance. Hereby *A. niger* has scored the highest, contributing for a stronger motivation for the use of this microorganism in second generation feedstocks (Rumbold *et al.*, 2009).

Monitoring and controlling the growth of microorganisms and their behaviour towards substrates and productivity needs careful kinetic studies, since a high concentration of substrate or product can lead to inhibitory effects, decreasing fermentation rates (Sivakumar, 1994). In addition, multiple and simultaneous substrate uptake is desired

to facilitate the use of second generation feedstocks where different monomers are present at low (limiting) concentrations (Lendenmann *et al.*, 1996).

1.4. Transport processes

For the proper functioning of a living cell, the cell membrane and embedded transport proteins are essential (Ramos *et al.*, 2016), as the transport system enables the metabolic homeostasis of the cell by uptaking nutrients, excreting unwanted products and establishing electrochemical gradients.

All eukaryotic cells contain a wide range of plasma membrane proteins which ensure the exchange (import and export) of molecules with the environment. To understand whether a compound can cross the plasma membrane freely, it is important to know that this membrane has a lipophilic nature. This means that charged and hydrophilic molecules need a mediator (transport protein).

1.4.1. Mechanisms

The transport systems can be divided in two types: non-coupled transport, and coupled transport – Fig. 1.5.

In case of a non-coupled mechanism no transporter protein is involved (passive diffusion), lipophilic and non-charged molecules like oxygen, carbon dioxide, ethanol and small undissociated organic acids can be exchanged across the membrane with as the only driving force the membrane concentration gradient. In case of facilitated diffusion, a membrane protein is present to mediate the non-coupled transport. In case of a non-charged molecule, only the membrane concentration gradient determines the transport rate. However, when a charged molecule is transported by a protein, the transport rate depends on the electrochemical gradient, influenced by the internal potential.

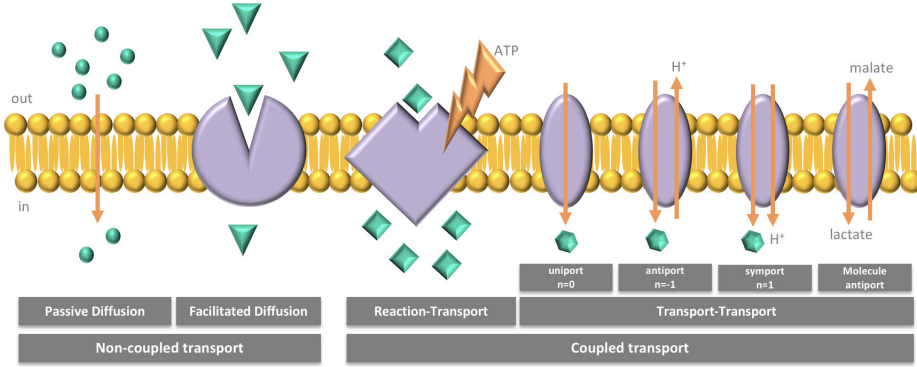


Fig. 1.5. Cellular transport mechanisms.

When the solubility of a molecule (charged, hydrophilic) in the lipid membrane is insufficient, or the transport has to occur against a concentration gradient, both a transporter and energy input (coupled transport) are needed. Coupled transport requires ATP (reaction-transport) or energy derived from a H⁺ gradient or gradient of another molecule or ion over the membrane (transport-transport). Examples of reaction-transport are the ATP-binding cassette (ABC) transporter and the phospho transferase system (PTS). In case of a transport-transport system the molecule is either translocated in the same direction together with one or more protons or another molecule (symport) or in opposite directions (antiport). The proton gradient involved in proton coupled transport needs to be balanced in terms of charge and therefore this mechanism involves the proton motive force (pmf). Finally, the H⁺ balance needs to be restored by H⁺-ATPase.

1.4.2. Thermodynamics

The described transport processes need to be accessed in terms of energetics. The Gibbs energy of the H⁺ coupled export of a charged compound (charge z) such as $C_{in}^z + nH_{in}^+ \rightleftharpoons C_{out}^z + nH_{out}^+$ can be written as:

$$\Delta_r G = \left[RT \ln \left(\frac{C_{out}^z}{1} \right) + 0 + nRT \ln \left(\frac{H_{out}^+}{1} \right) + 0 \right] - \left[RT \ln \left(\frac{C_{in}^z}{1} \right) + ZF\psi + nRT \ln \left(\frac{H_{in}^+}{1} \right) + nF\psi \right] \quad (1.1.)$$

Where $\ln(C^z/1)$ and $\ln(H^+/1)$ are the correction terms for concentrations different from 1 mol/L, $R = 8.314 \times 10^{-3}$ kJ/molK, T is the temperature in Kelvin (K); n is the number of protons (H^+ co-exported); and $ZF\psi$ is the correction for the electrical potential (Z is the charge of the transported molecule, F is the Faraday constant = 96.5 kJ/v e⁻mol and ψ is the inside membrane potential in volt).

The intracellular space has an electrical potential (the extracellular space has $\psi = 0$ by definition), of which the value depends on the extracellular pH to maintain a constant proton motive force (E_{pmf}). The relation between the electrical potential and the extracellular pH can be written as:

$$\psi = \frac{2.303RT}{F} (pH_{in} - pH_{out}) - E_{pmf} \quad (1.2.)$$

In this relation E_{pmf} and pH_{in} are homeostatic at values of $E_{pmf} = 0.15$ V and $pH_{in} = 7.6$ (Hesse *et al.*, 2002). With these assumptions, ψ only depends on the extracellular pH and becomes negative for high pH_{out} , and positive for low pH_{out} .

Assuming $\Delta_T G = 0$ in equation 1.1., one can calculate the logarithm of the equilibrium out/in equilibrium concentration ratio of the charged species of the transported compound according to equation 1.3.

$$\log \frac{C_{out}^z}{C_{in}^z} = z(pH_{out} - pH_{in}) + \frac{(n-z)(-E_{pmf})F}{2.303 RT} \quad (1.3.)$$

This ratio is the thermodynamic maximum value of the out/in ratio for a proton coupled export system.

1.4.3. Maximal out/in ratios of total acids

Organic acids can occur in a charged form depending on their pK_a value(s) and the ambient pH. Depending on the molecule to be transported, its charge (z), the mechanism (n) and the set extracellular pH, different scenarios have to be considered.

To achieve high extracellular concentrations of organic acids in a fermentation process, it is imperative to consider the presence of an efficient (high out/in ratio) exporter as well as metabolic reprogramming of the cell. Insufficient export results in intracellular accumulation and compromises the cell's homeostasis. The mechanisms of the transport process, and specially how much energy is demanded, is a research field in its own (Burgstaller, 2006; Karaffa and Kubicek, 2003; van Maris *et al.*, 2004).

Depending on the pH, there is an equilibrium between the four different species of tricarboxylic acids such as citric acid (H_3A , H_2A^- , HA^{2-} , A^{3-}), and three species for dicarboxylic acids as itaconic acid (H_2A , HA^- , A^{2-}).

It is therefore important to calculate, as function of the pH (Fig. S1.1.), the concentration ratios of the charged species with respect to the total acid – Fig. 1.6. In this figure the intersections between different species represent the values of the acid dissociation constants (citric acid: $pK_{a1}=3.13$, $pK_{a2}=4.76$, $pK_{a3}=6.39$; itaconic acid: $pK_{a1}=3.85$, $pK_{a2}=4.45$).

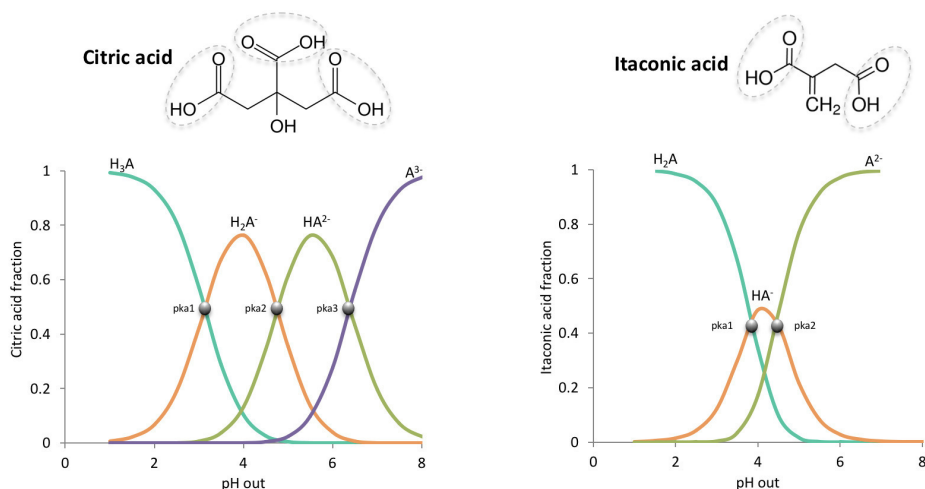


Fig. 1.6. Citric acid (left) and itaconic acid (right) fractions of different charged species depending on extracellular pH.

At the intracellular pH of *A. niger* (pH = 7.6), these carboxylic acids are near fully dissociated. In case of citric acid, 94% of the acid is fully dissociated (A^{3-}) and 6% of the acid is present in as the HA^{2-} species. For itaconic acid, 99.9% of the acid is fully dissociated A^{2-} and 0.1% in the HA^{-} species. Although different charged species of the acids can be exported, but given their abundance, the most likely exported species are the fully dissociated ones, which we will consider from this point on.

This also means that there is a metabolic production of H^{+} which must be exported as well: $3H^{+}$ per A^{3-} and $2H^{+}$ per A^{2-} for citric and itaconic acid respectively. Depending on the transport mechanism (uniport, symport, double symport and antiport), there could be export of additional H^{+} required.

It is important to understand the role of the extracellular pH and the different energy requirements (ATP expense) when considering different transport mechanisms. Fig. 1.7. shows the ATP cost of the export of A^{3-} and A^{2-} species for citric acid and itaconic acid respectively, depending on the type of mechanism.

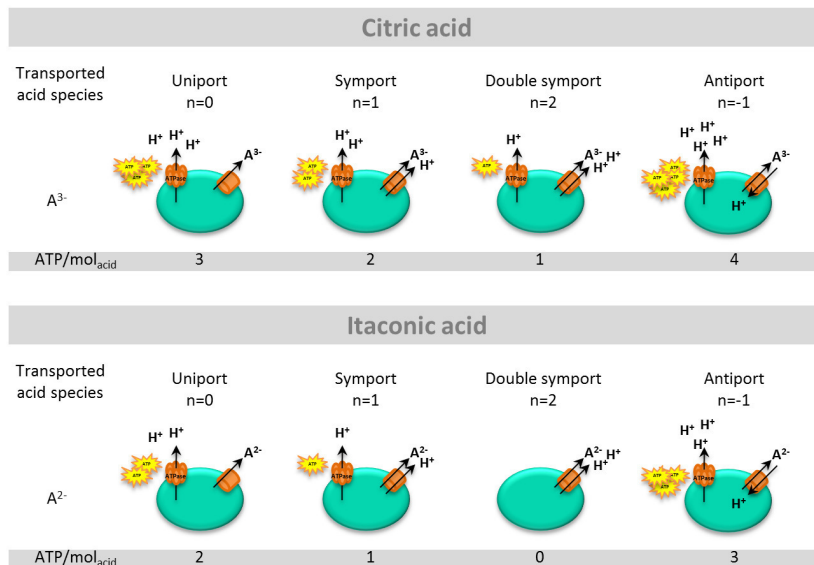


Fig. 1.7. Energy requirements for different export mechanisms in citric acid (upper panel) and itaconic acid (lower panel).

The ATP cost follows from the number of exported protons, using the eukaryotic H^+ -ATPase with a stoichiometry 1. When one proton (H^+) is imported, then there is a possible ATP benefit, assuming $1H^+$ per ATP synthesized.

Depending on the pH_{out} , different transport mechanisms will achieve different out/in ratios (Fig. 1.8.).

At neutral pH^{out} the uniport mechanism can achieve a high ratio (A_{out}/A_{in}) of about 10^6 when transporting the species A^{3-} of citric acid, but at the expense of 3 ATP. The symport system achieves lower ratios (10^3) but with less ATP expense.

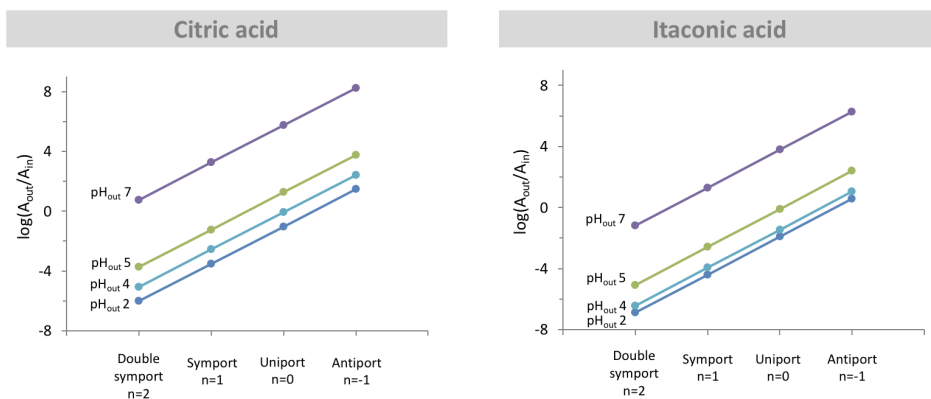


Fig. 1.8. Calculated equilibrium ratios of total acid (A_{out}/A_{in}) of citric acid (left) and itaconic acid (right) for fully dissociated transported species (A^{3-} and A^{2-}) by different transport mechanisms depending on the pH_{out}

However, at low $pH^{out} = 2$ ($pH < pK_a$) high out/in ratios require an antiport system, leading to the highest ATP expenses. Similar conclusions are obtained for the A^{2-} species of itaconic acid: to obtain high ratios out/in at low pH, an antiport mechanism is desired, but at higher ATP cost.

1.4.4. Organic acid solubility

A high organic acid titer in a fermentation process with a high producing industrial microorganism equipped with an efficient export system may result in acid

concentrations which approach, or even cross, the solubility limit. It is therefore important to consider these solubility limits.

The solubility of organic acids can be increased with increasing temperature (Fig. 1.9.).

At the pH where the acid is present predominantly in the undissociated form, the solubility limit of the undissociated acid is reached (Fig. 1.9.). At 25°C citric acid reaches this solubility limit of 3.366 M at pH 2, and itaconic acid reaches this limit (1.298 M) at pH 3. Below these pH values, the organic acids enter their solid state, which makes the low-pH approach very interesting from the recovery point of view (downstream processing).

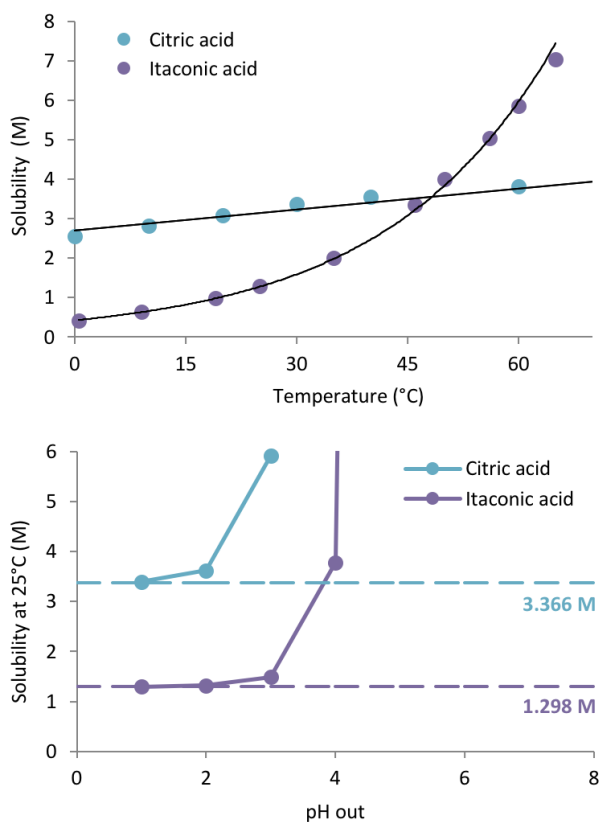


Fig. 1.9. Solubility of citric acid and itaconic acid depending on the temperature (upper panel) and pH (lower panel) (Sources: Kfivnkovi *et al.*, 1992; Mullin, 2001).

At low pH and temperature, not only the organic acids are closer to their solubility limits, which is economically advantageous because less alkali is required for pH control during the fermentation (no acidification is required in the downstream processing and as a result less waste salts are produced), but also because at low solubility the osmotic stress for the cells is less.

1.4.5. Futile cycle

It should also be noticed that in their undissociated form (H_3A for citric acid, and H_2A for itaconic acid), organic acids could diffuse freely over the cellular membrane. However, once imported into the cell and exposed to the intracellular pH which is close to neutral, weak acids dissociate into their fully charged species and H^+ . To maintain cell homeostasis and balance the charge intracellularly, the charged species are transported back by a required active export, generating a futile cycle – Fig. 1.10. This leads to extra energy consumption, hence more O_2 consumption, and thus lower yield and productivity.

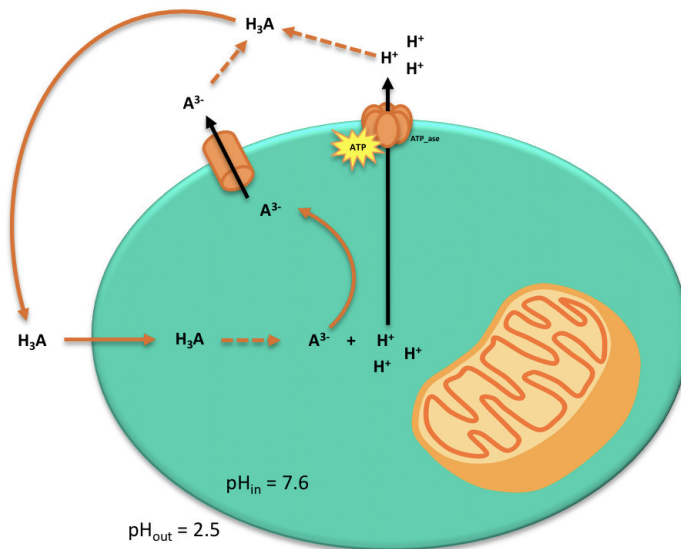


Fig. 1.10. Futile cycling of citric acid.

Unravelling the transport mechanisms is then crucial for the optimization of efficiency and economy of the process, and can help designing and developing strains better suited for the production of organic acids (Jamalzadeh, 2013).

The rate of diffusion of an undissociated acid as shown in Fig. 1.10. follows as:

$$q_{acid} = k \frac{6V}{d} (C_{acid\ out} - C_{acid\ in}) \quad (1.4.)$$

Where q_{acid} is the biomass specific uptake of the undissociated acid through passive diffusion (mol/h/Cmol), k is the permeability coefficient of the acid (m/h), V is the cell volume of *A. niger* ($32.8 \times 10^{-6} \text{ m}^3/\text{Cmol}$), d is the cell diameter ($10 \times 10^{-6} \text{ m}$), $C_{acid\ out}$ is the extracellular concentration of undissociated acid in mol/m³, and $C_{acid\ in}$ is neglected (= 0) as the intracellular concentration of undissociated acid is very low at $\text{pH}_{in} = 7.6$ (Hesse *et al.*, 2002).

The cell volume was estimated to be 1.2 ml/g_{DW} in *A. niger* (Ruijter and Visser, 1996), and the biomass molecular weight used was 27.3 ± 0.17 (Lameiras *et al.*, 2015), leading to $V = 32.8 \times 10^{-6} \text{ m}^3/\text{Cmol}$. The diameter of fungal hyphae varies between 5 µm to 15 µm, and therefore an average of 10 µm was considered in this approach (Geitmann and Emons, 2000). Note that in case of a solubility limit, there is a maximal rate

$$q_{acid,max} = k \frac{6V}{d} C_{acid\ out\ sol}.$$

1.4.6. Substrate transport mechanisms

For carbohydrate substrates, the eukaryotic fungal transport system has been extensively studied in *Saccharomyces cerevisiae* (Andre, 1995; Leandro *et al.*, 2009). The yeast hexose transporter (HXT family) contains at least 20 different proteins involved in the transport of glucose, and some of these transporters also have a broad specificity for other hexoses, as well as for pentoses. The main hexose transporters HXT1-7 and Gal2 from *S. cerevisiae*, are acting by facilitated diffusion (Flagfeldt *et al.*, 2009). In the filamentous fungus *Aspergillus nidulans* there are at least 17 putative HXT transporters identified in its genome (Wei *et al.*, 2004).

For *A. niger*, despite the 461 putative transporters from the major facilitator superfamily (MFS), from which 19 seem to be transporting glucose, only very few transporters have been identified and confirmed (genome sequencing reported by Pel *et al.*, 2007). A high affinity glucose/proton symporter MSTA was identified (van Kuyk *et al.*, 2004), as well as two other glucose proton symporters, MSTG and MSTH (Sloothaak *et al.*, 2015). In addition, a galacturonic acid transporter (unknown mechanism) GATA (Martens-Uzunova and Schaap, 2008; Sloothaak *et al.*, 2014), a fructose proton symporter FSY1 (Coelho *et al.*, 2013), a rhamnose proton symporter RHTA (Sloothaak *et al.*, 2016a) and three xylose transporters (unknown mechanism) XLTA, XLTB and XLTC (Sloothaak *et al.*, 2016b) were identified.

Details on the characteristics of some transporters of *A. niger* and their mechanisms are given in Table 1.2. It appears that substrate transporters are usually of the high affinity type using a proton symport mechanism, and are not specific for a single substrate.

Table 1.2. Summary of the known transporters and their mechanism in *A. niger*.

Transporter(s) name	Mechanism	Comment	Reference
n/a	unknown	High affinity glucose transporter (K_m 0.39 mM) at low concentrations and low-affinity transporter (K_m 3.67 mM) when grown on high concentration	Torres <i>et al.</i> , 1996
MSTA	Proton symporter	Transports fructose (K_m 4.5 ± 1.0 mM), xylose (K_m 0.3 ± 0.1 mM), mannose (K_m 0.06 ± 0.02 mM), and glucose (K_m 0.025 ± 0.01 mM).	van Kuyk <i>et al.</i> , 2004
FSY1	Proton symporter	two FSY1 homologues transport fructose (K_m 0.066 ± 0.011 mM and 0.10 ± 0.011 mM)	Coelho <i>et al.</i> , 2013
GATA	unknown	Galacturonic acid transporters	Martens-Uzunova and Schaap 2008; Sloothaak <i>et al.</i> , 2014
MSTG MSTH	Proton symporter	MSTG transports glucose (K_m 0.5 ± 0.04 mM), but also galactose, mannose and sucrose MSTH transports glucose (K_m 0.06 ± 0.005 mM), but also galactose, mannose, sucrose and fructose	Sloothaak <i>et al.</i> , 2015
RHTA	Proton symporter	Rhamnose transporter	Sloothaak <i>et al.</i> , 2016a
XLTA XLTB XLTC	unknown	Xylose transporters	Sloothaak <i>et al.</i> , 2016b

Nevertheless, there are at present no transporters described for the import of other 2nd generation feedstock monomers such as arabinose; however, the sequencing data from Pel and co-workers reveal many other potential transporters to be discovered (Pel *et al.*, 2007).

1.5. Scope and outline of this thesis

The aim of this project is to contribute to the knowledge of *A. niger* as a cell factory in the production of organic acids, in order to improve existing processes and to facilitate new ones. To this aim, fundamental studies were performed in two parts: the substrate and the product.

The objective of the former part is to understand the mechanism of uptake of different C5 and C6 substrates and how they interact in a simulated second generation feedstock mixture. For this, also the growth stoichiometry is relevant.

The objective of the product study is to address two important issues of industrial large scale production of organic acids: fermentation at low pH ($\text{pH} < \text{pK}_a$), which is desired because it allows cheaper downstream processing and avoids the consumption of expensive alkali and hence absence of stoichiometric salt production (Fig. 1.9.); and the achievement of high extracellular concentrations (high titers) which can be energetically demanding for the cell due to ATP dissipating futile cycling.

In Fig. 1.11., the scheme resumes the scope and flow of this thesis. In this study, both substrates and products of *A. niger* were studied. For that purpose, experimental approaches had to be designed and established.

Throughout this chapter (**chapter 1**), *A. niger* is the preferred filamentous fungus in fungal biotechnology. Although its cultivation under submerged fermentation had been shown possible by Kluyver's group in Delft (Kluyver and Perquin, 1932), there have been few process studies in the last 8 decades. One of the reasons is the difficulty of cultivation of this filamentous fungi: the high viscosity and pellet formation results in an insufficient mixed heterogeneous culture and low nutrient supply (Krull *et al.*, 2010). This issue is tackled in **chapter 2**, where a pellet-free homogeneous and well-defined continuous cultivation of *A. niger* was established in a dedicated bioreactor.

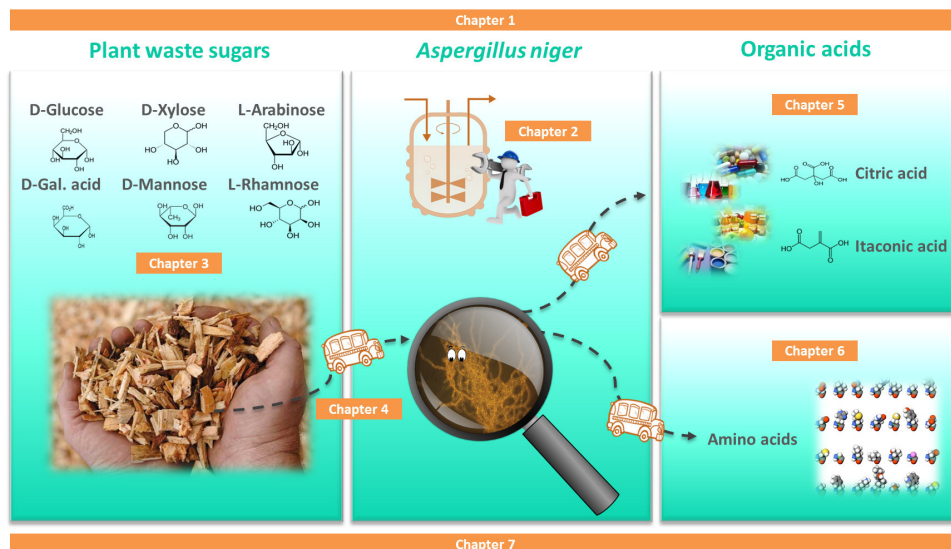


Fig. 1.11. Scope of this thesis.

Furthermore, to enable fundamental studies such as kinetics and transport characterizations with accurate quantification of inside and outside concentrations, a new rapid sampling and quenching protocol to obtain reliable intracellular metabolite levels was optimized (**chapter 2**), in order to obtain insights on both the intracellular and extracellular metabolome under steady state conditions.

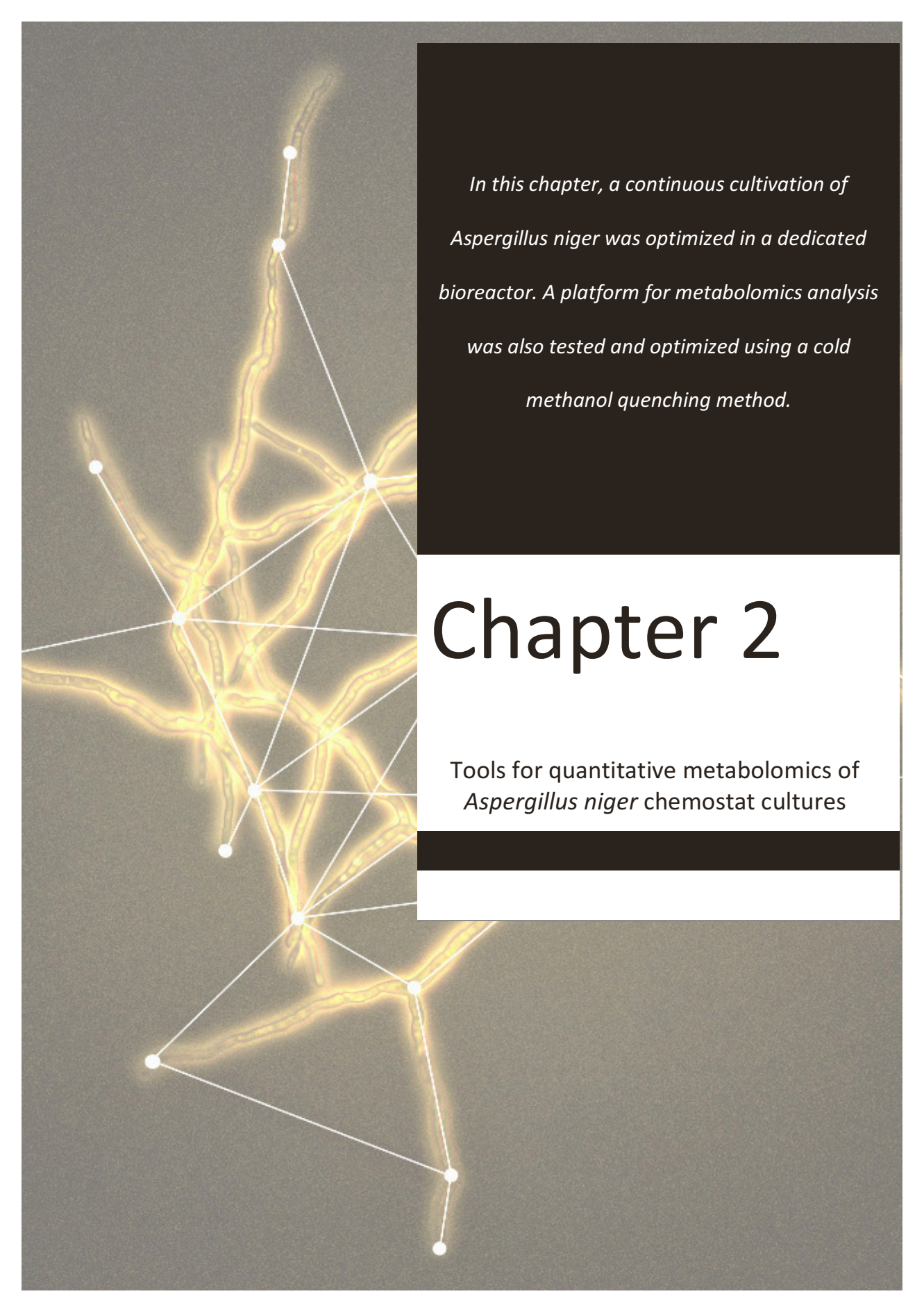
Once all experimental protocols and tools were established for *A. niger*, we focused on the substrate uptake and growth stoichiometry (**chapter 3 and 4**) and organic acid excretion and uptake (**chapter 5 and 6**).

Regarding the substrate uptake, in **chapter 3** we have characterized the growth of *A. niger* on different carbon sources from second generation feedstocks in single and mixed cultures with respect to growth stoichiometry and substrate uptake kinetics. In **chapter 4**, we have studied the stoichiometry of the metabolism of these sugars using stoichiometric modelling and metabolic flux analysis, together with an insight on the transport system of these molecules.

In **chapter 5** we study the impact of high concentrations and low pH of citric and itaconic acid on the uptake/secretion and transport energetics in two strains: *A. niger* NW185, a parental strain, and *A. niger* C3, an itaconic acid producer. Citric acid is a key product in Biotechnology being exploited for the last 120 years. Nevertheless, the transporters of this organic acid haven't been found and the effective extracellular acid accumulation it is still a mystery. Itaconic acid, has also its interest as it has been named one of the 12 top value added building blocks which can be obtained from biomass substrates (Werpy *et al.*, 2004). The production routes of both acids are relatively similar and their uptake/secretion, metabolism and transport are addressed in chapter 5.

Chapter 6, is related to a particular group of organic acids: the amino acids. In this chapter we disclose the function of a putative transporter and characterize it in *A. niger*. The transporter, which initially was hypothesized to be excreting carboxylic acids, was empirically revealed to be importing amino acids at low pH and low amino acid concentration (high affinity).

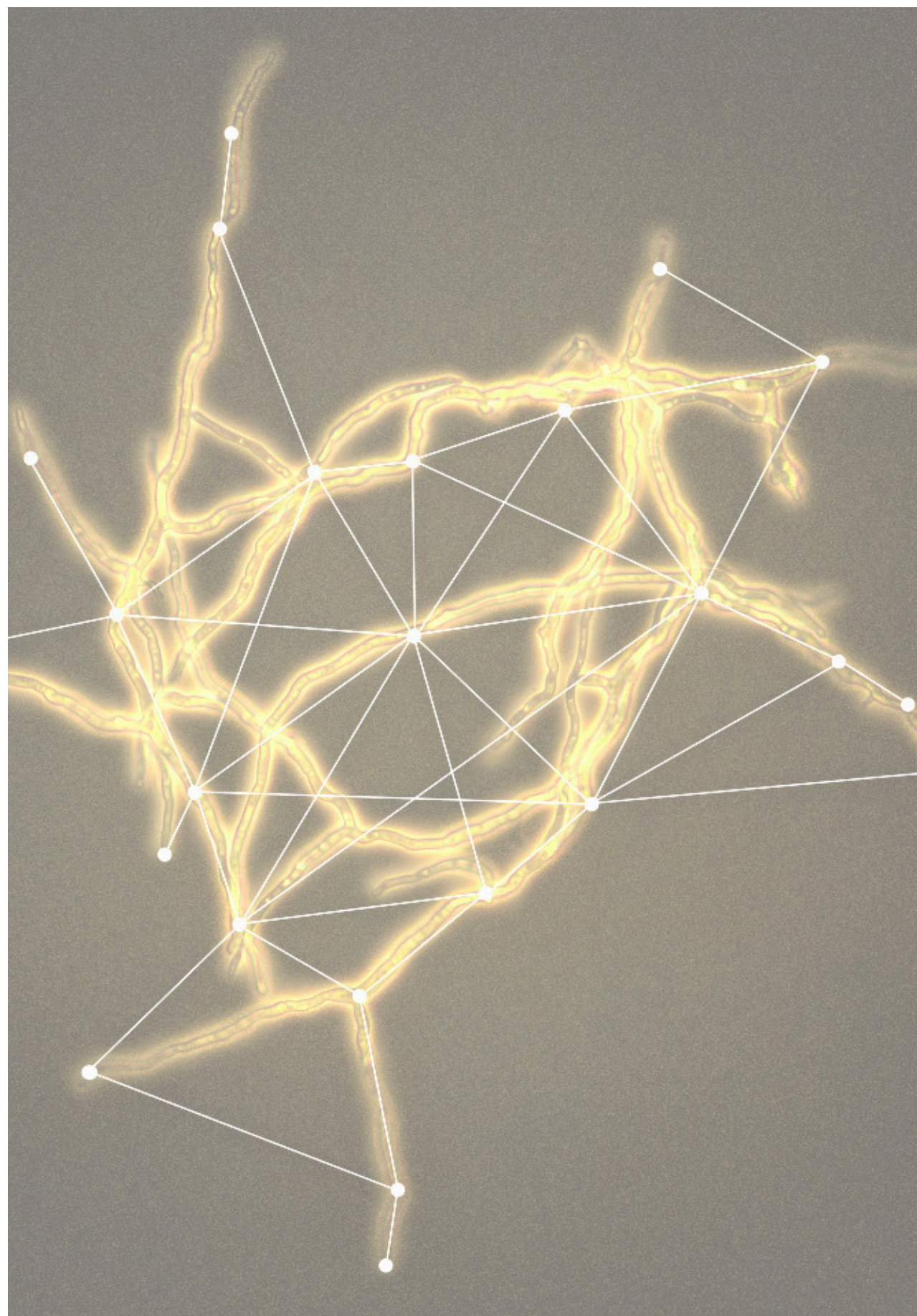
Finally, in **chapter 7**, general conclusions and guidelines for future research are explored, based on the obtained insights.

A microscopic image of *Aspergillus niger* hyphae, which are long, thin, and branching structures. Overlaid on the image is a network graph consisting of white dots (nodes) connected by thin white lines (edges). The nodes are positioned at various points along the hyphae, including at branch points and ends. The background is a dark, textured grey.

*In this chapter, a continuous cultivation of
Aspergillus niger was optimized in a dedicated
bioreactor. A platform for metabolomics analysis
was also tested and optimized using a cold
methanol quenching method.*

Chapter 2

Tools for quantitative metabolomics of
Aspergillus niger chemostat cultures



Abstract

Given the high citric acid production capacity of *Aspergillus niger*, it should be well suited as a cell factory for the production of other relevant acids such as succinic, fumaric, itaconic and malic acid. Quantitative metabolomics is an important *-omics* tool in a synthetic biology approach to develop *A. niger* for the production of these acids. Such studies require well defined and tightly controlled cultivation conditions and proper rapid sampling, sample processing and analysis methods. In this study we present the development of a chemostat for homogeneous steady state cultivation of *A. niger*, equipped with a new dedicated rapid sampling device. A quenching method for quantitative metabolomics in *A. niger* based on cold methanol was evaluated and optimized with the aim of avoiding metabolite leakage during sample processing. The optimization was based on measurements of the intermediates of the glycolysis, TCA and PPP pathways and amino acids, using a balance approach. Leakage was found to be absent at -20°C for a 40% (v/v) methanol concentration in water. Under these conditions the average metabolite recovery was close to 100%. When comparing *A. niger* and *P. chrysogenum* metabolomes, under the same cultivation conditions, similar metabolite fingerprints were found in both fungi, except for the intracellular citrate level which was higher for *A. niger*.

Keywords

Aspergillus niger, chemostat, rapid sampling, cold methanol quenching, quantitative metabolomics

2.1. Introduction

Filamentous fungi like *Aspergillus niger*, form a key step in the global carbon cycle by their capacity to degrade plant wastes efficiently, as they have one essential advantage: the massive secretion of enzymes that are capable of degrading plant cell wall constituents. In this manner sugars become available which can subsequently be taken up by the cells. This fungal characteristic is already exploited industrially for the production of enzymes such as glucoamylases and hemicellulases. Moreover, *A. niger* is applied in large scale industrial fermentations for the production of citric acid.

Considering the high citric acid production capacity of *A. niger* at low pH, it should be well suited for the production of other relevant organic acids, such as itaconic, succinic, fumaric and malic acid. Bio-based fermentative production of these acids from plant waste streams using *A. niger*, is an attractive alternative to their petroleum-based production. Moreover, the above mentioned dicarboxylic acids have a good potential as chemical building blocks in polymer synthesis (Werpy *et al.*, 2004). Overproduction of dicarboxylic acids in *A. niger* requires metabolic engineering of the fungus, not only with respect to the product pathway but also with respect to the import of lignocellulosic sugars (glucose, xylose, arabinose, etc.) and the export of the produced acids.

A. niger as a cell factory exhibits a flexible metabolism which enables growth on a wide range of substrates. Furthermore, its genome has been fully sequenced (Pel *et al.*, 2007) which facilitates metabolic engineering efforts for the development of strains for the production of new compounds and subsequent strain and process improvement. Hence, a systems biology approach can be applied for identifying and removing bottlenecks by combining different *-omics* levels.

Steady state as well as dynamic quantitative metabolomics with and without stable isotope labelling can be applied to identify kinetic and capacity bottlenecks in the product pathway, substrate import and product export. Such metabolomics studies

require well defined and tightly controlled cultivation conditions and proper rapid sampling, sample processing and analysis methods (van Gulik *et al.* 2000).

Unfortunately, the filamentous growth-form of *A. niger* poses problems, especially in bench-scale fermentors, due to the tendency of the organism to grow as pellets and to accumulate on the walls and probes of the fermentor, as well as in the outflow system in case of chemostat cultivation (Larsen *et al.*, 2004; Schrickx *et al.*, 1993). This should be avoided as a homogeneous culture is a prerequisite for proper metabolomics/fluxomics studies. Due to these practical difficulties, little work has been done with respect to chemostat cultivation of *A. niger*.

In one of the few chemostat studies on *A. niger*, changes in mycelium morphology and conidia formation were studied as a function of the growth rate (Schricks *et al.*, 1993). In the same work a *Teflon* covered ring bar magnet was used, which could be moved over the wall with an external horseshoe magnet, to remove wall growth. With a similar purpose, Swift *et al.* 1998 tried to reduce biomass accumulation on internal surfaces by periodically increasing the stirrer speed for 5 to 10 min.

Larsen *et al.* 2004 suggested the use of a custom made *variomixing* bioreactor, in which intermittently rotating baffles reduce the surface area susceptible to wall growth and probes were inserted below the surface level of the culture to prevent mycelium accumulation between the probes. With this technically complex bioreactor, wall growth was significantly reduced in batch cultivations of *Aspergillus oryzae*. Later on, this reactor was successfully used for steady state chemostat cultivation of *A. niger* (Jørgensen *et al.*, 2007). With the purpose of minimization of wall growth, Jørgensen *et al.* 2011 cooled the glass surface of the headspace of the bioreactor. Another problem when growing *A. niger* is its aggregation as pellets. It has been reported that when inoculating a culture with spores at pH values of 3.5 or higher, pellets were formed whereas free mycelium was formed when inoculation was done at pH 2.5 (Pedersen *et al.*, 2000).

In addition to a homogeneous cultivation, accurate sampling is required for quantitative metabolome analysis. Over the years, different rapid sampling devices have been developed (Schädel and Franco-Lara, 2009), to allow fast sampling of biomass from bioreactors for intracellular metabolomics studies. When constructing a sampling device, the residence time for the cells to pass from the reactor to a quenching fluid has to be considered and compared to the consumption rate of the available substrate (and oxygen for respiration-related processes). This residence time should be short enough to prevent any change in limitation to occur and thus to prevent changes in metabolite levels during sampling. Additionally, dead zones within the equipment must be avoided and the construction must permit aseptic use (Larsson and Törnkvist, 1996). In most of the described sampling devices the dead volume has been reduced by using channels with a small internal volume such as HPLC capillaries.

Currently, there is a sampling device built in house (Lange *et al.*, 2001), designed for *Saccharomyces cerevisiae*. This sampling device has been used for other metabolomics studies in different organisms, *e.g.* *Escherichia coli*, *Pichia pastoris* and even the filamentous *Penicillium chrysogenum* (Carnicer *et al.* 2012; Taymaz-Nikerel *et al.* 2009; de Jonge *et al.* 2012). However, *A. niger*, being a filamentous fungi, is not suited for the usage of such a device comprehending a sampling tube of 0.8 mm, and thus blocking the system due to the long hyphae (up to 100 μm) of the organism (Swift *et al.*, 1998).

Any changes in the environment of the cells directly influences their metabolism and thus also the outcome of a metabolome analysis. It is known that the turnover times of intracellular metabolites are generally small, in the order of seconds, considering their conversion rates and intracellular concentrations. Hence, quenching of cellular metabolism within a fraction of a second upon sampling is required, in order to avoid further (inter)conversion of metabolites and obtain a proper snapshot of the metabolic state.

The most critical assumption in quenching methods which allow separation of cells and extracellular medium and washing of the biomass, such as the cold methanol/water

method (de Koning and van Dam, 1992) is that intracellular metabolites will remain inside the cells during quenching, separation and washing. However it is known that some metabolites can leak from the cells into the quenching solution, which is later discarded, thus underestimating intracellular levels (Canelas *et al.*, 2008). For eukaryotic microorganisms, leakage can be avoided by adaptation of the composition of the quenching fluid (Carnicer *et al.* 2012; de Jonge *et al.* 2012; Canelas *et al.* 2008). Apart from quenching, also a proper extraction procedure is crucial, as it is not desired that the metabolites of interest are (inter)converted and/or degraded during this procedure. Only very few studies have been performed on the optimization of quenching and extraction procedures for metabolomics of *A. niger*.

Ruijter and Visser (1996) performed rapid sampling of *A. niger* cultures in a quenching solution of 60% aqueous methanol at -45°C and metabolite extraction was performed using a cold chloroform/methanol method. In this study it was stated that metabolites do not leak from the cells, as no significant concentrations were detected in the quenched filtrate. However, the detection limits of the analysis were not specified, and leakage cannot be quantified from intracellular concentrations only, as one needs to compare external and intracellular metabolite amounts. Jernejc (2004) evaluated different quenching methods and different extraction methods for metabolite recovery in *A. niger*. Quenching in liquid nitrogen or in a 60% methanol water solution at -40°C, gave similar results. For metabolite extraction, acid and alkali extractions were considered better methods than ethanol extraction, though recoveries of the different methods were not checked. In these previous protocols, the absence of leakage was not validated.

Here we describe the successful development of a chemostat protocol for homogeneous steady state cultivation of *A. niger*, based on a conventional turbine stirred bioreactor. We equipped the reactor with a dedicated rapid sampling device for fast and reproducible withdrawal of mycelium samples, allowing quantitative metabolome analysis. To obtain reliable snapshots of the metabolome, a cold methanol/water based quenching procedure was optimized and validated for absence

of leakage for *A. niger* using the metabolite balance approach as described by Canelas *et al.*, 2008. To this end, we quantified an extensive set of metabolites with different physicochemical properties in different sample fractions, using isotope dilution mass spectrometry (Mashego *et al.*, 2004; Wu *et al.*, 2005).

2.2. Materials and Methods

2.2.1. Strain and Inoculum

A. niger NW185 (*cspA1* short conidiospores, *fwA1* fawn coloured spores, *goxC17* glucose oxidase negative and *prtF28* oxalate non-producing) was used throughout. The conidial inocula for chemostat cultivation were obtained from cultures on complete medium agar plates at pH 6 containing 9 g/l glucose monohydrate as carbon source, 6 g/l NaNO₃ as N-source, 1.5 g/l KH₂PO₄, 0.5 g/l KCl, 0.5 g/l MgSO₄·7H₂O, 2 g/l meat peptone, 1 g/l yeast extract, 1 g/l tryptone and 15 g/l agar.

The agar medium was supplemented with 1 ml/l of trace elements solution, containing 10 g/l EDTA, 4.4 g/l ZnSO₄·7H₂O, 1.0 g/l MnCl₂·4H₂O, 0.32 g/l CoCl₂·6H₂O, 0.32 g/l CuSO₄·5H₂O, 0.22 g/l (NH₄)₆Mo₇O₂₄·4H₂O, 1.47 g/l CaCl₂·2H₂O and 1.0 g/l FeSO₄·7H₂O (Vishniac and Santer, 1957) and 1 ml/l of vitamins solution (containing 0.05 g/l D-biotin, 1 g/l CaD(+)panthotenate, 1 g/l nicotinic acid, 25 g/l myo-inositol, 1 g/l thiamine chloride hydrochloride, 1 g/l pyridoxol hydrochloride, 0.2 g/l p-aminobenzoic acid). Media were sterilized at 121°C for 20 min and the glucose solution was sterilized separately at 110°C. The trace elements and vitamin solutions were added sterile to the culture media by filtration through a 0.2 µm cartridge filter (Whatman FP 30/0.2 CA-S).

One week prior to inoculation of the fermentor cultures, the medium plates were inoculated with conidia from a stock culture kept at 4°C. Plates were incubated at 30°C for 4 days and then stored at 4°C. Spores were harvested and washed with saline solution containing 0.9% NaCl and 0.05% Tween 80 to enhance the release of the spores from the plates.

2.2.2. Fermentor set up

A 7 litre turbine-stirred bioreactor was used (Applikon, Delft, The Netherlands). The bioreactor was set up and operated as described in Nasution *et al.* (2006) with the following adaptations.

The broth level was chosen such that the baffles were completely covered (working volume of 4.5 ± 0.01 litre). A cooling tubing (4°C) was wrapped around the headspace of the fermentor to minimize growth of the fungus on the glass surface above the liquid. The exhaust gas of the fermentor was passed through a condenser (4°C) and a Nafion dryer (Permapure, Toms River, USA) before entering a NGA 2000 offgas analyser (Rosemount Analytical, Anaheim, USA) for measurement of the oxygen and carbon dioxide contents. Data acquisition was performed with MFCS/win 3.0 software.

The bioreactor was equipped with pH, temperature and dissolved oxygen probes, inserted in the metal bottom part of the fermentor, below the broth level.

The cultivation temperature was kept constant at 30.0°C (± 0.1), and the pH (Mettler Toledo InPro[®] 3030/120) was controlled at 3.0 (± 0.1) by addition of 4 M NaOH.

Sterile air was supplied via a mass flow controller (Brooks 58505 calibration at 0°C and 1 bar) at 1 l/min through a bottom sparger. Dissolved oxygen was monitored with an AppliSens Z010011020 probe.

To avoid biofilm formation on the wall, continuous media inflow was supplied at the bottom of the fermentor, along with the air supply. An overpressure of 0.3 bar was applied.

2.2.3. Batch cultivation

The fermentor, containing 4.5 kg of minimal medium, was inoculated with a conidial suspension to give a final concentration of 1×10^6 spores/ml, along with 0.003% (wt/wt) of yeast extract to induce conidia germination (Jørgensen *et al.*, 2011).

The glucose-limited minimal medium contained 0.5 g/l $(\text{NH}_4)_2\text{SO}_4$, 0.3 g/l KH_2PO_4 , 3 g/l $\text{NH}_4\text{H}_2\text{PO}_4$, 0.5 g/l $\text{MgSO}_4 \cdot 7\text{H}_2\text{O}$ and 1 ml/l trace elements solution (composition as described above), with a final pH of 4.6. Sterilization of the medium was performed by passing it through a 0.2 μm filter (*Sartorius stedim Sartopore 2*). The substrate concentration was 7.5 g/l of glucose monohydrate and the fermentor pH was controlled at 2.5 to prevent pellet formation.

Oxygen-sufficient growth was ensured by preventing the dissolved oxygen (DO) to decrease below 50%, of air saturation by automatic DO control through progressively increasing the stirrer speed from initial 100 rpm to a maximum of 450 rpm at the end of batch fermentation.

2.2.4. Chemostat cultivation

Continuous cultivation was started in the late exponential phase of the batch culture, approximately 30 hours after inoculation, by starting the medium feed. The composition of the chemostat medium was the same as the batch medium. Effluent was removed discontinuously via a pneumatic valve in the bottom of the reactor and a peristaltic effluent pump controlled by the broth weight. During chemostat cultivation the stirrer speed was kept constant at 450 rpm.

2.2.5. Sampling and analytical procedures

When a steady state was reached (after five residence times), at least 6 samples were taken for quantification of cell dry weight, concentrations of extracellular compounds and TOC (total organic carbon) content.

Broth samples for determination of the biomass dry weight concentration were taken from three different sections of the fermentation setup: the regular sampling port aside the fermentor vessel, the sampling port of the rapid sampling device and the outflow tube upstream the effluent vessel. In all cases, biomass dry weight was determined by filtration over glass fiber filters (47 mm, type A/E, Pall, USA),

subsequent washing with water and drying at 70°C until constant weight. All samples were analysed in triplicate.

Filtrate samples were obtained by quickly (within 3 s) withdrawing 5 ml of broth, via the over-pressure on the fermentor, into a syringe containing cooled steel beads (-20°C) to bring the sample temperature down to 0°C (Mashego *et al.* 2003). The broth was then immediately pressed through a 0.45 µm cartridge filter (Millex-HV durapore PVDF membrane) into a sampling tube, which was directly frozen in liquid nitrogen.

The total organic carbon content of the filtrate samples was quantified with a total organic carbon analyser (type TOC-L, Shimadzu, Kyoto, Japan). With this method, both total carbon (TC) and inorganic carbon (TIC) were measured. The latter representing the content of dissolved carbon dioxide and carbonic acid salts. Subtracting the inorganic carbon from the total carbon, yields the TOC.

The morphology of the hyphae was inspected by microscopy (Axiostarplus, Carl Zeiss, Jena, Germany) using a 10x objective, and biomass elemental composition was determined by combustion and subsequent gas analysis (carbon dioxide, water vapour and nitrogen mass fractions), gas chromatography (oxygen) and ICP-MS (phosphorus and sulphur) of washed and dried cells (Energy Research Centre of the Netherlands).

2.2.6. Rapid Sampling and quenching

A new customized rapid sampling device (Fig. 2.1.A and 2.1.B) designed such that pellet formation and/or long mycelia would not result in blockage of the device was built in house. The working principle is shown in Fig. 2.1.C.

Via a loop with an internal diameter of 8 mm and a peristaltic pump (Masterflex L/S, Cole-Parmer), the broth was pumped from the fermentor through the sampling device and back into the fermentor at a flow rate of 40 ml/s. The broth residence time in the part of the loop between the fermentor broth outflow and the sampling port was 0.25s. The broth residence time in the entire loop was 1.3 s. Whenever metabolite

dynamics had to be performed, the highest frequency of this device was 3 s, at which samples could be sequentially taken.

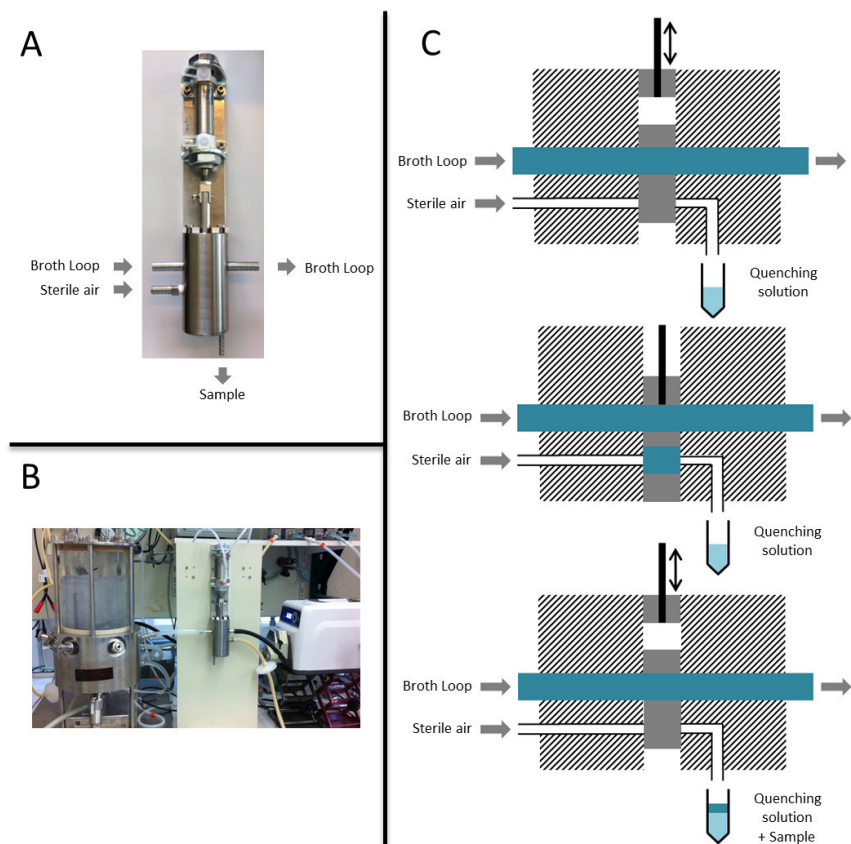


Fig. 2.1. Custom-made rapid sampling device and its working principle.

When sampling, the piston of the sampling device is pushed down and up again by a two-way pneumatic cylinder, removing a constant volume of broth from the loop. This constant volume is then pushed into a sampling vial containing the cold quenching fluid, by a constant flow of sterile air.

2.2.6.1. Rapid sampling and quenching for intracellular metabolome quantification

The procedure is described for the standard 60% aqueous/methanol quenching solution (at -40°C), however, the same procedure was applied for 50% (at -20°C) and 40% (at -20°C) aqueous/methanol mixtures (Fig. 2.2.).

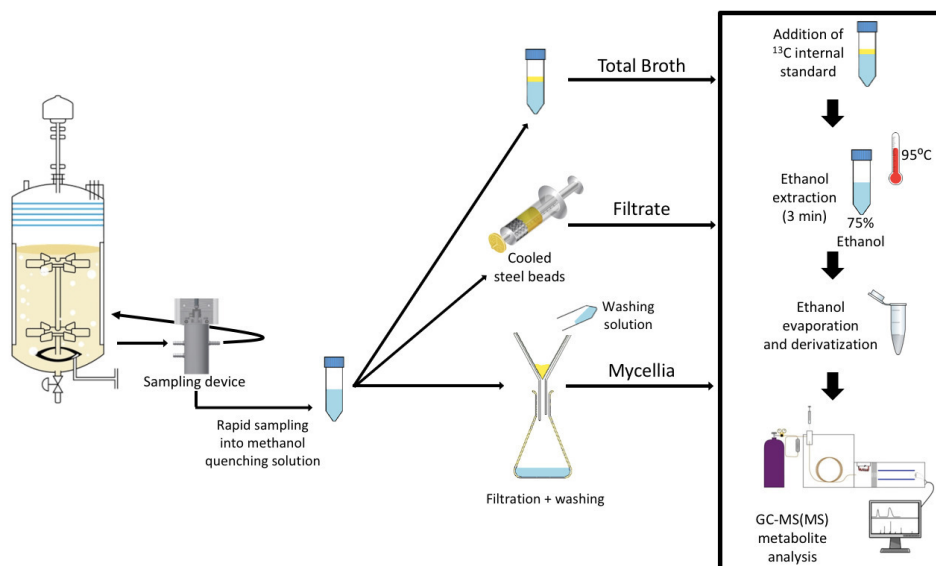


Fig. 2.2. Rapid sampling and quenching procedure of *A. niger*.

Two aliquots of $0.76 (\pm 0.04)$ g of broth was rapidly withdrawn from the broth loop with the sampling device and injected (< 1 s) into the same vial containing 10 ml of 60 % aqueous methanol (v/v) solution pre-cooled to -40°C . The exact sample weight was determined by weighing each tube before and after sampling. The content of each tube was quickly mixed by vortexing (1 s) and the tube was placed back in a cryostat (Lauda, Germany) at -40°C . A set of 3 replicates were taken within one minute.

The quenched cold mycelia samples were harvested and washed by cold filtration, according to a previously described method (Douma *et al.*, 2010) which was slightly modified. Filtration was performed using glass fiber filter disks (PALL glass fibre type E). To cool down the filter and filter unit, 20 ml of 60% aqueous methanol (v/v) solution pre-cooled to -40°C was poured onto the filter. Immediately thereafter the quenched mycelium sample was poured into the cold aqueous methanol on the filter. Then the vacuum pump was turned on and after the filter fell dry, 20 ml of cold (-40°C) 60% methanol was poured on the filter for a first washing followed by 40 ml of cold 60% methanol for a second washing of the mycelium sample.

2.2.6.2. Rapid sampling and quenching for extracellular metabolite quantification

Two aliquots of 0.76 (\pm 0.04) g of broth, withdrawn with the rapid sampling device, was quickly filtered through a syringe containing cooled steel beads (-20°C) and a 0.45 μm cartridge filter (Millex-HV durapore PVDF membrane) directly into the same tube containing 10 ml 40% methanol (v/v) at -20°C . The exact sample weights were determined by weighing all tubes before and after sampling.

2.2.6.3. Rapid sampling and quenching for metabolite quantification in whole broth

Sampling was done as for intracellular metabolites, by quenching two aliquots of 0.76 (\pm 0.04) g of broth in 10 mL of 40 % aqueous methanol (v/v) solution pre-cooled to -20°C , but the quenched cell suspension was not filtered. The exact sample weights were determined by weighing all tubes before and after sampling.

2.2.6.4. Extraction method

Boiling ethanol extraction was performed to ensure complete cell disruption and inactivation of enzyme activity, according to a method modified from Lange *et al.* 2001. The three sample fractions (described in 2.2.6.1. – 2.2.6.3.) were extracted immediately after sampling and quenching. For intracellular samples, the cooled filter paper with quenched mycelium was placed in a falcon tube containing 25 mL of 75% ethanol (pre-heated at 75°C), along with 100 μl of $\text{U-}^{13}\text{C}$ -labeled cell extract of *S. cerevisiae* as internal standard. Each tube was immediately vortexed and placed in a water bath at 95°C . After 3 min each tube was placed on ice, and later stored at -80°C . Extracellular and total broth fractions were also submitted to the same process, by adding the whole volume of quenched solution into 25 ml of 75% ethanol, with 100 μl of $\text{U-}^{13}\text{C}$ -labeled yeast extract, and boiled for 3 min at 95°C , as described for intracellular fractions.

2.2.6.5. Ethanol evaporation

All extracts were evaporated to dryness in a Rapid-Vap (Labconco, Kansas City, MO) under vacuum for 240 min, based on the protocol from Mashego *et al.* 2004. After evaporation, the residues were resuspended in 500 µl of water, and centrifuged at 1000 g to remove cell debris. The supernatants were stored at -80°C until further analysis.

2.2.6.6. Metabolite quantification

The concentrations of the metabolic intermediates from glycolytic, TCA and PPP pathways and aminoacids were measured by isotope dilution mass spectrometry (LC-IDMS/MS and GC-IDMS) according to the protocols of van Dam *et al.* 2002, de Jonge *et al.* 2011 and Cipollina *et al.* 2009 (Table S2.1.).

2.2.7. Balances, biomass specific rates and data reconciliation

From compound balances, the rates of substrate consumption (R_S), biomass formation (R_X), oxygen consumption (R_{O_2}), carbon dioxide production (R_{CO_2}) and by-products production (R_{TOC}) were calculated. From these rates, carbon and degree of reduction recoveries (equations 2.1. and 2.2.) were calculated wherein possible excretion of by-products was quantified by measurements of the total organic carbon content of the culture filtrate.

$$\text{Carbon recovery (\%)} = \frac{R_X + R_{CO_2} + R_{TOC}}{R_S} \times 100 \quad (2.1.)$$

$$\text{Degree of reduction (\%)} = \frac{Y_X R_X + Y_{TOC} R_{TOC} + Y_{O_2} R_{O_2}}{Y_S R_S} \times 100 \quad (2.2.)$$

The biomass specific net conversion rates (i.e. growth rate), glucose and oxygen consumption rates and carbon dioxide and TOC production rates, were calculated from the primary measurements of concentrations in gas and liquid phases, as well as gas and liquid flow rates, using the corresponding steady state mole balances. Data reconciliation was applied to obtain the best estimates of the measurements, within

their error margins, using the elemental and charge conservation relations as constraints (Verheijen, 2010).

2.2.8. Metabolite consistency check

The extent of metabolite leakage was evaluated by a metabolite balance approach according to Canelas *et al.* 2008. Each metabolite was quantified in different sample fractions, that is, in the mycelium fraction (intracellular; IC), the culture filtrate (extracellular; EC) and in the whole broth (WB). As the ^{13}C internal standard mix was added upstream the extraction step, any metabolite losses due to partial degradation could be corrected for. For each metabolite i , the following metabolite balances should be satisfied, if leakage of i from the cells into the quenching solution is absent:

$$M_i(\text{TB}) = M_i(\text{IC}) + M_i(\text{EC}) \quad (2.3.)$$

Here, M_i is the total amount of metabolite present per gram biomass dry weight.

If leakage occurs, the amount released from cells into the quenching solution can be calculated from:

$$M_i(\text{leakage}) = M_i(\text{TB}) - M_i(\text{IC}) - M_i(\text{EC}) \quad (2.4.)$$

Finally, the metabolite recovery can be calculated as:

$$\text{Recovery (\%)} = \frac{M_i(\text{IC})}{M_i(\text{TB}) - M_i(\text{EC})} \times 100 \quad (2.5.)$$

2.3. Results and Discussion

2.3.1. Chemostat cultivation of *A. niger*

2.3.1.1. Development of the chemostat protocol

A. niger was grown in a 7 litre turbine stirred bioreactor, specifically constructed for chemostat cultivation of filamentous fungi. The reactor vessel consisted of a glass upper part and a stainless steel bottom part in which all probes were inserted. The

stirrer was driven from the bottom, by means of a magnetic coupling. Feed medium was supplied continuously from the top of the reactor while effluent removal was discontinuous, accomplished with a pneumatic outflow device and a peristaltic pump which were controlled by broth weight.

Despite these features, a homogeneous steady state chemostat culture could not be achieved in this reactor, due to massive wall growth and accumulation of biomass in the headspace of the reactor (Fig. S2.1.), as also experienced in other studies (Larsen *et al.*, 2004; Schrickx *et al.*, 1993).

In order to obtain a homogeneous cultivation, avoiding accumulation of mycelium above the liquid surface and on the glass wall, as well as avoiding pellet formation, both the chemostat system and the way of operation had to be adapted.

As massive mycelium growth occurred in the headspace of the reactor below the medium inlet, which was positioned in the lid of the vessel, the medium inflow was moved to the sterile air supply, at the bottom of the fermentor. The broth level was chosen such that it covered the baffles to prevent biomass adhesion (4.5 litre working volume) and a cooling coil (4°C) was wrapped around the headspace of the fermentor with the same purpose. Moreover, a low cultivation pH (2.5) was used to prevent pellet formation.

During the preceding batch phase, the stirrer speed was progressively increased from 100 rpm to a maximum of 450 rpm through DO control (setpoint 50%), which minimized splashing and consequently biofilm formation on the fermentor wall. With these adaptations, homogeneous steady state chemostat cultivations could be achieved without significant wall growth. An illustrative figure can be found in the supplementary material Fig. S2.2.

Effluent broth was discontinuously removed via an 8 mm diameter tubing to assure homogeneous withdrawal of broth, where the biomass concentration in the broth outflow and in the fermentor should be the same. To verify this, in a previous

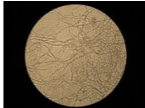

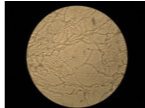
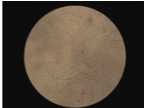
chemostat study at dilution rates of 0.045 h^{-1} and 0.087 h^{-1} (results not shown), the biomass concentration was measured in the outflow ($C_{x,\text{out}}$) and compared with the biomass concentration (C_x) inside the fermentor (Table S2.2.), showing no significant difference. Consequently, the important condition for a proper chemostat cultivation, that is, $C_x = C_{x,\text{out}}$, was satisfied.

2.3.1.2. Batch and chemostat cultivations

Using the optimized fermentor set up, *A. niger* was grown in aerobic glucose-limited chemostat culture. During the preceding batch phase, the pH was controlled at 2.5, which avoided the formation of pellets and assured exponential growth. The batch maximum growth rate on glucose was $0.26 (\pm 0.01) \text{ h}^{-1}$. This value is somewhat lower than the value of 0.29 h^{-1} reported in Jørgensen *et al.* 2007, for a different strain of *A. niger*.

During the late exponential phase, chemostat cultivation was initiated. Four different dilution rates were applied. Cultivations were assumed to be in steady state after 5 residence times under glucose limitation, which was verified by the measured carbon dioxide (Fig. S2.3.) and oxygen concentrations in the offgas being constant in time.

Table 2.1. Applied chemostat effluent flow rates and resulting dilution rates and obtained steady state biomass concentrations and respective biomass morphology.

Dilution rate (h^{-1})	0.043 ± 0.001	0.089 ± 0.001	0.134 ± 0.001	0.205 ± 0.003
Effluent flow rate (ml/h)	193	402	599	922
Residence time (h)	23.30	11.18	7.49	4.87
Biomass concentration ($\text{g}_{\text{DW}}/\text{Kg}_{\text{broth}}$)	3.02 ± 0.03	3.25 ± 0.04	3.38 ± 0.03	3.45 ± 0.05
Morphology (10x amplification)				

For all dilution rates, the biomass concentration was determined by dry weight, and the mycelium was examined microscopically, revealing no differences in morphology

(Table 2.1.), showing polarized growth of each hyphal tip and an increasing number of branches, resulting in freely dispersed mycelia in all cases.

2.3.1.3. Steady state and data reconciliation

For all dilution rates, residual glucose, biomass concentration, oxygen and carbon dioxide concentrations in the offgas were measured. In addition, the total organic carbon (TOC) concentration of the culture filtrate was determined in order to verify whether significant amounts of by-products were formed. From these measurements, it appeared that recoveries of the carbon and degree of reduction were on average > 90% and thus the biomass specific rates were calculated and reconciled (Table 2.2.). Moreover, the biomass elemental composition was determined from several chemostat samples and shown to be 27.3 ± 0.2 g/mol ($C_1H_{1.8}N_{0.12}O_{0.6}$) (Table S2.3.).

Table 2.2. Biomass specific net conversion rates and carbon and redox recoveries of steady state chemostat cultivations carried out at different dilution rates.

Dilution rate (h^{-1})	0.043		0.089		0.134		0.205	
	Unreconciled	Reconciled	Unreconciled	Reconciled	Unreconciled	Reconciled	Unreconciled	Reconciled
Carbon recovery (%)	99 \pm 3	-	94 \pm 3	-	96 \pm 2	-	92 \pm 2	-
Redox recovery (%)	95 \pm 2	-	89 \pm 4	-	90 \pm 3	-	88 \pm 3	-
q_x (mCmol/h)/Cmol	42.9 \pm 0.6	42.9 \pm 0.2	89.5 \pm 1.4	89.5 \pm 0.3	133.5 \pm 1.8	133.5 \pm 0.2	205.3 \pm 3.8	205.3 \pm 0.4
q_s (mmol/h)/Cmol	14.6 \pm 0.3	14.9 \pm 0.1	28.3 \pm 0.5	26.7 \pm 0.1	40.4 \pm 0.7	38.8 \pm 0.1	60.7 \pm 1.1	55.0 \pm 0.1
q_{O_2} (mmol/h)/Cmol	34.7 \pm 1.5	37.0 \pm 0.2	57.1 \pm 2.0	53.0 \pm 0.2	81.8 \pm 2.7	82.6 \pm 0.3	111.7 \pm 3.4	101.1 \pm 0.4
q_{CO_2} (mmol/h)/Cmol	37.7 \pm 1.5	39.4 \pm 0.3	61.8 \pm 2.0	55.4 \pm 0.2	90.4 \pm 2.3	81.3 \pm 0.2	118.5 \pm 3.5	90.1 \pm 0.2
q_{TOC} (mCmol/h)/Cmol	6.1 \pm 2.5	6.2 \pm 2.2	8.8 \pm 4.0	8.4 \pm 3.3	7.9 \pm 3.2	7.7 \pm 2.8	11.4 \pm 4.7	10.6 \pm 3.8

In further analysis, the *Herbert-Pirt* equation was obtained for this typical example of aerobic growth, whereby the yield and the maintenance coefficients were estimated (Fig. S2.4.) with respective values of 0.270 ± 0.002 mol_S/Cmol_X and $2.6 \times 10^{-3} \pm 0.3 \times 10^{-3}$ mol_S/h.Cmol_X (= 0.1 mmol_S/h.g_{DW}). These values are of the same order of magnitude with another glucose-limited chemostat study, where $Y_{X/S}$ and m_s were reported as 2.14 μmol/g_{DW} (\approx 0.2 mol_S/Cmol_X) and 0.16 μmol/h.g_{DW} (= 0.5 mmol_S/h.g_{DW}) respectively (Jørgensen *et al.*, 2007). In another study (Roels 1983), the maintenance coefficient for several microorganisms was also shown to be in the same order of magnitude as presented here.

Growth conditions were truly glucose-limited (residual glucose concentration around $0.6 \mu\text{Cmol/l}$ at 0.043 h^{-1}) and aerobic, however TOC measurements revealed that the culture filtrates contained a significant amount of organic carbon, corresponding to 2-7 % of the carbon supplied as glucose (15.8 mCmol/l at 0.043 h^{-1}). Higher TOC percentages were found for lower dilution rates (Fig. S2.5.). As the concentrations of residual glucose were considerably lower, the measured residual carbon was credited to cell lysis and excreted enzymes, since no significant amounts of organic acids were detected extracellularly (results not shown).

2.3.2. Rapid Sampling and quenching

2.3.2.1. Performance of the rapid sampling device

A proper sampling procedure is essential for unbiased quantification of the intracellular metabolome. Therefore, a sampling device that enables fast withdrawal of homogeneous broth samples which can in principle be operated at high sampling rates on a sub second scale was constructed (see materials and methods). High sampling rates are desired for future experiments, for capturing the short term dynamics of metabolite intermediates in response to pulse experiments. To avoid the risk of blocking of the system if clump or pellet formation would occur, the sampling device was connected to a fast broth loop with an internal diameter of 8 mm. With this sampling device a constant volume of broth (1 ml) could be removed from the loop.

The circulation speed of the broth in the loop was chosen such that the travel time of the broth through the sampling device was approximately 0.25 s. It was calculated that the change in the concentration of glucose was negligible within this time interval (Fig. S2.6.).

To test the functioning of the rapid sampling system the biomass concentrations in samples taken with the sampling device ($C_{x,SD}$) were compared with the biomass concentrations (C_x) in samples directly withdrawn from the fermentor (Table S2.4.). It was observed that even though the chamber size is 1 ml, the amount of liquid sampled

with the device is smaller because air is taken along. The average amount of liquid withdrawn was 0.76 (\pm 0.04) g. Remarkably, the biomass concentration was slightly lower (6-8%) in the samples withdrawn with the rapid sampling device. Therefore, the biomass concentrations determined in these samples were used to express metabolite levels per gram dry cell weight.

2.3.2.2. Optimization of cold methanol quenching fluid to avoid leakage in *A. niger*

The main purpose of this study was to develop a reliable, leakage free, quenching method for quantification of intracellular metabolites in *A. niger*, applicable to steady state chemostat cultivations as well as future dynamic pulse response experiments.

We choose the cold methanol based quenching procedure as this enables to remove extracellular metabolites, through cold centrifugation or filtration and subsequent washing with cold quenching solution. The centrifugation-based procedure for mycelia separation and washing appeared impracticable for *A. niger*, because no proper cell pellet was formed (results not shown). Therefore a quenching protocol based on cold filtration was developed, based on a previously developed procedure for *P. chrysogenum* (Douma et al., 2010).

Most importantly, the cold filtration based quenching and washing procedure, described in detail in the materials and methods section, enabled a significantly reduced contact time of the cells to the cold methanol compared to cold centrifugation, which should minimize possible leakage of metabolites. Furthermore, filtration compared to centrifugation, allows a much more efficient removal of the extracellular metabolites from the mycelium (Douma *et al.*, 2010).

Different variations (methanol concentration and temperature) of the filtration-based cold methanol quenching fluid were applied to samples withdrawn from glucose-limited chemostats carried out at dilution rates of 0.043 h⁻¹ and 0.089 h⁻¹.

Metabolite amounts were quantified in the mentioned sample fractions (intracellular, extracellular and total broth). For accurate quantification of leakage, the fraction of the washing solution should also be taken into account, however this measurement was shown to be impractical as the concentrations were too low to be quantified. Since the ^{13}C labelled internal standard was added to the fractions before the extraction step in 75% ethanol at 95°C, possible partial degradation of metabolites was corrected for.

Quantification was carried out using LC-MS/MS and GC-MS based on isotope dilution mass spectrometry (IDMS) (Canelas *et al.*, 2009). To enable comparison of metabolite amounts in different sample fractions, all amounts are expressed in μmol per gram biomass dry weight.

In a preliminary testing phase, 100% aqueous methanol (v/v) solution, as used by Canelas *et al.* 2008 for *S. cerevisiae*, was also tested, giving low recoveries, significant leakage and low intracellular metabolite amounts (results not shown). Therefore, this option was abandoned and for further optimization we zoomed in on methanol concentrations between 40% and 60%.

In Fig. 2.3., intracellular metabolite amounts are compared for quenching in different methanol concentrations (40%, 50% and 60%), at both dilution rates tested. Additional results can be found in the Tables S2.5. and S2.6. Clearly the intracellular metabolite level slightly dropped at 60% methanol, compared to 40% and 50%.

The extent of metabolite leakage brought about by the cold methanol quenching and washing of the mycelium was examined by carrying out metabolite measurements in different sample fractions (whole broth, extracellular and intracellular space). All the fractions were analysed in triplicate for this evaluation and the metabolite recoveries were calculated according to equation (2.5.). The results for the two dilution rates are shown in Tables S2.5. and S2.6.

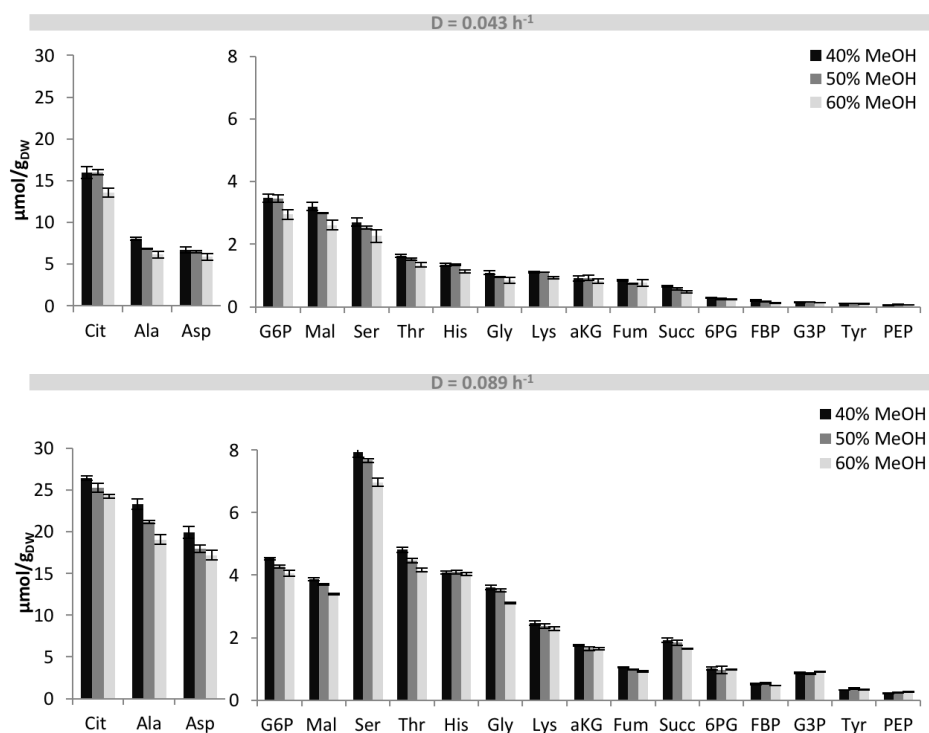


Fig. 2.3. Measured intracellular metabolite amounts for different methanol concentrations of the quenching solution for *A. niger* grown at dilution rates of 0.043 h⁻¹ (upper panel) and 0.089 h⁻¹ (lower panel).

Comparing different methanol concentrations, the average metabolite recovery and respective standard error was 79% ($\pm 10\%$) for 40% aqueous methanol (v/v), 77% ($\pm 9\%$) for 50% aqueous methanol (v/v), and 67% ($\pm 9\%$) for 60% aqueous methanol (v/v) for 0.043 h⁻¹ dilution rate. For the higher dilution rate (0.089 h⁻¹), the recoveries were: 95% ($\pm 4\%$) for 40% aqueous methanol (v/v), 93% ($\pm 5\%$) for 50% aqueous methanol (v/v), and 89% ($\pm 4\%$) for 60% aqueous methanol (v/v). Thus, for both dilution rates the recoveries were highest for the 40% aqueous methanol solution.

These results show that quenching at -20°C in 40% aqueous methanol (v/v) appears to be the best quenching procedure for *A. niger* intracellular metabolomics. From previous studies it can be inferred that the optimal cold methanol quenching conditions are quite different for different eukaryotic microorganisms, as it has been

found that for *S. cerevisiae*, *P. pastoris* and *P. chrysogenum* leakage was minimal for methanol concentrations of 100% (-40°C), 60% (-27°C) and 40% (-20°C) respectively (Canelas *et al.*, 2008; Carnicer *et al.*, 2012; de Jonge *et al.*, 2012). Remarkably, the optimal quenching condition found for *A. niger* in this study is the same as has been reported for *P. chrysogenum*.

Comparing the metabolite levels of the different dilution rates it is clear that the higher dilution rate leads to higher metabolite amounts, which is to be expected due to higher fluxes. Similar results were found in *S. cerevisiae* (Canelas *et al.*, 2009).

The levels of intra- and extracellular metabolites determined for *A. niger* grown in an aerobic glucose-limited chemostat at a dilution rate of 0.043h^{-1} , were compared with the levels reported for *P. chrysogenum* grown under similar chemostat conditions ($D = 0.05\text{h}^{-1}$), but at a significantly higher pH 6.5 (de Jonge *et al.*, 2012) (Fig. 2.4.). For *A. niger* the measured metabolite levels were between 0.02 (GAP) and $67\text{ }\mu\text{mol/g DW}$ (Tre) a difference of 4 orders of magnitude (Table S2.6.). Similarly, the published values for *P. chrysogenum* also vary 4 orders of magnitude between 0.09 (Met) and $12\text{ }\mu\text{mol/g}_{\text{DW}}$ (Cit).

Nevertheless, intracellular metabolite pools of both *A. niger* and *P. chrysogenum* are comparable. This is to be expected because, as both organisms were cultured at similar growth rates in glucose-limited chemostats, the fluxes in central metabolism in both systems should be very similar. Remarkable differences between both fungi are the intracellular levels of citrate, of which the level is 5 times higher in *A. niger* and threonine and aspartic acid, which are 5 and 6 times higher in *P. chrysogenum*. Citric acid is a known product in *A. niger* species as mentioned before, and threonine was found in other *Penicillium* studies, in the same range of intracellular amount here compared (Nasution *et al.*, 2006; Nasution, 2007).

For both organisms the extracellular metabolite amounts are considerably lower than the intracellular ones, with exception of citric acid and succinic acid which were both present in considerable amounts in the extracellular space of *P. chrysogenum*.

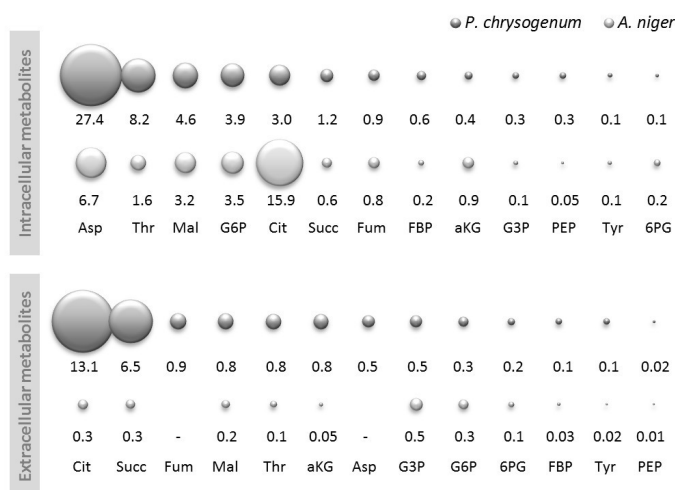
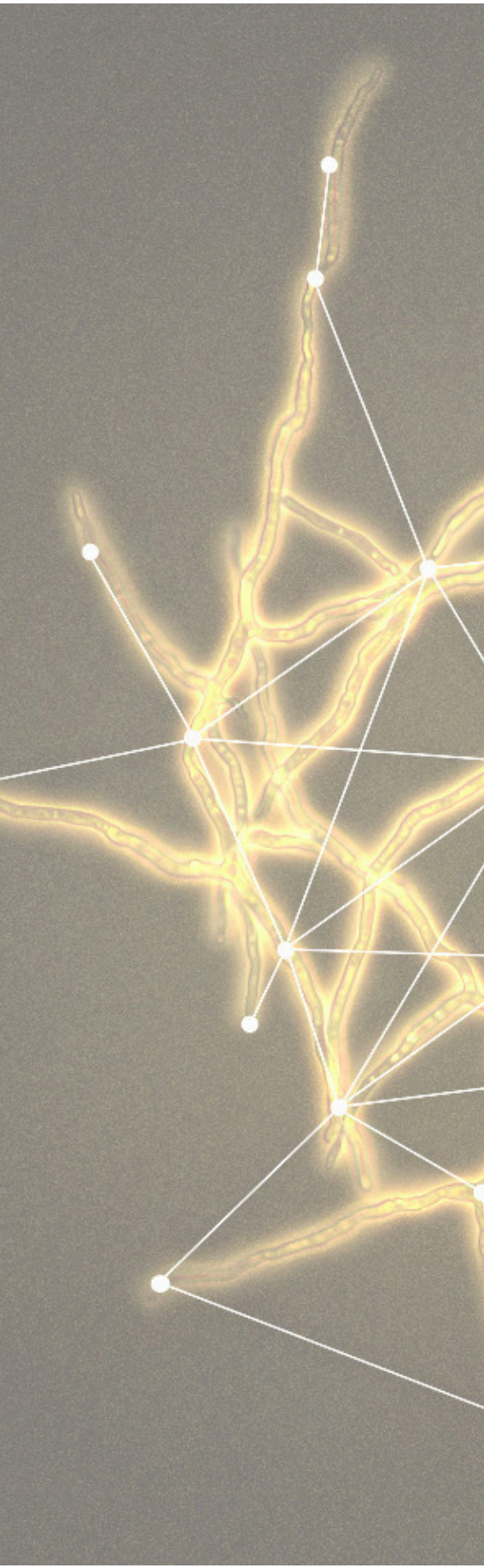


Fig. 2.4. Intra- and extracellular metabolite comparison of *A. niger* and *P. chrysogenum* at a comparable dilution rate. The bubble areas are proportional to the pool sizes of the metabolites ($\mu\text{mol/g}_{\text{DW}}$).

2.4. Conclusions

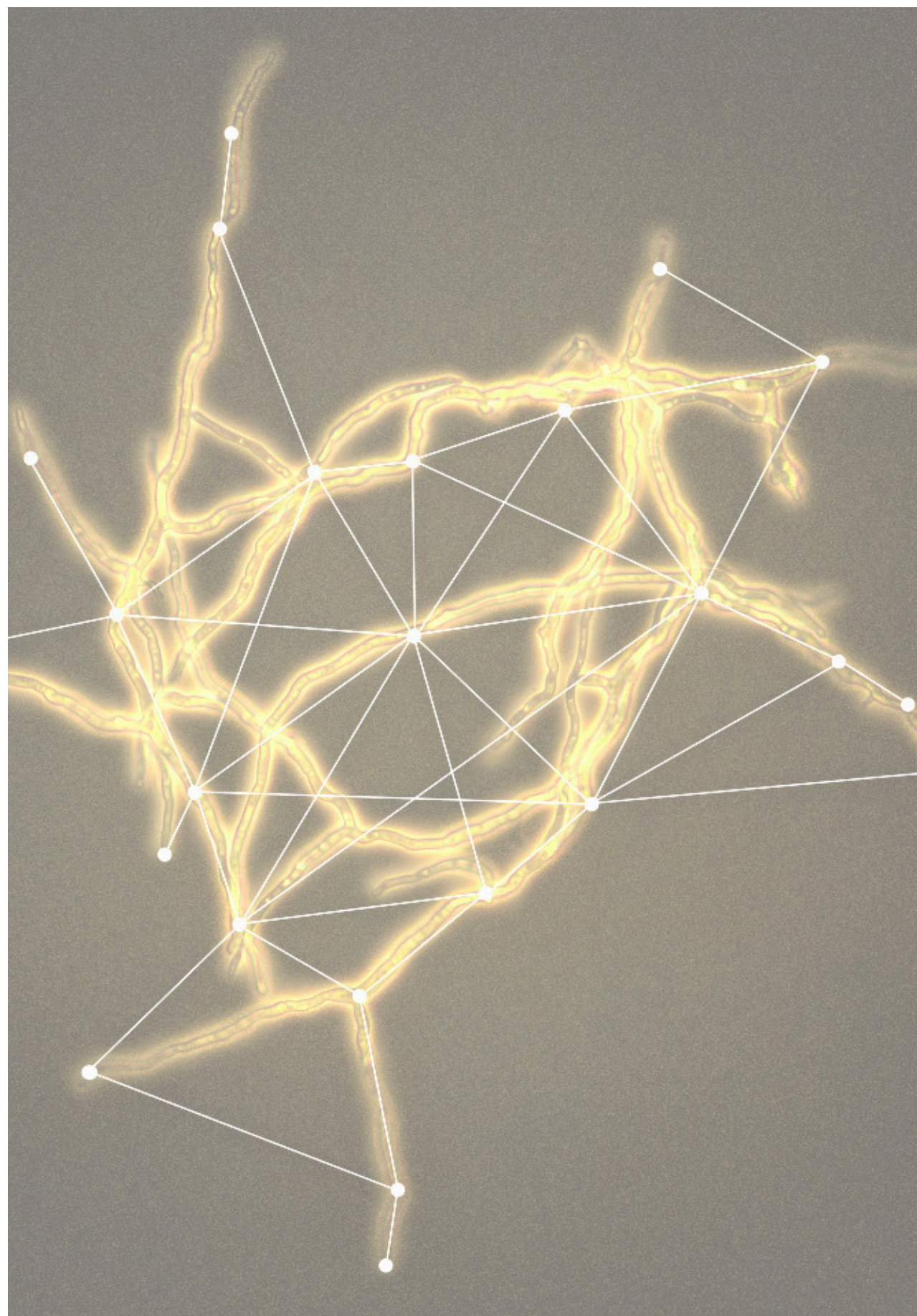
The purpose of this work was to develop a chemostat protocol for homogeneous steady state cultivation of *A. niger* in a conventional turbine stirred bioreactor, to develop and validate a robust rapid sampling device for filamentous fungi, and to perform a systematic investigation of cold methanol quenching combined with cold filtration to enable quantitative metabolomics studies of this organism. We demonstrated that *A. niger* is able to grow as homogeneous, finely dispersed mycelium in steady state glucose-limited chemostat cultures without significant wall growth. Furthermore, we developed a rapid sampling device and an efficient cold methanol quenching method combined with rapid cold filtration for rapid sampling, harvesting and washing of the mycelium enabling accurate quantitative metabolomics studies. A 40% (v/v) aqueous methanol mixture at -20°C resulted in minimal metabolite leakage. A comparison with published metabolome data of *P. chrysogenum*, grown in a similar chemostat, revealed similar metabolome profiles and some interesting differences. Overall, with this work we now have validated techniques for metabolomics studies of *A. niger*, as a starting point for further metabolomics and metabolite transport studies.



*In this chapter, we have characterized the growth of *A. niger* on different carbon sources from second generation feedstocks in single and mixed cultures with respect to growth stoichiometry and substrate uptake kinetics.*

Chapter 3

Stoichiometry and kinetics of single and mixed substrate uptake in *Aspergillus niger*



Abstract

In its natural environment the filamentous fungus *Aspergillus niger* grows on decaying fruits and plant material thereby enzymatically degrading the lignocellulosic constituents (lignin, cellulose, hemicellulose and pectin) into a mixture of mono- and oligosaccharides. To investigate the kinetics and stoichiometry of growth of this fungus on lignocellulosic sugars, we carried out batch cultivations on six representative monosaccharides (glucose, xylose, mannose, rhamnose, arabinose and galacturonic acid) and a mixture of these. Growth on these substrates was characterized in terms of biomass yields, oxygen/biomass ratios and specific conversion rates. Interestingly, some of the carbon sources were consumed simultaneously and some sequentially. With a previously developed protocol, a sequential chemostat cultivation experiment was performed on a feed mixture of the six substrates. We found that the uptake of glucose, xylose and mannose could be described with a Michaelis-Menten type kinetics. However these carbon sources seem to be competing for the same transport systems, while the uptake of arabinose, galacturonic acid and rhamnose appears to be repressed by the presence of other substrates.

Keywords

Aspergillus niger, plant waste streams, substrate uptake, kinetics, stoichiometry

3.1. Introduction

In white biotechnology, the feedstock represents the highest cost factor in the production of bulk chemicals. Therefore, there is an increasing interest in using cheaper biomass streams as feedstock for industrial biotechnology processes, the so called second generation feedstocks.

Second generation feedstocks have the advantage that they do not compete with food supplies but have the disadvantage that they are much more complex than first generation ones. Second generation feedstocks consist of mixtures of different fermentable carbon sources from plant biomass of agricultural crops waste, which are currently insufficiently used. Of the global 200×10^9 tons per year of plant biomass produced, over 90% is lignocellulose. About $8\text{--}20 \times 10^9$ tons of this biomass is potentially accessible but remains unexploited (Lin and Tanaka, 2006).

Rumbold *et al.*, 2009 tested the performance of six industrially relevant microorganisms by submitting them to growth conditions that they may encounter in a second generation feedstock based production process (mixture of substrates, inhibitors, extreme pH, etc.). The generated data were used to rank the organisms by relative performance, and *Aspergillus niger* scored the highest, leading to a stronger motivation for the use of this microorganism in second generation feedstocks (Rumbold *et al.*, 2009).

A. niger is known to grow on hexose as well as pentose substrates, and can also hydrolyse plant material due to high levels of excreted enzymes having the capacity to degrade the plant cell wall polysaccharides: mainly lignocellulose and pectin (Gouka, Punt and Van Den Hondel, 1997).

Lignocellulose contains three structural polysaccharides: cellulose (40% to 50%), hemicellulose (25% to 35%) and lignin (15% to 20%) (de Souza *et al.*, 2011). Besides glucose, sugar monomers in hemicellulose can include xylose, galactose, mannose and arabinose; pectins on the other hand are rich in galacturonic acid and rhamnose.

The shift of industrial biotechnology from highly refined sugar syrups (first generation feedstocks) to more sustainable and cheaper carbon and energy sources, requires a shift from single substrate to mixed substrate use (van Maris *et al.*, 2006).

To obtain a better understanding of the uptake of individual substrates in a complex mixture as well as the stoichiometry and kinetics of growth and product formation under those conditions, careful kinetic studies are required. Generally, the uptake and metabolism of different carbon sources in heterotrophic microorganisms is controlled through carbon catabolite repression (CCR). In many cases glucose is the preferred substrate for growth and thus the presence of glucose will repress the uptake and metabolism of other available carbon sources. Glucose repression was first studied in the bacterium *Escherichia coli* (Moses and Prevost, 1966) and later on also in yeasts and filamentous fungi (Ronne, 1995).

In this work we studied the capacity of *A. niger* for uptake of six selected monosaccharides present in lignocellulosic biomass, that is, three C6 sugars (glucose, mannose and rhamnose) two C5 sugars (xylose and arabinose) and a sugar acid (galacturonic acid). We investigated the stoichiometry and kinetics of substrate uptake and aerobic growth on these different carbon sources, under substrate-limited (sequential chemostat cultures) as well as substrate excess conditions (shake flask and batch cultivations), using single and mixed substrate feedstocks. With the application of *A. niger* for the production of organic acids in mind, we used a strain (*A. niger* NW185) not capable of producing gluconic and oxalic acid and carried out all cultivations at pH 2.5 for reasons outlined in the Materials and Methods.

3.2. Materials and Methods

3.2.1. Strain and Inoculum

A. niger NW185 (*cspA1* short conidiospores, *fwA1* fawn coloured spores, *goxC17* glucose oxidase negative and *prtF28* oxalate non-producing) was used throughout. Unless stated otherwise, the hyphal inocula for batch and continuous cultivations were

obtained from shake flask cultures. Spores for pre inoculum were grown on agar plates and harvested as described in Lameiras *et al.*, 2015. A concentration of 1×10^6 spores/ml was pre-inoculated in a 250 ml shake flask containing 100 ml of PM medium and 100 mM of sorbitol (Ruijter, van de Vondervoort and Visser, 1999) at pH 4.5. Sorbitol was used as a pre-substrate as it does not induce or repress any catabolic system (Sloothaak *et al.* 2014).

The shake flask was incubated overnight at 30°C in an orbital shaker (CERTOMAT BS-1, Sartorius group) at 250 rpm. The resulting mycelia suspension, was separated by centrifugation (*Heraeus Biofuge Stratos*, *Thermo Scientific*, USA) for 2 min at 10000 G, 4°C and washed two times with 50 ml PM medium without carbon source at room temperature and subsequently used to inoculate the bioreactor (one shake flask per bioreactor).

3.2.2. Shake flask cultivation

A. niger was inoculated in 250 ml shake flasks, containing 100 ml minimal medium (0.5 g/l $(\text{NH}_4)_2\text{SO}_4$, 0.3 g/l KH_2PO_4 , 3 g/l $\text{NH}_4\text{H}_2\text{PO}_4$ and 0.5 g/l $\text{MgSO}_4 \cdot 7\text{H}_2\text{O}$), at initial pH 2.5. The pH 2.5 for growth in continuous cultivation has high advantages in terms of morphology and broth homogeneity (Lameiras *et al.*, 2015) but is also highly relevant because we are interested in organic acid production.

In each shake flask, the medium was supplemented with one single carbon-source, such that the added amount of carbon was the same (total 228 mCmol/l), namely 38 mM of D-glucose, D-galacturonic acid, L-rhamnose and D-mannose; and 45.6 mM of D-xylose and L-arabinose. Furthermore, 1 ml/l of trace elements solution was added, containing 10 g/l EDTA, 4.4 g/l $\text{ZnSO}_4 \cdot 7\text{H}_2\text{O}$, 1.0 g/l $\text{MnCl}_2 \cdot 4\text{H}_2\text{O}$, 0.32 g/l $\text{CoCl}_2 \cdot 6\text{H}_2\text{O}$, 0.32 g/l $\text{CuSO}_4 \cdot 5\text{H}_2\text{O}$, 0.22 g/l $(\text{NH}_4)_6\text{Mo}_7\text{O}_{24} \cdot 4\text{H}_2\text{O}$, 1.47 g/l $\text{CaCl}_2 \cdot 2\text{H}_2\text{O}$ and 1.0 g/l $\text{FeSO}_4 \cdot 7\text{H}_2\text{O}$ (Vishniac and Santer, 1957).

Medium was sterilized at 121°C for 20 min and the carbon-source solutions were sterilized separately at 110°C. The trace elements were added sterile to the culture

media by filtration through a 0.2 µm cartridge filter (Whatman FP 30/0.2 CA-S).

One set of shake flasks was inoculated with spores and the second set with washed mycelia from one shake flask previously grown in PM medium as described above.

Cultures were incubated for 50 hours in an orbital shaker at 30°C and 250 rpm (CERTOMAT BS-1, Sartorius group).

3.2.3. Single carbon source batch cultivation

Batch cultivations were operated in a 2 litre bioreactor with 1 litre working volume (Applikon, Schiedam, The Netherlands), on minimal medium (section 3.2.2.) supplemented with either 38 mM D-glucose, 38 mM D-galacturonic acid, 38 mM L-rhamnose, 38 mM D-mannose, 45.6 mM of D-xylose or 45.6 mM L-arabinose.

The bioreactor was equipped with pH, temperature and dissolved oxygen probes. Throughout the cultivation, the pH was kept at 2.5 (± 0.1) by controlled addition of 1M NaOH and the temperature was controlled at 30°C (± 0.1).

Sterile air was supplied via a mass flow controller (Brooks 58505 calibration at 0°C and 1 bar) at 0.22 vvm through a bottom sparger, and an overpressure of 0.3 bar was applied.

The exhaust gas of the fermentor was passed through a condenser (4°C) and a Nafion dryer (Permapure, Toms River, USA) before entering a NGA 2000 offgas analyser (Rosemount Analytical, Anaheim, USA) for measurement of the oxygen and carbon dioxide contents. Data acquisition was performed with MFCS/win 3.0 software.

3.2.4. Mixture of carbon sources batch cultivation

Fermentation conditions and control were carried out as described for the single substrate batch fermentations (section 3.2.3.), with the difference that the minimal medium was supplemented with equimolar concentrations of carbon of six different carbon sources (6.3 mM D-glucose, 6.3 mM D-galacturonic acid, 6.3 mM L-rhamnose,

6.3 mM D-mannose, 7.6 mM of D-xylose and 7.6 mM L-arabinose), to a total of 228 mCmol/l.

3.2.5. Sequential chemostat cultures

In contrast to the batch fermentations (sections 3.2.3 and 3.2.4), the sequential chemostat cultures experiment was performed in a 7 litre bioreactor with a working volume of 4.5 litres. Fermentor set up and operating conditions were the same as described in Lameiras *et al.*, 2015, and temperature and pH were the same as the batch experiments.

The reactor was inoculated with pre grown and washed mycelia into minimal media supplemented with 12.6 mM D-glucose, 12.6 mM D-galacturonic acid, 12.6 mM L-rhamnose, 12.6 mM D-mannose, 15.2 mM of D-xylose and 15.2 mM L-arabinose. After the batch phase was finished, the feed was initiated with a starting dilution rate of 0.04h^{-1} . Subsequently, the dilution rate was increased to 0.21h^{-1} in eleven steps (0.04h^{-1} , 0.06h^{-1} , 0.08h^{-1} , 0.09h^{-1} , 0.11h^{-1} , 0.13h^{-1} , 0.14h^{-1} , 0.16h^{-1} , 0.17h^{-1} , 0.19h^{-1} and 0.21h^{-1}).

3.2.6. Sampling and analytical procedures

During batch cultivations (both single and mixture of substrates), at least 6 samples were taken for quantification of cell dry weight, biomass elemental composition, extracellular metabolites, and total organic carbon (TOC), during the exponential phase and at the end of the batch. During the sequential chemostat cultures experiment, a minimum of triplicate samples were withdrawn after 2 residence times, at each dilution rate.

Biomass dry weight was determined by filtration of 5 ml of broth over glass fiber filters (47 mm, type A/E, Pall, USA), subsequent washing with 10 ml of water and drying at 70°C until constant weight. All samples were analysed in quadruplicate.

Biomass elemental composition was determined by combustion and subsequent gas analysis (carbon dioxide, water vapour and nitrogen mass fractions), gas chromatography (oxygen) and ICP-MS (phosphorus and sulphur) from washed and dried cells (Energy Research Centre of the Netherlands).

Filtrate samples were obtained by quickly (within 3 s) withdrawing 5 ml of broth, via the over-pressure on the fermentor, into a syringe containing cooled steel beads (-20°C) to bring the sample temperature down to 0°C (Mashego *et al.* 2003). The broth was then immediately pressed through a 0.45 µm cartridge filter (Millex-HV durapore PVDF membrane) into a sampling vial, which was directly frozen in liquid nitrogen.

The total organic carbon content of filtrate samples was quantified with a total organic carbon analyser (type TOC-L, Shimadzu, Kyoto, Japan). With this method, both total carbon (TC) and inorganic carbon (TIC) were measured. The latter representing the content of dissolved carbon dioxide and carbonic acid salts. Subtracting the inorganic carbon from the total carbon, yielded the TOC in filtrate.

The residual concentration of the different carbon sources was measured by different methods.

For the batch cultivation on single substrates (section 3.2.3), analyses were implemented by a HPLC method, using a H⁺ exchange column at 60°C (Bio-Rad HPX-87H 300*7.8mm), employing phosphoric acid 1.5 mmol/l in Milli-Q water at 70°C as mobile phase with a refractive index detection (Waters 2414; sens =1024; temp = 30°C) and UV detection (Waters 2489; 210 nm).

For the mixture of carbon sources (section 3.2.4) both GC-IDMS/MS and HPLC methods were used. The concentrations of the sugars measured by isotope dilution mass spectrometry (GC-IDMS/MS) was according to the protocols of (Niedenführ *et al.*, 2016) with the following changes: temperature gradient was slower in order to have a better separation for xylose and arabinose and the temperature was increased to 5°C/min instead of 10°C/min. Glucose¹³, xylose¹³, mannose¹³ and arabinose¹³ were

added as internal standards (IS) for the same ^{12}C compounds, while for rhamnose and galacturonic acid, glucuronic acid and fumarate were used as IS respectively. The HPLC method used for the same measurements was performed in an ion exchange column in Lead (Pb) form column at 85°C (Bio-Rad HPX-87P300*7.8mm), employing milliQ water at 70°C as mobile phase with a refractive index detection (Waters 2414; sens =1024; temp = 30°C) and UV detection (Waters 2489; 210 nm).

The samples from the sequential chemostat cultivation experiment (section 3.2.5.) were analysed with a Dionex ICS – 5000 HPIC system with AS-AP sampler, SP pump, Carbopac PA-20 3*150 mm column and Aminotrap 3*30 mm precolumn employing 2 mM NaOH isocratic (for 17.5 min followed by a cleaning step of 5 min with 200 mM and equilibration for 15 min), 20 mM NaOH isocratic (15 min followed by 5 min cleaning with 200 mM NaOH and equilibration for 15 min) or gradient: 15 min 10 mM NaOH followed by a linear increase to 200 mM in 15 min, then a linear gradient in 20 min with 0.5 M sodium acetate in 200 mM NaOH from 4% to 40 % v/v, followed by a cleaning step of 5 min 200 mM NaOH and equilibration for 15 min (for acidic sugars). All eluents with a flow of 0.5 ml/min at 30°C. The detection was by electrochemical pulse at 15°C.

3.2.7. Balances, biomass specific rates and data reconciliation during single carbon source batch cultivation

Using the gas phase balances (O_2 and CO_2) and liquid phase balances (biomass and substrate), the batch cumulative amounts of consumed O_2 and substrate and produced CO_2 and biomass were calculated.

Subsequently, because the carbon and degree of reduction balances were close to 100%, the element reconciled cumulative amounts were calculated as function of time, as described in Cruz *et al.* 2012.

These reconciled amounts were used to calculate the maximum biomass specific conversion rates (μ^{\max} , q_s^{\max} , $q_{\text{CO}_2}^{\max}$, $q_{\text{O}_2}^{\max}$, i.e. the biomass specific conversion rates of

biomass, substrate, carbon dioxide and oxygen respectively) and the growth stoichiometric values.

The biomass elemental composition was analysed for each substrate and taken into account for the data reconciliation.

3.2.8. Balances, biomass specific rates and data reconciliation during sequential chemostat cultivation

Using the steady state mole balances, the rates of substrate (R_s), biomass (R_x), carbon dioxide (R_{CO_2}), oxygen (R_{O_2}) and by-products in the culture filtrate (R_{TOC}), were calculated from the primary measurements of concentrations in gas and liquid phases, as well as gas and liquid flow rates. From these rates, carbon and degree of reduction recoveries (equations 3.1. and 3.2.) were calculated.

$$\text{Carbon recovery (\%)} = \frac{R_x + R_{CO_2} + R_{TOC}}{\sum R_s} \times 100 \quad (3.1.)$$

$$\text{Degree of reduction (\%)} = \frac{Y_x R_x + Y_{TOC} R_{TOC} + Y_{O_2} R_{O_2}}{\sum Y_s R_s} \times 100 \quad (3.2.)$$

$\sum R_s$ is the weighted sum of all consumed carbon sources in Cmol/l, and R_{TOC} is the residual total organic carbon resulted from the subtraction of the concentration of the residual substrates to the measured TOC. After checking absence of relevant carbon and degree of reduction gaps, data reconciliation was applied to obtain the best estimates of the measurements, within their error margins, using the elemental and charge conservation relations as constraints (Verheijen, 2010).

3.2.9. Substrate uptake kinetics

Microbial growth studies report several different equations to define substrate uptake kinetics. The simplest and widely used equations follow the hyperbolic Michaelis-Menten model of enzyme kinetics (equation 3.3.).

$$q_s = q_{smax} \times \frac{C_s}{K_m + C_s} \quad (3.3.)$$

In a first approach of this study, the data obtained from the sequential chemostat cultivations were fitted to a Michaelis-Menten equation. When $C_s = K_s$, the value of q_s corresponds to 50% of the q_s^{\max} .

Depending on the outcome of the fitting of equation 3.3., two situations were considered: competition for the same transport system; or catabolite repression from other substrates.

To model the uptake of competing sugars, we assumed that these sugars are taken up by the same import systems and that their uptake could be described by competition, according to Schäuble *et al.*, 2013 - equation 3.4.

$$v_1 = \frac{v_{max1} S_1}{K_{m1} \left(1 + \sum_{i=2}^n \frac{S_i}{K_{mi}} \right) + S_1} \quad (3.4.)$$

Where, S_1 competes with $n-1$ substrates S_2, \dots, n for the binding site of the enzyme. The variables K_{mi} describe the Michaelis-Menten affinity constant for each substrate S_i .

Catabolite repression of the uptake/metabolism of different carbon sources can be described by a so called switch function, based on the Hill kinetics (equation 3.5.), whereby the expression of an enzyme (e.g. transport protein or rate controlling enzyme of a catabolic pathway) is repressed by the presence of another carbon source:

$$v_{max}(R) = v_{max}(U) \left(\frac{1}{1 + \left(\frac{R}{K_R} \right)^n} \right) \quad (3.5.)$$

Herein $v_{max}(R)$ and $v_{max}(U)$ are respectively the repressed and unrepressed enzyme rates, R is the repressor concentration and K_R the repression constant.

3.3. Results and Discussion

3.3.1. Shake flask cultivations on single carbon sources

As a preliminary experiment to investigate which carbon sources would sustain growth and whether growth on different carbon sources would lead to different morphologies, *A. niger* was cultivated on minimal medium in shake flasks with six different substrates. Two sets of shake flask cultivations were carried out. The first set was inoculated with spores, while the second set was inoculated with mycelia pre-grown on the same minimal medium with sorbitol as the carbon source (Fig. 3.1.).

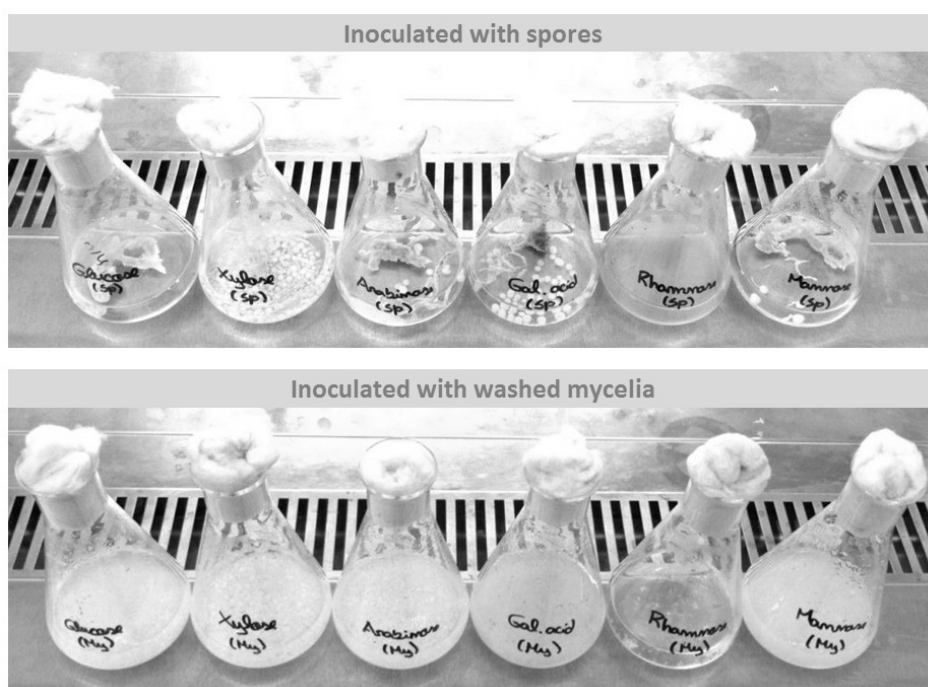


Fig. 3.1. *A. niger* morphology after 50h of growth in minimal media inoculated with spores (upper panel) and washed mycelia (lower panel). From left to right: glucose, xylose, arabinose, galacturonic acid, rhamnose and mannose.

After 50h of incubation, all shake flask cultures showed evident growth with the exception of rhamnose. This carbon source did not seem to induce spore germination

nor further growth of pre-grown mycelia. Nevertheless, growth has been observed on L-rhamnose as a sole carbon source for *A. niger* in minimal media (Fries and Kallstromer, 1965; Sloothaak *et al.*, 2016a).

Further comparison between the sets of shake flask cultivations indicated that inoculation with spores generates heterogeneity in the morphology of the mycelia among the different carbon sources with sometimes the formation of pellets, while inoculation with mycelia induces a uniform and similar, pellet free, morphology for all the different carbon sources (Fig. 3.1.). Such pellet free morphology is preferred in kinetic studies to avoid diffusion limitation.

3.3.2. Bioreactor batch cultivations on single carbon sources

To be able to study growth and substrate uptake of *A. niger*, batch cultures were performed on each single substrate, in 2 litres' bench scale bioreactors. All bioreactor cultures were inoculated with washed mycelia pre-grown on minimal media with sorbitol as the carbon source. During the batch cultivations samples were taken for quantification of the concentrations of biomass and residual carbon source. The concentrations of O₂ and CO₂ in the offgas were measured online for the calculation of the O₂ consumption and CO₂ production rates as a function of time. The obtained profiles for the different batch cultures are shown in Fig. 3.2.

In contrast to what was observed for the shake flask cultivations, *A. niger* did grow on minimal media with rhamnose as sole carbon source in the bioreactor.

The first striking differences between the batch cultivations carried out on the different carbon sources were the duration of the lag phase and the total duration of the batch. The rhamnose cultivation had the longest lag phase (around 50 hours, and therefore explaining the absence of growth in shake flasks) and longest duration (85 hours). In contrast, the glucose, arabinose and mannose cultivations had short or no lag phases and were finished after about 30 hours.

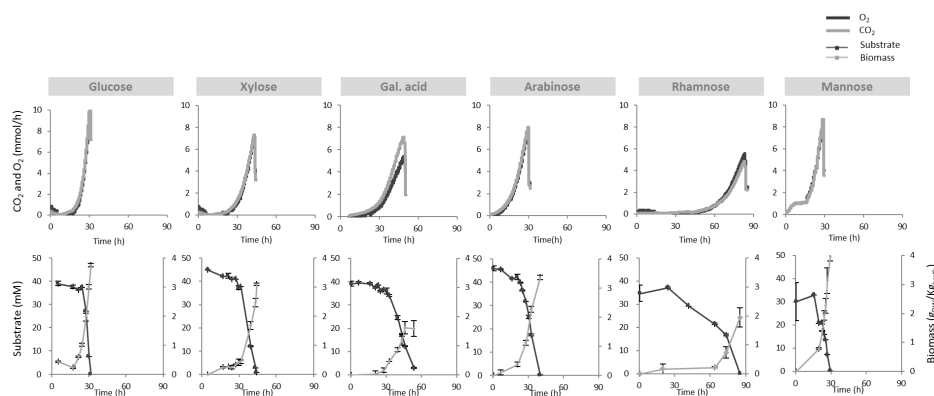


Fig. 3.2. Carbon dioxide production and oxygen consumption rates (upper panel) and biomass production - right axis - and carbon source consumption - left axis (lower panel) during batch phase using single different carbon sources.

It should be realized that the degree of reduction of the used carbon sources is not the same for all of them (Roels, 1983). For the sugars glucose, mannose, xylose and arabinose, the generalized degree of reduction is 4 electrons per Cmol ($\gamma_s = 4e^-/C$). However, galacturonic acid is more oxidized ($\gamma_s = 3.333 e^-/C$) and rhamnose is more reduced ($\gamma_s = 4.333 e^-/C$). This can clearly be seen from the respiratory quotients (Table 3.1.), i.e. the ratios of the biomass specific carbon dioxide production (q_c^{\max}) and oxygen consumption (q_o^{\max}) rates. As expected, for the substrates with a degree of reduction of $4 e^-/C$ the respiratory quotients have a value slightly higher than one, however, for the more oxidized substrate galacturonic acid the value is significantly higher than one, while for the more reduced substrate rhamnose the value is significantly lower than one.

The obtained measurements show in general that carbon and degree of reduction balances have recoveries of more than 90% (Table 3.1.), indicating that by-product formation is either absent or insignificant.

The cumulative O_2 , CO_2 , substrate and biomass data obtained during exponential growth (Fig. S3.1.) were used to obtain the best estimates of the biomass yield and

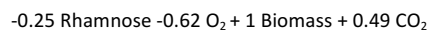
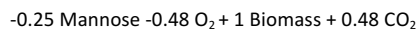
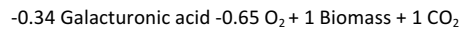
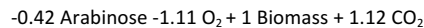
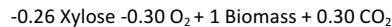
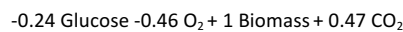
biomass specific conversion rates (Table 3.1.) using data reconciliation (method explained in section 3.2.7). The biomass elemental composition was analysed for each substrate and taken into account for the data reconciliation (Table S3.1.).

Table 3.1. Carbon and degree of reduction recoveries, reconciled biomass yield and maximum biomass specific conversion rates for different carbon sources in *A. niger*, in single batch cultivation.

Carbon source	RQ Respiratory Quotient	Carbon balance (%)	Degree of reduction balance (%)	$Y_{x/s}$ Biomass yield (Cmol _x /Cmol _s)	μ^{\max} max. growth rate (h ⁻¹)	q_s^{\max} max. substrate uptake rate (mol _s /h)/(Cmol _x)	q_O^{\max} max. O ₂ uptake rate (mol _{O₂} /h)/(Cmol _x)	q_C^{\max} max. CO ₂ production rate (mol _{CO₂} /h)/(Cmol _x)
Glucose	1.03 ± 0.04	94 ± 2	94 ± 2	0.68 ± 0.03	0.221 ± 0.004	0.054 ± 0.001	0.101 ± 0.003	0.104 ± 0.003
Xylose	1.02 ± 0.07	87 ± 2	83 ± 2	0.77 ± 0.06	0.149 ± 0.007	0.039 ± 0.002	0.044 ± 0.002	0.045 ± 0.002
Arabinose	1.01 ± 0.04	98 ± 3	94 ± 5	0.47 ± 0.01	0.097 ± 0.001	0.041 ± 0.001	0.108 ± 0.003	0.109 ± 0.003
Gal acid	1.53 ± 0.07	93 ± 4	88 ± 10	0.50 ± 0.06	0.092 ± 0.005	0.031 ± 0.001	0.060 ± 0.002	0.092 ± 0.003
Mannose	1.00 ± 0.06	96 ± 2	92 ± 2	0.68 ± 0.03	0.151 ± 0.004	0.037 ± 0.001	0.072 ± 0.003	0.072 ± 0.003
Rhamnose	0.79 ± 0.05	101 ± 5	96 ± 7	0.67 ± 0.03	0.116 ± 0.003	0.029 ± 0.001	0.072 ± 0.003	0.057 ± 0.003

Large differences in biomass yields and maximum biomass specific conversion rates were observed for the different single substrate cultivations. Glucose, xylose and mannose were the substrates on which the highest biomass yield, maximum growth rate, and maximum substrate uptake rate were obtained.

From Table 3.1., the growth stoichiometry for unlimited exponential growth on the different substrates can be obtained by dividing the biomass specific conversion rates of substrate, oxygen, biomass (= maximum growth rate) and carbon dioxide by the maximum growth rate. This yields the overall reaction equations for the formation of 1mol of biomass from substrate and oxygen:



From an energy point of view, looking at the consumed oxygen per produced biomass, it is observed that xylose has the lowest oxygen consumption (about $0.30 \text{ mol}_{\text{O}_2}/\text{mol}_{\text{biomass}}$). Glucose and mannose have a higher oxygen requirement (about $0.47 \text{ mol}_{\text{O}_2}/\text{mol}_{\text{biomass}}$) while galacturonic acid and rhamnose have an even higher oxygen demand of respectively 0.65 and $0.62 \text{ mol}_{\text{O}_2}/\text{mol}_{\text{biomass}}$. Finally, arabinose has the highest oxygen consumption of $1.1 \text{ mol}_{\text{O}_2}/\text{mol}_{\text{biomass}}$. These differences representing the differences in net energy expenditure for the formation of biomass for these different substrates, maybe due to different metabolic pathways. In case of arabinose, the energy and oxygen requirements are quite puzzling when compared to xylose, as this substrate has a very similar assimilation pathway in *A. niger*. These outputs ought to be further explored and confirmed by metabolic flux analysis.

3.3.3. Bioreactor batch cultivations on a mixture of carbon sources

The metabolic versatility of *A. niger* was investigated during growth on a mixture of all six carbon sources. Remarkably, in this cultivation, the CO_2 profile resembled the typical pattern of diauxic growth (Fig. 3.3.). This could indicate that some of the substrates were taken up and metabolised simultaneously, while the uptake and metabolism of other substrates was repressed and occurred only after the repressing substrates were depleted, as explored later.

Quantification of the residual concentrations of the different carbon sources at different time points during the batch cultivation was carried out with two methods (HPLC and GC-IDMS/MS), which gave essentially the same results. Here, we only show the results obtained with GC-IDMS/MS. We plotted each substrate in a different graph to facilitate visualization (Fig. 3.3.). From these plots it can be seen that glucose consumption started immediately, while the other carbon sources were not consumed during the first 10 hours after inoculation, indicating that the presence of glucose repressed the metabolism of all other carbon sources. The repression of the transport and metabolism of less preferred substrates in the abundance of a sugar which is easily metabolized, e.g. glucose, is a well-known phenomenon amongst

microorganisms, also in case of filamentous fungi (Flipphi *et al.*, 2003; Schneider and Wiley, 1971 and Portnoy *et al.*, 2011).

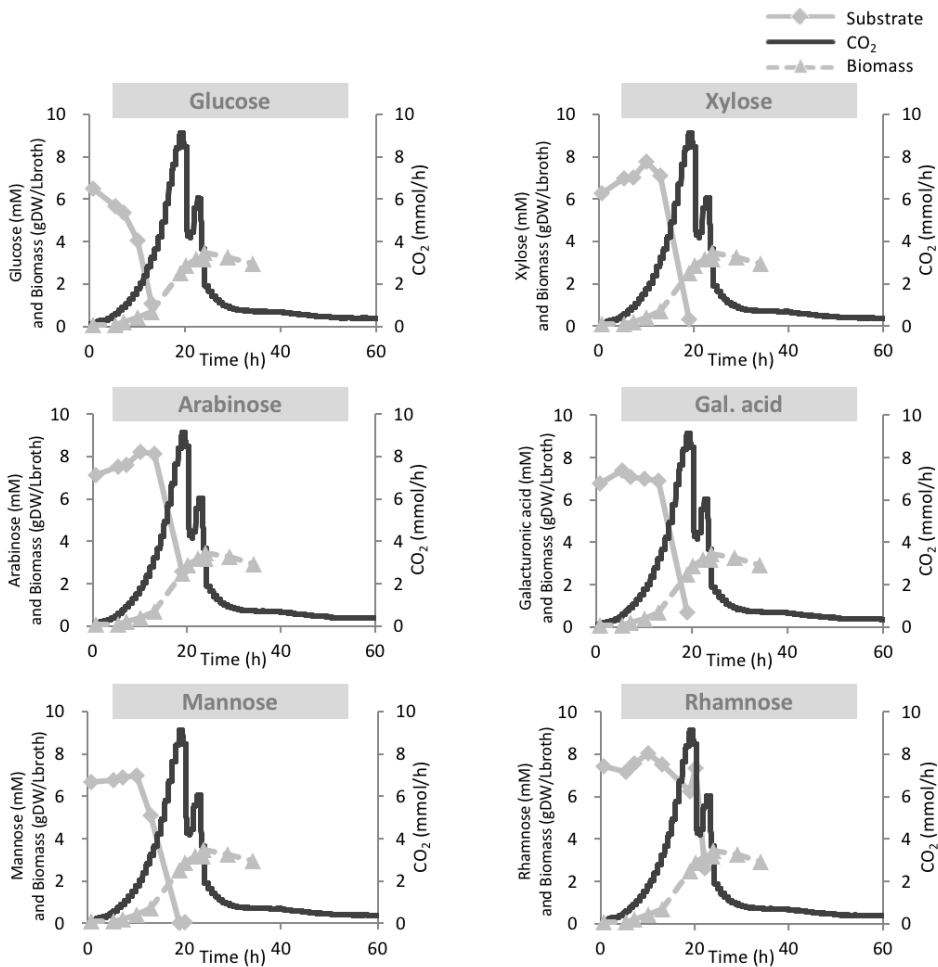


Fig. 3.3. Carbon dioxide production rate and carbon source and biomass concentrations during batch phase in a mixture of six carbon sources.

After glucose was almost depleted, mannose consumption started. At the sixth sample point, when mannose was depleted, consumption of arabinose, galacturonic acid and xylose occurred. Finally, rhamnose consumption started only after 20 hours of cultivation when all other carbon sources were depleted, which coincided with a sharp decrease of the O₂ consumption and CO₂ production rates. In the period during which

rhamnose was consumed, the respiration rate increased again for a short period of time and decreased sharply after depletion of this last substrate.

During the batch cultivation the specific growth rate could be obtained from the online measurement of the respiration rate, that is either oxygen consumption or carbon dioxide production. During exponential growth the respiration rate also increases exponentially and thus from a plot of the natural logarithm of e.g. the CO₂ production rate, the growth rate can be obtained. From this it was calculated that during the initial 10 hours of the batch cultivation, when glucose was the only carbon source consumed, the specific growth rate was $0.264 \pm 0.005 \text{ h}^{-1}$. Between 10 and 18 hours, during the consumption of mannose, arabinose, galacturonic acid and xylose, the growth rate was $0.201 \pm 0.005 \text{ h}^{-1}$ (Fig. S3.2.). The initial growth rate during the first 10 hours on glucose was slightly higher than measured in the single substrate batch cultivation, while the growth rate obtained during consumption of mannose, arabinose, galacturonic acid and xylose was significantly higher than the growth rates obtained from the single substrate batches (Table 3.1.). This suggests that these carbon sources have individual uptake systems, which act in parallel.

3.3.4. Sequential chemostat cultures

To obtain a more detailed insight in the kinetics of substrate uptake in *A. niger* at low carbon source concentrations, a carbon-limited sequential chemostat experiment was performed on a mixture of the six substrates used for the single and mixed substrate batch cultivations. The experiment was carried out in a 7 litres bioreactor designed for homogeneous chemostat cultivation of *A. niger*, without pellet formation and/or wall growth (Lameiras *et al.*, 2015). The feed medium of the chemostat was minimal medium complemented with an equimolar mixture of the six carbon sources as described in section 3.2.5.

After achieving steady state, the dilution rate was increased stepwise and the chemostat was run until a new steady state was obtained. The initial dilution rate was 0.04 h^{-1} which was sufficiently lower than the lowest maximum growth rate

determined for the single substrate batch cultivations (Table 3.1.), to enable growth on all carbon sources in carbon-limited chemostat cultures.

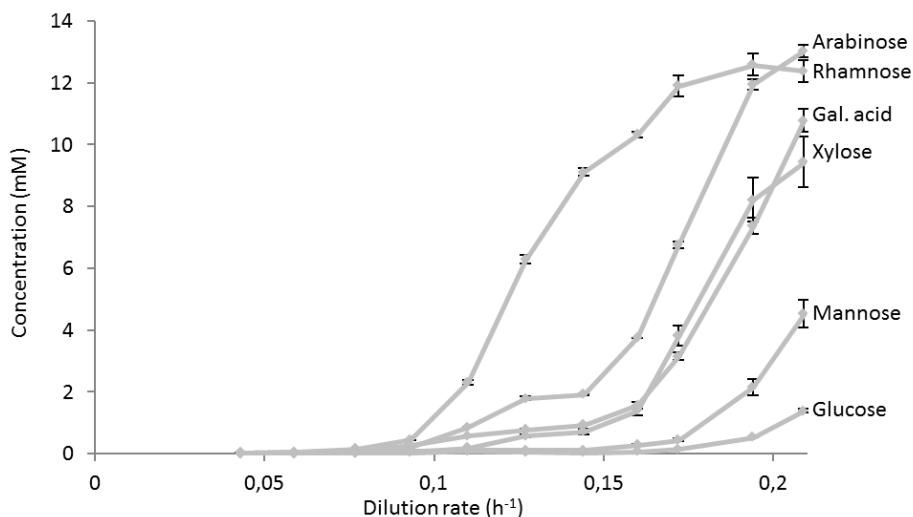


Fig. 3.4. Residual concentration of carbon sources for different dilution rates during sequential chemostat cultures.

For all dilution rates, measurements of the concentrations of residual substrates (Fig. 3.4. and Table S3.3.), biomass dry weight, and oxygen and carbon dioxide levels (Fig. 3.5.) were performed. In addition, the total organic carbon (TOC) contents of the culture filtrate samples were determined. From these values the measured amounts of residual substrates were subtracted to calculate the residual filtrate organic carbon, to verify whether amounts of by-products were formed (Fig. S3.3.). It was found that the in this way, determined residual carbon in the filtrate samples did not increase with increasing dilution rate, and was equal to an average value of 32 ± 8 mCmol/l, which was about 7% of the carbon supplied as mixed substrate to the culture. No attempts were undertaken to analyse the composition of the released carbon, as it was assumed that it mainly consisted of cell lysis products.

From the mentioned measurements (substrate, biomass, oxygen and carbon dioxide), it appeared that recoveries of carbon and degree of reduction were higher than 90%

and thus the biomass specific rates were calculated and reconciled (Table 3.2. and Table S3.2.).

From the quantification of the residual concentrations of the carbon sources in the chemostat it can be seen that during the first four steady states, up to a dilution rate of 0.093 h^{-1} , all six carbon sources were consumed simultaneously (Fig. 3.4.). From the fifth steady state ($D = 0.11 \text{ h}^{-1}$) the residual concentrations of rhamnose, arabinose and galacturonic acid started to increase, from $D=0.127 \text{ h}^{-1}$ also xylose, from $D=0.16 \text{ h}^{-1}$ mannose and finally at $D=0.194 \text{ h}^{-1}$ also glucose started accumulating.

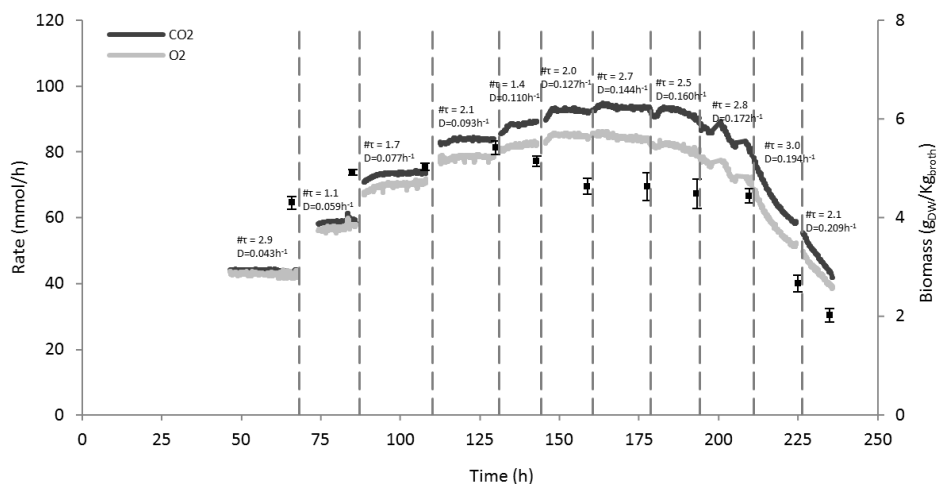


Fig. 3.5. Oxygen and carbon dioxide consumption/production rates, biomass concentration (■) and number of residence times ($\# \tau$) during sequential chemostat cultivation.

At increasing dilution rate of the sequential chemostat fermentation the increase of the residual concentrations of the different carbon sources occurred in the reverse order as the consumption of substrates in the multi substrate batch fermentation. In these fermentations, L-rhamnose was only consumed after all other substrates were depleted, and appeared as the first increasing substrate at increasing dilution rate in the sequential chemostat cultivation. The observed increases of residual carbon source concentrations also imply that the total amount of residual carbon source released from the chemostat via the effluent gradually increased with increasing dilution rate,

and thus the amount of consumed carbon gradually decreased. The result of this was that after an initial increase, the biomass specific respiration rate and steady state biomass concentration levelled off, and finally decreased with increasing dilution rate (Fig. 3.5.).

Table 3.2. Biomass concentration, respiratory quotient, carbon and degree of reduction recoveries, and reconciled biomass specific net conversion rates at different dilution rates.

Dilution rate (h ⁻¹)	0.04	0.06	0.08	0.09	0.11	0.13	0.14	0.16	0.17	0.19	0.21
Biomass (g _{dw} /g _{dw} h)	4.30 ± 0.13	4.92 ± 0.06	5.03 ± 0.07	5.42 ± 0.14	5.15 ± 0.11	4.63 ± 0.16	4.63 ± 0.29	4.48 ± 0.30	4.44 ± 0.14	2.66 ± 0.17	2.01 ± 0.14
RQ	1.03 ± 0.04	1.04 ± 0.04	1.07 ± 0.04	1.09 ± 0.04	1.10 ± 0.04	1.11 ± 0.04	1.14 ± 0.04	1.18 ± 0.04	1.19 ± 0.04	1.20 ± 0.05	1.16 ± 0.04
Carbon balance (%)	92 ± 2	95 ± 1	94 ± 1	91 ± 2	92 ± 1	89 ± 2	92 ± 2	93 ± 3	98 ± 1	97 ± 2	99 ± 1
Degree of reduction recovery (%)	86 ± 3	93 ± 2	88 ± 2	83 ± 3	87 ± 2	83 ± 2	87 ± 5	90 ± 3	97 ± 2	98 ± 2	102 ± 2
q _{Glucose} (mmol/h)/Cmol _x	3.05 ± 0.07	4.00 ± 0.06	5.14 ± 0.09	5.22 ± 0.09	6.62 ± 0.11	7.08 ± 0.09	8.78 ± 0.17	10.32 ± 0.21	12.66 ± 0.30	22.81 ± 1.12	31.39 ± 1.92
q _{Xylose} (mmol/h)/Cmol _x	3.67 ± 0.08	4.81 ± 0.07	6.19 ± 0.11	6.27 ± 0.11	7.91 ± 0.13	8.23 ± 0.11	10.09 ± 0.20	11.32 ± 0.25	11.41 ± 0.39	12.53 ± 1.26	15.72 ± 2.17
q _{Arabinose} (mmol/h)/Cmol _x	3.67 ± 0.08	4.80 ± 0.07	6.16 ± 0.11	6.21 ± 0.11	7.56 ± 0.13	7.54 ± 0.10	9.25 ± 0.18	9.38 ± 0.20	8.50 ± 0.25	5.98 ± 0.51	5.90 ± 0.76
q _{Galactid} (mmol/h)/Cmol _x	2.80 ± 0.06	3.67 ± 0.06	4.70 ± 0.08	4.71 ± 0.09	5.83 ± 0.10	6.43 ± 0.09	7.46 ± 0.15	8.25 ± 0.18	8.56 ± 0.24	7.90 ± 0.61	2.21 ± 1.07
q _{Mannose} (mmol/h)/Cmol _x	3.31 ± 0.07	4.34 ± 0.07	5.58 ± 0.10	5.65 ± 0.10	7.17 ± 0.12	7.66 ± 0.10	9.50 ± 0.18	11.05 ± 0.22	13.48 ± 0.32	21.74 ± 1.12	25.60 ± 1.85
q _{Rhamnose} (mmol/h)/Cmol _x	3.35 ± 0.07	4.38 ± 0.07	5.59 ± 0.10	5.57 ± 0.10	6.07 ± 0.11	3.75 ± 0.09	3.24 ± 0.13	2.83 ± 0.14	1.75 ± 0.35	2.11 ± 0.71	3.97 ± 1.06
q _{O₂} (mmol/h)/Cmol _x	57.8 ± 2.1	72.7 ± 1.7	93.9 ± 2.6	85.2 ± 2.8	97.1 ± 2.9	78.1 ± 1.1	93.3 ± 3.6	95.0 ± 3.8	99.3 ± 3.7	129.4 ± 7.5	134.5 ± 9.2
q _{CO₂} (mmol/h)/Cmol _x	60.3 ± 2.1	76.1 ± 1.7	98.3 ± 2.6	89.9 ± 2.8	103.4 ± 2.9	86.5 ± 1.2	103.8 ± 3.7	3.7 ± 3.9	112.6 ± 3.9	143.8 ± 8.0	144.1 ± 9.4
q _X (mmol/h)/Cmol _x	42.5 ± 0.0	59.1 ± 0.0	76.6 ± 0.0	93.5 ± 0.0	109.7 ± 0.0	127.4 ± 0.0	143.9 ± 0.0	159.7 ± 0.0	172.0 ± 0.0	193.8 ± 0.0	209.2 ± 0.0
q _{TOC} (mmol/h)/Cmol _x	8.9 ± 0.2	11.1 ± 0.2	12.9 ± 0.2	5.9 ± 0.1	18.3 ± 0.5	14.4 ± 0.8	22.9 ± 1.2	1.2 ± 1.9	33.7 ± 3.6	82.4 ± 12.0	133.8 ± 20.4

The observed increases of the residual concentrations of the different carbon sources, indicates that the supply rate becomes higher than the uptake rate by the cells. In case of rhamnose, arabinose, galacturonic acid and xylose this already happened at biomass specific uptake rates of only 20% of the maximum value determined in the single substrate batch cultivations (see Table 3.1. and Table 3.2.). In principle this could have been caused by a very low affinity of the import systems for these substrates, however, it is to be expected that under carbon-limited chemostat conditions high affinity importers are expressed. Other possible explanations are catabolite repression and/or competition of multiple substrates for the same import system(s).

As mentioned above, glucose repression is likely to have occurred in the multi substrate batch cultivations, as only after glucose was almost depleted the consumption of the other carbon sources started. In the carbon-limited chemostat cultivation, however, the residual glucose concentration was very low until a dilution

rate of about 0.17 h^{-1} (Fig. 3.4.). Nevertheless, the residual glucose concentration increased with increasing dilution rate (= growth rate) from 0.0125 mM at the lowest growth rate of 0.043 h^{-1} to 1.4 mM at the highest growth rate of 0.21 h^{-1} (Table S3.3.). If glucose repression would have been responsible for the limited uptake of the other carbon sources, this would imply that already at very low glucose concentrations repression of the uptake of the other substrates occurs. In Ilyés *et al.*, 2004 it was reported that in glucose-limited chemostat cultivations of *Aspergillus nidulans* CreA mediated carbon catabolite repression increased with increasing dilution rate and thus specific growth rate. However, it follows from chemostat theory that the residual concentration of the growth limiting substrate increases with increasing dilution rate (Herbert, Elsworth and Telling, 1956). It can therefore not be excluded that the observed CreA mediated carbon catabolite repression at higher dilution rates observed by Ilyés *et al.*, 2004 was in fact caused by the onset of glucose repression due to the increase of the residual glucose concentration.

As the last substrate which was depleted, before rhamnose consumption started in the multi substrate batch was arabinose (Fig. 3.3.), and the second substrate appearing with rhamnose was also arabinose (Fig. 3.4.), arabinose is a possible candidate repressor of L-rhamnose transport/metabolism. It has indeed been observed that in *Aspergillus nidulans* the α -L-rhamnosidase genes are strongly repressed by arabinose but also by glucose, ethanol and sorbitol through a CreA independent mechanism (Tamayo-Ramos *et al.*, 2012; Sloothak *et al.* 2016a). It might be that the uptake and/or metabolism of the other substrates (arabinose, galacturonic acid, xylose and mannose) is repressed by glucose only, via a CreA dependent mechanism. However, from the results of the multi substrate batch cultivations it appears that also mannose represses the metabolism of xylose, arabinose and galacturonic acid. A better zoom in on the kinetics and putative catabolite repression systems is advanced in the following section.

3.3.5. Substrate uptake kinetics

To obtain a clearer picture on possible catabolite repression in *A. niger*, the biomass specific uptake rates of the different substrates in the sequential chemostat cultivations are plotted as a function of the residual substrate concentration (Fig. 3.6.).

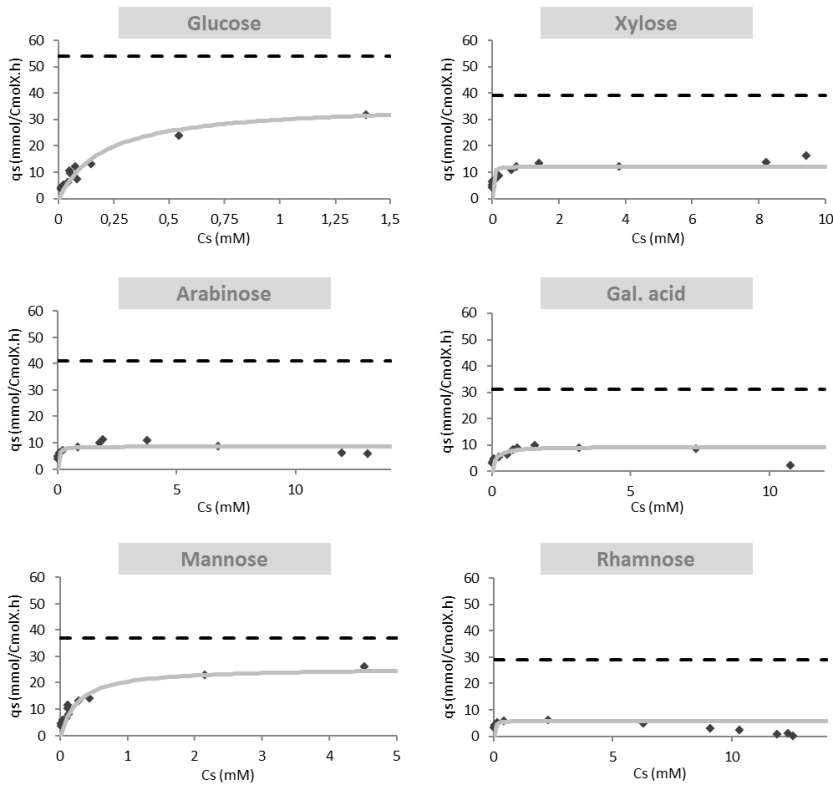


Fig. 3.6. Biomass specific uptake rate of different substrates against residual substrate concentration during sequential chemostat cultivation. Maximum substrate uptake specific rate fitting using the Michaelis-Menten equation. Dotted line represents V_{max} .

In these plots the maximum specific substrate uptake rate measured in the single substrate batch cultivations is indicated with a broken line. A Michaelis-Menten function (equation 3.3.) was fitted to the data to obtain apparent V_{max} and K_m values

for uptake of the different carbon sources in the multi carbon source chemostat cultivation.

It can be seen from these plots that for all carbon sources the maximum uptake rate is lower than observed in the single carbon source batch cultivations. Especially the uptake/metabolism of galacturonic acid, arabinose and rhamnose seems to be repressed, as at a certain point the uptake rates of these carbon sources level off far below their q_s^{\max} values and subsequently decrease at increasing substrate concentration. In case of glucose, mannose and xylose, repression does not seem to take place, however, with increasing substrate concentration, the specific substrate uptake does not reach the determined q_s^{\max} . A possibility could be that glucose, mannose and xylose are taken up by the same transport systems, resulting in competition between those substrates for the same transporters. Until now three glucose import systems of *A. niger* have been characterized, namely MSTA, MSTG and MSTH. MSTA ($K_{m,\text{glucose}} 0.025 \pm 0.010$ mM) also imports mannose ($K_m 0.06 \pm 0.02$ mM) and xylose ($K_m 0.3 \pm 0.1$ mM) (van Kuyk *et al.*, 2004). MSTG ($K_{m,\text{glucose}} 0.50 \pm 0.04$ mM), also imports mannose and possibly xylose, while MSTH ($K_{m,\text{glucose}} 0.06 \pm 0.005$ mM) also imports mannose and fructose (Sloothaak *et al.*, 2015). In addition, also three xylose import systems have been identified in *A. niger*, namely XTLA, XTLB and XTLC (Sloothaak *et al.*, 2016b). XTLA ($K_m 0.09 \pm 0.03$ mM) also imports glucose ($K_m 0.07 \pm 0.01$ mM) with the same V_{\max} as for xylose. XTLB seems specific for xylose ($K_m 15.0 \pm 4.50$ mM) and XTLC ($K_m 4.71 \pm 1.04$ mM) imports glucose with a much higher affinity ($K_m 0.11 \pm 0.02$ mM) and a roughly ten times higher V_{\max} and should therefore be called a glucose importer.

From the published kinetic information on the sugar transporters of *A. niger* characterized to date, it appears that five of them are not very specific and import several sugars. Therefore, to model the uptake of glucose, mannose and xylose, we assumed that these sugars are taken up by the same import systems and that their uptake could be described by competition (equation 3.4.). Also in other filamentous fungi and yeasts, transport systems have been characterized that import several

monosaccharides. In *Aspergillus nidulans* the xylose transporter XTRD also imports glucose, galactose and mannose (Colabardini *et al.* 2014) while the glucose transporters HXTB, HXTC and HXTE also import fructose, mannose and galactose (dos Reis *et al.* 2013). A functional survey carried out by Young *et al.* 2011 found that the hexose transporter HXT7 and galactose transporter GAL2 of *Saccharomyces cerevisiae* are able to import glucose, xylose, galactose, fructose and mannose while GAL2 in addition also imports ribose. Similar results were obtained for the sugar importers GXF1 and GXS1 of *Candida intermedia*, DEHA0D02167 and XylHP of *Debaryomyces hansenii* and XUTt1 and XUT3 of *Scheffersomyces stipites*.

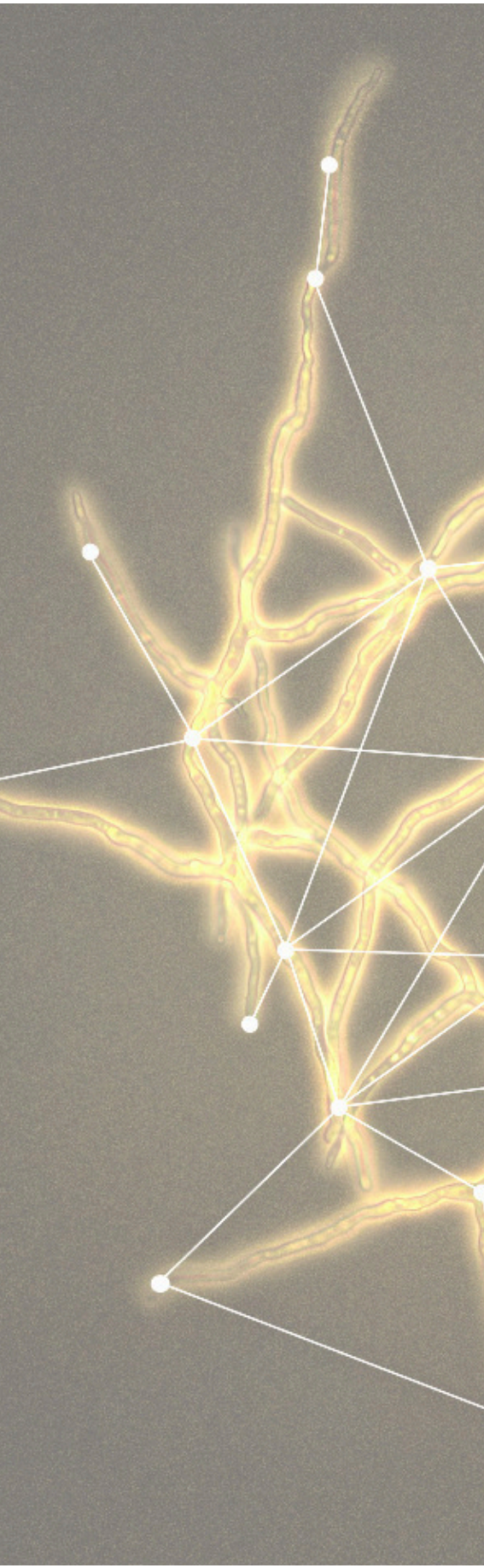
To model the uptake of glucose, mannose and xylose, we assumed that these sugars are taken up by the same import systems and that their uptake could be described by competition (equation 3.4). Both the specific uptake rate of glucose and mannose could be described well with this equation. For the specific uptake of xylose, no good fit could be obtained, indicating that besides competition probably also catabolite repression of xylose uptake and/or metabolism occurred (Fig. S3.4.).

The switch function (equation 3.5.) was used to model glucose repression of the uptake of xylose, arabinose, galacturonic acid and rhamnose in the sequential chemostat cultivation. The specific uptake rates of xylose, arabinose and galacturonic acid could be described reasonably well by glucose repression (Fig. S3.5.), however, no fit could be obtained for the uptake of rhamnose (result not shown). As it is known that in *A. nidulans* the α -L-rhamnosidase genes are strongly repressed by arabinose (Tamayo-Ramos *et al.*, 2012), the same switch function (equation 3.5.) was used to describe the repression of rhamnose uptake/metabolism by arabinose, which gave a reasonable fit (Fig. S3.5.). Further experiments using simultaneous substrate cultivation, i.e. with and without competitor/repressing substrates, would be advantageous to validate the mentioned hypothesis.

3.4. Conclusions

Large differences in q_{Smax} and μ_{max} for individual substrates was observed, but in combination, some carbon sources were consumed simultaneously and some sequentially. We found that the uptake of glucose, xylose and mannose seems to be competing for the same transport systems, while the uptake of arabinose, galacturonic acid and rhamnose appeared to be repressed by the presence of other substrates.

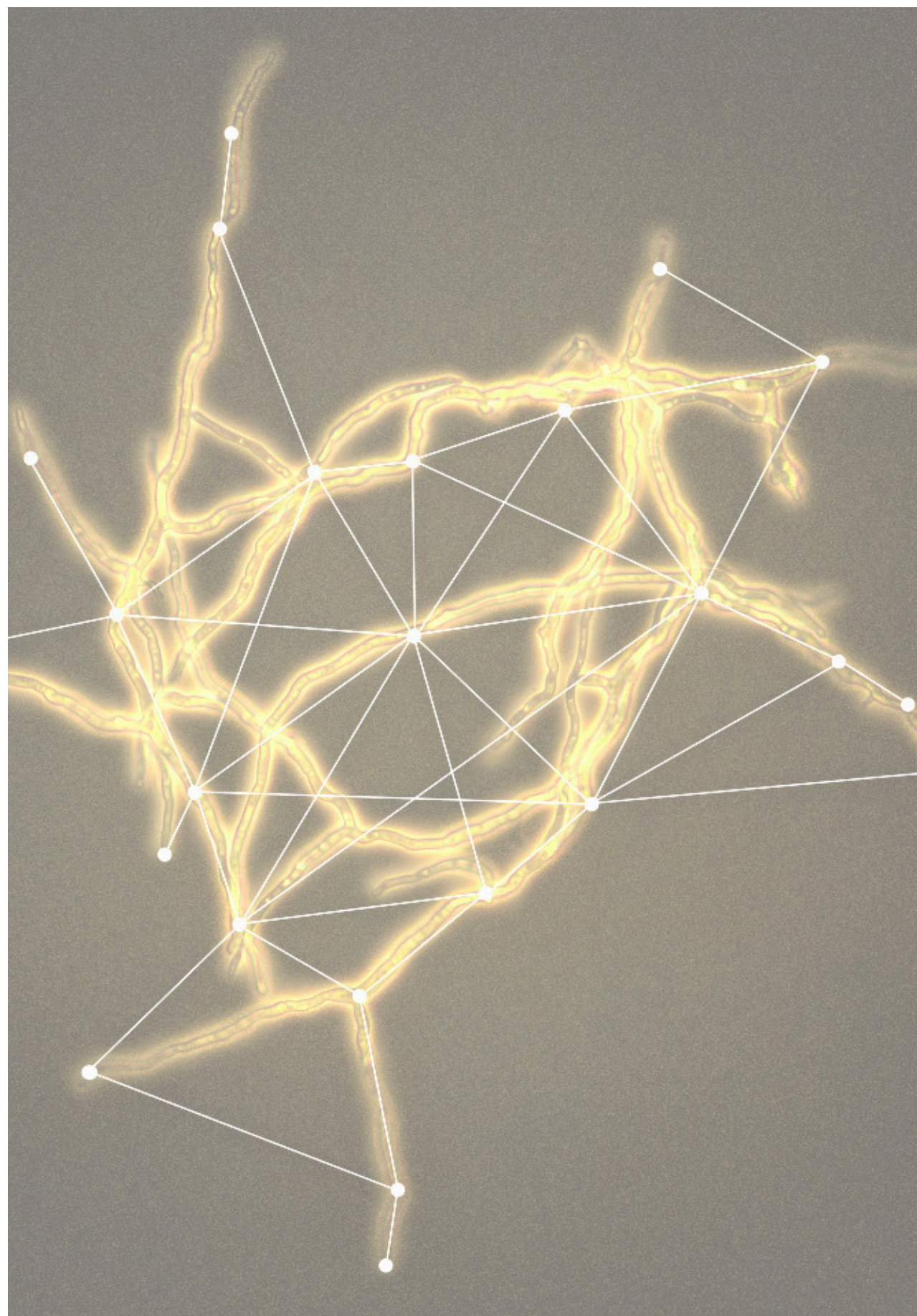
The stoichiometric and kinetic parameters of growth on different carbon sources, and the role of substrates as repressors or competitors during cultivation, should be taken into account in the design of a fermentation process based on plant waste feedstocks. In addition, the transition from simple carbon sources to more complex substrate mixtures requires careful attention.



In this chapter, we construct a stoichiometric model and perform flux analysis based on estimations of import mechanisms for six carbon sources, and on the steady state data from a carbon-limited chemostat experiment.

Chapter 4

Metabolic network analysis and transport mechanisms of lignocellulosic substrates in *Aspergillus niger*



Abstract

As a follow-up of previous stoichiometric and kinetic studies, we open in this chapter the black box model of chapter 3. In addition, we measured intracellular and extracellular concentrations of the six selected substrates which allowed an assessment of the most plausible import mechanism for the substrate transport systems, based on measured in/out ratios. A proton symport mechanism seems to be the most likely importer for all substrates with exception of galacturonic acid. The results from eleven carbon-limited chemostat steady states of *Aspergillus niger* on a mixture of six substrates at different growth rates were used as input for a flux analysis from which we obtained estimations of ATP costs for mycelium growth. The energetics of growth of *A. niger* were based on well-known pathways for some substrates and possible pathways for others. Finally, the metabolic flux analysis revealed a much higher flux into the oxidative PPP branch with the mixed substrate sequential chemostat cultivation as compared to carbon-limited chemostat cultivations on glucose as the sole carbon and energy source.

Keywords

Aspergillus niger, metabolic network, flux analysis, growth energetics, transport

4.1 Introduction

Metabolic network analysis enables insights in the ATP stoichiometry of growth and product formation and metabolic flux distributions through different pathways of an organism. In *Aspergillus niger*, a large metabolic network has been reconstructed by integration of the genome, metabolome and reactome (Andersen *et al.*, 2008; David *et al.* 2003), which were supported by the genome sequencing of two *Aspergillus niger* strains (Pel *et al.*, 2007; Andersen *et al.*, 2011). These *omics* analyses provided information on metabolic fluxes, storage compounds and available machinery in the cell (Kromer, Nielsen and Blank, 2014). However, the transportome, i.e. the transporters and channels which regulate influx and efflux of molecules to and from the cell, has not yet been included in current metabolic network models of *A. niger*.

A cell's survival depends on its membrane and transporters (Ramos, Sychrová and Kschischo, 2016), as the transport system enables the cell to obtain metabolic homeostasis by uptaking up nutrients, excreting unwanted products and establishing electrochemical gradients across membranes. The eukaryotic fungal transport system has been extensively studied in *Saccharomyces cerevisiae* (Andre, 1995; Leandro, Fonseca and Goncalves, 2009). As an example, the yeast hexose transporters (HXT family) consist of at least 20 different proteins involved in the transport and sensing of glucose, while some of these transporters also have a broad specificity for other hexoses, as well as for pentoses. The main hexose transporters HXT1-7 and Gal2 from *S. cerevisiae*, are acting by facilitated diffusion (Flagfeldt *et al.*, 2009).

In the filamentous fungi *Aspergillus nidulans* there are at least 17 putative HXT transporters identified in its genome (Wei *et al.*, 2004). However, for *A. niger*, despite the reported 461 putative transporters from the MFS family (major facilitator superfamily), from which 19 seem to be transporting glucose (Pel *et al.*, 2007), only very few transporters have been identified and confirmed. A high affinity glucose/proton symporter MSTA was identified (van Kuyk *et al.*, 2004), as well as two other glucose proton symporters, MSTG and MSH (Sloothaak *et al.*, 2015). In

addition, a galacturonic acid transporter (unknown mechanism) GATA (Martens-Uzunova and Schaap, 2008; Sloothak *et al.*, 2014), a fructose proton symporter FSY1 (Coelho *et al.*, 2013), a rhamnose proton symporter RHTA (Sloothak *et al.*, 2016a) and three xylose transporters (unknown mechanism) XLTA, XLTB and XLTC (Sloothak *et al.*, 2016b) were identified. A summary of the known transporters of *A. niger* and their mechanisms was already given in Table 1.2. (chapter 1). It appears that substrate transporters are most of the time of the high affinity type using a proton symport mechanism, and are generally not specific for a single substrate.

In addition to the insufficient knowledge on transport systems, also metabolic pathways for the used substrates are not completely unraveled. *A. niger* has the ability to grow on the most abundant lignocellulosic monomers, i.e. glucose, xylose, arabinose, galacturonic acid, mannose and rhamnose (chapter 3). In addition, this fungus has been shown to be able to metabolize xylose and arabinose (Witteveen *et al.*, 1989), apart from glucose. Later, Mojzita *et al.* 2010 identified the reductase genes of D-xylose and L-arabinose in *A. niger*. Both sugars are able to induce the expression of the genes of the pentose phosphate pathway (Mojzita, Penttilä and Richard, 2010). Martens-Uzunova and Schaap 2008 proposed a galacturonic acid degradation pathway in filamentous fungi (Martens-Uzunova and Schaap, 2008). Mannose and rhamnose pathways, on the other hand, have not been confirmed or characterized in *A. niger*.

Having in mind the metabolic pathway gaps and little knowledge on the substrate transport systems in *A. niger*, in this study we focused on these two topics.

To this aim, we measured intra- and extracellular substrate concentrations during a sequential chemostat experiment on a mixture of six lignocellulosic substrates (see chapter 3) and we calculated the corresponding in/out ratio's. From a comparison with the thermodynamic equilibrium ratio's the most plausible import mechanism for each substrate could be identified.

Subsequently we constructed a simplified version of a metabolic network for *A. niger*, based on the genome scale stoichiometric model published by David *et al.* 2003. The

thus obtained model was extended with the pathways for the metabolism of six lignocellulosic carbon sources and their most plausible import mechanisms. Using a dataset obtained from a carbon-limited sequential chemostat cultivation on a mixture of these six lignocellulosic substrates at eleven different dilution rates, a metabolic flux analysis was performed for each growth rate. The results of the flux analysis were used to obtain more insight in the ATP requirements for growth and maintenance of the cells, the stoichiometry of growth on each single substrate and to identify possible metabolic bottlenecks for the simultaneous consumption of lignocellulosic carbon sources in *A. niger*.

4.2 Materials and Methods

4.2.1. Sequential chemostat cultivation

4.2.1.1. Strain, inoculum and fermentation

The strain used was *A. niger* NW185 (*cspA1* short conidiospores, *fwA1* fawn coloured spores, *goxC17* glucose oxidase negative, *prtF28* oxalate non-producing). The hyphal inocula for continuous cultivation were obtained from shake flask cultures. Spores for initiating the pre inoculum were obtained by growing the fungus on agar plates and the spores were harvested as described in Lameiras *et al.*, 2015. A concentration of 1×10^6 spores/ml was pre-inoculated in a 250 ml shake flask containing 100 ml of PM media with 100 mM of sorbitol (Ruijter, van de Vondervoort and Visser, 1999) at pH 4.5. The shake flask was incubated overnight at 30°C in an orbital shaker (CERTOMAT BS-1, Sartorius group) at 250 rpm. The resulting mycelial suspension, was separated by centrifugation (*Heraeus Contifuge stratos* for 2 min at 10000G, 4°C) washed two times with 50 ml PM medium without carbon source at room temperature and subsequently used to inoculate the bioreactor.

A sequential chemostat cultivation was performed in a 7 litres bioreactor with a working volume of 4.5 litres. Fermentor set up and operating conditions were the same as described in Lameiras *et al.*, 2017.

The reactor was inoculated with pre grown and washed mycelia into minimal media supplemented with a mixture of 12.6 mmol/L D-glucose, 12.6 mmol/L D-galacturonic acid, 12.6 mmol/L L-rhamnose, 12.6 mmol/L D-mannose, 15.2 mmol/L of D-xylose and 15.2 mmol/L L-arabinose (note that each sugar represents 76 mmol/L of carbon). After the batch phase was finished, the feed was initiated with a starting dilution rate of 0.04h^{-1} . Subsequently, the dilution rate was increased to 0.21h^{-1} in eleven steps (0.04h^{-1} , 0.06h^{-1} , 0.08h^{-1} , 0.09h^{-1} , 0.11h^{-1} , 0.13h^{-1} , 0.14h^{-1} , 0.16h^{-1} , 0.17h^{-1} , 0.19h^{-1} and 0.21h^{-1}), as described in Lameiras *et al.*, 2017.

4.2.1.2. Rapid sampling and quenching for extracellular substrate quantification

For each dilution rate, after steady state was reached (observed from the constant CO_2 and O_2 levels in the offgas of the chemostat), filtrate samples were obtained by quickly (within 3 s) withdrawing 5 ml of broth, via the over-pressure on the fermentor, into a syringe containing cooled steel beads (-20°C) to bring the sample temperature quickly down to 0°C (Mashego *et al.* 2003). The broth was then immediately pressed through a $0.45\text{ }\mu\text{m}$ cartridge filter (Millex-HV durapore PVDF membrane) into a filtrate sampling vial, which was directly frozen in liquid nitrogen.

4.2.1.3. Rapid sampling and quenching for intracellular substrate quantification

For each dilution rate, after steady state was reached, intracellular samples were obtained by a rapid sampling, quenching and washing method previously developed for filamentous broth, with the difference that the customized rapid sampling device described in Lameiras *et al.*, 2015, was now substituted by another one with the same working principle but a bigger sampling chamber, allowing higher volumes of broth to be withdrawn (1.4 g of broth), in comparison with the old device (0.7g of broth).

1.4 g of broth was rapidly withdrawn from the broth loop with the sampling device and injected ($< 1\text{ s}$) into a vial containing 10 ml of 40 % aqueous methanol (v/v) solution pre-cooled to -40°C . The exact sample weight was determined by weighing each tube before and after sampling. The content of each tube was quickly mixed by vortexing (1

s) and the tube was placed back in a cryostat (Lauda, Germany) at -40°C . A set of 3 replicates were taken within one minute. The quenched cold mycelia samples were harvested and washed in two steps by cold filtration, according to a previously described method Lameiras *et al.*, 2015. It has been shown previously that the washing efficiency of this method was sufficient for *S. cerevisiae* (Shah, 2016) and *P. chrysogenum* (Douma *et al.*, 2010).

After the rapid sampling, washing and quenching procedure, samples were submitted to boiling ethanol extraction, evaporation and concentration, as described in Lameiras *et al.*, 2015.

4.2.1.4. Analytical procedures and data reconciliation

In addition to intracellular and extracellular substrate quantification, during each steady state, at least 3 samples were taken for quantification of cell dry weight (four replicates) and total organic carbon (TOC) content of the culture filtrate. Furthermore, the oxygen and carbon dioxide volume percentage in the offgas of the chemostat were measured continuously (Lameiras *et al.*, 2017).

Both the intracellular and extracellular concentrations of each substrate were determined with a Dionex ICS – 5000 HPIC system with AS-AP sampler, SP pump, Carbopac PA-20 3*150 mm column and Aminotrap 3*30 mm precolumn employing 2 mM NaOH isocratic, 20 mM NaOH isocratic or gradient with 0.5 M sodium acetate in 200 mM NaOH (for acidic sugars) as eluents with a flow of 0.5 ml/min at 30°C . The detection was by electrochemical pulse at 15°C . A factor of 1.2 ml intracellular volume/g dry weight was used to calculate intracellular concentrations from the extracted amounts of metabolites (Ruijter and Visser, 1996).

Using the steady state mole balances, the net conversion rates (mol/h) of substrate (R_S), biomass (R_X), carbon dioxide (R_{CO_2}), oxygen (R_{O_2}) and TOC in the culture filtrate (R_{TOC}), and the corresponding covariance matrix were calculated from the primary measurements of concentrations in the gas and liquid phases, as well as gas and liquid

flow rates. From these rates, carbon and degree of reduction recoveries were calculated according to the description in Lameiras *et al.*, 2017. After checking absence of relevant carbon and degree of reduction gaps, data reconciliation was applied to obtain the best estimates of the measurements, within their error margins, using the elemental and charge conservation relations as constraints (Verheijen, 2010).

4.2.2. Thermodynamics of uptake processes

An extensive elucidation on the thermodynamics of transport mechanisms was already given in chapter 1. Summarising, when the solubility of a molecule (charged, hydrophilic) in the lipid membrane is insufficient, or the transport has to occur against a concentration gradient, then a transporter and energy input (coupled transport) are needed. These transport processes need to be accessed in terms of energetics. The Gibbs energy of the H^+ coupled import of a charged compound (charge z) such as $C_{out}^z + nH^+_{out} \Leftrightarrow C_{in}^z + nH^+_{in}$ can be written as:

$$\Delta_r G = \left[RT \ln \left(\frac{C_{in}^z}{1} \right) + ZF\psi + nRT \ln \left(\frac{H_{in}^+}{1} \right) + nF\psi \right] - \left[RT \ln \left(\frac{C_{out}^z}{1} \right) + 0 + nRT \ln \left(\frac{H_{out}^+}{1} \right) + 0 \right] \quad (4.1.)$$

Where $\ln(C^z/1)$ and $\ln(H^+/1)$ are the correction term for concentrations different from 1 mol/L, $R = 8.314 \times 10^{-3}$ kJ/(mol.K), T is the temperature in Kelvin (K); n is the number of protons (H^+ co-imported); and $ZF\psi$ is the correction for the intracellular electrical potential (Z is the charge of the transported molecule, F is the Faraday constant = 96.5 kJ/v e⁻mol and ψ is the inside membrane potential in volt).

The intracellular space has an electrical potential (the extracellular space has $\psi = 0$ by definition), of which the value depends on the extracellular pH to maintain a constant proton motive force (E_{pmf}). The relation between the electrical potential and the extracellular pH was already shown in chapter 1 (equation 1.2.). In that relation E_{pmf} and pH_{in} are homeostatic at values of $E_{pmf} = 0.15$ V and $pH_{in} = 7.6$ (Hesse *et al.*, 2002). Therefore, ψ only depends on the extracellular pH and becomes negative for high pH_{out} , and positive for low pH_{out} .

Assuming $\Delta rG = 0$ in equation 4.1., one can calculate the logarithm of the in/out equilibrium concentration ratio of the charged species of the imported compound according to equation 4.2.

$$\log \frac{C_{in}^Z}{C_{out}^Z} = z(pH_{in} - pH_{out}) - \frac{(n-z)(-Epmf)F}{2.303 RT} \quad (4.2.)$$

This ratio is the thermodynamic maximum value of the out/in ratio for a proton coupled import system.

In case of glucose, xylose, arabinose, mannose and rhamnose, there is no charge on the molecules, which means that the in/out ratio is not dependent on the pHout. Equation 4.2. simplifies then to:

$$\log \frac{C_{in}}{C_{out}} = \frac{n \times Epmf \times F}{2.303 RT} \quad (4.3.)$$

The equilibrium in/out ratios for these five carbon sources can be estimated for the different transport mechanisms.

$$\text{Antiport } n=-1 \log \frac{C_{in}}{C_{out}} = -1 \times 2,57 \equiv \frac{C_{in}}{C_{out}} = 10^{-2.57} = 0.003$$

$$\text{Uniport } n=0 \log \frac{C_{in}}{C_{out}} = 0 \times 2,57 \equiv \frac{C_{in}}{C_{out}} = 10^0 = 1$$

$$\text{Symport } n=1 \log \frac{C_{in}}{C_{out}} = 1 \times 2,57 \equiv \frac{C_{in}}{C_{out}} = 10^{2.57} = 372$$

In case of galacturonic acid, depending on the pH, this sugar acid can dissociate ($pK_a=3.48$) and therefore different species can coexist (Fig. S4.1.). At pHout = 2.5 about 90% of the acid is present in its undissociated form (HA) and 10% of the acid in its protonated form (A^-). It could therefore be that the undissociated acid is imported by passive diffusion.

4.2.3. Metabolic Network Analysis

4.2.3.1. Data Processing and metabolic flux analysis

From the sequential chemostat cultivations, the primary measurements (concentrations in the liquid and gas phase and liquid and gas flow rates) for each steady state were used to calculate the net conversion rates (mmol/h) and the corresponding covariance matrix, using the corresponding steady state mole balances.

The obtained conversion rates and the corresponding covariance matrix for each steady state were used as input for the flux analysis using the constructed stoichiometric model (see below) with as metabolic flux analysis software MNA PR 3.0 (van der Heijden *et al.* 1994a; van der Heijden *et al.* 1994b; Verheijen 2010).

4.2.3.2. Stoichiometric model

The metabolic network used for the flux analysis was based on a published genome scale stoichiometric model for *A. niger* (David *et al.* 2003). Here a simplified version was used but the model contained all anabolic reactions from the genome scale model, furthermore the assimilation reactions for the six different sugars were incorporated. The resulting model contained 200 reactions, and 173 compounds in 3 compartments (Fig. S4.3) - see supplementary material for a complete listing of the model. The most plausible import mechanisms (see results section) for glucose, xylose, arabinose, mannose, rhamnose and galacturonic acid were incorporated in the model. The biomass formation reaction of the published genome scale model also included the hydrolysis of 61 mol ATP to ADP per kg of dry biomass produced (1.64 mol ATP per Cmol biomass) as growth dependent maintenance energy requirements (David *et al.* 2003). In our version of the model this additional ATP hydrolysis was removed from the biomass reaction, instead we used the obtained flux data to estimate this ATP demand (see results and discussion section).

4.3. Results and Discussion

4.3.1. Sequential chemostat cultivation

A sequential chemostat experiment was performed on an equimolar carbon mixture of the six substrates. After achieving steady state, the dilution rate was increased stepwise and the chemostat was run until a new steady state was obtained. The initial dilution rate was 0.04 h^{-1} which was significantly lower than the lowest maximum growth rate determined for the single substrate batch cultivations (Lameiras *et al.*, 2017) to enable simultaneous uptake on all carbon sources.

For all dilution rates, measurements of residual substrates, biomass dry weight, oxygen and carbon dioxide concentrations in the offgas were performed. In addition, the measured total organic carbon (TOC) concentration of the culture filtrate minus the residual concentrations of the six carbon sources was used to verify whether significant amounts of unknown by-products were formed. The extensive analysis of this experiment in terms of substrate uptake kinetics and black box stoichiometric parameters is described in chapter 3.

Fig. 4.1. presents the extracellular and intracellular concentrations of all six substrates measured in each steady state achieved at the different dilution rates of the sequential chemostat cultivation.

The observed significant increases of the extracellular concentrations of the different carbon sources, indicates that in case of rhamnose, arabinose, galacturonic acid and xylose this already happened at biomass specific uptake rates of only 20% of the maximum value determined in the single substrate batch cultivations (Lameiras *et al.*, 2017). This increase of residual concentrations occurred in the reverse order as the consumption of substrates in the multi substrate batch fermentation (Lameiras *et al.*, 2017).

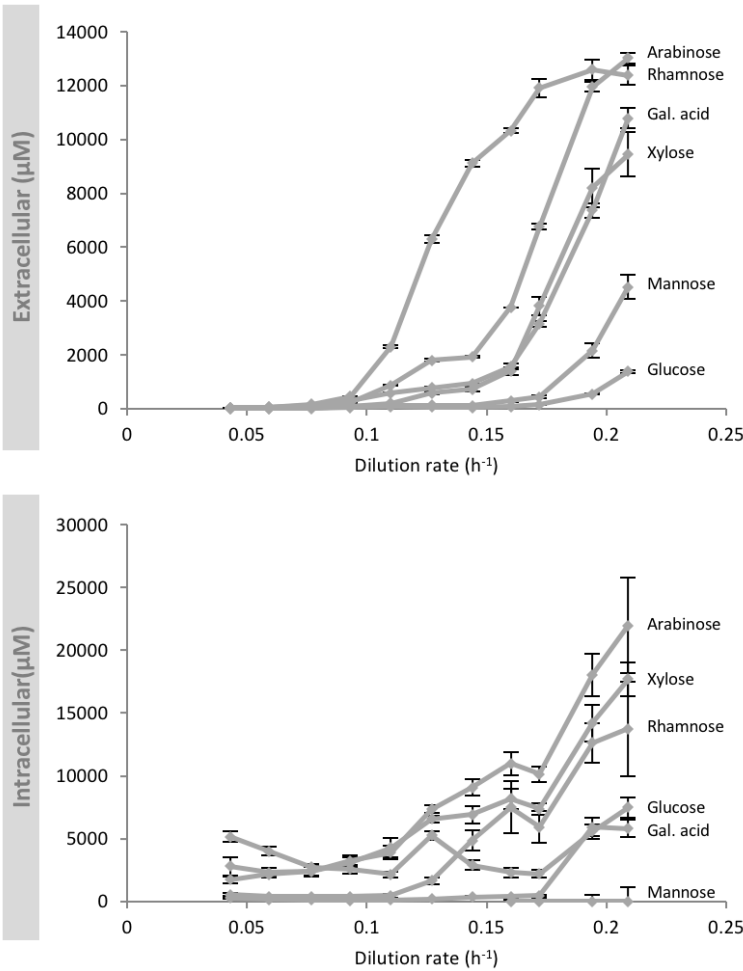


Fig. 4.1. Extracellular (upper panel) and intracellular (lower panel) carbon sources concentration, at different dilution rates of the sequential chemostat cultivation in *A. niger*.

More interesting is to know what is happening simultaneously to the intracellular levels of the different carbon sources. In Fig. 4.1. it can be seen that intracellular concentrations of carbon typically increase with increasing dilution rate, except for glucose which oscillates around a concentration of 20 µM.

4.3.2. Thermodynamics of transport processes

In order to have some insight on the transport mechanism of each carbon source, we determined the in/out ratios at each dilution rate – Table 4.1. Unfortunately, the measurements of the intracellular mannose concentration were corrupted for part of the samples taken and therefore the corresponding in/out ratio's could not be estimated.

Table 4.1. In/Out ratios of different carbon sources for each dilution rate of the sequential chemostat cultivation in *A. niger*.

Dilution rate (h ⁻¹)	Glucose	Xylose	Arabinose	Gal. acid	Mannose	Rhamnose
0.043	414.0 ± 77.9	709.5 ± 185.4	72.4 ± 11.1	5.52 ± 0.71	-	19.89 ± 5.12
0.059	260.0 ± 45.3	501.1 ± 117.8	56.5 ± 4.9	2.52 ± 0.25	-	5.69 ± 1.07
0.077	107.6 ± 19.8	184.1 ± 33.3	25.8 ± 3.6	1.09 ± 0.12	-	2.25 ± 0.47
0.093	59.6 ± 9.7	36.9 ± 6.4	14.1 ± 1.9	0.36 ± 0.02	-	0.92 ± 0.23
0.110	25.4 ± 2.8	20.7 ± 4.1	4.5 ± 0.6	0.22 ± 0.03	-	0.20 ± 0.06
0.127	96.8 ± 9.5	11.2 ± 1.0	4.1 ± 0.2	0.28 ± 0.04	-	0.27 ± 0.04
0.144	54.7 ± 8.2	9.5 ± 1.5	4.7 ± 0.3	0.40 ± 0.06	-	0.53 ± 0.09
0.160	29.2 ± 5.6	5.8 ± 0.9	2.9 ± 0.2	0.25 ± 0.05	6.7 ± 0.9	0.73 ± 0.20
0.172	14.6 ± 2.4	1.9 ± 0.2	1.5 ± 0.1	0.15 ± 0.03	5.1 ± 0.8	0.50 ± 0.11
0.194	10.2 ± 1.1	1.7 ± 0.2	1.5 ± 0.1	0.81 ± 0.10	2.4 ± 0.4	1.00 ± 0.13
0.209	5.4 ± 0.6	1.9 ± 0.2	1.7 ± 0.3	0.54 ± 0.07	1.5 ± 0.3	1.11 ± 0.31

In Fig. 4.2. the substrate in/out ratios are plotted against their corresponding specific substrate uptake rates (q_s). Note that equilibrium ratios were already discussed in the materials and methods section and galacturonic acid, being a sugar acid presents different equilibrium values.

For glucose, xylose, arabinose, mannose and rhamnose, the values plotted in Fig. 4.2. are on (or below) the expected equilibrium value of 372 for proton symport and decrease with increased flux to achieve a higher driving force, as to be expected. This is mostly in agreement with the findings stated in Table 1.2. where most of the known transporters for these substrates are indeed proton symporters.

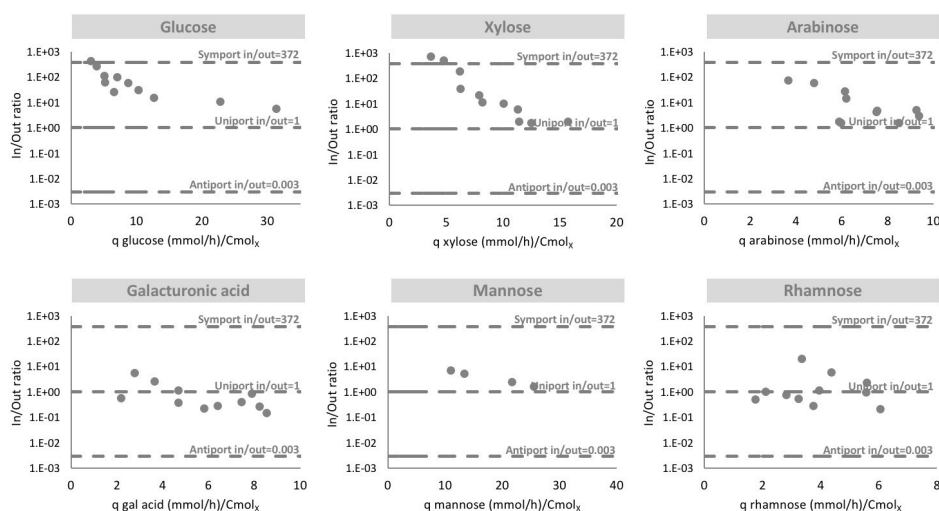


Fig. 4.2. In/Out ratios of different carbon sources in relation to their substrate specific uptake rate (q_s).

Dashed lines represent the equilibrium in/out ratios for different import mechanisms.

Because at pH 2.5 90% of the galacturonic acid is present in the undissociated lipophilic form, we assume that passive diffusion is the most probable import mechanism of this sugar acid at this pH. This finding is actually confirmed by the in/out ratios, which are close to 1 (equilibrium) – Table 4.1 and Fig. 4.2.

4.3.3. Metabolic Network Analysis

The C5 substrates, xylose and arabinose, were well studied in *A. niger* since the late 80s (Witteveen *et al.* 1989; vanKuyk *et al.* 2001; de Groot *et al.* 2003 and de Groot *et al.* 2005). Martens-Uzunova & Schaap, 2008 have described the evolutionary conserved D-galacturonic acid metabolic pathway in *A. niger*, allowing the degradation of pectin. The degradation of mannose is a quite straightforward pathway, and well known in eukaryotes (Panneman *et al.*, 1998), although not confirmed in *A. niger*. Finally, the fungal pathway of rhamnose was described for *Pichia stipitis* and *Debaryomyces hansenii* but not yet confirmed in *A. niger* (Fries and Kallstromer 1965 and Gruben *et al.* 2014). Nevertheless, with this information (Fig. S4.2.) we

incorporated metabolic pathways for the catabolism of the six substrates studied here in the stoichiometric model of *A. niger*.

4.3.3.1. Model description

From the measured in/out ratio's for the different sugars measured in the sequential chemostat experiment, the most plausible transport mechanisms are proton symport for glucose, xylose, arabinose, rhamnose and mannose; and passive diffusion for galacturonic acid at the cultivation pH of 2.5. These mechanisms were incorporated in the stoichiometric model, which was based on the model of David *et al.* (2003) and was extended with the import mechanisms and the catabolic pathways of the 6 different sugars used in the sequential chemostat experiment.

4.3.3.2 Experimental results

In Fig. 4.3 the biomass specific uptake rates of the six different substrates are plotted as a function of the dilution rate for the sequential chemostat cultivation.

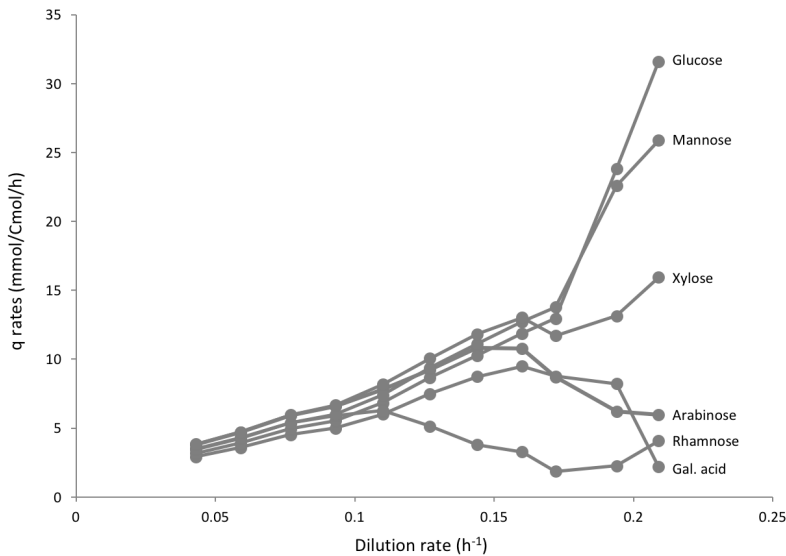


Fig. 4.3. Biomass specific substrate uptake rates in relation to different dilution rates (h⁻¹).

Until a dilution rate of 0.11 h^{-1} all sugars were consumed simultaneously. Above a dilution rate (D) of 0.11 h^{-1} rhamnose consumption decreased. Above $D = 0.16 \text{ h}^{-1}$ the consumption rates of arabinose and galacturonic acid decreased, while the biomass specific consumption rates of glucose, mannose and xylose increased.

Interestingly, in spite of the changes in the biomass specific uptake rates of the individual substrates the total substrate uptake rate, expressed in mmol carbon per Cmol biomass per hour, increased linearly with increasing dilution rate (Fig. 4.4.).

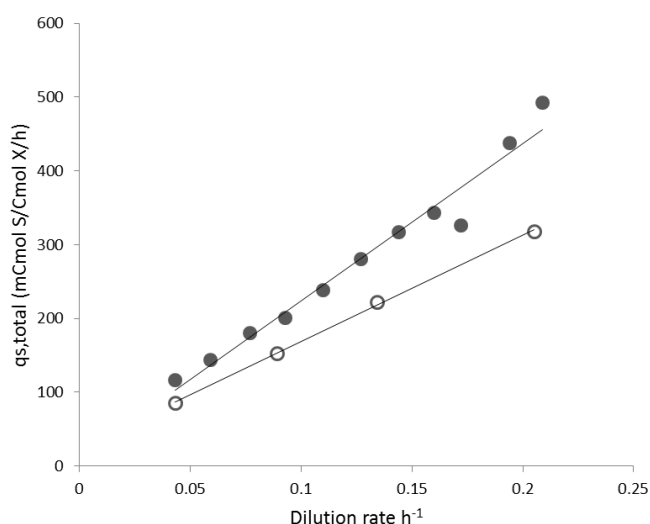


Fig. 4.4. Total biomass specific uptake rate of the six selected substrates in the mixed sugar sequential chemostat (closed circles) and in glucose-limited chemostat cultures (open circles) vs dilution rate (h^{-1}).

A similar linear relation was found for the glucose-limited chemostat cultivations (data retrieved from chapter 2). However, as can be seen from Fig. 4.4 the slope of this q_S vs D plot is smaller than for the mixed substrate chemostat. This indicates that the yield of biomass on glucose (expressed as Cmol biomass produced per Cmol of substrate consumed) is higher for growth on glucose than for growth on the six mixed substrates. This can have several causes. First of all, the average electron content of the mixed substrate used is slightly lower ($3.94 \text{ e}^-/\text{C}$) than for glucose ($4 \text{ e}^-/\text{C}$). Secondly, the ATP requirements for import of the different substrates can be different.

Based on our experimental data we assumed that import of glucose, xylose, arabinose, mannose and rhamnose occurred via proton symport while galacturonic acid entered the cells via passive diffusion. Having the same import system for a C5 and C6 substrate results in almost 20% higher transport costs per carbon atom for the C5 sugars. Using the metabolic network model with the estimated ATP stoichiometry parameters (see section 4.3.3.2) we calculated that the maximum yields of biomass for the different substrates ranged between 0.52 and 0.65 Cmol biomass/Cmol substrate (for galacturonic acid and rhamnose respectively) with an average yield of 0.60 for the mixed substrate, which is slightly lower than for glucose (0.62).

When the biomass specific oxygen consumption and carbon dioxide production rates (qO_2 and qCO_2) are plotted against the dilution rate it can be seen that they only increase linearly until $D = 0.127 \text{ h}^{-1}$ (Fig. 4.5.).

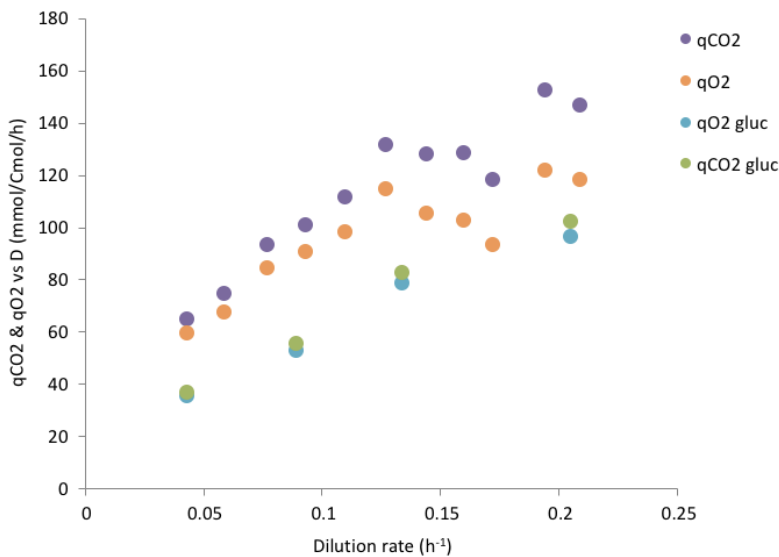


Fig. 4.5. Oxygen consumption and carbon dioxide production rates, filled symbols: mixed substrate sequential chemostat, open symbols: glucose-limited chemostat.

At higher dilution rates, the respiration rate slightly decreases in the following 3 steady states and increases again in the last two. This would indicate that at dilution rates

above 0.127h^{-1} the growth becomes more efficient in terms of ATP requirements, e.g. due to a change in biomass composition (accumulation of storage compounds). A comparison with the biomass specific oxygen consumption and carbon dioxide production rates in a glucose-limited chemostat (see chapter 2) shows that these rates are higher in the mixed carbon source cultivation. This corresponds with the lower yield of biomass on the mixed substrate discussed above.

4.3.3.2. Metabolic flux analysis and estimation of the ATP stoichiometry parameters K_x , m_{ATP} and P/O -ratio.

Flux analysis was performed for the 11 steady states of the mixed sugar sequential chemostat experiment (Fig. S4.1. to Fig. S4.11.).

An issue is that the residual carbon (TOC - residual sugars) detected in the effluent of the chemostat, is quite significant, especially for the higher dilution rates (Fig. 4.6.). For the flux analysis it was assumed that all non identified carbon in the effluent is the result of cell lysis. So this adds up to the biomass formation rate. We can, however, not exclude that also byproducts have been excreted at higher dilution rates.

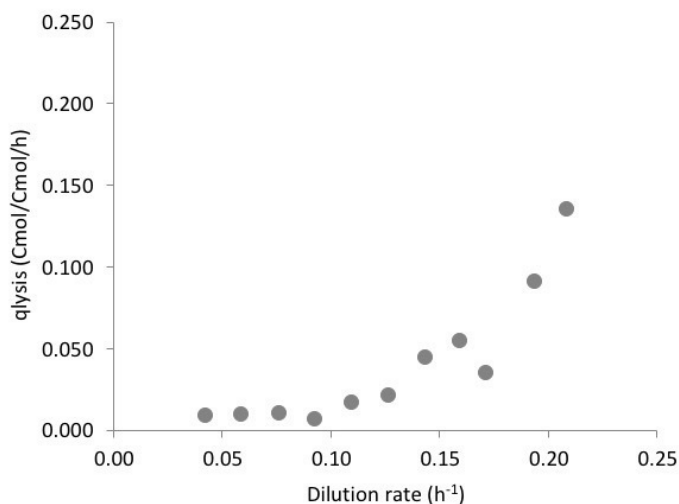


Fig. 4.6. Biomass specific rate of cell lysis, calculated from unaccounted total organic carbon content of the culture filtrate.

From the results of the flux analysis it was calculated that the operational P/O-ratio was on average 2.1 mol ATP per 2 mol of electrons. The fraction of mitochondrial NADH entering the respiratory chain was about 0.62 and the fraction of cytosolic NADH and FADH was about 0.38. Using the P/O ratios used in the genome scale model of David *et al.*, (2.46 mol ATP/2 mol electrons for mitochondrial NADH and 1.64 for cytosolic NADH and FADH) the operational P/O ratio would be $0.62 \cdot 2.46 + 0.38 \cdot 1.64 = 2.15$. We conclude that the operational P/O ratio calculated from the current flux analysis corresponds with the one used in the published genome scale model.

It should be realized that the anabolic ATP requirement obtained from a stoichiometric model is always an underestimation because several ATP requiring processes are not incorporated in these models, e.g. proofreading, posttranslational modification of enzymes, phosphorylation/dephosphorylation and protein turnover. This additional ATP requirement can be divided in a growth dependent and a growth independent part, respectively K_x (mol ATP/Cmol biomass) and m_{ATP} (mol ATP per Cmol biomass per hour).

To estimate these parameters from the experimental data the stoichiometric model contains an ATP hydrolysis reaction which represents this additional ATP demand for growth and maintenance of the cells. If a plot is made of the rate of additional ATP hydrolysis against specific growth rate a linear relationship is expected between the growth rate and the biomass specific additional ATP demand (mol ATP per Cmol biomass per hour with slope K_x (mol ATP/Cmol biomass) and intercept m_{ATP} (mol ATP/Cmol/h). It should be noted, however, that this only holds if no significant changes in the biomass composition occur as a function of the growth rate.

When such a plot of additional ATP consumption against growth rate ($\mu + q_{ATP}$) was made based on the results of the metabolic flux analysis for the sequential chemostat cultivation on the mixed substrate a linear relationship was only obtained for the first 6 steady states (Fig. 4.7.). From these data a K_x of 1.53 ± 0.21 mol ATP/Cmol biomass (about 56 ± 8 mmol ATP/gDW) and an m_{ATP} of 0.157 ± 0.021 mol ATP/Cmol.h (about

5.6 ± 0.8 mmol/gDW/h) can be estimated. Compared to the values published by David *et al.* ($K_x = 61$ mmol ATP/gDW and $m_{ATP} = 1.9$ mmol/gDW/h), the estimated K_x is somewhat lower while m_{ATP} is higher.

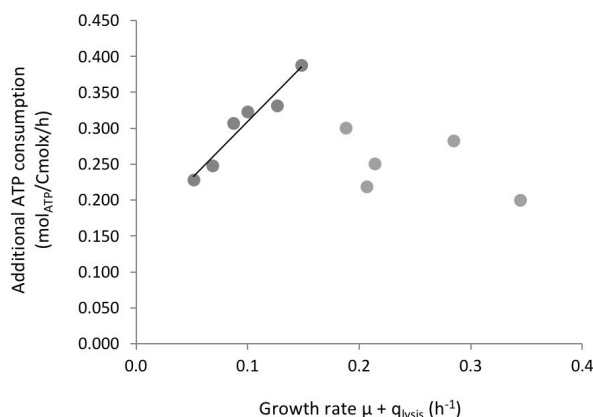
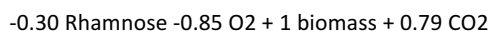
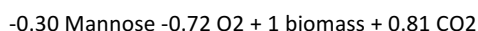
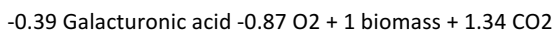
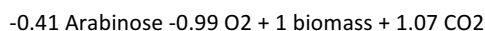
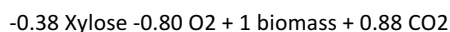
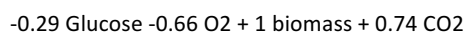


Fig. 4.7. Additional ATP consumption (mol ATP/Cmol/h) vs growth rate ($\mu + q_{\text{lys}}$).

Calculation of the stoichiometry of batch growth

Using the estimated values for the growth dependent and independent maintenance parameters K_x and m_{ATP} (see above), the stoichiometric model was used to calculate the overall reactions for the formation of one mol biomass from the six different substrates during growth in batch culture at the corresponding maximum growth rates.



It was calculated from the standard errors of the estimated values of K_x and m_{ATP} that the standard errors of the stoichiometric coefficients for substrate, oxygen and carbon dioxide are approximately $\pm 5\%$, $\pm 10\%$ and $\pm 8\%$ respectively. If we now compare the above obtained stoichiometric relations with the ones obtained from the single substrate batch cultivations (see chapter 3) only the one for arabinose as substrate corresponds with the one derived from the batch culture data. In all other cases the substrate and oxygen requirement and the carbon dioxide produced are lower in substrate excess batch cultivations than could be estimated from the ATP stoichiometry obtained from the carbon-limited multi substrate sequential chemostat cultivation. This could be caused by a different biomass composition, e.g. containing more storage materials, in unlimited batch cultures compared to C-limited chemostat cultivations. Since the synthesis of storage compounds generally costs less ATP, the substrate and oxygen requirement as well as carbon dioxide production for the synthesis of biomass with a high storage content is lower.

PPP pathway flux

Several of the six substrates in the feed of the sequential chemostat culture require NADPH for their metabolism. Per mol of arabinose this is 2 mol NADPH while 2 mol NADH is produced, for xylose this is 1 NADPH while 1 NADH is produced, for galacturonic acid this is 2 NADPH with no production of NADH while metabolism of rhamnose requires 2 NADPH and produces 1 NADH (see supplementary material Fig. S4.2). Therefore, due to the simultaneous consumption of arabinose, xylose, galacturonic acid and rhamnose the NADPH demand in the sequential chemostat experiment is large.

The main source of cytosolic NADPH is the oxidative branch of the pentose phosphate pathway (PPP). Therefore, it follows from the metabolic flux analysis that the flux into the oxidative PPP branch must be much higher in the mixed substrate sequential chemostat cultivation as compared to carbon-limited chemostat cultivations on glucose as the sole carbon source (Fig. 4.8).

The oxidative PP branch connects to the glucose-6-phosphate (G6P) node which has an inflow from glucose and outflows to the oxidative PPP branch and the glycolysis. In the mixed substrate sequential chemostat cultivation only one sixth of the carbon is supplied in the form of glucose, which implies that the inflow into the G6P pool is only one sixth compared to the situation where glucose is the sole carbon source. This means that due to the fact that in the mixed substrate cultivation the flux towards the oxidative PPP is large while the influx into the G6P pool is small an additional influx is required, which can only come from fructose-6-phosphate, requiring a reversal of phosphoglucose isomerase (PGI) (Fig. 4.9.) while the fluxes through phosphofructokinase and fructose biphosphate aldolase are strongly reduced. This is not observed for the flux distributions calculated for the carbon-limited chemostat cultivations where glucose is the sole carbon source (chapter 2).

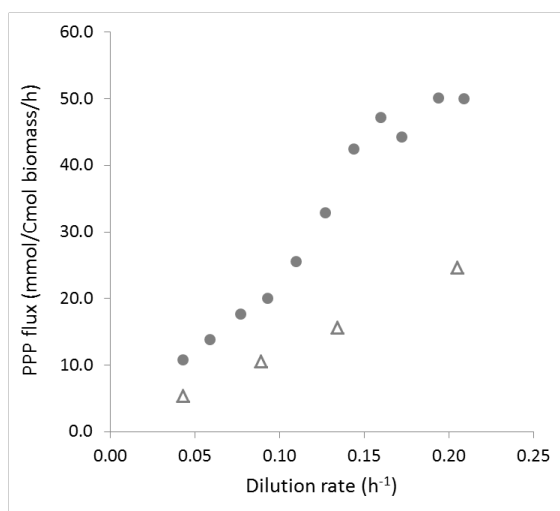


Fig. 4.8. PPP flux as a function of dilution rate in the mixed carbon source sequential chemostat (filled circles) and glucose-limited chemostat (open triangles).

It can be seen from Fig. 4.8. that the highest flux from F6P to G6P through PGI occurs at a steady state eight, at a dilution rate of 0.16 h^{-1} , just before the steep increase in the biomass specific consumption rates of glucose and mannose, which do not require

NADPH to be metabolized, and the decrease in the consumption rates of arabinose, galacturonic acid, rhamnose and to a lesser extent, xylose (Fig. 4.3.).

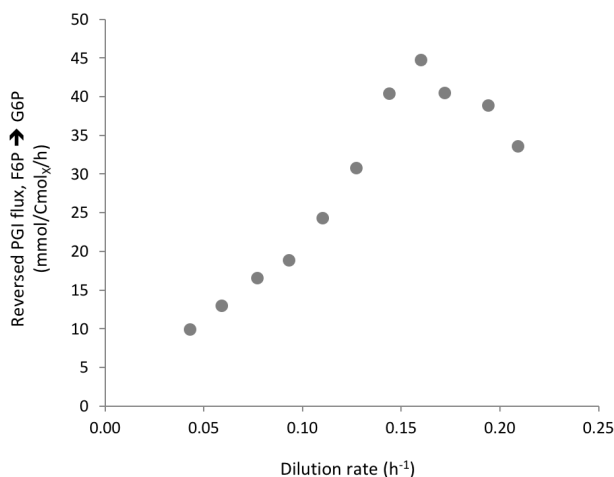


Fig. 4.9. Reversed PGI flux, F6P → G6P (mmol/Cmol/h) vs dilution rate in the mixed carbon source sequential chemostat.

The imbalance between inflow into the G6P pool in the form of glucose and outflow towards the oxidative PPP branch is also seen from the PPP split ratio, which is the ratio between the PPP outflow and the glucose inflow which is between 3.5 and 4 for the first eight steady states (until $D = 0.16 \text{ h}^{-1}$) and steeply decreases at higher dilution rates (Fig. 4.10.) due to the decrease of the relative contribution of substrates which require NADPH for their metabolism (Fig. 4.3.).

However, for all steady states of the sequential chemostat experiment the PPP split ratio is much higher compared to carbon-limited chemostat cultivations on glucose as the sole carbon source.

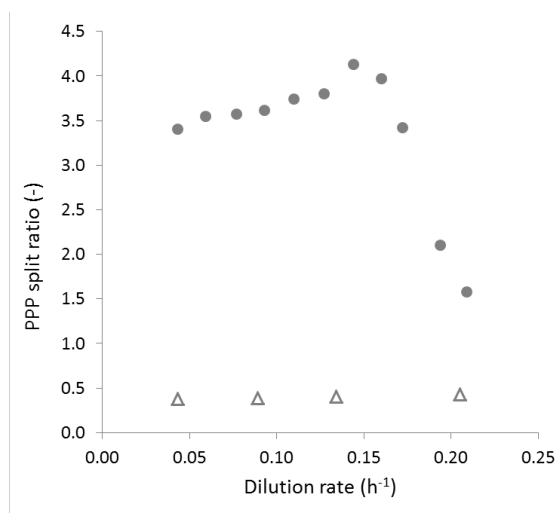
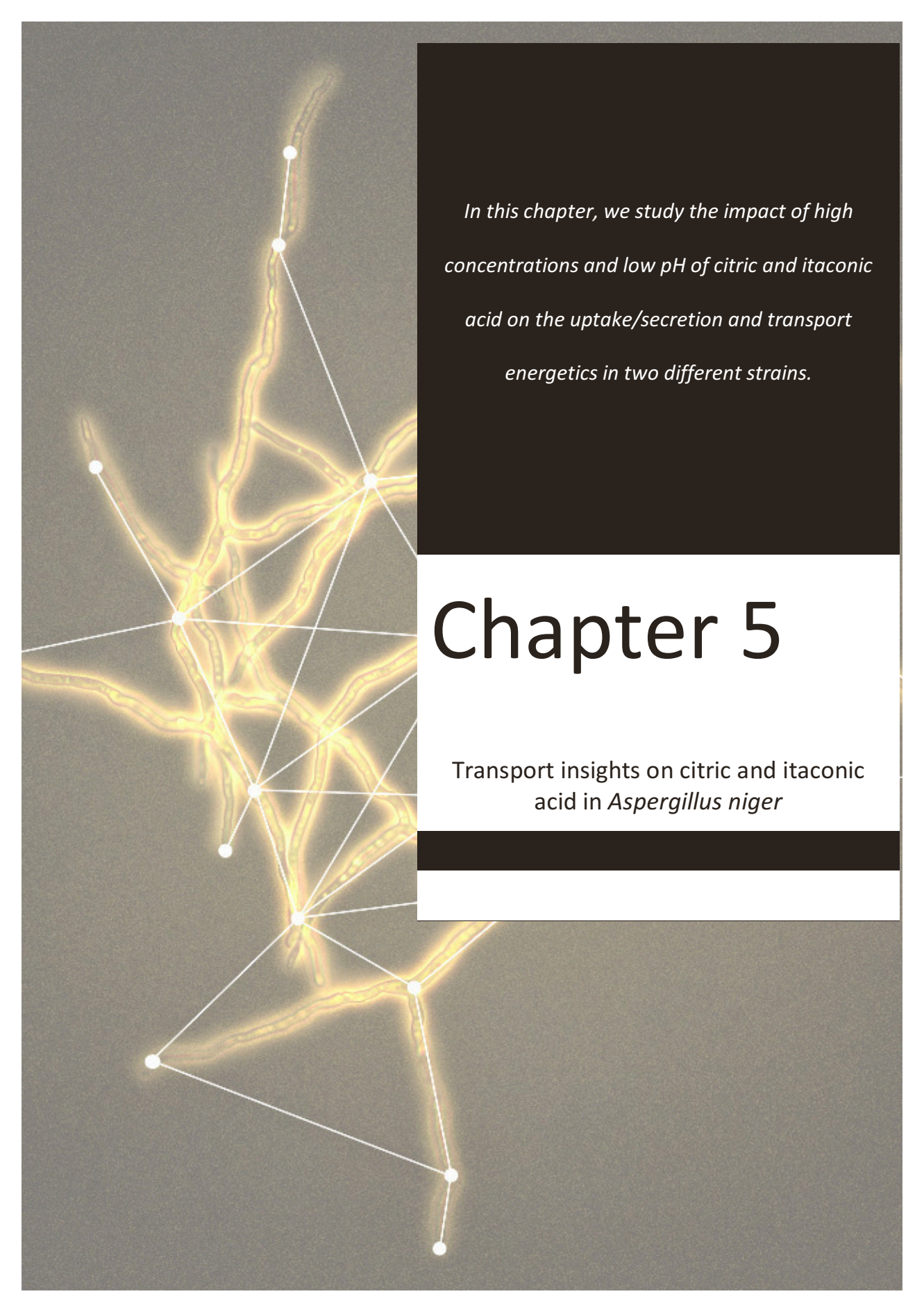


Fig. 4.10. Ratio between the flux entering the pentose phosphate pathway (glucose 6 phosphate dehydrogenase) and the flux entering the glycolysis (hexokinase) in the mixed carbon source sequential chemostat (filled circles) and glucose-limited chemostat (open triangles).

4.4. Conclusions

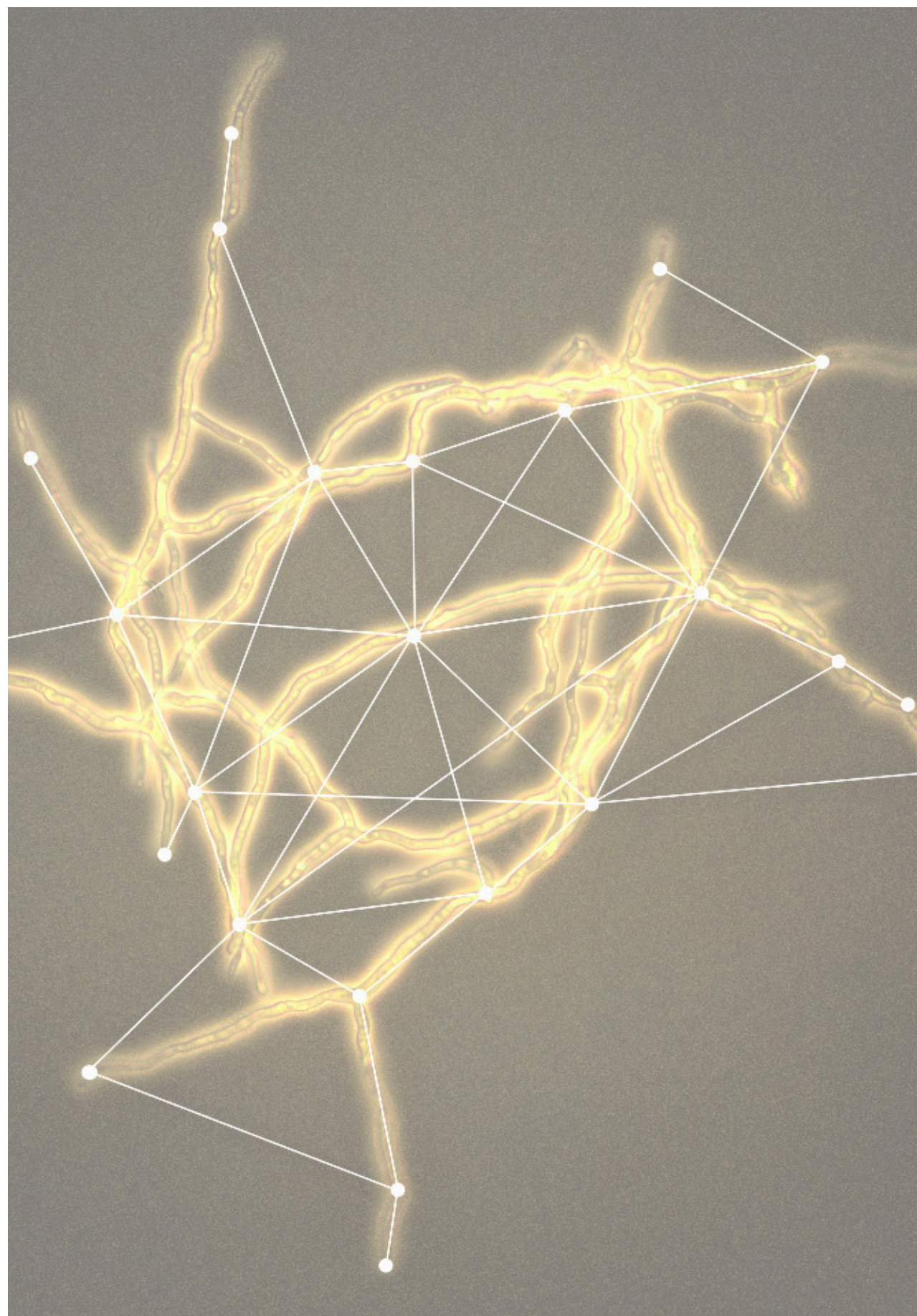
By the use of metabolomics tools, we have estimated the most plausible import mechanism for six selected substrates, based on measured in/out ratios. In addition to the predicted import system, and data from eleven carbon-limited chemostat steady states, we have built a stoichiometric model and carried out metabolic flux analysis for *A. niger* growth on a mixture of six different carbon sources. We have observed a different ATP stoichiometry for the first six steady states compared to the five last ones, possibly due to changes in biomass composition and/or the accumulation of storage compounds. The batch stoichiometry (chapter 3) obtained from the estimated ATP stoichiometry for the first six steady states obtained at relatively low growth rates, appeared different from the experimental one except for arabinose. Also this could have been caused by changes in the biomass composition. Based on the flux analysis, we observed a large pentose pathway flux and reversal of PGI during growth on a mixture of lignocellulosic sugars, due to a strongly increased NADPH demand.

A microscopic image of *Aspergillus niger* hyphae, which are long, branching, and filamentous structures. The hyphae are stained with a fluorescent dye, appearing as bright yellow-orange lines against a dark background. A network graph is overlaid on the image, with white dots representing nodes at the intersections and ends of the hyphae, and white lines representing the edges connecting these nodes.

In this chapter, we study the impact of high concentrations and low pH of citric and itaconic acid on the uptake/secretion and transport energetics in two different strains.

Chapter 5

Transport insights on citric and itaconic acid in *Aspergillus niger*



Abstract

In this study we focused on two organic acids: citric acid, essential for the food and beverage industries; and itaconic acid, used in the chemical and polymer industries. *Aspergillus niger*, as a cell factory, is capable of producing citric acid in high quantities, but can also produce itaconic acid when metabolically engineered. The objective of this work was to study the membrane transport of these acids in *A. niger* and focus on two important aspects at industrial scale: high product concentrations and a low cultivation pH, which is beneficial for the downstream processing (facilitating acid recovery and avoiding the use of titrants and associated massive waste production). Using an optimized continuous cultivation protocol for a 7 litres lab scale bioreactor (Chapter 2), we performed acid addition experiments with citric and itaconic acid at pH 2.5 and 5.5. We observed that citric acid uptake at pH=2.5 was much higher than at pH=5.5, which points to passive diffusion. However, the calculated permeability was a factor 100 higher than the expected value based on the octanol water partition coefficient, indicating that active uptake could have played a role. Itaconic acid uptake, on the other hand, was very low both at high and low cultivation pH, probably due to the absence of a pathway for the metabolism of this acid. Nevertheless, itaconic acid accumulated in the cells to levels which were affecting the physiology of the cells and resulted in increased levels of the growth limiting substrate in chemostat cultivations. Furthermore, we investigated the uptake and metabolism of itaconic acid in an itaconic acid producing and non-producing strain at high concentrations of this acid and low pH (2.5). Measurements of the in/out ratios of the acid and thermodynamic considerations indicated that export of the produced itaconic acid in the producing strain is most likely through a proton antiport mechanism.

Keywords

Aspergillus niger, chemostat, passive diffusion, citric acid, itaconic acid, thermodynamics of transport mechanisms

5.1. Introduction

Organic acids are important chemical building blocks because their functional groups are extremely valuable as starting materials for the production of polymers and resins. To move from petroleum-based production of these acids to a more sustainable industry, requires the use of renewable feedstocks.

Organic acids produced from microorganisms are divided in two groups: the TCA cycle derived acids (citric, itaconic, malic, fumaric, succinic and oxalic acid) and the glucose derived acids (gluconic and kojic acid). For high production of TCA cycle related organic acids there are four important aspects to consider: a high substrate import rate; a high flux through glycolysis and TCA cycle; the ATP, redox cofactors and electrical charge should be balanced intracellularly; and the produced acids and protons must be exported efficiently and at a high rate through the plasma membrane (Witteveen, 1993). In this work we focus on membrane transport of two organic acids: citric and itaconic acid.

Citric acid is applied in the food and beverage industries as an acidulant, and a flavouring and chelating agent. For the last 120 years, citric acid is a key product in Biotechnology and has been produced from *Aspergillus niger* submerged fermentations. *A. niger* converts glucose to citric acid with more than 80% efficiency and a titer of 300 g/l can be obtained. A reason for the efficient production of citric acid in this filamentous fungus is still not completely clear but believed to reside in the fact that *A. niger* did not evolve tight regulatory mechanisms to control acid production, as the substrate concentration in the natural environment of this organism is generally low (Magnuson and Lasure, 2004). Furthermore, the acid production capacity is thought to confer a competitive advantage for this organism, because of the chelation capacity of citric acid which facilitates the solubility of metals, and allows *A. niger* to grow in environments where metals are limited (Karaffa and Kubicek, 2003). Citric acid production by *A. niger* has been reviewed by several authors (Karaffa and Kubicek, 2003; Papagianni, 2007; Sauer *et al.*, 2008; Max *et al.*, 2010).

Itaconic acid is a dicarboxylic acid which also has industrial interest: it is among the top 12 value added building blocks which can be produced from biomass substrates (Werpy *et al.*, 2004). Itaconic acid is used for synthesis of resins, plastics, rubbers, surfactants and oils. Itaconic acid is naturally produced by *Aspergillus terreus* with a titer of up to 80 g/l on glucose (Okabe *et al.*, 2009). Since citric acid is the metabolic precursor for itaconic acid biosynthesis, many research efforts have focused on *A. niger* as a potential itaconic acid producer. This requires the heterologous expression of the enzyme cis-aconitate decarboxylase (*cadA*) from *A. terreus*, the introduction of a mitochondrial and a plasma membrane transporter and re-routing of central carbon metabolism (van der Straat and de Graaff, 2016).

The production processes of these acids are relatively similar and can be conducted in the same manufacturing facility. Both low pH and high extracellular concentrations are relevant for industrial scale production of organic acids. In this work we have focussed on membrane transport of these acids and studied the uptake of citric acid and production and uptake of itaconic acid in *A. niger* in aerobic chemostat cultures at low and high pH, and in the presence of high extracellular acid concentrations in a non transformed strain and in an itaconic acid producing strain of *A. niger*. The membrane transport and metabolism of the acids was investigated by measuring intracellular and extracellular concentrations of these acids as well as the intermediates of central metabolism. Import/export of these acids is studied as well to obtain insight on their possible transport mechanism, based on experimental data and thermodynamic considerations.

5.2. Materials and Methods

5.2.1. Strains and Inoculum

The strains used in this study were *A. niger* NW185 (*cspA1*, *goxC17*, *prtF28*, *fwA1*), and an itaconic acid producing strain *A. niger* C3 (*cspA1*, *goxC17*, *prtF28*, Δ *argB*, *mfsA*, *mttA*, *cadA*) containing the enzyme cis-aconitate decarboxylase (*cadA*) and a

mitochondrial and a plasma membrane transporter from *A. terreus* (*mttA* and *mfsA*) (van der Straat *et al.*, 2013, 2014).

Spores for pre inoculum were grown on agar plates and harvested as described in Lameiras *et al.*, 2015, with the difference that strain C3 required addition of arginine (0.2 g/l). All fermentations were inoculated with a concentration of 1×10^6 spores/ml.

5.2.2. Chemostat cultivations

A 7 litre turbine-stirred bioreactor with 4.5 litre working volume was used (Applikon, Delft, The Netherlands). To obtain a homogeneous and pellet free suspension, a special protocol was developed. The media composition, bioreactor set up and operation are described in Lameiras *et al.*, 2015.

Two sets of aerobic chemostat fermentations were performed at an intended dilution rate (D) of 0.1 h^{-1} . In experiments A and B (Fig. 5.1.), carried out with *A. niger* NW185, either citric or itaconic acid was added to the glucose based feed medium to study their uptake at pH 2.5 and 5.5 – as described below in section 5.2.2.1., while in experiments C and D (Fig. 5.2.) the cultivation pH was kept at 2.5 and itaconic acid was added to the xylose based feed medium to study possible itaconic acid uptake and metabolism in two different strains (non-producing strain *A. niger* NW185 and producing strain *A. niger* C3) - section 5.2.2.2.

5.2.2.1. Experiments A and B: Citric and itaconic acid uptake studies at pH 2.5 and 5.5 (*A. niger* NW185)

Two experimental set ups were designed for the study of the uptake of citric and itaconic acid in *A. niger* NW185 - Fig. 5.1. For the preceding batch phase minimal medium (Lameiras *et al.*, 2015) was supplemented with 38 mM of glucose. Temperature and pH were 30 ± 0.1 °C and 2.5 ± 0.05 respectively.

In these experiments continuous cultivation was initiated at the late exponential part of the batch phase by starting the medium feed at a dilution rate of 0.1 h^{-1} . After the

first steady state was achieved using medium containing 38 mM glucose as the growth limiting carbon source, the medium was exchanged for a medium of which, on a carbon basis, 50% of the glucose was replaced by citric acid and which was otherwise identical (experiment A). A similar experiment was carried out with itaconic acid in the feed medium (experiment B). In both experiments the pH was initially controlled at 2.5 to be sure that both acids were predominantly present in the fully undissociated form. After the second steady state was achieved and measurements were carried out, the cultivation pH was increased to 5.5 and a third steady state was obtained.

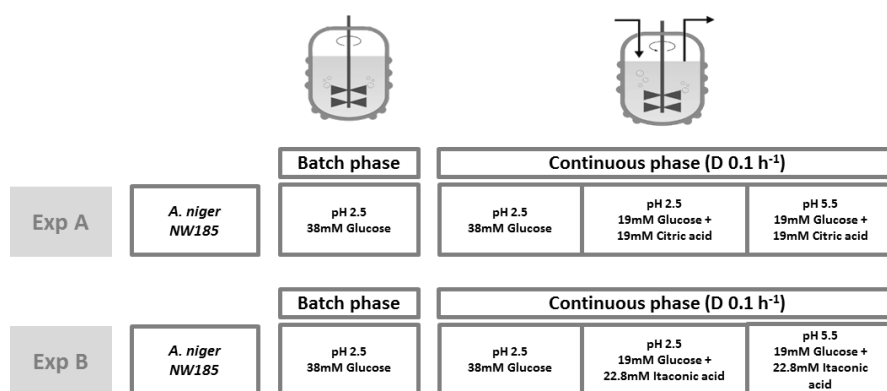


Fig. 5.1. Experiments A and B: chemostat design for the study of citric acid (Exp A) and itaconic acid (Exp B) uptake in *A. niger* NW185 at pH 2.5 and 5.5, using glucose as the limiting carbon source.

5.2.2.2. Experiments C and D: Itaconic acid production and uptake at pH 2.5 (*A. niger* NW185 and *A. niger* C3)

In order to further investigate the membrane transport of itaconic acid in *A. niger*, we compared the non-producing strain *A. niger* NW185 with the itaconic acid producing strain *A. niger* C3 (Fig. 5.2.). In these experiments the minimal medium used for the chemostat cultivation as well as the preceding batch phase was supplemented with 45.6 mM of xylose, thereby supplying the same amount of carbon source as in experiments A and B. The reason that xylose was used instead of glucose was that the promotor of the CAD gene in the C3 strain is xylose induced.

Both batch and continuous cultivation were run at temperature and pH of 30 ± 0.1 °C and 2.5 ± 0.1 respectively. Continuous cultivation was started in the late exponential phase of the batch culture by starting the medium feed at a dilution rate of 0.1 h^{-1} . For *A. niger* NW185 (experiment C), the feed composition was changed, after obtaining a first steady state, by adding 100 mmol/l of itaconic acid to the feed. Later on the itaconic acid concentration was increased further to 200 mmol/l. In case of the itaconic acid producing strain (experiment D), after cultivation with 100 mmol/l and 200 mmol/l of itaconic acid in the feed, the concentration was raised further to 300 mmol/l (fourth steady state).

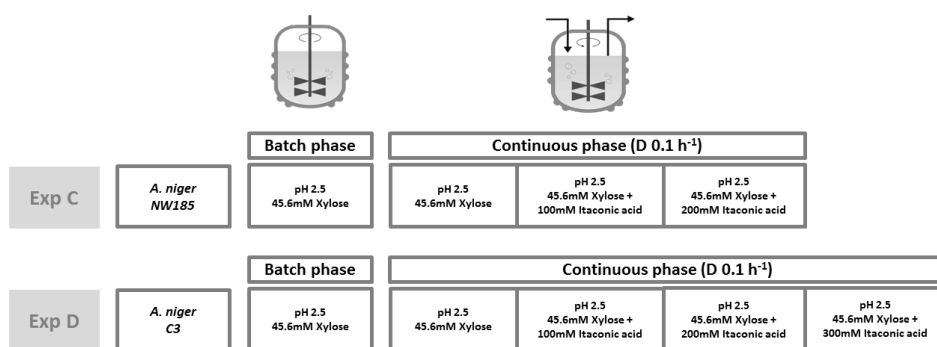


Fig. 5.2. Experiments C and D: chemostat design for the study of itaconic acid production and uptake using a stepwise increase in the itaconic acid feed concentration. Two strains were compared: *A. niger* NW185 (Exp C) and the itaconic acid producer *A. niger* C3 (Exp D), at pH 2.5, using xylose as the limiting carbon source.

5.2.3. Sampling and analytical procedures

During each steady state at least 3 samples were taken for quantification of biomass dry weight, filtrate TOC (total organic carbon) content, and concentrations of extracellular and intracellular compounds.

Biomass dry weight was determined by filtration over glass fibre filters (47mm, type A/E, Pall, USA), subsequent washing with water and drying at 70°C until constant weight. All samples were analysed in four replicates.

Filtrate samples were obtained by quickly (within 3 s) withdrawing 5 ml of broth, via the over-pressure (0.3 bar) of the fermentor, into a syringe containing a proper amount of cooled steel beads (-20 °C) to bring, within a fraction of a second, the sample temperature down to 0°C (Mashego *et al.* 2003). The cold broth was then immediately pressed through a 0.45 µm cartridge filter (Millex-HV durapore PVDF membrane) into a sampling tube, which was directly frozen in liquid nitrogen. Total organic carbon content and extracellular concentrations of organic acids (citric and itaconic acid) were measured from these filtrate samples.

The total organic carbon content of the filtrate samples was quantified with a total organic carbon analyser (type TOC-L, Shimadzu, Kyoto, Japan). With this method, both total carbon (TC) and inorganic carbon (TIC) were measured. The latter representing the content of dissolved carbon dioxide and carbonic acid salts. Subtracting the inorganic carbon from the total carbon, yields the TOC.

Extracellular concentrations of organic acids (citric and itaconic acid) were measured with a HPLC method, using a H⁺ exchange column at 60°C (Bio-Rad HPX-87H 300*7.8mm), employing phosphoric acid 1.5 mmol/l in Milli-Q water at 70°C as mobile phase. Quantification was performed with refractive index (Waters 2414; sens =1024; temp = 30°C) and UV detection (Waters 2489; 210 nm).

Samples for extracellular and intracellular metabolites were obtained by rapid sampling at -20° C in a 40% (v/v) methanol concentration in water, by the use of a custom-made sampling device. Both the protocol for rapid sampling and quenching, as well as the function of the sampling device are described in Lameiras *et al.*, 2015. The concentrations of the metabolic intermediates from glycolytic, TCA and PPP pathways were measured by isotope dilution mass spectrometry (LC-IDMS/MS and GC-IDMS/MS) according to the protocols of van Dam *et al.* 2002, de Jonge *et al.* 2011 and Cipollina *et al.* 2009.

5.2.4. Balances, biomass specific rates and data reconciliation

From the primary data (concentrations and flow rates) and compound balances, the biomass specific rates ((mol/h)/Cmol_x) of limiting substrate ($q_{\text{substrate}}$, representing glucose or xylose), organic acids ($q_{\text{organic acid}}$, representing citric or itaconic acid), and oxygen (q_{O_2}), and production rates of biomass (q_{biomass}), carbon dioxide (q_{CO_2}), cell lysis products (q_{lysis}), and organic acid (q_p) were calculated. From these biomass specific rates, carbon and degree of reduction recoveries (equations 5.1. and 5.2.) were calculated.

$$\text{Carbon recovery (\%)} = \frac{q_{\text{biomass}} + q_{\text{CO}_2} + q_{\text{lysis}} + q_p}{q_{\text{substrate}} + q_{\text{organic acid}}} \times 100 \quad (5.1.)$$

$$\text{Degree of reduction (\%)} = \frac{Y_{\text{biomass}} q_{\text{biomass}} + Y_{\text{lysis}} q_{\text{lysis}} + Y_{\text{O}_2} q_{\text{O}_2} + Y_p q_p}{Y_{\text{substrate}} q_{\text{substrate}} + Y_{\text{organic acid}} q_{\text{organic acid}}} \times 100 \quad (5.2.)$$

$q_{\text{organic acid}}$ is the consumed organic acid whereas the q_p represents acid production. The biomass composition used was the same as measured in chapter 3. For Y_{lysis} we used the degree of reduction of the biomass, assuming that unknown carbon came from biomass lysis. The produced q_p applies to the itaconic acid producing strain *A. niger C3*.

When recoveries of carbon and degree of reduction were close to 100%, data reconciliation was applied to obtain the best estimates of the measurements, within their error margins, using the elemental and charge conservation relations as constraints (Verheijen, 2010).

In addition, we estimated the ratio (here denominated β) between the flux of electrons transferred to the electron acceptor oxygen and the flux of electrons supplied by the electron donor, using the degree of reduction concept, according to equation 5.3.

$$\beta = \frac{Y_{\text{O}_2} \times q_{\text{O}_2}}{Y_{\text{glucose or xylose}} \times q_{\text{glucose or xylose}} + Y_{\text{organic acid}} \times q_{\text{organic acid}}} \quad (5.3.)$$

In this relation the denominator represents the electrons available for growth and catabolism, which is corrected for the electrons associated with organic acid production (or consumption).

This ratio gives relevant information on extra energy dissipation that might happen in case of organic acid uncoupling effect (futile cycling principles discussed in chapter 1).

5.2.5. Thermodynamics of transport mechanisms

From the acid dissociation constants (citric acid: $pK_{a1} = 3.13$, $pK_{a2} = 4.76$, $pK_{a3} = 6.39$; itaconic acid: $pK_{a1} = 3.85$, $pK_{a2} = 4.45$), the extracellular pH and the acid dissociation equilibria, the fractions of the four species of citric acid (H_3A , H_2A^- , HA^{2-} , A^{3-}) and the three species of itaconic acid (H_2A , HA^- , A^{2-}) can be calculated – Fig. 1.6 (chapter 1). In Table 5.1. the fractions of different species of citric acid and itaconic acid that coexist at pH 2.5., 5.5 and 7.6. (the relevant pH values in this study) are given.

Table 5.1. Fractions of different species of citric acid (upper panel) and itaconic acid (lower panel) for pH 2.5, 5.5 and 7.6.

Citric acid				
	H_3A	H_2A^-	HA^{2-}	A^{3-}
pH = 2.5	80.9%	19.0%	0.1%	0.0%
pH = 5.5	0.1%	13.9%	76.2%	9.8%
pH = 7.6	0.0%	0.0%	5.8%	94.2%

Itaconic acid			
	H_2A	HA^-	A^{2-}
pH = 2.5	95.7%	4.3%	0.0%
pH = 5.5	0.2%	8.2%	91.6%
pH = 7.6	0.0%	0.1%	99.9%

Depending on the pH, different species are present and can be transported, possibly along with protons (H^+) in order to maintain homeostasis of the intracellular pH. To

enable calculations on possible transport mechanisms, intracellular and extracellular conditions must be first defined.

5.2.5.1. Uptake by passive diffusion and permeability coefficient – pH_{out} 2.5

At an extracellular pH of 2.5, approximately 81% of citric acid and 96% of the itaconic acid are present in their undissociated forms (Table 5.1.), which are thus likely candidate species to be imported into the cell by passive diffusion due to their lipophilic properties. Note that at $pH=5.5$ the extracellular concentration of undissociated acid is so low (approx. 0.1%) that passive diffusion can be neglected as a transport mechanism.

For passive diffusion, the influx of an acid can be calculated by the following equation:

$$q_{acid} = k \frac{6V}{d} (C_{acid\ out} - C_{acid\ in}) \quad (5.4.)$$

Where q_{acid} is the biomass specific influx of the undissociated acid through passive diffusion (mol/h/Cmol), k is the permeability coefficient of the acid (m/s), V is the cell volume of *A. niger* ($32.8 \times 10^{-6} \text{ m}^3/\text{Cmol}$), d is the cell diameter ($10 \times 10^{-6} \text{ m}$), $C_{acid\ out}$ is the extracellular concentration of undissociated acid in mol/m^3 , and $C_{acid\ in}$ is neglected (= 0) as the intracellular undissociated acid concentration is virtually zero at $pH_{in} = 7.6$ (Hesse *et al.*, 2002). The cell surface area per Cmol biomass follows then as $154 \text{ m}^2/\text{Cmol}$.

The cell volume was estimated to be $1.2 \text{ mL}/g_{DW}$ in *A. niger* (Ruijter and Visser, 1996), and the biomass molecular weight used was $27.3 \pm 0.17 \text{ g/Cmol}$ (Lameiras *et al.*, 2015), leading to $V = 32.8 \times 10^{-6} \text{ m}^3/\text{Cmol}$. The diameter of fungal hyphae varies between $5 \text{ }\mu\text{m}$ to $15 \text{ }\mu\text{m}$, and therefore an average of $10 \text{ }\mu\text{m}$ was used for the permeability calculation (Geitmann and Emons, 2000).

However, at pH 2.5, also significant fractions of H_2A^- and HA^- are present for both citric acid and itaconic acid: 19% and 4% respectively (Table 5.1.). It should be realized that negatively charged molecules cannot passively diffuse over the membrane, so for

import/export a transport protein has to be present, as we elaborate in following section.

5.2.5.2. Import of charged organic acids across a cell membrane – pH_{out} 5.5 and 2.5

In case the extracellular pH is 5.5, it should be noticed (Table 5.1.) that for citric acid 76% of the acid is present as the HA^{2-} species, 14% as H_2A^- species and 10% as the fully dissociated form (A^{3-} species); for itaconic acid 8% of the acid is present as the HA^- species and 92% is present in the fully dissociated form (A^{2-} species). This means that the most abundant species are charged and cannot passively diffuse over the membrane, therefore a transporter protein has to be present. The anionic species (charge z) can be imported together with nH^+ according to the import process $C_{out}^z + nH^+_{out} \rightleftharpoons C_{in}^z + nH^+_{in}$, with n representing the different possible transport mechanisms. For uniport $n=0$, symport $n=1$, double symport $n=2$, antiport $n=-1$ (Fig. 1.5. - chapter 1).

At $pH_{out}=5.5$, we will consider that the mono- and di-anions (the most abundant ones) are the imported species, that is H_2A^- and HA^{2-} in case of citric acid and HA^- and A^{2-} in case of itaconic acid.

The thermodynamic driving force for the transport of a double anion ($z=-2$) linked to H^+ transport across the cell membrane can be defined according to equation 5.5.

$$\Delta_r G = 2.303 RT \log \left(\frac{A_{in}^{2-}}{A_{out}^{2-}} \right) - 2.303 n RT (pH_{in} - pH_{out}) + (n - 2) F \psi \quad (5.5.)$$

We have described previously (chapter 1) how the membrane potential ψ depends on the extracellular pH (equation 1.2.). Rearranging equation 5.5., by elimination of ψ , leads to an expression (equation 5.6.) giving the in/out ratio A_{in}^{2-}/A_{out}^{2-} for different transport mechanisms as a function of pH_{out} and temperature for $\Delta_r G=0$ (equilibrium). Herein n represents the stoichiometry of proton coupled transport, that is $n=-1, -2$ etc. for proton antiport, $n=0$ for uniport and $n=1, 2$, etc. for proton symport.

$$\log \frac{A_{in}^{2-}}{A_{out}^{2-}} = 2(pH_{in} - pH_{out}) - \frac{(n-2)(-E_{pmf})F}{2.303 RT} \quad (5.6.)$$

For the case of transport of an anion ($z=-1$) ($\text{pH}=2.5$), equations similar to 5.5 and 5.6 can be derived to obtain the $A_{\text{in}}^-/A_{\text{out}}^-$ ratio. The total in/out equilibrium ratio of the acid is related to the in/out ratio of the transported double anion A^{2-} and follows from the dissociation relations, e.g. for itaconic acid (Fig. S1.1.):

$$\frac{A_{\text{in}}}{A_{\text{out}}} = \left(\frac{10^{\text{p}ka_1 + \text{p}ka_2 - 2\text{pH}_{\text{in}} + 10^{\text{p}ka_2 - \text{pH}_{\text{in}} + 1}}}{10^{\text{p}ka_1 + \text{p}ka_2 - 2\text{pH}_{\text{out}} + 10^{\text{p}ka_2 - \text{pH}_{\text{out}} + 1}}} \right) \left(\frac{A_{\text{in}}^{2-}}{A_{\text{out}}^{2-}} \right) \quad (5.7.)$$

Equation 5.7 can be applied in an experimental context, as the measured in/out ratio's represent total acid ratio's.

A similar equation can be derived for citric acid, with as only difference that three anionic species have to be taken into account:

$$\frac{A_{\text{in}}}{A_{\text{out}}} = \left(\frac{10^{\text{p}ka_1 + \text{p}ka_2 - 2\text{pH}_{\text{in}} + 10^{\text{p}ka_2 - \text{pH}_{\text{in}} + 10^{\text{pH}_{\text{in}} - \text{p}ka_3 + 1}}}{10^{\text{p}ka_1 + \text{p}ka_2 - 2\text{pH}_{\text{out}} + 10^{\text{p}ka_2 - \text{pH}_{\text{out}} + 10^{\text{pH}_{\text{out}} - \text{p}ka_3 + 1}}} \right) \left(\frac{HA_{\text{in}}^{2-}}{HA_{\text{out}}^{2-}} \right) \quad (5.8.)$$

In table 5.2. the total in/out equilibrium ratios of the acids (obtained from equations 5.6 and 5.7 or 5.8) can be found for pH_{out} values of 2.5 and 5.5, for proton coupled transport mechanisms with different H^+ stoichiometries for the transported species H_2A^- and HA^{2-} (citric acid) and HA^- and A^{2-} (itaconic acid) and according to the thermodynamic relations elaborated. Here, $\text{pH}_{\text{in}} = 7.6$ (Hesse *et al.*, 2002), $T = 303 \text{ K}$ (30°C), $E_{\text{pmf}} = 0.15 \text{ V}$, $R = 8.314 \times 10^{-3} \text{ kJ/molK}$ and $F = 96.5 \text{ kJ/v e}^- \text{mol}$.

Because also passive diffusion can be considered as a relevant transport mechanism at low pH (section 5.2.5.1.), the in/out equilibrium ratios for passive diffusion of the fully undissociated species are included in Table 5.2 for an extracellular pH of 2.5.

At $\text{pH}_{\text{out}}=2.5$, in/out ratios of total acid higher than one are calculated for import of H_2A^- via double symport for citric acid and import of HA^- via single and double symport for itaconic acid, which shows that these are feasible import mechanisms for this pH. At $\text{pH}_{\text{out}}=5.5$, in/out ratios of total acid higher than one are calculated for single and double symport of HA^{2-} for citric acid and A^{2-} for itaconic acid, showing that these are feasible import mechanisms at pH 5.5.

Table 5.2. Equilibrium in/out ratios of total acid for $pH_{in} = 7.6$, considering import of the undissociated and mono-anionic species of citric and itaconic acid at $pH_{out} = 2.5$ and the mono and di-anionic species of citric and itaconic acid at pH_{out} .

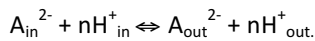
$A_{in}/A_{out} (pH_{out} = 2.5)$				
Transport mechanism	Citric acid		Itaconic acid	
	imported species: H_3A	imported species: H_2A^-	imported species: H_2A	imported species: HA^-
Antiport $n = -1$	-	2.9×10^3	-	78
Uniport $n = 0$	-	9.1×10^5	-	2.4×10^4
Symport $n = 1$	-	2.9×10^8	-	7.6×10^6
Double symport $n = 2$	-	8.9×10^{10}	-	2.4×10^9
Passive diffusion	2.9×10^8	-	7.6×10^6	-

$A_{in}/A_{out} (pH_{out} = 5.5)$				
Transport mechanism	Citric acid		Itaconic acid	
	imported species: H_2A^-	imported species: HA^{2-}	imported species: HA^-	imported species: A^{2-}
Antiport $n = -1$	2.1	6.8×10^{-3}	0.15	4.8×10^{-4}
Uniport $n = 0$	6.7×10^2	2.1	47	0.15
Symport $n = 1$	2.1×10^5	6.7×10^2	1.5×10^4	47
Double symport $n = 2$	6.5×10^7	2.1×10^5	4.5×10^6	1.5×10^4

5.2.5.3. Export of organic acids – $pH_{in} 7.6$

Weak acids inside the cell will dissociate because of the near neutral intracellular pH. At an intracellular pH of 7.6 (Hesse *et al.*, 2002) almost all acid, approximately 94.2% of the citric acid and 99.9% of the itaconic acid are present in their fully dissociated form: A^{3-} and A^{2-} respectively (Table 5.1). Therefore, we assume that only the fully dissociated species are exported.

In the case of itaconic acid, the export can be described by:



Similarly to what was derived in the previous section for acid import, we can obtain a relation for the out/in ratio of total acid at equilibrium if the di-anionic species of itaconic acid is exported.

$$\Delta_r G = 2.303 RT \log(A_{out}^{2-}/A_{in}^{2-}) - 2.303 n RT (pH_{out} - pH_{in}) - (n - 2) F \psi \quad (5.9.)$$

$$\log \frac{A_{out}^{2-}}{A_{in}^{2-}} = 2(pH_{out} - pH_{in}) + \frac{(n-2)(-E_{pmf})F}{2.303 RT} \quad (5.10.)$$

$$\frac{A_{out}}{A_{in}} = \left(\frac{10^{pka1+pka2-2pH_{out}+1} 10^{pka2-pH_{out}+1}}{10^{pka1+pka2-2pH_{in}+1} 10^{pka2-pH_{in}+1}} \right) \left(\frac{A_{out}^{2-}}{A_{in}^{2-}} \right) \quad (5.11.)$$

An analogous equation can be derived for export of the triple anionic species of citric acid.

$$\Delta_r G = 2.303 RT \log(A_{out}^{3-}/A_{in}^{3-}) - 2.303 nRT(pH_{out} - pH_{in}) - (n-3)F\psi \quad (5.12.)$$

Which can be rewritten as:

$$\log \frac{A_{out}^{3-}}{A_{in}^{3-}} = 3(pH_{out} - pH_{in}) + \frac{(n-3)(-E_{pmf})F}{2.303 RT} \quad (5.13.)$$

And further as:

$$\frac{A_{out}}{A_{in}} = \left(\frac{10^{pka1+pka2+pka3-3pH_{out}+1} 10^{pka2+pka3-2pH_{out}+1} 10^{pka3-pH_{out}+1}}{10^{pka1+pka2+pka3-3pH_{in}+1} 10^{pka2+pka3-2pH_{in}+1} 10^{pka3-pH_{in}+1}} \right) \left(\frac{A_{out}^{3-}}{A_{in}^{3-}} \right) \quad (5.14.)$$

In table 5.3 the total acid out/in ratios at equilibrium can be found for the exported species (A^{3-} and A^{2-} for citric and itaconic acid respectively) for different transport mechanisms, and according to the thermodynamic relations here elaborated. Here, $pH_{in} = 7.6$ (Hesse *et al.*, 2002), $T = 303$ K (30°C), $E_{pmf} = 0.15$ V, $R = 8.314 \times 10^{-3}$ kJ/molK and $F = 96.5$ kJ/v e⁻mol.

Table 5.3. Equilibrium out/in ratios of total acid considering export of the anionic species A^{3-} and A^{2-} for citric and itaconic acid respectively at $pH_{out} = 2.5$ and $pH_{out} = 5.5$.

Transport mechanism	A_{out}/A_{in} ($pH_{out} = 2.5$)		A_{out}/A_{in} ($pH_{out} = 5.5$)	
	Citric acid exported species: A^{3-}	Itaconic acid exported species: A^{2-}	Citric acid exported species: A^{3-}	Itaconic acid exported species: A^{2-}
Antiport $n = -1$	33	4.0	4.6×10^4	2.1×10^3
Uniport $n = 0$	1.1×10^{-1}	1.3×10^{-2}	1.5×10^2	6.7
Symport $n = 1$	3.4×10^{-4}	4.1×10^{-5}	0.47	2.1×10^{-2}
Double symport $n = 2$	1.1×10^{-6}	1.3×10^{-7}	1.5×10^{-3}	6.9×10^{-5}

It is obvious that for a significant extracellular accumulation of both acids at low pH_{out} (2.5), at least an antiport system is needed (total acid out/in ratio's significantly above 1). At moderate pH_{out} (5.5) a uniport system could work for both acids.

From these thermodynamic calculations it can be inferred that the export of the fully dissociated species of these organic acids at low pH must be accompanied by the export of 3 to 4 protons (for itaconic and citric acid respectively). Considering a $\text{H}^+/\text{ATP}=1$ stoichiometry of the plasma membrane H^+ -ATPase this goes at the expense of 3 to 4 mol of ATP per mol of acid exported, which is very significant (the ATP cost associated to each transport mechanism is explored in more detail in chapter 1).

5.3. Results and Discussion

5.3.1. Experiments A and B: Citric and itaconic acid uptake studies at pH 2.5 and 5.5

Two carbon-limited chemostat fermentations were carried out in parallel (Fig. 5.1.), indicated as experiments A and B. The strain *A. niger* NW185 was cultivated on chemically defined medium with glucose as the limiting carbon and energy source. The chemostat phase was started in the late exponential part of the preceding batch phase by starting the medium feed at an intended dilution rate of 0.1h^{-1} .

In experiment A, the pH was initially controlled at 2.5, and after the first steady state on glucose as the only carbon source was achieved, the feed medium was changed to a feed medium containing, with respect to the amount of carbon, an equimolar mixture of glucose and citric acid, which was otherwise identical to the previous one. Subsequently, when a second steady state was reached, measurements and samples were taken as described in the Materials and Methods. Next, the pH setpoint was changed from 2.5 to 5.5 and the chemostat was run until a third steady state was reached and another set of samples and measurements could be taken.

Experiment B was carried out in the same way, but now citric acid was substituted by itaconic acid (Fig. 5.1.).

5.3.1.1. General observations

In both experiments A and B, the biomass concentration was measured at least four times during each steady state and the concentrations of O_2 and CO_2 in the offgas were measured online for the calculation of the O_2 consumption and CO_2 production rates (Fig. 5.3.).

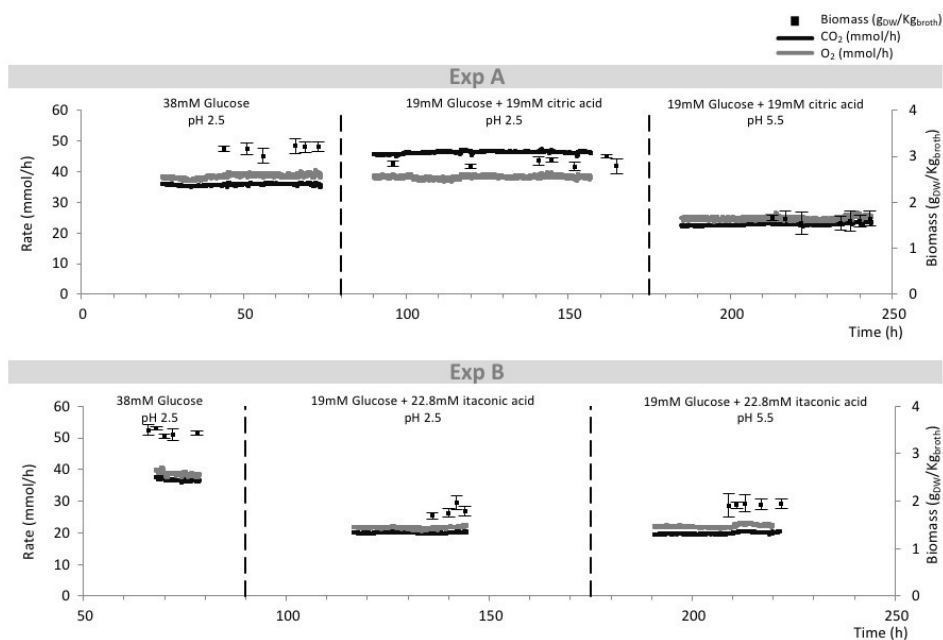


Fig. 5.3. Biomass concentration (right axis) and molar rates of carbon dioxide and oxygen (left axis) in experiment A (upper panel) and B (lower panel).

In addition, the total organic carbon (TOC) content of the filtrate samples was quantified as well as the concentrations of glucose and organic acids - Fig S5.1. In the first steady state (no organic acid present), the difference between TOC and glucose carbon was used to calculate the rate of cell lysis (see also Lameiras *et al.*, 2015).

In the three steady states, the carbon balance using TOC filtrate indicates that there is no other by-product formation. Therefore, the TOC concentration of the filtrate samples ($TOC_{filtrate}$) should equal the carbon sum of the residual concentration of the

limiting substrate ($C_{\text{glucose out}}$), the organic acid concentration ($C_{\text{organic acid out}}$), and cell lysis products (C_{lysis}), according to the equation:

$$\text{TOC}_{\text{filtrate}} = C_{\text{glucose out}} + C_{\text{organic acid out}} + C_{\text{lysis}} \text{ (in mCmol/L)} \quad (5.15.)$$

In the first steady state of experiment A and B, where only glucose was present, the measured concentration of lysis products (C_{lysis}) was around 11 mCmol/l and 14 mCmol/l of carbon respectively, which is in agreement with what was measured previously (12 mCmol/l of cell lysis products with glucose as sole carbon source and the same feed concentration at dilution rate 0.1h^{-1}) (Lameiras *et al.*, 2015). These concentrations of lysis products correspond to biomass specific rates of $q_{\text{lysis}} = 9.75$ (mCmol/h)/Cmol and 7.95 (mCmol/h)/Cmol for experiments A and B.

Based on this result, we consider the biomass specific rate of cell lysis products (q_{lysis}) constant during the chemostat cultivations, i.e. during the following two steady states for each experiment A and B.

Evaluating the HPLC measurements of organic acids (in light red) in relation to the measured filtrate TOC, it was found that these were in most cases overestimated and in addition contained significant standard errors. Therefore, we chose to estimate more realistic values for the organic acid concentrations ($C^*_{\text{organic acid out}}$), from the TOC measurements represented in light green in Fig. S5.1.

$$C^*_{\text{organic acid out}} = \text{TOC}_{\text{filtrate}} - C_{\text{glucose out}} - C_{\text{lysis}} \text{ (in mCmol/L)} \quad (5.16.)$$

In this relation C_{lysis} was calculated using a constant q_{lysis} as discussed before. From this point on, we consider the residual organic acids concentration as estimated from TOC measurements ($C^*_{\text{organic acid out}}$).

The data set of all primary measurements (concentration and flow rates), before and after reconciliation, as well as the molar rates, carbon and redox balances can be found in Tables S5.1. and S5.2.

From the substrate, biomass, O₂, CO₂, and TOC measurements, it was calculated that the recoveries of carbon and degree of reduction were close to 100% and thus the best estimates of the biomass specific rates were calculated using data reconciliation (Table 5.4.).

Table 5.4. Concentrations of residual biomass organic acid and glucose; biomass specific net conversion rates, respiratory quotient and ratio β of steady state chemostat cultivations in experiment A (upper panel) and experiment B (lower panel) chemostats.

Exp A						
	38mM Glucose pH 2.5		19mM Glucose + 19mM citric acid pH 2.5		19mM Glucose + 19mM citric acid pH 5.5	
	Unreconciled	Reconciled	Unreconciled	Reconciled	Unreconciled	Reconciled
C _{biomass} (g/l)	3.19±0.05	3.32±0.03	2.86±0.03	2.83 ± 0.03	1.60±0.06	1.90±0.03
C _{*citric acid out} (mmol/l)	0.00±0.00	0.00±0.00	2.43±0.92	1.57 ± 0.32	15.38±0.14	15.79±0.13
C _{glucose out} (mmol/l)	0.29±0.08	0.35±0.08	0.18±0.06	0.16 ± 0.06	0.14±0.02	0.15±0.02
q _{CO2} (mmol/h)/Cmol	69.6±19.4	78.5±1.0	100.7±1.5	102.9 ± 1.3	88.2±1.3	79.4±1.0
q _{O2} (mmol/h)/Cmol	-79.2±14.9	-77.1±1.0	-78.8±16.7	-76.2 ± 1.0	-99.8±30.1	-71.7±1.0
q _{biomass} (mmol/h)/Cmol	98.4±1.4	98.4±1.0	98.6±1.1	98.7 ± 1.1	98.6±3.5	98.6±1.5
q _{lactis} (mCmol/h)/Cmol	9.75±0.44	9.73±0.42	9.75±0.44	9.69 ± 0.50	9.75±0.44	9.22±0.73
q _{citric acid} (mmol/h)/Cmol	0.00±0.00	0.00±0.00	-17.79±0.12	-16.93 ± 0.31	-5.76±1.41	-4.26±0.19
q _{glucose} (mmol/h)/Cmol	-32.40±0.08	-31.11±0.07	-18.12±0.06	-18.29 ± 0.07	-31.91±0.30	-26.95±0.04
RQ (R _{CO2} /R _{O2})	0.88±0.21	1.02±0.02	1.28±0.27	1.35 ± 0.02	0.88±0.27	1.11±0.02
β (X _{O2} /X _{glucose} +X _{citric acid})	0.41±0.08	0.41±0.01	0.42±0.09	0.41 ± 0.01	0.46±0.14	0.40±0.01
Exp B						
	38mM Glucose pH 2.5		19mM Glucose + 22.8mM itaconic acid pH 2.5		19mM Glucose + 22.8mM itaconic acid pH 5.5	
	Unreconciled	Reconciled	Unreconciled	Reconciled	Unreconciled	Reconciled
C _{biomass} (g/l)	3.45±0.04	3.47±0.03	1.87 ± 0.06	1.95±0.03	1.93 ± 0.06	1.82±0.03
C _{*itaconic acid out} (mmol/l)	0.00±0.00	0.00±0.00	18.94 ± 0.17	19.39±0.16	19.47 ± 0.18	19.59±0.17
C _{glucose out} (mmol/l)	0.13±0.02	0.13±0.02	0.13 ± 0.02	0.14±0.02	0.19 ± 0.03	0.19±0.03
q _{CO2} (mmol/h)/Cmol	66.2±1.0	67.9±0.7	66.6 ± 1.0	64.0±0.8	64.0 ± 0.9	65.4±0.8
q _{O2} (mmol/h)/Cmol	-72.8±13.8	-66.6±0.7	-74.9 ± 25.9	-60.3±0.8	-73.9 ± 25.0	-62.0±0.9
q _{biomass} (mmol/h)/Cmol	95.3±1.0	95.4±0.7	101.5 ± 3.0	101.6±1.3	95.1 ± 3.0	95.2±1.2
q _{lactis} (mCmol/h)/Cmol	7.95±0.23	9.70±0.23	7.95 ± 0.46	10.09±0.41	7.95 ± 0.41	10.92±0.41
q _{itaconic acid} (mmol/h)/Cmol	0.00±0.00	0.00±0.00	-5.83 ± 1.32	-4.57±0.22	-4.24 ± 1.23	-4.01±0.23
q _{glucose} (mmol/h)/Cmol	-29.23±0.06	-28.83±0.03	-28.60 ± 0.28	-25.47±0.04	-25.59 ± 0.32	-25.23±0.05
RQ (R _{CO2} /R _{O2})	0.91±0.17	1.02±0.01	0.89 ± 0.31	1.06±0.02	0.87 ± 0.29	1.05±0.02
β (X _{O2} /X _{glucose} +X _{itaconic acid})	0.42±0.08	0.39±0.00	0.38 ± 0.13	0.35±0.00	0.43 ± 0.15	0.37±0.01

Using an optimized rapid sampling and quenching protocol (Chapter 2), intra- and extracellular concentrations of glucose and organic acids were determined in order to obtain insight in their transport mechanisms (Table 5.6.). The thermodynamics of different possible transport systems, using these measurements, is explored in more detail in section 5.3.3. Additionally, the metabolome, in terms of glycolytic, TCA and PPP intermediates, was also quantified, both with respect to intra- and extracellular concentrations, for experiments A and B (Fig. S5.3. and Fig. S5.4.).

In the following two subsections, experiments A and B are explored individually in terms of offgas profiles (Fig. 5.3.), biomass specific uptake and production rates (Table 5.4.); while intra- and extracellular concentrations, as well as the related thermodynamics of transport mechanisms are presented in section 5.3.3. (Table 5.6.).

5.3.1.2. Experiment A: Citric acid uptake in *A. niger* NW185

In the first steady state of experiment A, recovery of carbon and degree of reduction are close to 100% (Table S5.1) and the respiratory quotient (CO_2/O_2) is slightly above one, as expected for glucose being the only electron donor. The concentration of biomass was consistently measured around $3.19 \pm 0.05 \text{ g}_{\text{DW}}/\text{Kg}_{\text{broth}}$, close to what was observed in previous comparable experiments: $3.25 \pm 0.04 \text{ g}_{\text{DW}}/\text{Kg}_{\text{broth}}$ (chapter 2). Analysing Table 5.4., residual glucose is found to be below 1 mM. In fact, in all three steady states, the extracellular levels of glucose are very low, indicating that glucose is the growth limiting nutrient and is practically fully consumed in all cases.

During the second steady state at pH 2.5, glucose and citric acid were fed to the chemostat in equal amounts with respect to their carbon content. A first observation of the offgas measurements (Fig. 5.3.) indicated that citric acid is consumed as the respiratory quotient is significantly higher than one. This is expected because citric acid is a more oxidized substrate ($3 \text{ e}^-/\text{C}$) than glucose ($4 \text{ e}^-/\text{C}$). Also in this case no significant gaps were found in the carbon and degree of reduction balances. Another clear evidence of citric acid uptake is the low residual concentration and estimated high uptake rate ($16.9 \text{ mmol/h}/\text{Cmol}$), which is nearly the same as the glucose uptake

rate (18.2 mmol/h)/Cmol) - Table 5.4. The glucose uptake rate was 43% lower than during the previous steady state and not 50%, which would have been expected because the glucose concentration in the feed was also a factor two lower. However, the biomass concentration, and thus the yield of biomass on the mixed substrate, was also lower (15%). An explanation for the decreased biomass yield in the second steady state is that in spite of the fact that the same amount of carbon is supplied, the supply of electrons is less. Because $4\text{ e}^-/\text{C}$ are supplied in case of glucose and $3\text{ e}^-/\text{C}$ in case of citric acid, feeding a 1:1 mixture of glucose and citric acid results in the supply of $3.5\text{ e}^-/\text{C}$. This represents 12.5% less electrons than for glucose as the sole carbon and electron source, which is very well reflected in the decreased biomass concentration.

In the last steady state of experiment A, the pH_{out} setpoint was increased to 5.5 without changing the medium feed composition (thus no change in the feed concentrations of glucose and citric acid). The calculated carbon and degree of reduction recoveries do not show evidence of gaps (Fig. S5.1). The offgas profile indicates some consumption of citric acid, as the carbon dioxide production and oxygen consumption rates were slightly higher than half of what was observed for the first steady state (Fig. 5.3.). In addition, the residual concentration of citric acid (Table 5.4.), was estimated to be 17% lower than the concentration in the feed, showing that indeed at pH 5.5 some consumption of citric acid occurred. The biomass specific uptake rate of citric acid was estimated to be 4.26 (mmol/h)/Cmol (Table 5.4.), which is 4 fold lower than at $\text{pH}=2.5$. Also in this case, the increased value of the RQ compared to growth on glucose only, indicates consumption of citric acid as carbon and energy source.

In table 5.4. it is shown that the ratios of catabolized electrons (β) are very similar in all three steady states of experiment A (0.41, 0.41 and 0.39), which suggests that there is no extra energy dissipation due to uncoupling related to the presence of citric acid (19 mM) – second and third steady states. This would imply that the citric acid which is taken up is fully metabolized into biomass and is not exported (which would create a futile cycle). Also, the metabolome data supports this observation (see below).

5.3.1.3. Experiment B: Itaconic acid uptake in *A. niger* NW185

In experiment B, citric acid was substituted by itaconic acid. In the first steady state, with glucose as the only substrate, the results with respect to measured concentrations of biomass, substrate, O₂ and CO₂ and calculated biomass specific conversion rates are very similar as obtained for experiment A, as expected.

In this experiment, the most interesting steady states are the last two where glucose and itaconic acid are fed in an equimolar carbon ratio at pH 2.5 and 5.5. Looking at the carbon dioxide production and oxygen consumption rates, there might be a small consumption of itaconic acid, both at pH 2.5 and 5.5, which is also visible from the O₂ and CO₂ rates (Fig. 5.3.) which are both slightly higher than half that of the first steady state. The same holds for the measured biomass concentration (Fig. 5.3.). These indications that itaconic acid is taken up is also supported by the estimations of residual itaconic acid in the filtrate samples (Table 5.4.). The biomass specific uptake rate of this acid was estimated to be 4.6 and 4.0 (mmol/h)/Cmol at pH 2.5 and 5.5 respectively. In contrast with previous experiment (exp A), the extracellular pH does not seem to have a large effect on the uptake rates of the acid.

Comparing the β ratio, these values for all three steady states (0.38, 0.34 and 0.36) are very close to the ones calculated in experiment A, rejecting any hypothesis of acid uncoupling, and thus extra energy dissipation.

The above presented evidence indicated that itaconic acid is taken up in *A. niger* NW185 at low rates. However, there is no pathway known in *A. niger* for itaconic acid metabolism. In *Pseudomonas* sp., itaconic acid is metabolized by activation through itaconyl-CoA hydratase or itaconate-CoA transferase, followed by hydration and cleavage to acetyl-CoA and pyruvate (Cooper and Kornberg, 1964) – Fig. S5.7. Here in this work we did not investigate further on the possible degradation pathway of itaconic acid.

5.3.2. Experiments C and D: Itaconic acid production and uptake at pH 2.5

In order to further investigate itaconic acid transport and possible metabolism in *A. niger*, two chemostat fermentations were run in parallel (Fig. 5.2.) with two different strains: *A. niger* NW185 (experiment C) and the itaconic acid producing strain *A. niger* C3 (experiment D). Both strains were cultivated on minimal medium in the presence of xylose. Subsequently, high levels of itaconic acid were added to the chemostat feed. The chemostat phase was started in the late exponential phase of the batch by starting the feed at an intended dilution rate of 0.1h^{-1} while the pH was controlled at 2.5 ± 0.05 .

5.3.2.1. General observations

In both experiments, the first steady state was obtained on xylose as the only carbon source, while during the following two itaconic acid was added to the feed media at concentrations of 100 and 200 mM, respectively. In experiment D, a fourth steady state was achieved by increasing the itaconic acid concentration further to 300 mM. In both experiments C and D, the biomass concentration was measured at least four times during each steady state and the concentrations of O_2 and CO_2 in the offgas were measured online for the calculation of the O_2 consumption and CO_2 production rates as a function of time (Fig. 5.4.).

In addition, total organic carbon was quantified from filtrate samples and compared to the measured carbon residuals of xylose and itaconic acid - Fig S5.2. Similarly to experiment A and B, also here the biomass specific rate of lysis products was considered constant throughout each experiment ($q_{\text{lysis}} = 17 \text{ (mCmol/h)/Cmol}$ in experiment C and $15 \text{ (mCmol/h)/Cmol}$ in experiment D). The concentration of itaconic acid ($C^*_{\text{itaconic acid out}}$) was obtained from the TOC measurements as explained previously.

$$C^*_{\text{itaconic acid out}} = \text{TOC}_{\text{filtrate}} - C_{\text{xylose out}} - C_{\text{lysis}} \text{ (in mCmol/L)} \quad (5.17.)$$

The complete data set of all primary measurements, before and after reconciliation, as well as the molar rates, carbon and redox balances can be found in Tables S5.3. and S5.4.

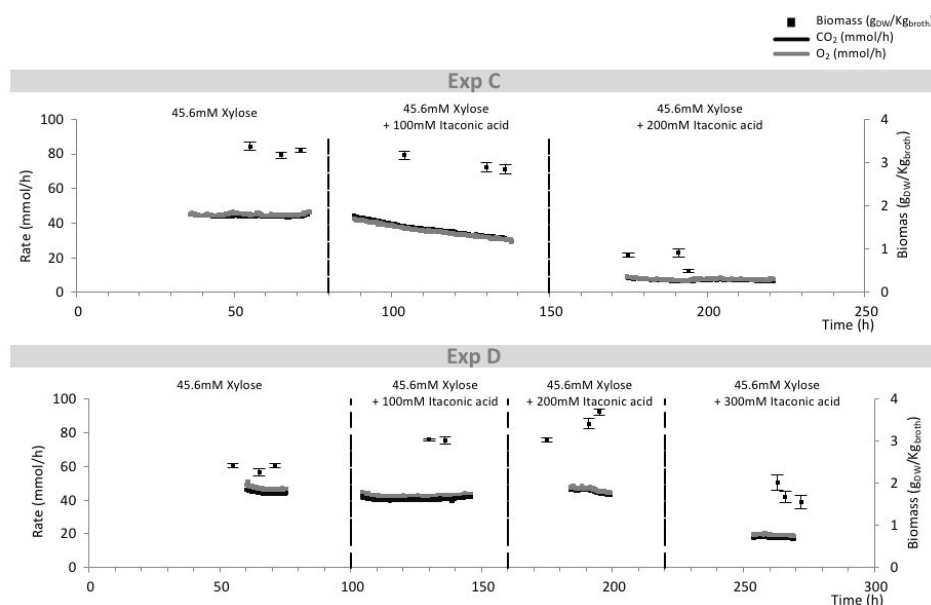


Fig. 5.4. Biomass concentration (right axis) and molar rates of carbon dioxide and oxygen (left axis) in experiment C (upper panel) and D (lower panel).

From the substrate, biomass, O₂, CO₂, and TOC measurements, it was calculated that the recoveries of carbon and degree of reduction were close to 100% and thus the biomass specific rates were calculated using data reconciliation (Table 5.5.).

Finally, using an optimized rapid sampling and quenching protocol, intra- and extracellular concentrations of xylose and organic acids were determined in order to get an insight in their transport mechanisms (Table 5.6.). The thermodynamics of transport systems is explored in detail in section 5.3.3. In addition, the metabolome, in terms of glycolytic, TCA and PPP intermediates, was also evaluated for experiments C and D (Fig. S5.5. and Fig. S5.6.).

In the following two subsections, these two experiments are explored individually in terms of offgas profiles (Fig. 5.4.), biomass specific uptake and production rates (Table 5.5.); Intra- and extracellular concentration levels, as well as thermodynamics of transport mechanisms are addressed in section 5.3.3. (Table 5.6.).

5.3.2.2. Experiment C: Itaconic acid uptake in *A. niger* NW185

The same strain used in experiments A and B was also used in C but with xylose as a carbon source. The idea behind this set up was to investigate whether the increase of the itaconic acid concentration (from 19 mM to 200 mM) would trigger higher uptake of itaconic acid at pH 2.5.

The first steady state in experiment C is similar to the first steady state of experiments A and B; this is validated by the comparable data on offgas profiles, biomass concentration, and β ratios. After the first steady state, xylose was fed at the same concentration of 45.6 mM, but now together with itaconic acid which was increased from 100 mM (second steady state) to 200 mM. The last condition however (200 mM), was not considered further for biomass specific rate analysis or transporter calculations, as a steady state was not obtained. Although we did not consider this last condition further, the measured concentrations can be found in the appendix (Table S5.3.).

Table 5.5. Concentrations of residual biomass itaconic acid and xylose; biomass specific net conversion rates, respiratory quotient and ratio β of steady state chemostat cultivations in strains *A. niger* NW185 (upper panel) and *A. niger* C3 (lower panel).

Exp C				Exp D			
45.6mM Xylose pH 2.5				45.6mM Xylose + 100mM itaconic acid pH 2.5			
	Unreconciled	Reconciled	Reconciled		Unreconciled	Reconciled	Reconciled
$C_{biomass}$ (g/l)	3.28±0.05	3.22±0.04	2.97±0.07	2.97±0.07	2.97±0.07	2.97±0.07	2.97±0.07
C^* itaconic acid out (mmol/l)	0.00±0.00	0.00±0.00	97.90±2.45	97.55±1.83	97.90±2.45	97.55±1.83	97.55±1.83
C_{xylose} out (mmol/l)	0.29±0.04	0.28±0.04	8.77±2.22	8.53±1.77	8.77±2.22	8.53±1.77	8.53±1.77
q_{CO2} (mmol/h)/Cmol	83.3±1.2	84.1±1.1	76.2±1.1	76.2±1.1	76.2±1.1	76.2±1.1	76.2±1.1
q_{O2} (mmol/h)/Cmol	-85.6±14.7	-83.6±1.2	-73.7±17.0	-74.8±1.4	-73.7±17.0	-74.8±1.4	-74.8±1.4
$Q_{biomass}$ (mmol/h)/Cmol	92.0±1.3	92.0±1.4	121.3±2.9	121.3±3.0	121.3±2.9	121.3±3.0	121.3±3.0
Q_{xylose} (mCmol/h)/Cmol	17.29±3.60	3.92±1.71	17.29±5.23	17.07±5.05	17.29±5.23	17.07±5.05	17.07±5.05
$Q_{itaconic\ acid}$ (mmol/h)/Cmol	0.00±0.00	0.00±0.00	-0.96±2.97	-1.45±1.98	-0.96±2.97	-1.45±1.98	-1.45±1.98
Q_{xylose} (mmol/h)/Cmol	-35.12±0.07	-35.99±0.08	-41.14±2.54	-41.46±1.95	-35.12±0.07	-41.46±1.95	-41.46±1.95
RQ (R_{CO2}/R_{O2})	0.97±0.17	1.01±0.02	1.03±0.24	1.02±0.02	0.97±0.17	1.03±0.24	1.02±0.02
β ($X_{O2}/X_{xylose}+X_{itaconic\ acid}$)	0.49±0.08	0.46±0.01	0.35±0.08	0.35±0.02	0.49±0.08	0.35±0.08	0.35±0.02

45.6mM Xylose pH 2.5				45.6mM Xylose + 200mM itaconic acid pH 2.5				45.6mM Xylose + 300mM itaconic acid pH 2.5			
	Unreconciled	Reconciled	Reconciled		Unreconciled	Reconciled	Reconciled		Unreconciled	Reconciled	Reconciled
$C_{biomass}$ (g/l)	2.37±0.04	2.29±0.04	2.95±0.12	2.95±0.12	3.39±0.09	3.11±0.08	3.11±0.08	1.75±0.10	1.66±0.09	1.66±0.09	1.66±0.09
C^* itaconic acid out (mmol/l)	17.92±1.04	10.68±0.70	100.57±0.74	100.57±0.74	197.96±0.77	196.28±0.63	196.28±0.63	283.53±2.87	297.04±0.90	297.04±0.90	297.04±0.90
C_{xylose} out (mmol/l)	3.75±0.51	1.60±0.47	0.11±0.01	0.11±0.01	1.50±0.23	1.27±0.22	1.27±0.22	17.93±1.54	15.26±1.04	15.26±1.04	15.26±1.04
q_{CO2} (mmol/h)/Cmol	115.3±1.7	120.8±1.4	75.4±1.1	90.0±1.0	80.9±1.2	90.6±1.0	90.6±1.0	61.6±0.9	66.7±0.9	66.7±0.9	66.7±0.9
q_{O2} (mmol/h)/Cmol	-124.6±19.7	-127.2±1.3	-80.9±14.1	-89.5±0.9	-84.0±13.8	-90.5±0.9	-90.5±0.9	-70.1±27.1	-73.2±0.8	-73.2±0.8	-73.2±0.8
$Q_{biomass}$ (mmol/h)/Cmol	105.2±1.7	105.2±1.8	101.9±6.1	101.9±4.1	105.2±2.9	105.0±2.7	105.0±2.7	105.2±6.0	105.2±6.0	105.2±6.0	105.2±6.0
Q_{xylose} (mCmol/h)/Cmol	15.17±4.54	12.96±3.90	15.17±3.15	13.72±3.22	15.17±3.18	4.89±2.86	4.89±2.86	15.17±6.14	10.00±6.02	10.00±6.02	10.00±6.02
$Q_{itaconic\ acid}$ (mmol/h)/Cmol	22.08±1.28	13.74±0.91	-1.04±0.76	-2.09±0.71	-2.62±0.75	0.75±0.62	0.75±0.62	-9.39±4.81	-14.13±1.50	-14.13±1.50	-14.13±1.50
Q_{xylose} (mmol/h)/Cmol	-51.32±0.63	-56.33±0.61	-38.33±0.04	-43.01±0.05	-37.07±0.20	-40.83±0.22	-40.83±0.22	-43.38±2.57	-50.52±1.83	-50.52±1.83	-50.52±1.83
RQ (R_{CO2}/R_{O2})	0.92±0.15	0.95±0.01	0.93±0.16	0.99±0.01	0.96±0.16	1.00±0.01	1.00±0.01	0.88±0.34	0.91±0.02	0.91±0.02	0.91±0.02
β ($X_{O2}/X_{xylose}+X_{itaconic\ acid}$)	0.35±0.06	0.37±0.01	0.41±0.07	0.40±0.00	0.43±0.07	0.45±0.01	0.45±0.01	0.27±0.11	0.23±0.01	0.23±0.01	0.23±0.01

It was noticed that the residual xylose concentration strongly increased with the increase of the itaconic acid concentration in the fermentor (Fig. 5.5), which indicates that high concentrations of itaconic acid have an inhibitory effect on xylose uptake and/or on the metabolism as a whole (Table S5.3.).

From the offgas measurements (Fig. 5.4.) the same conclusion can be drawn, as the CO₂ production and O₂ consumption rates decreased with increased itaconic acid concentrations in the feed. This can also be seen from the biomass concentration, which decreased due to the decreased substrate uptake. High extracellular itaconic acid concentrations result in high intracellular itaconic acid levels, up to 800 mM (Fig. 5.5.), which somehow interferes with the metabolism of the cells.

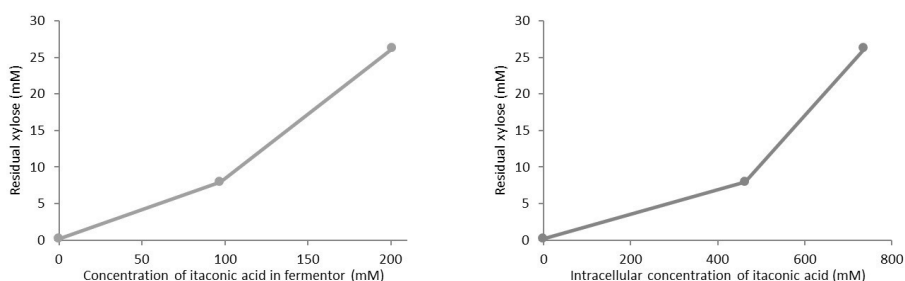


Fig. 5.5. Experiment C: Residual xylose as a function of the itaconic acid concentration in the fermentor (left) and intracellular itaconic acid concentration (right).

The uptake rate of itaconic acid by *A. niger* NW185 at an extracellular acid concentration of 100 mM appeared to be insignificant at pH 2.5 (Table 5.5). However, a high level of intracellular itaconic acid was present, showing that the acid entered the cells and accumulated intracellularly, without being metabolized.

The observation that the itaconic acid uptake rate remains small and insensitive to the extracellular itaconic acid concentration at pH=2.5, provides further evidence that a metabolic pathway for itaconic acid metabolism seems absent in *A. niger* NW185.

5.3.2.3. Experiment D: Itaconic acid production and uptake in *A. niger* C3

In experiment D we used an itaconic acid producing strain (*A. niger* C3) in the same experimental set up as in experiment C, although we increased the concentration of itaconic acid in the feed to a higher final level of 300 mM – fourth steady state.

In the presence of xylose as the only carbon source, the first observation is the production of itaconic acid at a titer of 11 mM. The itaconic acid yield is about $0.2 \text{ mol}_{\text{itaconic acid}}/\text{mol}_{\text{xylose}}$. In addition, the biomass concentration decreased when compared to experiment C, which is to be expected as 23% of the carbon fed ends up in itaconic acid. Itaconic acid production also leads to an increased substrate uptake rate, high energy demand (high q_{O_2}) and an increased consumption of the supplied electrons in catabolism ($\beta=0.58$) - Table 5.5.

The observed itaconic acid production rate of 14 mmol/h/Cmol requires, assuming export by proton antiport and $H^+/ATP=1$, an extra ATP demand of $3 \times 14 = 42 \text{ mmol}_{ATP}/\text{h}/\text{Cmol}$, which is equivalent to an extra oxygen consumption (assuming $P/O = 1.25$) of $42/2.5 = 17 \text{ mmol}/\text{h}/\text{Cmol}$. This could explain partially the very high q_{O_2} in the first steady state of experiment D.

During the first steady state there was significant itaconic acid production while the extracellular concentration of the acid in the chemostat was about 11 mM. However, increasing the extracellular concentration to 100 mM (second steady state) and further to 200 mM (third steady state) completely stopped itaconic acid production, while at the final concentration of 300 mM (fourth steady state) there appeared to be some itaconic acid uptake - Table 5.5.

These low itaconic acid uptake rates are in agreement with the results of experiment C. Most remarkable is the observation that, at higher extracellular itaconic acid concentrations (increase from 11 mM to 100 and 200 mM), the itaconic acid production stops. The fourth steady state shows that in the presence of 300 mM of itaconic acid, the residual xylose level strongly increases, which agrees with the

observed inhibitory effect of high itaconic acid concentrations in the non-producing strain, although in the producer *A. niger* C3 inhibition only occurs at the highest itaconic acid concentration of 300 mM - Table S5.4. The β ratios at 100 and 200 mM of itaconic acid are about 0.42 and are the same as in experiments A and B, and do not indicate uncoupling due to itaconic acid uptake and export.

5.3.3. Transport mechanisms

To characterize membrane transport systems for import of substrates (either glucose, xylose, citric or itaconic acid depending on the considered experiment), in/out ratios were calculated from the measured intra- and extracellular concentrations (Table 5.6).

Table 5.6. In/out ratios estimation from intra- and extracellular concentrations (mM) of glucose, xylose, citric acid and itaconic acid.

Experiment A				
	Glucose pH2.5	Glucose + 18 mM citric acid pH2.5	Glucose + 18 mM citric acid pH5.5	
Glucose	IC	4.57	7.72	2.38
	EC	0.35	0.16	0.15
	in/out ratio	13	48	16
Citric acid	IC	-	34.78	91.07
	EC	-	1.38	15.68
	in/out ratio	-	25	6
Experiment B				
	Glucose pH2.5	Glucose + 22.8 mM itaconic acid pH2.5	Glucose + 22.8 mM itaconic acid pH5.5	
Glucose	IC	5.62	6.69	8.27
	EC	0.13	0.13	0.18
	in/out ratio	44	51	46
Itaconic acid	IC	-	28.70	14.14
	EC	-	19.20	19.43
	in/out ratio	-	1.50	0.73
Experiment C				
	Xylose pH2.5	Xylose + 100 mM itaconic acid pH2.5		
Xylose	IC	20.70	30.00	
	EC	0.28	8.02	
	in/out ratio	73	4	
Itaconic acid	IC	-	462.2	
	EC	-	97.0	
	in/out ratio	-	4.8	
Experiment D				
	Xylose pH2.5	Xylose + 100 mM itaconic acid pH2.5	Xylose + 200 mM itaconic acid pH2.5	Xylose + 300 mM itaconic acid pH2.5
Xylose	IC	27.44	21.13	28.26
	EC	1.60	0.11	1.30
	in/out ratio	17	195	22
Itaconic acid	IC	19	267	478
	EC	10.68	100.77	196.58
	in/out ratio	1.8	2.7	2.4
				0.4

Regarding glucose and xylose transport, it is useful to plot the in/out ratios against the substrate uptake rate (Fig. 5.6.). The values are below the expected equilibrium value of 372 (for proton symport – described in chapter 4) and decrease with increased flux (leading to a higher driving force), as expected.

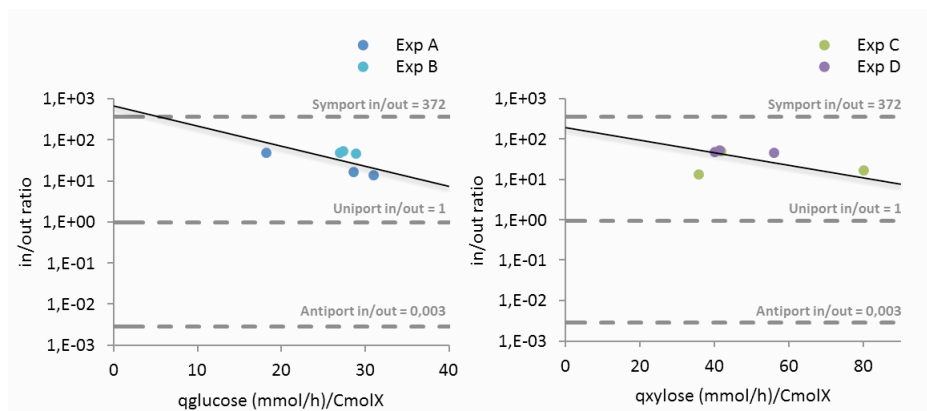


Fig. 5.6. In/out ratios of imported carbon limiting substrates: glucose (left) and xylose (right), against their biomass specific uptake rate (mmol/h)/Cmol_x. Dashed line represents equilibrium in/out ratios of H⁺ symport.

The transport of citric acid was studied in experiment A. Assuming passive diffusion of the undissociated species we calculated the permeability coefficient as $k = 1.9 \times 10^{-7}$ m/s at pH 2.5. This leads to a log k value of -6.7. The octanol/water partition coefficient for undissociated citric acid equals 0.02, leading to a log k_{ow} of -1.7 (INCHEM, 2017).

We can compare the obtained permeability coefficient for citric acid with values for different mono- and di-carboxylic acids (Shah *et al.*, 2016) and a published correlation between Log k and Log K_{ow} for a variety of different compounds (Escher *et al.*, 2008), see Fig. 5.7. It can be seen from this figure that the monocarboxylic acids have higher permeability coefficients than the dicarboxylic acids.

According to the correlation the k -value for passive diffusion of undissociated citric acid (log $K_{ow} = -1.7$) can be estimated to be around 10^{-10} m/s. This is about three

orders of magnitude smaller than the above calculated value. This would indicate that citric acid uptake does not occur by passive diffusion of undissociated acid only, but could be mediated by a transporter as well. The most abundant dissociated species of citric acid at pH 2.5 is the mono anion H_2A^- (19 %), while at pH 5.5 the most abundant species are H_2A^- (14 %) and HA^{2-} (76 %). These are therefore candidate species to be transported by a protein.

The total acid in/out ratio's at equilibrium for the transport of these species are listed in Table 5.2. Comparing the obtained in/out ratio of 25 at pH 2.5 (Table 5.6.) with the theoretical in/out ratios for the species H_2A^- (Table 5.2.), a possible import mechanism could be a proton antiporter of H_2A^- .

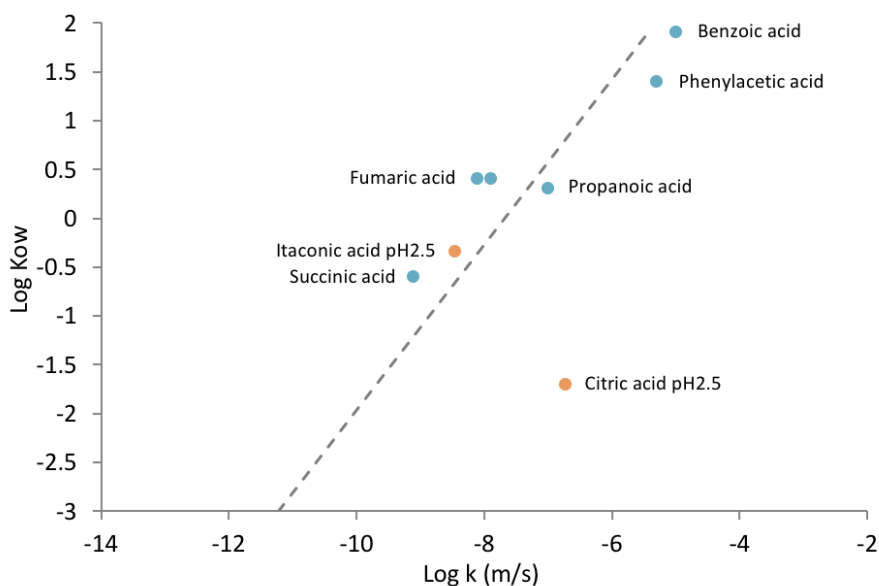


Fig. 5.7. Permeability coefficient (Log k, k is in m/s) with the water octanol partition coefficient (Log kow) for benzoic acid, phenylacetic acid, propanoic acid, fumaric acid, and succinic acid (in blue) - data retrieved from Shah, 2016; in comparison with citric acid and itaconic acid in this study (in orange).

The itaconic acid uptake rates calculated from the reconciled data vary a lot and show little relation to the pH and extracellular itaconic acid concentration. This is caused by the fact that probably *A. niger* lacks the pathway to metabolize itaconic acid.

However, Table 5.6 shows that in absence of extracellular itaconic acid, the intracellular itaconic acid is absent and in the presence of extracellular itaconic acid at pH = 2.5, high intracellular levels of itaconic acid are found.

This shows that itaconic acid is transported over the membrane, but probably is not metabolized. From the intracellular itaconic acid levels, an uptake rate can be calculated as well as a k value, assuming passive diffusion (Fig. S5.8). This gives $k = 3.5 \times 10^{-9}$ m/s, or $\log k = -8.5$ for itaconic acid which has an octanol/water coefficient partition of $k_{ow} = 0.46$, or $\log k_{ow} = -0.34$ (Verviers, 2012). Fig. 5.7 shows that this result is not far from the correlation, thus, passive diffusion of itaconic acid is a possible import mechanism.

Table 5.6 (experiments B and C) shows that at pH=2.5 the in/out ratios of itaconic acid are in the range 1.5 to 4.8 which is very far away from the equilibrium ratio for passive diffusion of the undissociated acid (Table 5.2) indicating the import is diffusion limited.

In experiment D an itaconic acid transporter was present which should facilitate the export of the produced itaconic acid. Comparing the out/in ratio of itaconic acid (first steady state) of $1/1.8 = 0.56$ (Table 5.6) with the possible export mechanisms (Table 5.2), it is clear that a proton antiport mechanism of the fully dissociated species with a maximal out/in ratio of 4 can act as the exporter. As above discussed, this transport mechanism represents substantial energy load (3 ATP per mol of itaconic acid). Moreover, because of the reversibility, it can be understood that production changes to zero at high extracellular itaconic acid levels.

Finally, the metabolite analysis (Fig. S5.3 to S5.6) shows that in experiment D (compared to A-C), very high levels of other dicarboxylic acids (succinic, fumaric and malic) occur, indicating that the itaconic acid transporter, implemented in strain C3,

may be a general dicarboxylic acid transporter. More detailed analysis can be found in the supplementary material.

5.4. Conclusions

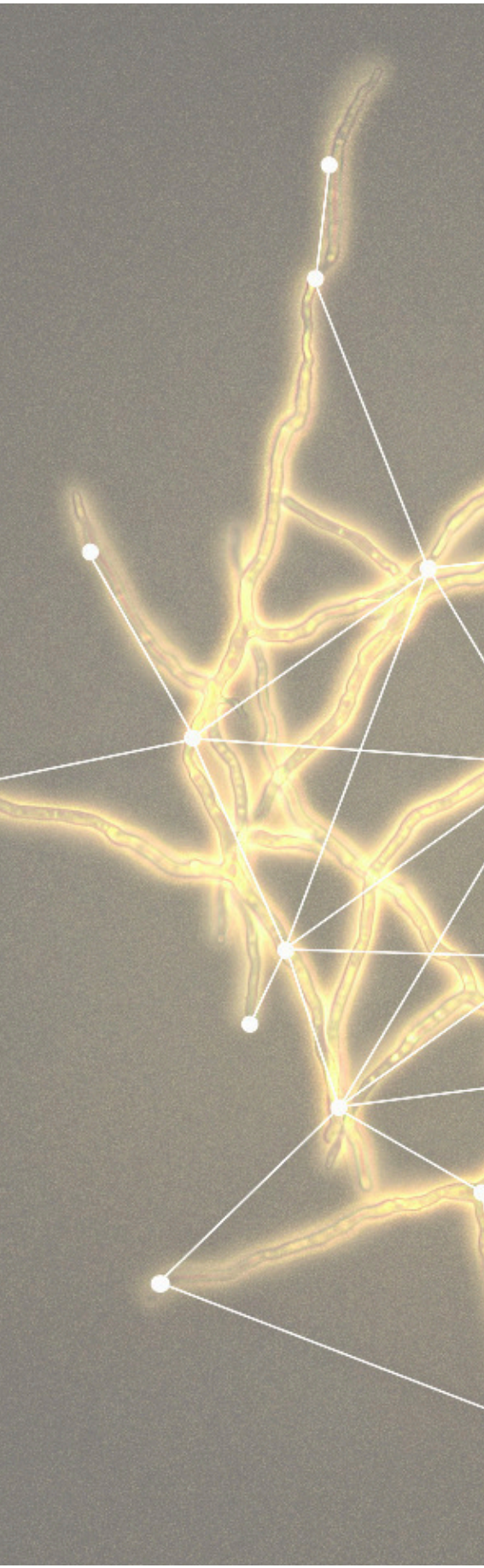
Continuous cultivation of *A. niger* enables fundamental studies on this cell factory, such as the study and understanding of its substrate and product transport mechanisms, in order to improve/develop industrial processes.

From four different chemostat set ups we studied the transport of citric and itaconic acid at low and high pH and compared producing and non-producing itaconic acid strains at high extracellular concentrations of the acid. We observed that citric acid uptake was much higher at pH 2.5 when compared to pH 5.5 (Exp A), which would indicate that the uptake was through passive diffusion of the undissociated acid. However, the calculated permeability coefficient appeared to be much higher than expected from the octanol/water partition coefficient, indicating the presence of another transport mechanism. Uptake of itaconic acid, on the other hand, was low both at pH 2.5 and 5.5 (Exp B).

Additionally, the production rate of itaconic acid decreased at higher intracellular itaconic acid concentration. We concluded that at low pH and high itaconic acid concentrations (Exp C and D), passive diffusion is most likely the import mechanism in *A. niger*.

In addition, the transporter engineered in *A. niger* C3 is acting as a A^{2-} proton antiporter in the production phase of experiment D. The production showed a yield of about 0.2 mol/mol and a $q_{\text{itaconic acid}} = 14 \text{ mmol/h/Cmol}$. From observed extracellular accumulation of other dicarboxylic acids, it follows that the transporter seems a general dicarboxylic acid transporter.

Finally, regarding the probable transport mechanisms acting on the uptake of glucose and xylose, a proton symporter appeared to be the most plausible mechanism in both cases, in agreement with previous findings.

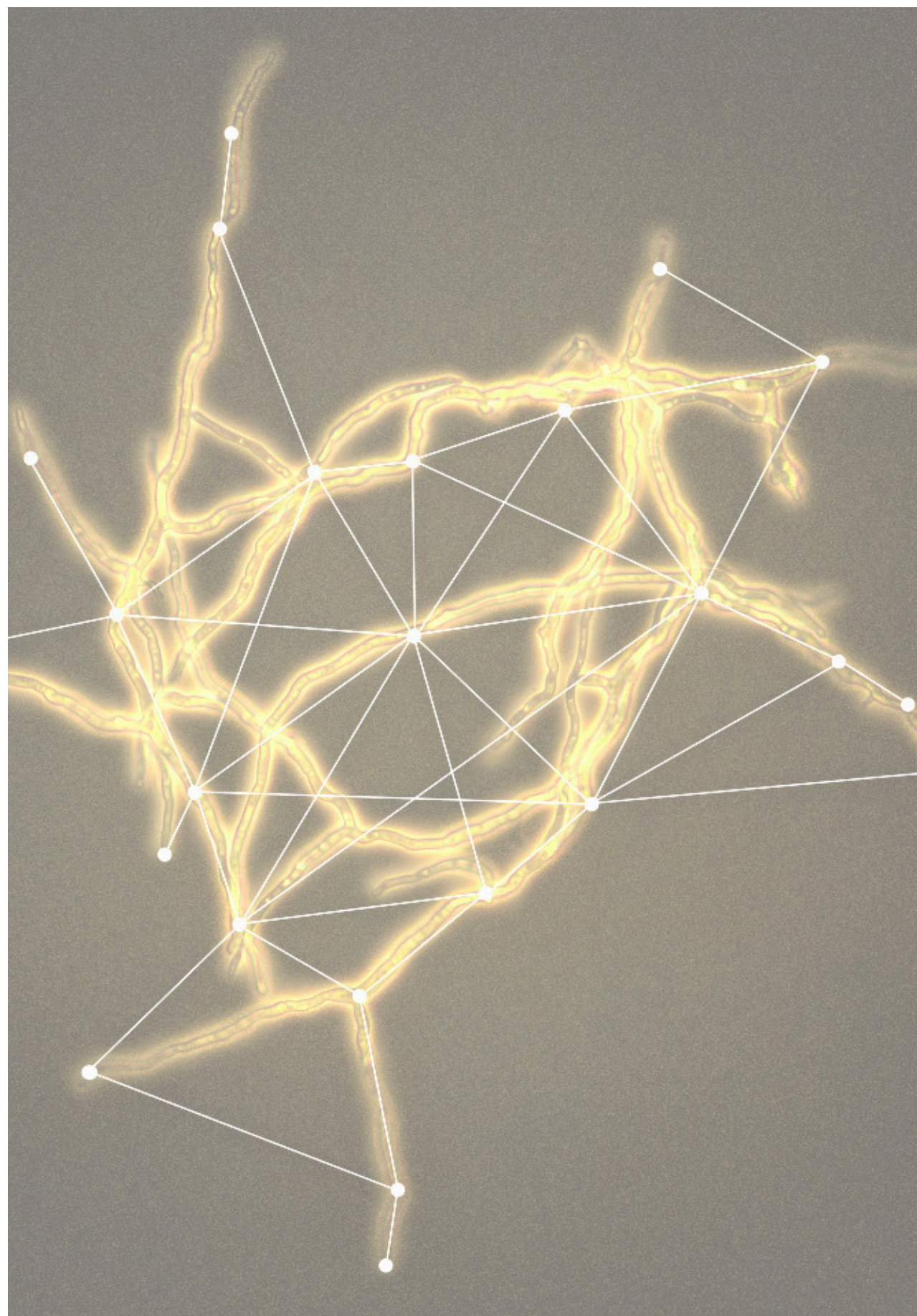


*In this chapter, by the use of a metabolomics approach and a dynamic pulse experiment, we disclose the function of a putative transporter of *Rhizopus delemar*, which was overexpressed in *A. niger*.*

Chapter 6

A metabolomics study in *Aspergillus niger* reveals a putative amino acid transporter

This work was done in collaboration with Wageningen University, and partly published as Odoni *et al.* 2017



Abstract

Together with metabolic engineering approaches, metabolomics studies are a powerful tool in the characterization of microbial processes. *Aspergillus niger*, as a cell factory for the production of organic acids like fumaric acid, requires efficient import and export mechanisms for substrate and product respectively. With help of quantitative metabolomics tools and dynamic experiments, we aimed to disclose the function of a putative fumaric acid transporter (*fumT*) isolated from *Rhizopus delemar*, which was overexpressed in *A. niger*. It was found that under aerobic xylose-limited continuous cultivation, amino acids were imported into the cellular space in the mutant strains which carry *fumT*. From the metabolomics analysis and an amino acid pulse experiment, we hypothesized that this transporter might be a high affinity general amino acid permease using a proton symport system.

Keywords

Aspergillus niger, chemostat pulse, rapid sampling, amino acid, transporter

6.1. Introduction

The use of *Aspergillus niger* for production of organic acids (like citric and glutamic acids) and enzymes (glucoamylases and hemicellulases) is a well-known industrial application (Kubicek, Punt, & Visser, 2010; de Vries, Visser, Ronald, de Vries, R., & P., 2001; Pedersen, Beyer, & Nielsen, 2000).

Additionally, this organism is known to be a well suited host for production of heterologous proteins (Punt *et al.*, 2002). Recently, production of other organic acids such as itaconic acid was accomplished in *A. niger* by overexpressing cis-aconitate carboxylase from *Aspergillus terreus* (van der Straat *et al.*, 2013). Considering the capacity of *A. niger* to produce citric acid and its tolerance to low pH, it would in principle be a suitable host for the production of such other organic acids.

An important aspect in the metabolic engineering of *A. niger* for the overproduction of organic acids is to realize efficient import of the substrate into and export of the produced acid from the cells. Unfortunately, little is known about transport systems in *A. niger*, as discussed extensively in chapters 4 and 5. For this reason, and aiming for the possible production of fumaric acid and its efficient export in *A. niger*, the potential of another filamentous fungus, *Rhizopus delemar*, was considered.

The industrial production of fumaric acid in *R. delemar* (former *R. oryzae*), dates from 1989, when duPont patented a fermentation process for the production of fumaric and other carboxylic acids by dissolved oxygen control (Lorraine and Thomas, 1989). Nevertheless, *R. delemar* has disadvantages as a production host in large scale fermentations, which is related to the high broth viscosity (Zhou *et al.*, 2000).

That said, studies on transport systems which aim at improved industrial productivities, are our research objective. To achieve fumaric acid production in *A. niger* (or other organisms), its exporter needs to be identified. In this study we investigated a putative fumaric acid transporter (*fumT*) obtained from the natural producer *R. delemar*. This transporter was then expressed in *A. niger*. By using an

homogeneous and pellet-free continuous cultivation protocol, as well as a metabolomics analytical platform previously optimized (Lameiras *et al.*, 2015), we provide insight on the function of this putative fumaric acid transporter.

6.2. Materials and Methods

6.2.1. *R. delemar* growth conditions and RNA sequencing

Pre-cultures of *R. delemar* ATCC 20344 were grown in shake flasks on a chemically defined medium containing 1% (w/v) D-glucose, 0.21% (w/v) urea, 0.06% (w/v) KH_2PO_4 , 0.05% (w/v) $\text{MgSO}_4 \cdot 7\text{H}_2\text{O}$ and 0.0018% (w/v) $\text{ZnSO}_4 \cdot 7\text{H}_2\text{O}$. Approximately 10^6 spores/mL were inoculated in 1 litre Erlenmeyer flasks containing 500 ml of pre-culture medium and cultivations were carried out at 35°C and 250 rpm for 24 hours. Subsequently the obtained mycelium (≈ 25 g of wet biomass) was washed with demineralized water and transferred to production medium, containing 10% (w/v) D-glucose, 0.06% (w/v) KH_2PO_4 , 0.05% (w/v) $\text{MgSO}_4 \cdot 7\text{H}_2\text{O}$, 0.0018% (w/v) $\text{ZnSO}_4 \cdot 7\text{H}_2\text{O}$, and 1% (w/v) CaCO_3 (used as a neutralizing agent). Batch fermentations were performed at 35°C and 600 rpm in 2.5 litres fermentors (Applikon, Schiedam, the Netherlands), with a working volume of 1.75 litres. Before inoculation, 85 μL antifoam 204 (Sigma Aldrich) were added to each fermentor. The fermentation medium was gassed with either with air (aerobic condition) or N_2 gas (anaerobic condition) at a gassing rate of 1.75 l/min and pH 7.

6.2.1.1. RNA seq and quality check

RNA extraction of *R. delemar* ATCC 20344 was performed by submerging frozen mycelium (≈ 100 mg) in 1 ml of Trizol reagent in a 2 ml tube, prefilled with a mix of glass beads with the following diameters: 0.1 mm (0.37 g), 1 mm (0.25 g) and 5 mm (1 bead). Mycelium samples were disrupted using a FastPrep-24 Instrument (MP Biomedicals). After disruption, 200 μL of chloroform were added and the mix was homogenated for 10 seconds. The mix was poured into phase-lock gel tubes (2 ml), and centrifuged at maximum speed in a table-top centrifuge. The RNA present in the

water phase was purified using the RNeasy Mini Kit (Qiagen), following the manufacturer's instructions. RNA integrity was assessed with an Experion system (Bio-Rad), and only high quality samples (RIN value ≥ 8) were selected for whole transcriptome shotgun sequencing.

Illumina RNA sequencing (RNA seq) using the Casava pipeline version 1.8.2 and subsequent quality analysis of the FASTQ sequence reads was performed by BaseClear (Leiden, the Netherlands). The number of reads obtained was 20'539'199 for the aerobic and 24'519'028 for the anaerobic condition, with an average quality score (Phred) of 37.59 and 37.91, respectively. The raw data has been submitted to the EMBL-EBI database, and can be found under the accession number PRJEB14210.

6.2.1.2. RNA seq data processing

The RNA seq reads were filtered using SortMeRNA v1.9 (Kopylova *et al.*, 2012), cutadapt v1.2.1 (Martin, 2011) and PRINSEQ v0.20.2 (Schmieder and Edwards, 2011). De novo assembly of the reads that passed the quality filtering was performed using the IDBA-UD assembler v1.1 (Peng *et al.*, 2012). Read mapping and transcript coverage calculations were performed using Bowtie2 v 2.2.2 (Langmead and Salzberg, 2012) and BEDTools (Quinlan 2010).

6.2.2. *A. niger* strain construction

The background strain used for the genetic constructions was *A. niger* NW186 (*cspA1* short conidiospores, Δ *argB* arginine auxotrophic, *pyrA6* phosphopantetheine binding, *goxC17* glucose oxidase negative, *prtF28* oxalate non-producing), which is a derivative strain of *A. niger* NW185 (*cspA1* short conidiospores, *fwA1* fawn coloured spores, *goxC17* glucose oxidase negative, *prtF28* oxalate non-producing).

Two transformant strains were constructed. The control strain (872.11emp) was transformed with plasmid pGW635, carrying the *pyrA* gene of *A. niger*. This complements the *pyrA6* transformation marker and restores the uridine prototrophy,

so that it only keeps the arginine auxotrophy (due to the $\Delta argB$ mutation). The other strain was transformed with the plasmid pFB401, carrying both the *R. delemar fumT* transporter coding gene, and the *pyrA* gene of *A. niger*. The construction of the pFB401 plasmid was performed by cloning an *A. niger* codon optimized version of the *fumT* gene in the expression vector pWA423, under the control of the *A. niger xlnD* promoter and terminator. One *A. niger* transformant carrying the empty vector pGW635 and two *A. niger* transformants (T2 and T5) carrying the pFB401 plasmid were selected for the experiments (strains 872.11emp, 872.11T2 and 872.11T5).

6.2.3. Chemostat cultivations

The negative control strain (872.11emp) was first compared to one transformant strain containing the putative fumaric acid transporter (872.11T5) – experiment A; and thereafter compared to another transformant (872.11T2) – experiment B. At the end of experiment B also a pulse experiment was performed (Fig. 6.1.).

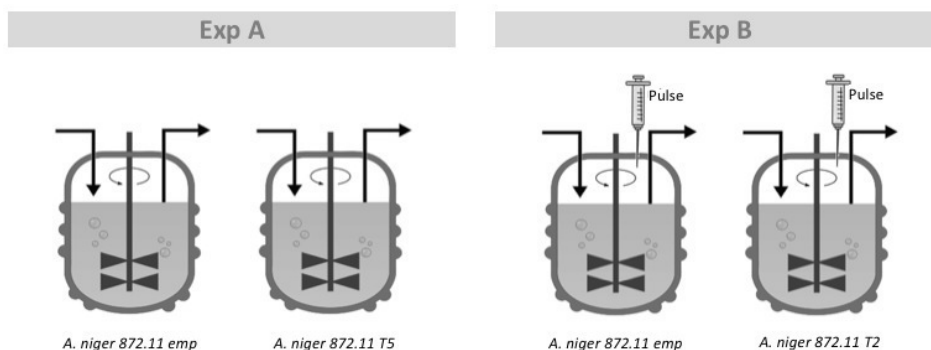


Fig. 6.1. Overview of used strains, chemostat cultivations and dynamic pulse experiments performed in both experiments A and B.

In all experiments, a 7 litres turbine-stirred bioreactor, with 4.5 litre working volume, was used (Applikon, Delft, The Netherlands). The aerobic bioreactor was set up, inoculated and operated as described in Lameiras *et al.*, 2015. Minimal medium was complemented with 38 mM of xylose as a substrate (because the heterologous

transporter is xylose induced). The temperature and pH were 30.0 ± 0.1 °C and 3.0 ± 0.1 respectively. The applied dilution rate was 0.05h^{-1} .

Continuous cultivation was started in the late exponential phase of the batch culture, approximately 100 hours after inoculation, by starting the medium feed.

6.2.4. Sampling and analytical procedures during steady state

When steady state was reached (after five residence times), at least 6 samples were taken for quantification of cell dry weight, 3 samples for concentrations of intra and extracellular compounds, and 3 samples for filtrate TOC (total organic carbon) content.

Biomass dry weight was determined by filtration over glass fiber filters (47 mm, type A/E, Pall, USA), subsequent washing with water and drying at 70°C until constant weight. All samples were analysed in triplicate.

Filtrate samples were obtained by quickly (within 3 s) withdrawing 5 ml of broth, via the over-pressure on the fermentor, into a syringe containing cooled steel beads (-20 °C) to bring the sample temperature down to 0°C, within a fraction of a second (Mashego *et al.* 2003). The cool filtrate was then immediately pressed through a 0.45 µm cartridge filter (Millex-HV durapore PVDF membrane) into a sampling tube, which was directly frozen in liquid nitrogen.

In addition, for the metabolome analysis, intracellular samples were obtained by rapid sampling at -20°C in a 40% (v/v) methanol/water quenching solution, followed by a two-step washing procedure. The protocol is described in Lameiras *et al.*, 2015. A factor of 1.2 ml intracellular volume/g dry weight was used to calculate intracellular concentrations from the extracted amounts of metabolites (Ruijter and Visser, 1996).

Both intra- and extracellular concentrations of the metabolic intermediates from glycolytic, TCA and PPP pathways and amino acids, were measured by isotope dilution mass spectrometry (LC-IDMS/MS and GC-IDMS) according to the protocols of van Dam *et al.* 2002, de Jonge *et al.* 2011 and Cipollina *et al.* 2009.

The total organic carbon content of the filtrate samples was quantified with a total organic carbon analyser (type TOC-L, Shimadzu, Kyoto, Japan). With this method, both total carbon (TC) and total inorganic carbon (TIC) were measured. The latter representing the content of dissolved carbon dioxide and carbonate acid salts. Subtracting the inorganic carbon from the total carbon, yields the TOC of the filtrate.

6.2.5. Balances, biomass specific rates and data reconciliation

Using steady state mole balances, the rates of substrate (R_s), biomass (R_x), carbon dioxide (R_{CO_2}), oxygen (R_{O_2}) and wherein possible by-products (excretion or cell lysis) in the culture filtrate (R_{TOC}) were calculated from the primary measurements of concentrations in gas and liquid phases, as well as gas and liquid flow rates. From these rates, carbon and degree of reduction recoveries (equations 6.1. and 6.2.) were calculated.

$$\text{Carbon recovery (\%)} = \frac{R_x + R_{CO_2} + R_{TOC}}{R_s} \times 100 \quad (6.1.)$$

$$\text{Degree of reduction (\%)} = \frac{Y_x \cdot R_x + Y_{TOC} \cdot R_{TOC} + Y_{O_2} \cdot R_{O_2}}{Y_s \cdot R_s} \times 100 \quad (6.2.)$$

Data reconciliation was applied to obtain the best estimates of the measurements, within their error margins, using the elemental and charge conservation relations as constraints (Verheijen, 2010).

The biomass composition used was the same as measured in Lameiras *et al.*, 2017 for xylose chemostat cultivations. The Y_{TOC} used was the degree of reduction of the biomass, assuming that filtrate TOC generates from biomass lysis.

6.2.6. Pulse experiment

After steady state was achieved, a concentrated pulse containing a mixture of 18 amino acids (alanine, asparagine, aspartic acid, cysteine, glutamine, glutamic acid, glycine, histidine, iso-leucine, methionine, leucine, lysine, phenylalanine, proline,

threonine, tryptophan, tyrosine and valine) was given in both fermentations of experiment B (872.11emp and 872.11T2 strains).

All amino acids were dissolved in 0.1M HCl aqueous solution with exception of asparagine, glutamine and tryptophan which were dissolved in MilliQ water. From this concentrated amino acid solution (Table 6.1.), 40 ml was quickly injected into the bioreactor, bringing the extracellular levels of amino acids roughly ten times higher than the steady-state extracellular concentrations measured before addition.

Table 6.1. Amino acid concentration in pulse solutions (40ml).

	Ala	Gly	Val	Leu	Ile	Pro	Thr	Met	Asp	Phe	Cys	Glu	Lys	Asn	Gln	Tyr	His	Trp	Total added (mCmol/Kg)
Concentration (mM)	19.5	60.5	8.0	10.4	5.1	2.3	10.4	1.1	10.3	4.3	1.0	10.5	10.3	7.8	14.1	5.8	5.2	1.3	
<i>A. niger</i>	±	±	±	±	±	±	±	±	±	±	±	±	±	±	±	±	±	±	6.9
<i>872.11emp</i>	0.7	2.4	0.3	0.2	0.2	0.1	0.4	0.0	0.3	0.2	0.0	0.4	0.4	0.2	0.5	0.4	0.2	0.0	
Concentration (mM)	15.9	48.5	6.5	8.9	4.1	1.9	8.5	0.9	8.2	3.5	0.9	8.4	8.4	6.2	11.2	4.5	4.0	1.0	
<i>A. niger</i>	±	±	±	±	±	±	±	±	±	±	±	±	±	±	±	±	±	±	5.6
<i>872.11T2</i>	2.3	7.2	1.0	1.2	0.6	0.3	1.2	0.1	1.2	0.5	0.1	1.2	1.3	0.9	1.7	1.7	0.6	0.2	

Time zero (steady state) samples were collected before the pulse. After the pulse, samples for extracellular amino acid measurements, using the rapid sampling and quenching protocol described below, were collected with the following time schedule (in minutes): 0.08, 0.17, 0.25, 0.33, 0.42, 0.67, 1, 2, 5, 10, 20, 40, 60, 120, 180, 270 and 330. Intracellular samples were collected less frequently (in minutes): 0.08, 0.25, 1 and 2.

6.3. Results and Discussion

6.3.1. Identification of the putative fumaric acid transporter in *R. delemar*

The *R. delemar* ATCC 20344 strain was cultured in high (aerobic) and low (anaerobic) fumarate production conditions in order to identify candidate fumaric acid exporters, of which we assumed that these would be significantly upregulated under fumaric acid producing conditions. The largest difference in fumarate yield ($\text{g}_{\text{product}}/\text{g}_{\text{substrate}}$) was observed 24 hours after mycelium transfer, being $0.35 \pm 0.06 \text{ g/g}$ in the aerobic condition, and $0.03 \pm 0.02 \text{ g/g}$ in the anaerobic condition (Odoni *et al.* 2017). At this

point, mycelium samples were obtained for RNA isolation and RNAseq analysis. A full description of the RNA seq analysis can be found elsewhere (Odoni *et al.* 2017).

Based on the differential expression profile of *R. delemar* transporter proteins under high and low fumarate producing conditions, we selected a promising candidate (here named *fumT*) as putative fumarate exporter. *fumT* is classified as a member of the sodium-dicarboxylate symporter family (SDF), which belongs to the DAACS (dicarboxylate amino acid:cation symporter) family of transporters. The members of the DAACS family catalyse Na^+ and/or H^+ symport together with: a Krebs cycle dicarboxylate (malate, succinate, or fumarate); a dicarboxylic amino acid (glutamate or aspartate); a small, semipolar, neutral amino acid (Ala, Ser, Cys, Thr); both neutral and acidic amino acids; or most zwitterionic and dibasic amino acids (TCDB.org, 2016).

The *fumT* gene was expressed in *A. niger*, under the control of the strong and inducible promoter *xlnD_p* to verify whether this transporter indeed functioned as a fumaric acid exporter, and if not, which compound(s) it would transport other than fumaric acid.

6.3.2. Chemostat cultivation of *A. niger*

Using the optimized fermentor set up, three transformed strains of *A. niger* (872.11emp (x2), 872.11T2 and 872.11T5) were grown in four aerobic xylose-limited chemostat cultures. All four fermentations were characterized by a very long lag phase of approximately 100 hours preceding the batch phase. This was not observed in previous xylose cultivations with similar strains of *A. niger* (Lameiras *et al.*, 2017) where the lag phase typically took about 30 hours.

The fermentation profiles characterization during steady state can be found in Fig. 6.2. The estimated dilution rate was equivalent for all four fermentations, which enables a direct comparison of strains and experiments. The offgas data obtained during steady state are also shown in Fig. 6.2. Due to anomalies in the offgas analyser, in the strain 872.11T5 of experiment A, the oxygen concentration could not be measured.

For all fermentations, measurements of residual xylose (C_S), biomass concentration (C_X), oxygen and carbon dioxide concentrations in the offgas were performed. In addition, the total organic carbon concentration (C_{TOC}) of the culture filtrate was determined in order to verify whether significant amounts of by-products were excreted.

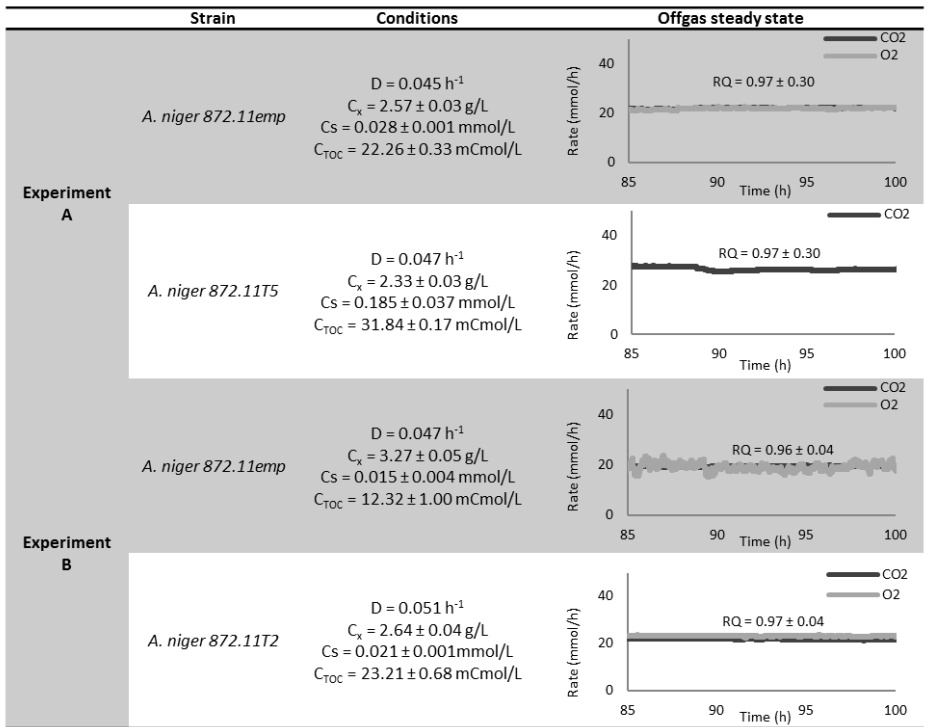


Fig. 6.2. Fermentation characterization and steady-state profiles for different experiments.

The main differences found were in biomass and TOC concentrations. For the control strain of experiment B the steady state biomass concentration was on average 30% higher in comparison with the other three fermentations, while the TOC concentration measured in the filtrate was significantly lower. These two observations could be explained by a lower extent of cell lysis in the chemostat cultivation of the control strain of experiment B.

From the substrate, biomass, CO₂, O₂ and TOC measurements, it was estimated that the recoveries of carbon and degree of reduction were larger than 90% and thus the biomass specific rates were calculated using data reconciliation (Table 6.2.). Due to anomalies in the oxygen measurements of the experiment with transformant 5, it was not possible to calculate the redox balance, nevertheless the carbon balance closed satisfactory (Table 6.2.). Notice that even though oxygen measurements were not available for transformant 5, we have used the reconciled data to estimate RQ values, as well as the redox balance.

Table 6.2. Carbon and redox recoveries, and biomass specific net conversion rates during steady state chemostat cultivations, using xylose as a carbon source.

		<i>A. niger</i> 872.11emp		<i>A. niger</i> 872.11T5	
		Unreconciled	Reconciled	Unreconciled	Reconciled
Experiment A	Carbon recovery (%)	100 ± 2	-	110 ± 7	-
	Redox recovery (%)	102 ± 3	-	-	-
	Respiratory Quotient	0.96 ± 0.05	0.97 ± 0.30	-	0.97 ± 0.30
	Cs (mmol/L)	0.028 ± 0.001	0.028 ± 0.001	0.185 ± 0.037	0.168 ± 0.037
	C _{TOC} (mCmol/L)	22.26 ± 0.33	22.31 ± 0.33	31.84 ± 0.17	31.76 ± 0.17
	D (mCmol/h)/Cmol	45.2 ± 0.1	45.2 ± 0.1	47.0 ± 0.1	47.0 ± 0.1
	q _s (mmol/h)/Cmol	22.0 ± 0.4	21.7 ± 0.3	23.8 ± 0.4	25.1 ± 0.4
	q _{o2} (mmol/h)/Cmol	51.4 ± 16.1	51.1 ± 1.3	-	59.3 ± 1.5
	q _{co2} (mmol/h)/Cmol	53.8 ± 1.6	52.6 ± 1.3	55.3 ± 1.6	61.0 ± 1.5
	q _{TOC} (mCmol/h)/Cmol	10.8 ± 0.3	10.6 ± 0.2	16.8 ± 0.3	17.6 ± 0.3
		<i>A. niger</i> 872.11emp		<i>A. niger</i> 872.11T2	
		Unreconciled	Reconciled	Unreconciled	Reconciled
Experiment B	Carbon recovery (%)	97 ± 4	-	93 ± 5	-
	Redox recovery (%)	98 ± 3	-	95 ± 3	-
	Respiratory Quotient	0.94 ± 0.33	0.96 ± 0.04	0.92 ± 0.26	0.97 ± 0.04
	Cs (mmol/L)	0.015 ± 0.004	0.015 ± 0.004	0.021 ± 0.001	0.021 ± 0.001
	C _{TOC} (mCmol/L)	12.32 ± 1.00	12.90 ± 0.95	23.21 ± 0.68	23.93 ± 0.67
	D (mCmol/h)/Cmol	46.9 ± 0.1	46.9 ± 0.1	50.6 ± 0.1	50.6 ± 0.1
	q _s (mmol/h)/Cmol	18.2 ± 0.4	17.7 ± 0.2	25.7 ± 0.6	23.6 ± 0.4
	q _{o2} (mmol/h)/Cmol	36.8 ± 13.0	35.3 ± 1.1	59.8 ± 16.8	53.4 ± 1.7
	q _{co2} (mmol/h)/Cmol	39.3 ± 1.7	36.7 ± 1.1	64.8 ± 2.9	55.1 ± 1.7
	q _{TOC} (mCmol/h)/Cmol	4.9 ± 0.4	5.0 ± 0.4	13.1 ± 0.5	12.5 ± 0.4

As shown in Table 6.2., and in agreement with previous discussion, the q_{TOC} rate is considerably lower in the control strain of experiment B, suggesting that lysis is the explanation for the lower biomass concentrations in the other cultivations. Another

remarkable difference in the control strain of experiment B is the substrate conversion rate q_s , which is higher in the experiments where lysis is present.

To confirm the different behaviour of the control strain in experiment B, we plotted the biomass specific rates of oxygen consumption, carbon dioxide production and substrate consumption as a function of the true growth rate $\mu = D + q_{\text{TOC}}$ (Fig. 6.3.). Hereby it was assumed that the measured filtrate total organic carbon only consisted of cell lysis products and thus the biomass specific TOC production rate, q_{TOC} , equaled the cell lysis rate. It can be seen from figure 6.3. that the *A. niger* 872.11emp strain from experiment B clearly deviates from the cluster of the three other strains.

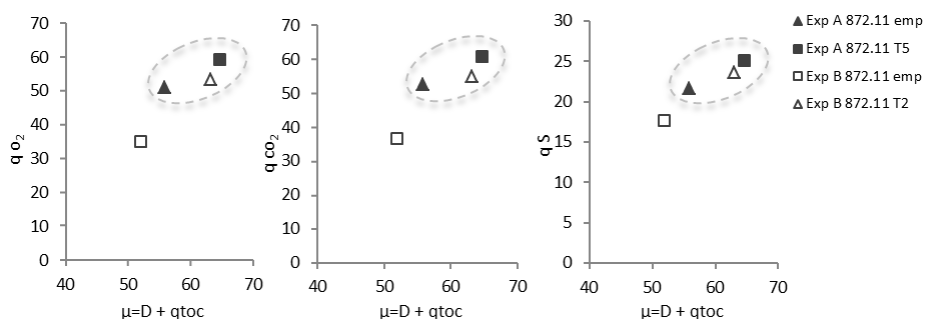


Fig. 6.3. Herbert-Pirt relations for all four chemostat cultivations.

6.3.2.1. Metabolomics

Recalling the initial objective of the expression of *fumT* in *A. niger*, we wanted to confirm whether this putative organic acid transporter would function as a fumaric acid exporter. To this end, we analysed and compared both the endo- and exometabolome of the control and mutant strains during steady state chemostat cultivation.

For all four fermentations, after a steady state was reached, both the levels of intra- and extracellular metabolites were quantified by isotope dilution mass spectrometry.

Initially, using the rapid sampling and quenching protocol, we compared the metabolomics results obtained for both fermentations with the control strain 872.11emp of experiment A and B, which should appear as replicate experiments. The fermentation of experiment B consistently showed much lower extracellular amino acid concentrations (2 to 5 fold, Fig 6.4.). This might have been caused by the lower extent of cell lysis in this cultivation. The same difference was observed for the group of metabolites from glycolytic, TCA and PPP pathways (results not shown). Because only experiments with a comparable extent of cell lysis can be compared, we did not include the results of the control strain of experiment B in the analysis described below.

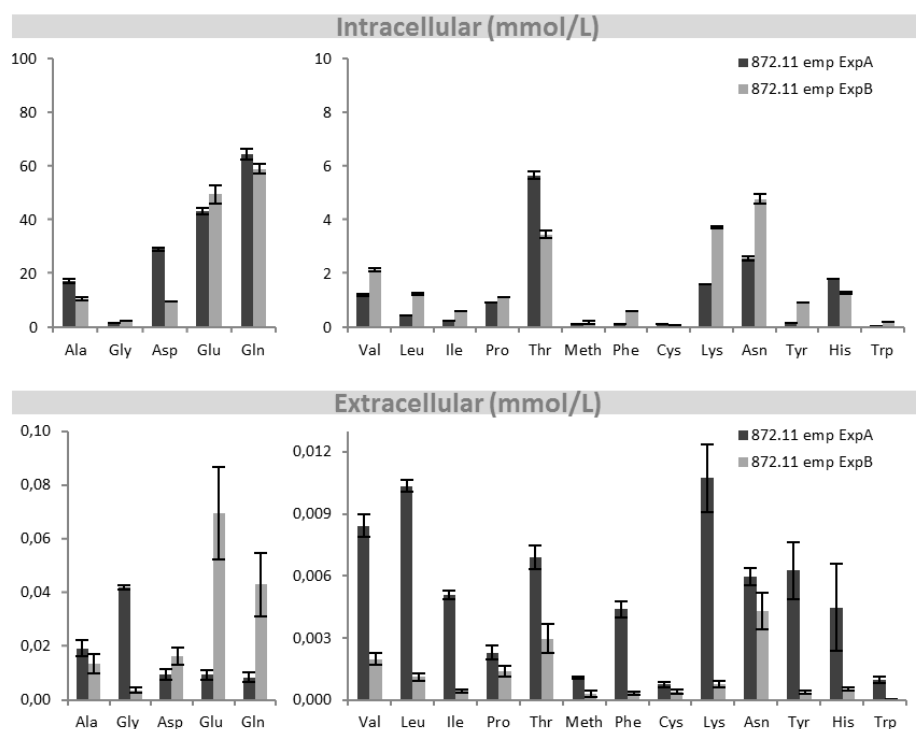


Fig. 6.4. Comparison of amino acid levels in *A. niger* 872.11 + empty in experiment A and B.

Therefore, the results obtained with both mutant strains (from experiments A and B) were compared with the results obtained with the control strain from experiment A, (Fig. 6.5. and 6.6.).

With respect to the intracellular glycolytic, TCA and PPP metabolites (Fig. 6.5.), no significant differences were found for all three strains. This is expected because intracellular fluxes were the same. More specifically, both transformant strains carrying the *fumT* did not show different levels (not inside nor outside) of fumaric acid or other organic acids compared with the control strain, indicating that ability of *fumT* to export organic acids is at least questionable.

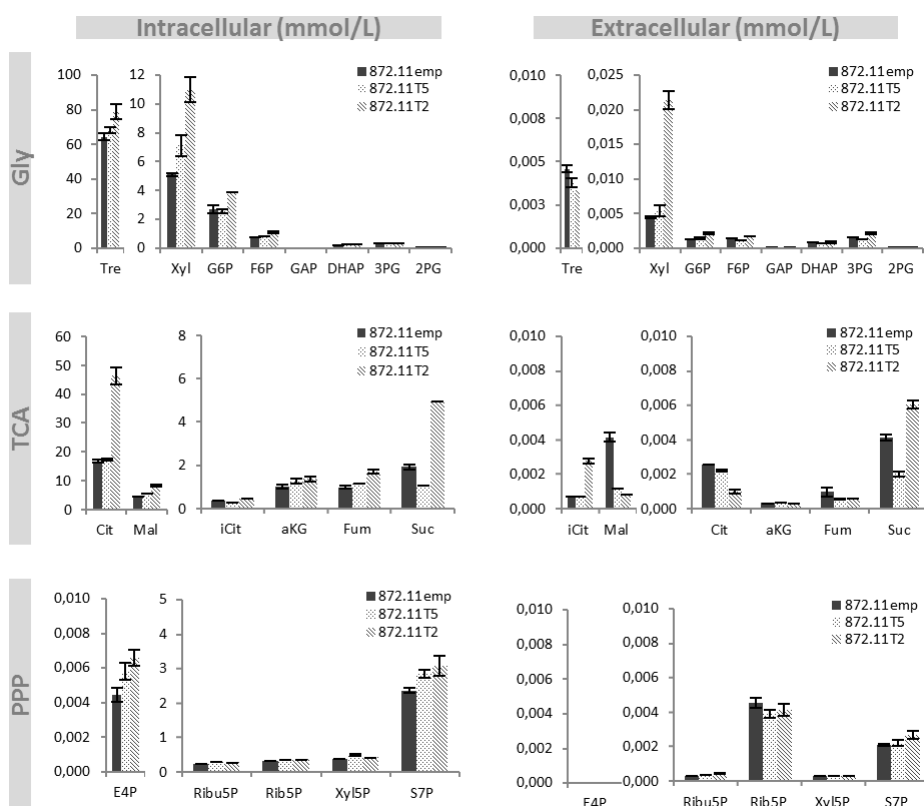


Fig. 6.5. Comparison of glycolytic (upper panel), TCA (middle panel) and PPP (lower panel) metabolites between different strains *A. niger* 872.11emp (experiment A), *A. niger* 872.11T5 (experiment A) and *A. niger* 872.11T2 (experiment B).

Surprisingly, the extracellular levels of free amino acids showed significant differences (Fig. 6.6.). In both mutant strains T2 and T5 containing *fumT*, the extracellular levels of almost all amino acids were considerably lower than for the control strain. In spite of this the intracellular amino acid levels in both strains were very similar (Table 6.2.), which is again to be expected because fluxes in the amino acid pathways are the same.

Comparing both transformant strains (Fig. 6.6.), the intracellular amino acid concentrations in T2 and T5 are nearly the same. Concentration differences between transporters (T2 and T5) can be due to different transporter levels in different transformants.

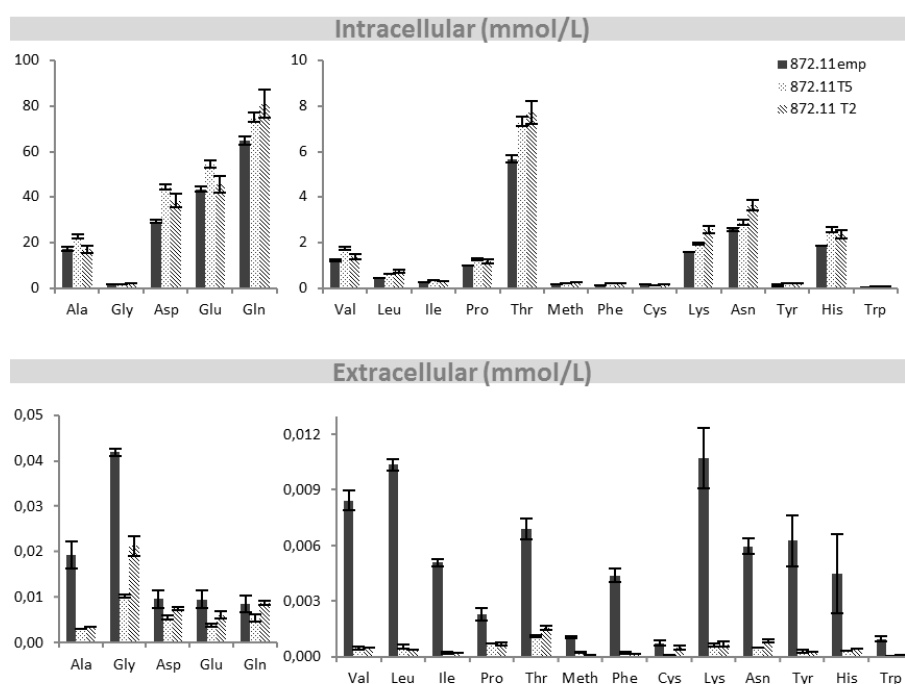


Fig. 6.6. Comparison of amino acid levels between different strains *A. niger* 872.11emp (experiment A), *A. niger* 872.11T5 (experiment A) and *A. niger* 872.11T2 (experiment B).

Considering these differences, we hypothesize that the expressed transporter is a general amino acid permease which imports amino acids into the cell, resulting as a

consequence, in significantly lower extracellular concentrations of amino acids during chemostat cultivation.

From the fact that for both mutant strains the extracellular amino acid concentrations are in the micromolar range, it can be concluded that it must be a high affinity transporter.

6.3.3. Transporter characterization

6.3.3.1. Import ratios of amino acids

To obtain some indication about the mechanism of this transporter, we calculated the in/out ratios of all amino acids for the empty plasmid strain (experiment A) and compared them to the averages of the in/out ratios obtained for transformants 5 and 2 (Table 6.3.).

Table 6.3. Comparison between empty plasmid strain and transformants: intracellular and extracellular concentrations and respective in/out ratios.

	Empty plasmid			Transformants						
	872.11 emp (Exp A)			872.11 T5 (Exp A)			872.11 T2 (Exp B)			Average In/out
	IC (mM)	EC (μ M)	In/out	IC (mM)	EC (μ M)	In/out	IC (mM)	EC (μ M)	In/out	
Ala	17.319	19.359	895	22.665	3.143	7212	17.080	3.585	4764	5988
Gly	1.548	41.923	37	1.827	10.253	178	2.201	21.276	103	141
Val	1.212	8.443	144	1.739	0.483	3601	1.390	0.533	2607	3104
Leu	0.462	10.367	45	0.652	0.562	1161	0.742	0.388	1911	1536
Ile	0.249	5.091	49	0.338	0.220	1535	0.316	0.221	1429	1482
Pro	0.965	2.295	420	1.280	0.787	1626	1.177	0.705	1668	1647
Thr	5.666	6.911	820	7.296	1.130	6453	7.699	1.574	4892	5673
Meth	0.152	1.088	140	0.203	0.271	751	0.277	0.117	2360	1556
Asp	29.259	9.590	3051	44.328	5.625	7880	38.317	7.587	5051	6466
Phe	0.142	4.393	32	0.193	0.223	867	0.211	0.188	1122	995
Cys	0.138	0.758	182	0.099	0.104	945	0.160	0.493	325	635
Glu	43.390	9.528	4554	54.320	3.952	13743	45.607	6.150	7415	10579
Lys	1.624	10.733	151	1.964	0.661	2969	2.564	0.684	3751	3360
Asn	2.565	5.967	430	2.883	0.521	5536	3.636	0.866	4197	4867
Gln	64.620	8.556	7552	74.894	5.454	13733	80.829	8.876	9106	11420
Tyr	0.158	6.275	25	0.231	0.290	799	0.233	0.310	752	776
His	1.848	4.489	412	2.559	0.358	7151	2.359	0.480	4913	6032
Trp	0.040	0.976	41	0.056	0.051	1099	0.050	0.085	585	842

From these calculations it appeared that the in/out ratios for all amino acids are consistently lower for the empty plasmid strain compared to the transformants, confirming its possible role as general amino acid permease. Because in/out ratios are for most amino acids larger than 1000 it must be an active transporter, more specifically a proton symporter, confirming the characteristics of a transporter from the DAACS family (see section 6.3.1.).

6.3.3.2. Amino acid Pulse experiment

To further shed light on the amino acid related properties of the transporter, a short-term pulse experiment was performed. In experiment B, an amino acid pulse was injected in the bioreactor during steady state cultivation of both the empty plasmid strain and transformant 2. The total amount of carbon (in the amino acid pulse) was calculated to be 40-50% in addition to the substrate feed, in terms of carbon uptake rate.

The temporal profiles of oxygen and carbon dioxide before and after the pulse are represented in Fig. 6.7. The pulse clearly resulted in similar temporary decrease in the oxygen and increase in the carbon dioxide levels of the offgas for the mutant strain and transformant, showing metabolism of the supplied amino acids after the pulse, for both strains.

Sampling from a fermentor with the aim to capture highly dynamic changes of intracellular metabolites in a pulse response experiment is achieved by rapid sampling and subsequent fast quenching, as described in the materials and methods section. With this method, samples were collected during a period of five hours after injection of the amino acid pulse.

Fig. S6.1. presents the dynamic of the intracellular and extracellular profiles of the 18 amino acids measured. It is seen that half of the amino acids in both strains have similar amino acid uptake rates which generally slow down at amino acid concentrations of the order 10-100 μ M. However, in the other half of the amino acids,

the empty plasmid strain has a higher uptake rate as the extracellular amino acids levels decrease more rapidly. The above mentioned putative amino acid transporter clearly has no contribution at high amino acid levels, as both strains perform similarly. This suggests that the putative transporter only transports amino acids at a low rate (low capacity). Considering the low extracellular amino acid levels during the preceding steady state chemostat phase of the transformant, the expressed transporter could be of a high affinity and low capacity type.

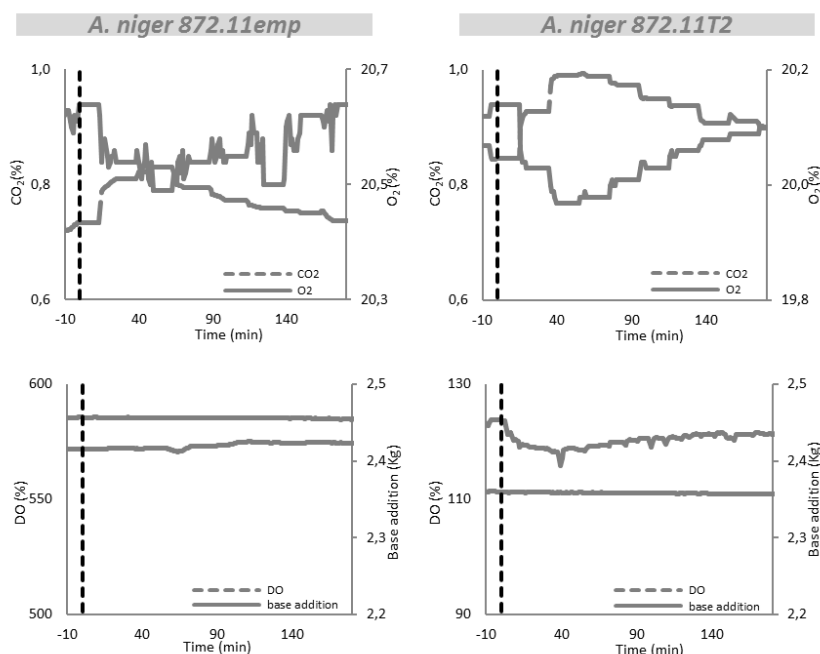
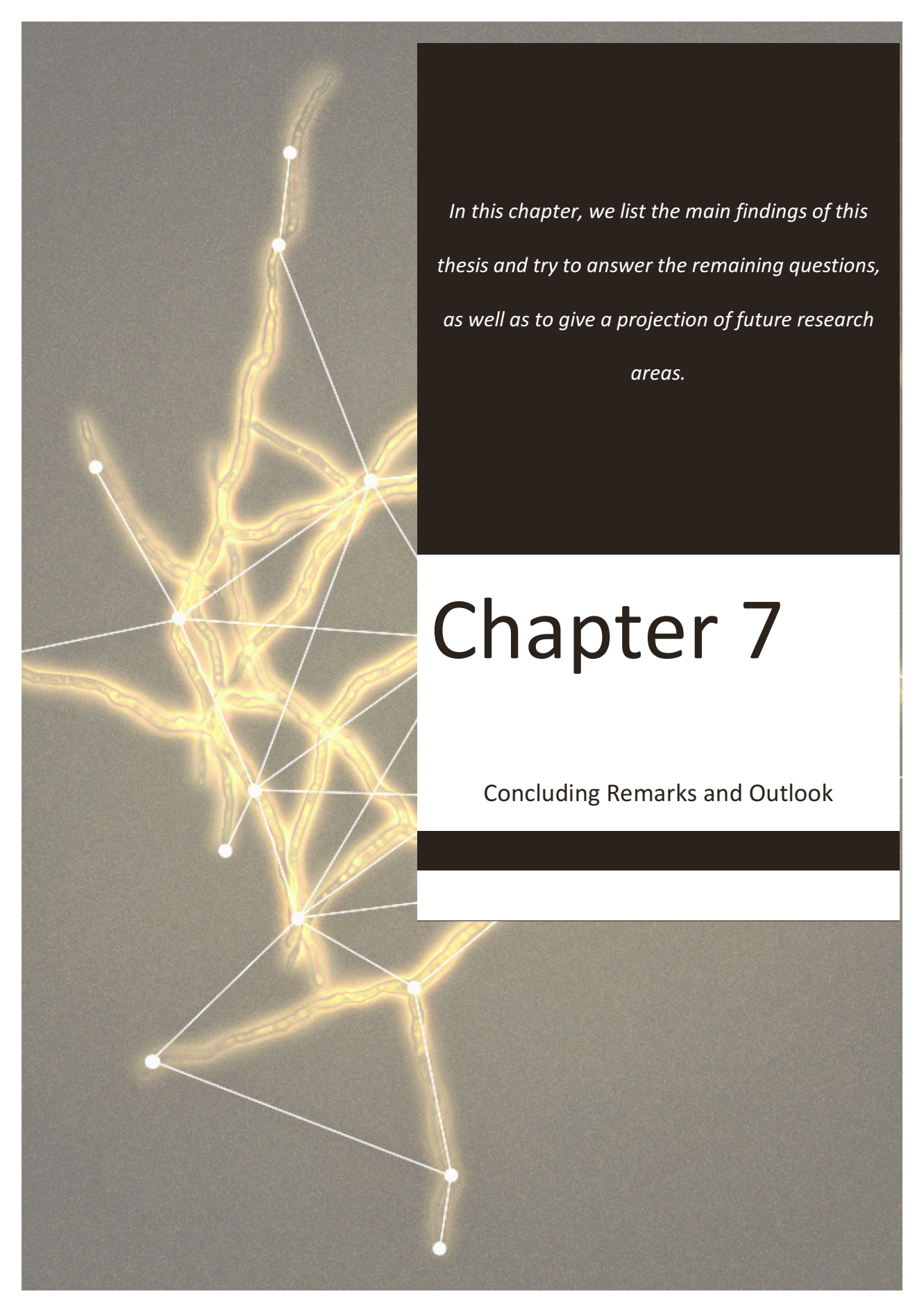


Fig. 6.7. Online data before (steady state) and after pulse experiment in experiment B: *A. niger* 872.11 + empty plasmid (left) and transformant 2 (right). Dotted line indicates moment of amino acid pulse addition.

From the pulse experiment and analysis of Fig. S6.1., the decreasing slope in amino acid concentrations suggests the activity of a low affinity high capacity transporter. This exporter might be acting in the pulse experiment in both strains (872.11emp and 872.11T2), explaining the fast uptake in both strains. Thus, as a hypothesis, the high affinity amino acid uptake transporter expressed, is not evident in this pulse experiment.

6.4. Concluding Remarks

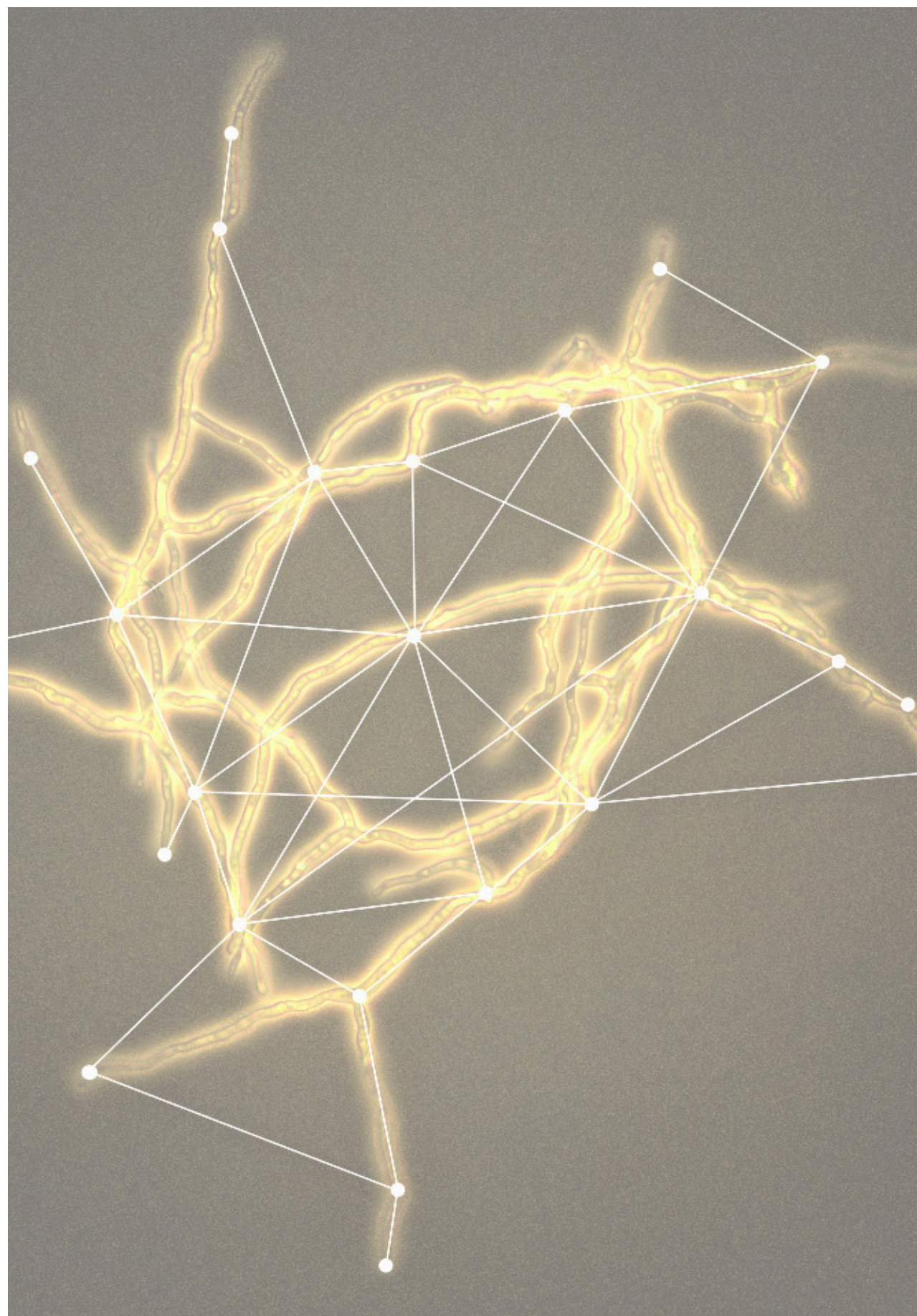
By the use of metabolomics tools and dynamic experiments we have gained information on the function of a putative fumaric acid transporter expressed in *A. niger*. The transporter is not a dicarboxylic acid carrier, but is probably a high affinity general amino acid permease. The putative production of amino acids in *A. niger* can be achieved by the metabolic reprogramming of this filamentous fungi. Nevertheless, here we show the importance of the presence of an efficient transport system, as the intrinsic capacity of a certain organism to excrete the targeted product can become a barrier when improving productivity. Adding up to the performed experiments, it would be necessary to carry on validation experiments and confirm the function of the amino acid transporter.



In this chapter, we list the main findings of this thesis and try to answer the remaining questions, as well as to give a projection of future research areas.

Chapter 7

Concluding Remarks and Outlook



This work represents an effort on the study of a non-conventional organism (i.e. not *Saccharomyces cerevisiae*, nor *Escherichia coli*) aimed at its use as an industrial workhorse for the production of organic acids. This implies a lot of technical challenges and the development of new tools. Nevertheless, one should recognize the necessity of exploring new platforms and the natural advantages of a non-conventional microorganisms such as *Aspergillus niger*.

Throughout this chapter we pinpoint the remaining open questions and different directions for further research, by focusing on five main topics:

- Fermentation technology, quenching and analytical protocols;
- Mycelia heterogeneity, apical growth, lysis and single cell studies;
- Second generation feedstocks;
- Production of organic acids;
- Intracellular and extracellular conditions - Thermodynamics assumptions;

Fermentation technology, quenching and analytical protocols

In chapter 2, using a 7 litres bench scale bioreactor, we have successfully optimized a continuous cultivation at pH 2.5 with a pellet-free and homogeneous *A. niger* mycelia. The most important feature on the chemostat protocol was the implementation of the feed solution along with the air sparger in the bottom of the bioreactor, and thus avoid splashing and wall growth. In addition, we developed a dedicated rapid sampling device for intracellular metabolite analysis, specifically suited for filamentous fungi, which was crucial for the transport studies elaborated in this thesis. However, when proceeding to industrial processes, the scale up would need careful attention and readjustment of these protocols.

In order to predict cellular systems behaviour, quantitative evaluations are required. That being said, in chapter 2 we also focused on developing a rapid sampling and

quenching protocol which we optimized for *A. niger* NW185. For our strain, and for the conditions applied, quenching the cells in a 40% methanol/aqueous solution at -20°C turned out to be optimal. At these conditions leakage of intracellular metabolites was absent and 95 ± 4 % of the metabolome was found back. Nevertheless, different organisms, or even different strains, require different quenching solutions, and therefore, these protocols ought to be validated for other microorganisms/strains. The reason for the variations in the optimal quenching conditions for different microbes is not well known, but most probably related to differences in membrane composition.

Mycelia heterogeneity, apical growth, lysis and single cell studies

A critical assumption we did in this study was to consider homogeneity throughout *A. niger*'s mycelia, while it is known that the secretion of proteins and growth are located at the tips of growing hyphae (apical growth) (Wösten *et al.*, 1991). This leads us to assume that organic acid secretion is probably also site dependent, and concentration gradients of intracellular metabolites throughout the hyphae should not be despised.

In case of single cell studies, this heterogeneity should be taken into account and further investigated. For the very reason that we see heterogeneity in eukaryotic and prokaryotic populations, observations obtained from bulk cultivations will not reveal unknown but interesting mechanisms and thus studies more and more aim at investigating the single cell level (Altschuler and Wu, 2010) to reveal culture heterogeneity.

Another direction for further studies is to investigate cell lysis. Throughout this work, we continuously faced an existing and unknown amount of filtrate (possibly excreted?) carbon which we attributed to cell lysis. What is the reason for the observed lysis which seem to be somehow predetermined and growth rate dependent? Understanding this mechanism with the aim to find ways to minimize cell death and subsequent lysis would increase productivities and decrease costs.

Second generation feedstocks

In many microbial ecosystems, the availability of carbon and energy sources are usually limited, and their uptake capacity and kinetics determine the microbial growth performance. The carbon-limited chemostat cultivations at low dilution rate are therefore resembling these natural environments, and help us to understand microorganisms' intrinsic characteristics. Also, the ability to take up several carbon sources simultaneously is an important asset for microbial fitness and survival.

Following this insight, in chapters 3 and 4 we have studied different carbon sources that can be found in lignocellulosic feedstocks. We obtained insights on the stoichiometry and kinetics of these substrates in single and mixed substrate conditions, and found that in the latter case, some substrates are consumed simultaneously and some sequentially. We also obtained some perceptions on repression systems acting on the uptake of arabinose, galacturonic acid and rhamnose. The stoichiometric and kinetic characterization of growth on different carbon sources, and the role of substrates as repressors or competitors during cultivation, should be included when it comes to designing a fermentation process based on plant waste feedstocks.

To better grasp the repression phenomena at the substrate level, we propose experiments of two substrates at the time. This implies that 15 fermentations are required when studying six substrates. In addition, one should realize the difference between repression and inhibition. In short, repression can be measured by gene expression at the mRNA or protein levels, while inhibition happens at the enzyme level only.

We suggest as follow-up of this work, to test the same six substrates, but in the actual ratios and concentrations as found on lignocellulosic feedstocks. Keeping in mind the fact that their proportion also changes seasonally, makes this a rather complex study to tackle. Finally, and ideally, one should substitute synthetic substrates for real lignocellulosic waste crops in a substrate uptake study.

Production of organic acids

Nine of the twelve building blocks identified by the US Department of Energy, are organic acids (Werpy *et al.*, 2004), which illustrate the industrial relevance of these molecules in the last decade. However, large scale fermentative production has seldomly been applied, as these processes are economically still not competing with current petro-chemical production routes of organic acids. Future metabolic engineering strategies for improvement of production of organic acids in *A. niger* should focus more on quantitative proteomics and transcriptomics studies, in order to establish a suitable platform for investigation of transport systems.

In chapter 5 we have seen that itaconic acid can be taken up in *A. niger*, but it is unknown how it is metabolized (if even possible). Most probably this itaconic acid is accumulated rather than assimilated. Nevertheless, we suggested a plausible metabolic route which is known for certain bacteria, that for *A. niger* still needs to be confirmed. For that purpose, we suggest ^{13}C labelled experiments where labelled itaconic acid would be fed to the culture, followed by a full scan analysis of the central carbon intermediates.

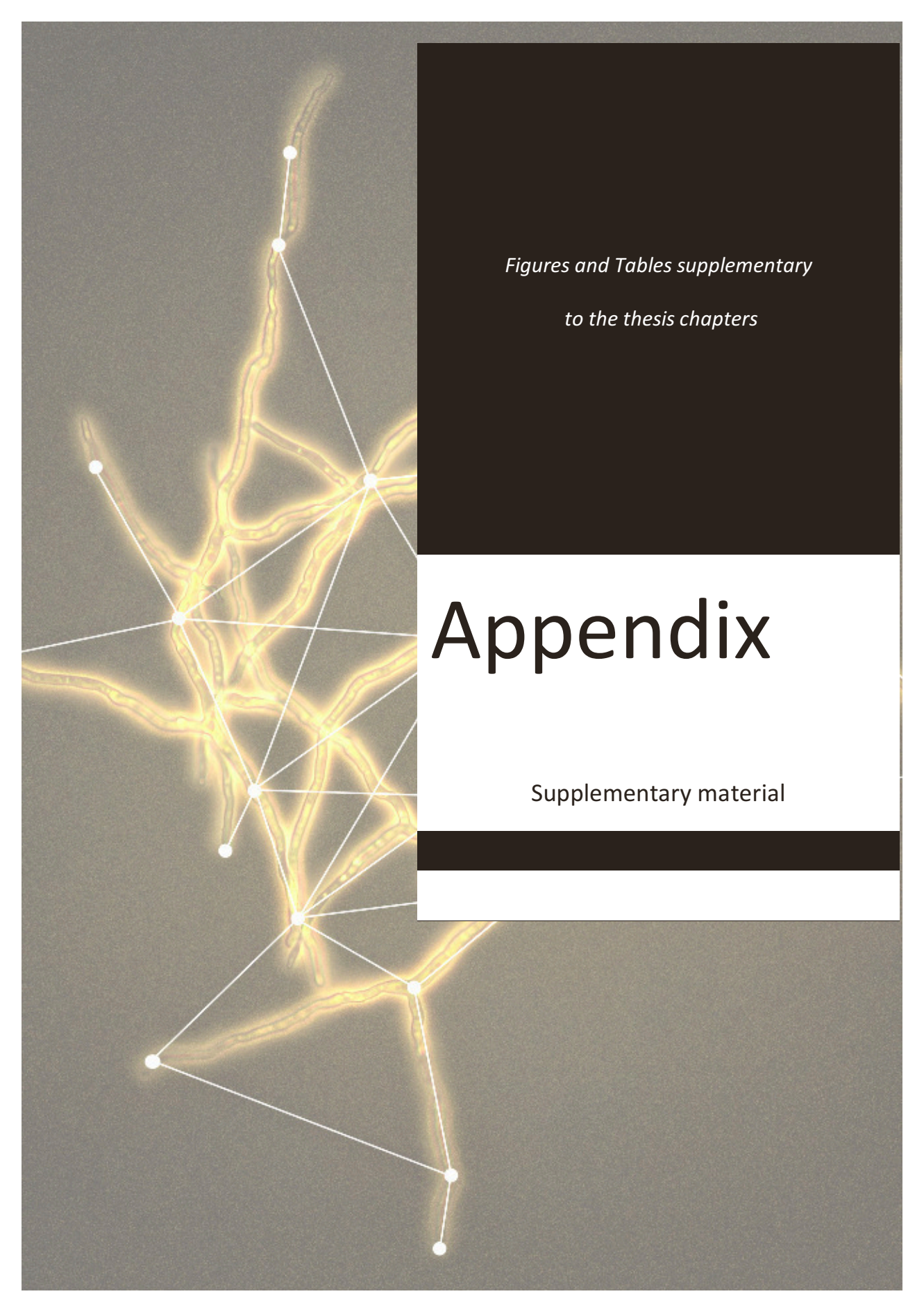
As discussed both in chapters 1 and 5, a low pH is preferred for organic acid production, however one should be aware that passive diffusion can happen under these conditions and therefore quantification of futile cycling is extremely relevant to improve yield and productivity. As we have seen in chapter 5, permeabilities were shown to be very low, indicating that a protein acting as a transporter is required. In addition, as we have been discussing throughout this thesis, one important challenge for organic acid production is implementing an efficient transport protein for product export in order to achieve high out/in ratios. Studies on the molecular biology and the use of genetic engineered strains with efficient proton antiport mechanisms are paramount of this approach.

Intracellular and extracellular conditions - Thermodynamics assumptions

For the investigation of transport systems and determine out/in (or in/out) ratios, it is very important to define the intracellular and extracellular conditions of the cell. Since these conditions cannot be known in all details however, one should be aware of the limitations/weaknesses of the thermodynamic assumptions.

The proton motive force and intracellular pH are here assumed to be homeostatic at 0.15V and 7.6 respectively. In case of the pmf this is not constant throughout the membrane, nor independent of the extracellular pH. Therefore, studies for *in vivo* determination of the proton motive force are required. With respect to the intracellular pH, it is expected that at low extracellular pH, its value is expected to be lower. However, in this thesis (and in other studies), independently of the extracellular pH, a constant intracellular pH is assumed. Therefore, efforts for better estimations and *in vivo* measurements of these values are a subject for further investigation. It should be borne in mind that variations on both pmf and pH_{in} affect thermodynamically calculated in/out ratios.

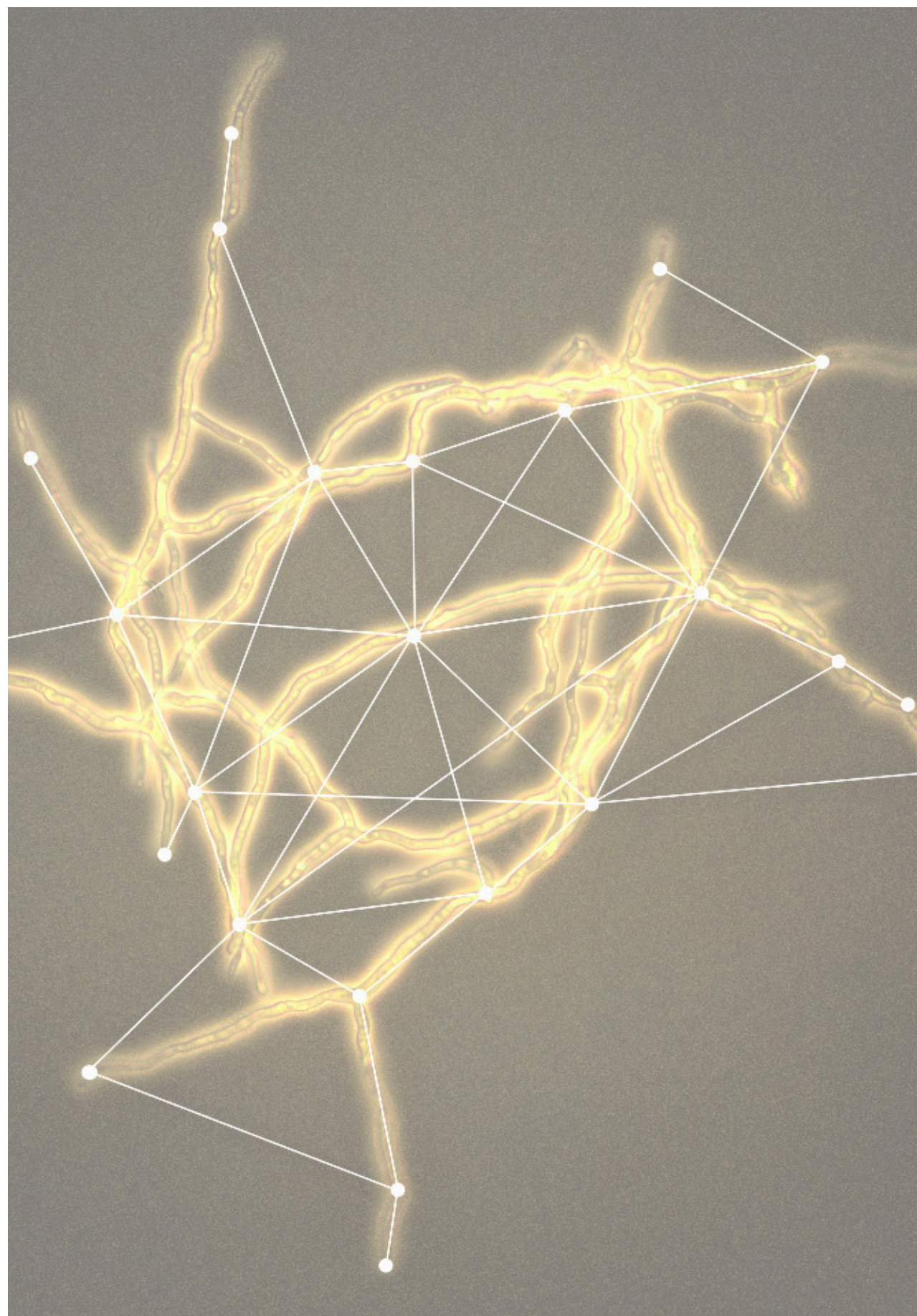
Another subject for further research is cellular compartmentalization. In this study we determine the out/in ratios to have insights on the transport mechanism, however we did not consider compartmentalization, neither metabolic pools.



*Figures and Tables supplementary
to the thesis chapters*

Appendix

Supplementary material



Appendix Chapter 1

Citric acid

$$\frac{H_3A}{A} = \frac{1}{1 + 10^{pH_{out}-pka1} + 10^{2pH_{out}-pka1-pka2} + 10^{3pH_{out}-pka1-pka2-pka3}}$$

$$\frac{H_2A^-}{A} = \frac{10^{pH_{out}-pka1}}{1 + 10^{pH_{out}-pka1} + 10^{2pH_{out}-pka1-pka2} + 10^{3pH_{out}-pka1-pka2-pka3}}$$

$$\frac{HA^{2-}}{A} = \frac{10^{2pH_{out}-pka1-pka2}}{1 + 10^{pH_{out}-pka1} + 10^{2pH_{out}-pka1-pka2} + 10^{3pH_{out}-pka1-pka2-pka3}}$$

$$\frac{A^{3-}}{A} = \frac{10^{3pH_{out}-pka1-pka2-pka3}}{1 + 10^{pH_{out}-pka1} + 10^{2pH_{out}-pka1-pka2} + 10^{3pH_{out}-pka1-pka2-pka3}}$$

Itaconic acid

$$\frac{H_2A}{A} = \frac{1}{1 + 10^{pH_{out}-pka1} + 10^{2pH_{out}-pka1-pka2}}$$

$$\frac{HA^-}{A} = \frac{10^{pH_{out}-pka1}}{1 + 10^{pH_{out}-pka1} + 10^{2pH_{out}-pka1-pka2}}$$

$$\frac{A^{2-}}{A} = \frac{10^{2pH_{out}-pka1-pka2}}{1 + 10^{pH_{out}-pka1} + 10^{2pH_{out}-pka1-pka2}}$$

Figure S1.1. Calculation of concentration ratio of charged acid species to total acid.

Appendix Chapter 2

Table S2.1. Parameters of the 43 metabolites identified in the investigated samples.

	Metabolite	Abbr.	PubChem CID	Method	Derivate	Quantification ion ¹² C (precursor/product) [m/z]	Quantification ion internal standard ¹³ C (precursor/product) [m/z]
1	2-phosphoglycerate	2PG	59	Cipollina <i>et al.</i> 2009	4TMS	459.1	462.1
2	3-phosphoglycerate	3PG	724	Cipollina <i>et al.</i> 2009	4TMS	459.1	462.1
3	6-phosphogluconate	6PG	91493	Van Dam <i>et al.</i> 2002	n.a.	275/96.7	281/96.7
4	Ketoglutarate	aKG	51	Cipollina <i>et al.</i> 2009	2TMS 1MOX	304.0	309.0
5	Alanine	Ala	5950	de Jonge <i>et al.</i> 2011	2TBDMS	260.1	263.1
6	Asparagine	Asn	6267	de Jonge <i>et al.</i> 2011	3TBDMS	417.2	421.2
7	Aspartic acid	Asp	424	de Jonge <i>et al.</i> 2011	3TBDMS	418.2	422.2
8	Citrate	Cit	311	Cipollina <i>et al.</i> 2009	4TMS	465.1	471.1
9	Cysteine	Cys	5862	de Jonge <i>et al.</i> 2011	3TBDMS	406.1	409.1
10	Dihydroxyacetone phosphate	DHAP	668	Cipollina <i>et al.</i> 2009	3TMS 1MOX	400.1	403.1
11	Erythrose-4-phosphate	E4P	122357	Cipollina <i>et al.</i> 2009	4TMS 1MOX	357.1	359.1
12	Fructose-6-phosphate	F6P	69507	Cipollina <i>et al.</i> 2009	6TMS 1MOX	459.1	462.1
13	Fructose-1,6-bis phosphate	FBP	10267	Van Dam <i>et al.</i> 2002	n.a.	339/96.7	345/96.7
14	Fumaric acid	Fum	44972	Cipollina <i>et al.</i> 2009	2TMS	245.0	249.0
15	Glycerol-3-phosphate	G3P	754	Van Dam <i>et al.</i> 2002	n.a.	171/78.8	174/78.8
16	Glucose-6-phosphate	G6P	5958	Cipollina <i>et al.</i> 2009	6TMS 2MOX	471.0	475.0
17	Glyceraldehyde-3- phosphate	GAP	729	Cipollina <i>et al.</i> 2009	3TMS 1MOX	400.1	403.1
18	Glucose	Glc	79025	Cipollina <i>et al.</i> 2009	5TMS 1MOX	319.1	323.1
19	Glutamine	Gln	5961	de Jonge <i>et al.</i> 2011	3TBDMS	431.2	436.2
20	Glutamic acid	Glu	611	de Jonge <i>et al.</i> 2011	3TBDMS	474.3	479.4
21	Glycine	Gly	750	de Jonge <i>et al.</i> 2011	2TBDMS	246.1	148.1
22	Histidine	His	6274	de Jonge <i>et al.</i> 2011	3TBDMS	440.3	446.3
23	isocitrate	iCit	1198	Cipollina <i>et al.</i> 2009	4TMS	465.1	471.1
24	isoleucine	Ile	6306	de Jonge <i>et al.</i> 2011	2TBDMS	274.1	279.1
25	Leucine	Leu	74840	de Jonge <i>et al.</i> 2011	2TBDMS	274.1	279.1
26	Lysine	Lys	5962	de Jonge <i>et al.</i> 2011	3TBDMS	431.3	437.1
27	Malate	Mal	525	Cipollina <i>et al.</i> 2009	3TMS	335.0	339.0
28	Methionine	Meth	6137	de Jonge <i>et al.</i> 2011	2TBDMS	320.1	325.1
29	Phosphoenolpyruvate	PEP	1005	Van Dam <i>et al.</i> 2002	n.a.	167/78.8	170/78.8
30	Phenylalanine	Phe	6140	de Jonge <i>et al.</i> 2011	2 TBDMS	336.2	345.2
31	Proline	Pro	145742	de Jonge <i>et al.</i> 2011	2 TBDMS	286.1	291.1

Table S2.1. Parameters of the 43 metabolites identified in the investigated samples (cont.).

	Metabolite	Abbr.	PubChem CID	Method	Derivate	Quantification ion ^{12}C (precursor/product) [<i>m/z</i>]	Quantification ion internal standard ^{13}C (precursor/product) [<i>m/z</i>]
32	Ribose-5-phosphate	Rib5P	21115541	Cipollina <i>et al.</i> 2009	5TMS 1MOX	459.1	462.1
33	Ribulose-5-phosphate	Ribu5P	439184	Cipollina <i>et al.</i> 2009	5TMS 1MOX	357.1	359.1
34	Sedoheptulose-7-phosphate	S7P	165007	Cipollina <i>et al.</i> 2009	7TMS 1MOX	471.1	475.1
35	Serine	Ser	5951	de Jonge <i>et al.</i> 2011	3 TBDMS	390.2	393.2
36	Succinate	Succ	160419	Van Dam <i>et al.</i> 2002	n.a.	117/72.7	121/75.7
37	Trehalose6-phosphate	T6P	122336	Van Dam <i>et al.</i> 2002	n.a.	421.2/78.8	433.2/78.8
38	Threonine	Thr	6288	de Jonge <i>et al.</i> 2011	3TBDMS	404.2	408.2
39	Trehalose	Tre	7427	Cipollina <i>et al.</i> 2009	8TMS	361.1	367.1
40	Tryptophan	Trp	6305	de Jonge <i>et al.</i> 2011	2TBDMS	375.2	386.2
41	Tyrosine	Tyr	6057	de Jonge <i>et al.</i> 2011	3TBDMS	466.3	475.3
42	Valine	Val	6287	de Jonge <i>et al.</i> 2011	2TBDMS	288.1	293.1
43	Xylulose-5-phosphate	Xyl5P	5459820	Cipollina <i>et al.</i> 2009	5TMS 1MOX	357.0	359.0

A**B****Figure S2.1.** *A. niger* wall growth accumulation in the fermentor during fermentation (A) and before cleaning (B).

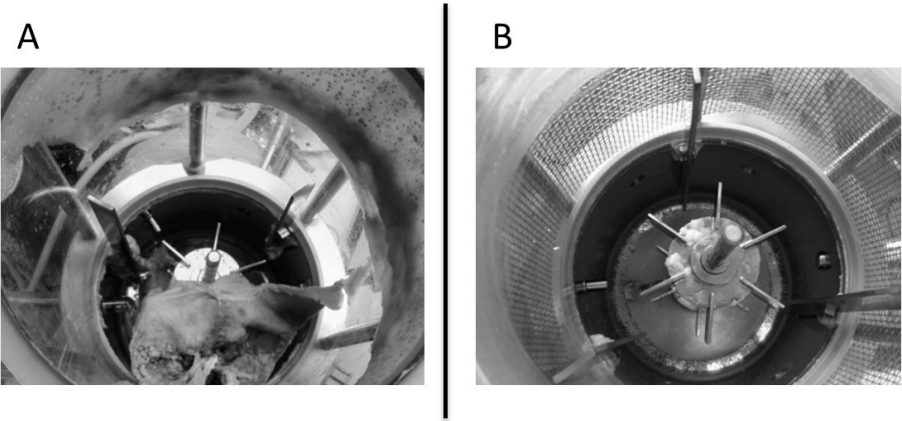


Figure S2.2. Top view of the fermentor. Massive aggregation of biomass with a conventional fermentor set up (A) in comparison to a biofilm-free bioreactor after optimization of the fermentor setup (B).

Table S2.2. Biomass concentration.

Dilution rate (h ⁻¹)	C _x (g _{DW} /l _{broth})	C _{x,out} (g _{DW} /l _{broth})
0.045	3.04 ± 0.03	3.03 ± 0.03
0.087	3.68 ± 0.04	3.57 ± 0.05

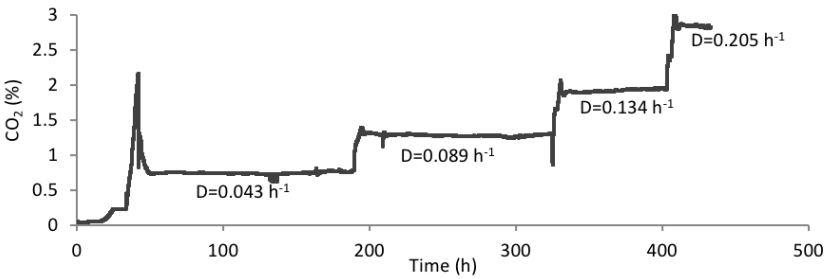


Figure S2.3. CO₂ profile during chemostat phase: consecutive steady states.

Table S2.3. Average biomass elemental composition of *A. niger*
(calculation based on three different chemostats).

	C (mol _c /Cmol _x)	H (mol _H /Cmol _x)	N (mol _N /Cmol _x)	O (mol _O /Cmol _x)	P (mol _P /Cmol _x)	MW
Chemostat 1 D=0,05h ⁻¹	1.0000	1.8062	0.1125	0.6624	0.0080	26.2529
Chemostat 2 D=0,05h ⁻¹	1.0000	1.8249	0.1120	0.6594	0.0074	26.1982
Chemostat 2 D=0,10h ⁻¹	1.0000	1.8331	0.1164	0.6284	0.0080	25.7915
Chemostat 3 D=0,10h ⁻¹	1.0000	1.8480	0.1389	0.6082	0.0099	25.8566
Average	1.0000	1.8280	0.1200	0.6396	0.0083	26.0248
Standard error	0.0000	0.0087	0.0064	0.0130	0.0005	0.1172

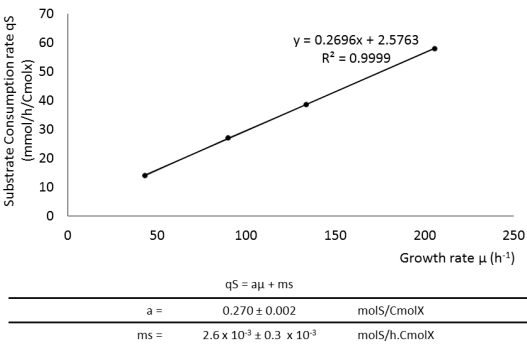


Figure S2.4. Herbert Pirt relation.

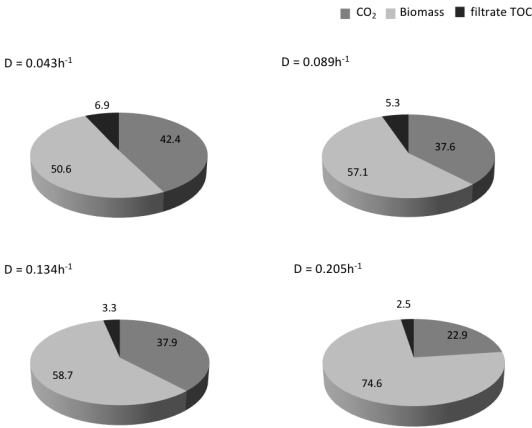


Figure S2.5. Distribution of carbon supplied as substrate (glucose).

Device specifications:

Length of the loop: 105 cm

Diameter: 8 mm

Volume of the loop: $\pi \times 0.4^2 \times 105 \approx 52$ ml

Volume between broth inflow in loop and sampling device: $\pi \times 0.4^2 \times 20 \approx 10$ ml

Applied flow rate: 40 ml/s

Residence time in whole loop: $\tau = \frac{V}{F} = \frac{52 \text{ ml}}{40 \text{ ml/s}} = 1.3$ s

Residence time between fermentor and sampling device: $\tau = \frac{V}{F} = \frac{10 \text{ ml}}{40 \text{ ml/s}} = 0.25$ s

Is glucose depleted during the circulation in the fast loop?

$D = 0.043 \text{ h}^{-1}$ (flow rate 0.193 l/h)

$[\text{Glu}]_{\text{ex}} = 0.74 \text{ mg/l}$ (at 0.043 h^{-1})

Consumption rate of glucose is calculated as

$R_{\text{Glu}} = C_{\text{S in}} \times F_{\text{in}} - C_{\text{S out}} \times F_{\text{out}} = 7.5 \text{ g/l} \times 0.193 \text{ l/h} - 0.74 \text{E-3 g/l} \times 0.193 \text{ l/h} \approx 1.45 \text{ g/h}$

$$t = \frac{0.74 \times 10^{-3} \text{ g} \times 4.5 \times 3600 \text{ s}}{1.45 \text{ g}} = 8.27 \text{ s}$$

3% of the residual glucose was consumed during the 0.25 s in the loop.

Figure S2.6. Example calculation of glucose depletion in the broth loop.

Table S2.4. Biomass concentration inside the fermentor C_x and in samples from the sampling device $C_{x,SD}$.

Dilution rate (h^{-1})	C_x ($\text{g}_{\text{DW}}/\text{l}_{\text{broth}}$)	$C_{x,SD}$ ($\text{g}_{\text{DW}}/\text{l}_{\text{broth}}$)
0.043	3.02 ± 0.03	2.84 ± 0.08
0.089	3.25 ± 0.04	3.02 ± 0.04

Table S2.5. Measured metabolite amounts in different sample fractions ($\mu\text{mol/g}_{\text{DW}}$) at dilution rate 0.043 h^{-1} .

Averages and standard errors of triplicate samples are shown. In light grey are measurements which were judged to be inconsistent due to concentrations being close to the detection limit, and in (<), measurements below the detection limit.

	IC 40%	IC 50%	IC 60%	EC	WB	WB-EC	Recovery 40%	Recovery 50%	Recovery 60%
G1P	0.070 ± 0.004	0.068 ± 0.006	0.058 ± 0.005	0.016 ± 0.001	0.103 ± 0.005	0.086 ± 0.005	81,642 ± 6,563	78,582 ± 8,096	67,715 ± 6,727
G6P	3.482 ± 0.131	3.452 ± 0.120	2.955 ± 0.150	0.302 ± 0.002	4.523 ± 0.368	4.221 ± 0.368	82,484 ± 7,823	81,776 ± 7,673	70,000 ± 7,052
F6P	0.843 ± 0.040	0.887 ± 0.024	0.779 ± 0.052	0.534 ± 0.013	1.695 ± 0.139	1.161 ± 0.140	72,672 ± 9,379	76,473 ± 9,428	67,169 ± 9,254
FBP	0.212 ± 0.023	0.167 ± 0.006	0.112 ± 0.009	0.035 ± 0.002	0.248 ± 0.032	0.213 ± 0.032	99,601 ± 18,440	78,751 ± 12,288	52,682 ± 9,084
GAP	0.018 ± 0.003	0.023 ± 0.004	0.023 ± 0.002	0.010 ± 0.001	0.060 ± 0.008	0.050 ± 0.009	35,789 ± 8,122	45,340 ± 10,797	45,197 ± 8,526
DHAP	0.238 ± 0.025	0.247 ± 0.011	0.224 ± 0.024	0.287 ± 0.010	0.701 ± 0.059	0.414 ± 0.060	57,463 ± 10,380	59,611 ± 9,074	54,268 ± 9,806
3PG	0.542 ± 0.043	0.561 ± 0.052	0.490 ± 0.044	0.544 ± 0.009	1.322 ± 0.100	0.778 ± 0.101	69,663 ± 10,568	72,105 ± 11,494	62,960 ± 9,909
2PG	0.049 ± 0.003	0.055 ± 0.003	0.046 ± 0.005	0.019 ± 0.001	0.086 ± 0.006	0.067 ± 0.006	73,193 ± 7,450	81,908 ± 8,526	67,770 ± 9,495
PEP	0.054 ± 0.007	0.067 ± 0.006	0.060 ± 0.005	0.015 ± 0.000	0.138 ± 0.010	0.123 ± 0.010	43,535 ± 7,035	54,650 ± 6,748	48,826 ± 6,039
Tre	66,730 ± 3,377	67,127 ± 1,542	61,249 ± 1,947	1,121 ± 0.005	76,736 ± 5,724	75,614 ± 5,724	88,251 ± 8,036	88,776 ± 7,023	81,002 ± 6,651
T6P	0.061 ± 0.007	0.062 ± 0.005	0.046 ± 0.003	0.015 ± 0.003	0.113 ± 0.013	0.098 ± 0.014	62,261 ± 11,135	63,398 ± 10,084	46,708 ± 7,374
G3P	0.147 ± 0.005	0.156 ± 0.004	0.130 ± 0.005	0.511 ± 0.004	0.652 ± 0.052	0.141 ± 0.052	104,486 ± 39,061	110,344 ± 41,186	91,982 ± 34,451
6PG	0.283 ± 0.015	0.251 ± 0.014	0.244 ± 0.013	0.104 ± 0.005	0.533 ± 0.029	0.430 ± 0.030	65,955 ± 5,744	58,370 ± 5,172	56,765 ± 4,923
Rbu5P	0.144 ± 0.003	0.149 ± 0.012	0.126 ± 0.005	0.087 ± 0.006	0.213 ± 0.014	0.126 ± 0.016	114,314 ± 14,641	118,308 ± 17,863	100,426 ± 13,297
Rib5P	0.329 ± 0.010	0.311 ± 0.007	0.260 ± 0.014	1.958 ± 0.080	2,574 ± 0.224	0.616 ± 0.238	53,375 ± 20,695	50,531 ± 19,558	42,269 ± 16,504
Xyl5P	0.252 ± 0.009	0.255 ± 0.005	0.206 ± 0.006	0.046 ± 0.001	0.295 ± 0.035	0.249 ± 0.035	101,262 ± 14,548	102,284 ± 14,390	82,799 ± 11,756
S7P	1,102 ± 0.041	1,077 ± 0.031	0,932 ± 0.041	0,348 ± 0.005	1,639 ± 0.132	1,291 ± 0.133	85,316 ± 9,309	83,419 ± 8,896	72,148 ± 8,063
E4P	0.008 ± 0.000	0.009 ± 0.000	0.007 ± 0.000	0.004 ± 0.000	0.010 ± 0.001	0.006 ± 0.001	142,377 ± 26,536	153,965 ± 28,829	132,143 ± 24,980
Cit	15,982 ± 0.723	16,012 ± 0.352	13,579 ± 0.524	0.310 ± 0.016	19,038 ± 1,549	18,728 ± 1,549	85,337 ± 8,046	85,497 ± 7,318	72,507 ± 6,620
iCit	0.215 ± 0.010	0.219 ± 0.007	0.177 ± 0.004	0.090 ± 0.003	0.344 ± 0.035	0.255 ± 0.035	84,225 ± 12,134	85,897 ± 12,080	69,310 ± 9,600
aKG	0.906 ± 0.087	0.926 ± 0.086	0.828 ± 0.071	0.051 ± 0.001	1,627 ± 0.133	1,576 ± 0.133	57,504 ± 7,350	58,763 ± 7,380	52,511 ± 6,335
Succ	0.649 ± 0.025	0.572 ± 0.026	0.481 ± 0.030	0.276 ± 0.046	0.944 ± 0.084	0.667 ± 0.096	97,226 ± 14,436	85,756 ± 12,880	72,047 ± 11,270
Fum	0.844 ± 0.034	0.740 ± 0.008	0.762 ± 0.117	< ± 0.241	1,007 ± 0.087	- ± -	83,855 ± 7,968	73,504 ± 6,394	75,731 ± 13,359
Mal	3,203 ± 0.131	2,993 ± 0.018	2,615 ± 0.150	0.212 ± 0.018	4,009 ± 0.345	3,797 ± 0.345	84,351 ± 8,414	78,825 ± 7,188	68,877 ± 7,412
His	1,351 ± 0.050	1,339 ± 0.022	1,127 ± 0.054	< ± <	1,565 ± 0.156	- ± -	86,307 ± 9,167	85,594 ± 8,643	72,036 ± 7,963
Ile	0.181 ± 0.003	0.174 ± 0.002	0.145 ± 0.008	0.014 ± 0.000	0.221 ± 0.018	0.207 ± 0.018	87,145 ± 7,872	83,767 ± 7,482	69,909 ± 7,344
Leu	0.272 ± 0.006	0.261 ± 0.002	0.221 ± 0.013	0.034 ± 0.007	0.342 ± 0.026	0.308 ± 0.027	88,382 ± 8,095	84,848 ± 7,600	71,595 ± 7,704
Lys	1,106 ± 0.032	1,106 ± 0.009	0,934 ± 0.039	< ± <	1,381 ± 0.184	- ± -	80,075 ± 10,913	80,106 ± 10,692	67,633 ± 9,436
Meth	0.106 ± 0.005	0.100 ± 0.002	0.087 ± 0.004	0.038 ± 0.002	0.151 ± 0.006	0.113 ± 0.007	93,828 ± 6,949	88,556 ± 5,594	77,036 ± 5,541
Phe	0.156 ± 0.005	0.146 ± 0.001	0.127 ± 0.009	0.021 ± 0.004	0.180 ± 0.014	0.160 ± 0.015	97,708 ± 9,447	91,702 ± 8,513	79,716 ± 9,203
Thr	1,636 ± 0.045	1,523 ± 0.031	1,345 ± 0.072	0.143 ± 0.003	2,149 ± 0.159	2,006 ± 0.159	81,555 ± 6,832	75,949 ± 6,210	67,039 ± 6,414
Trp	0.034 ± 0.001	0.032 ± 0.001	0.028 ± 0.002	< ± <	0.039 ± 0.003	- ± -	86,784 ± 8,056	82,719 ± 7,581	71,458 ± 8,360
Val	0.508 ± 0.016	0.473 ± 0.005	0.410 ± 0.025	0.000 ± 0.000	0.651 ± 0.056	0.651 ± 0.056	78,065 ± 7,180	72,600 ± 6,334	63,031 ± 6,705
Ala	8,068 ± 0.169	6,823 ± 0.037	6,161 ± 0.406	< ± <	11,271 ± 0.931	- ± -	71,583 ± 6,100	60,531 ± 5,011	54,659 ± 5,777
Asn	1,360 ± 0.061	1,405 ± 0.029	1,169 ± 0.070	0.055 ± 0.001	1,868 ± 0.151	1,813 ± 0.151	74,980 ± 7,108	77,459 ± 6,657	64,477 ± 6,628
Asp	6,707 ± 0.325	6,504 ± 0.117	5,861 ± 0.401	< ± <	9,954 ± 0.756	- ± -	67,377 ± 6,069	65,336 ± 5,098	58,874 ± 6,015
Cys	0.057 ± 0.001	0.054 ± 0.003	0.047 ± 0.003	0.025 ± 0.002	0.069 ± 0.005	0.044 ± 0.005	129,281 ± 15,266	120,888 ± 15,720	106,447 ± 14,347
Gln	26,219 ± 1,076	24,998 ± 0.548	22,433 ± 1,291	< ± <	36,259 ± 2,986	- ± -	72,312 ± 6,654	68,944 ± 5,876	61,869 ± 6,216
Glu	31,990 ± 1,683	30,454 ± 1,127	26,904 ± 1,399	< ± <	42,592 ± 3,537	- ± -	75,107 ± 7,383	71,502 ± 6,500	63,167 ± 6,189
Gly	1,090 ± 0.052	0.953 ± 0.004	0.845 ± 0.098	< ± <	1,675 ± 0.110	- ± -	65,096 ± 5,280	56,888 ± 3,748	50,459 ± 6,730
Pro	0.531 ± 0.018	0.488 ± 0.008	0.431 ± 0.030	0.060 ± 0.001	0.771 ± 0.060	0.711 ± 0.060	74,664 ± 6,820	68,679 ± 5,938	60,657 ± 6,652
Ser	2,707 ± 0.125	2,527 ± 0.045	2,265 ± 0.204	< ± <	> ± >	- ± -	- ± -	- ± -	- ± -
Tyr	0.110 ± 0.003	0.104 ± 0.001	0.090 ± 0.007	0.017 ± 0.004	0.123 ± 0.008	0.105 ± 0.009	104,288 ± 9,303	98,720 ± 8,581	85,187 ± 10,012
Total							79 ± 10	77 ± 9	67 ± 9

Table S2.6. Measured metabolite amounts in different sample fractions ($\mu\text{mol/g}_{\text{DW}}$) at dilution rate 0.089 h^{-1} .

Averages and standard errors of triplicate samples are shown. In light grey are measurements which were judged to be inconsistent due to concentrations being close to the detection limit, and in (<), measurements below the detection limit.

	IC 40%	IC 50%	IC 60%	EC	WB	WB-EC	Recovery 40%	Recovery 50%	Recovery 60%
G1P	0.186 ± 0.005	0.178 ± 0.006	0.179 ± 0.006	0.025 ± 0.004	0.229 ± 0.014	0.204 ± 0.014	91.081 ± 6.937	87.160 ± 6.799	87.872 ± 6.892
G6P	4.531 ± 0.031	4.277 ± 0.049	4.065 ± 0.090	0.355 ± 0.018	5.106 ± 0.077	4.751 ± 0.079	95.363 ± 1.721	90.024 ± 1.826	85.558 ± 2.367
F6P	1.085 ± 0.016	1.016 ± 0.020	1.014 ± 0.023	0.278 ± 0.016	1.467 ± 0.050	1.189 ± 0.052	91.234 ± 4.228	85.419 ± 4.091	85.289 ± 4.206
FBP	0.513 ± 0.019	0.533 ± 0.023	0.467 ± 0.001	0.077 ± 0.007	0.597 ± 0.027	0.520 ± 0.027	98.549 ± 6.308	102.506 ± 7.049	89.735 ± 4.740
GAP	0.020 ± 0.001	0.022 ± 0.001	0.022 ± 0.002	0.015 ± 0.002	0.077 ± 0.005	0.062 ± 0.006	31.932 ± 3.815	35.898 ± 3.476	35.521 ± 4.257
DHAP	0.391 ± 0.010	0.366 ± 0.014	0.447 ± 0.036	0.224 ± 0.017	0.734 ± 0.015	0.510 ± 0.022	76.673 ± 3.873	71.691 ± 4.228	87.634 ± 8.119
3PG	0.303 ± 0.006	0.294 ± 0.013	0.282 ± 0.002	0.347 ± 0.025	0.602 ± 0.011	0.255 ± 0.028	119.039 ± 13.208	115.258 ± 13.622	110.847 ± 12.144
2PG	0.078 ± 0.002	0.076 ± 0.002	0.084 ± 0.001	0.014 ± 0.002	0.097 ± 0.003	0.083 ± 0.003	94.320 ± 4.316	92.365 ± 4.517	101.596 ± 4.097
PEP	0.218 ± 0.010	0.232 ± 0.014	0.264 ± 0.003	0.029 ± 0.005	0.273 ± 0.010	0.243 ± 0.011	89.398 ± 5.923	95.427 ± 7.124	108.293 ± 5.204
Tre	74.253 ± 0.988	72.164 ± 1.252	72.346 ± 1.185	1.708 ± 0.214	73.848 ± 0.882	72.140 ± 0.908	102.929 ± 1.885	100.033 ± 2.144	100.286 ± 2.071
TPP	0.248 ± 0.005	0.226 ± 0.003	0.206 ± 0.003	0.015 ± 0.001	0.281 ± 0.005	0.266 ± 0.005	93.365 ± 2.531	85.150 ± 1.830	77.655 ± 1.788
G3P	0.876 ± 0.019	0.849 ± 0.026	0.906 ± 0.020	0.236 ± 0.012	1.076 ± 0.025	0.841 ± 0.028	104.278 ± 4.084	100.984 ± 4.535	107.835 ± 4.253
6PG	1.008 ± 0.046	0.972 ± 0.120	0.978 ± 0.012	0.238 ± 0.010	1.345 ± 0.019	1.107 ± 0.021	91.063 ± 4.526	87.783 ± 10.969	88.295 ± 2.035
Rbu5P	0.174 ± 0.008	0.173 ± 0.006	0.172 ± 0.012	0.053 ± 0.004	0.235 ± 0.004	0.182 ± 0.006	95.666 ± 5.240	95.117 ± 4.374	94.279 ± 7.347
Rib5P	0.385 ± 0.010	0.383 ± 0.007	0.366 ± 0.005	1.044 ± 0.034	1.492 ± 0.012	0.448 ± 0.036	85.851 ± 7.264	85.410 ± 7.021	81.569 ± 6.644
Xyl5P	0.363 ± 0.013	0.366 ± 0.004	0.338 ± 0.007	0.056 ± 0.002	0.429 ± 0.005	0.373 ± 0.006	97.402 ± 3.836	98.147 ± 1.890	90.496 ± 2.309
S7P	1.161 ± 0.004	1.116 ± 0.008	1.063 ± 0.015	0.191 ± 0.008	1.396 ± 0.020	1.205 ± 0.022	96.366 ± 1.776	92.567 ± 1.799	88.231 ± 2.045
E4P	0.007 ± 0.000	0.008 ± 0.000	0.007 ± 0.001	0.002 ± 0.000	0.009 ± 0.000	0.007 ± 0.000	104.554 ± 6.401	111.946 ± 7.809	106.608 ± 10.800
Cit	26.420 ± 0.274	25.289 ± 0.532	24.267 ± 0.242	0.641 ± 0.124	26.509 ± 0.387	25.868 ± 0.406	102.134 ± 1.920	97.761 ± 2.567	93.810 ± 1.744
iCit	0.851 ± 0.014	0.835 ± 0.015	0.770 ± 0.015	0.045 ± 0.005	0.868 ± 0.014	0.823 ± 0.015	103.449 ± 2.550	101.439 ± 2.555	93.625 ± 2.462
aKG	1.758 ± 0.025	1.647 ± 0.064	1.646 ± 0.044	0.050 ± 0.002	2.371 ± 0.044	2.321 ± 0.044	75.755 ± 1.798	70.984 ± 3.083	70.908 ± 2.332
Succ	1.921 ± 0.063	1.837 ± 0.081	1.643 ± 0.006	1.168 ± 0.462	1.698 ± 0.039	0.530 ± 0.464	362.502 ± 317.603	346.629 ± 303.876	310.072 ± 271.482
Fum	1.054 ± 0.007	0.978 ± 0.008	0.920 ± 0.028	0.113 ± 0.022	1.119 ± 0.015	1.005 ± 0.027	104.844 ± 2.880	97.252 ± 2.716	91.532 ± 3.691
Mal	3.871 ± 0.055	3.706 ± 0.028	3.389 ± 0.019	0.183 ± 0.050	4.313 ± 0.080	4.130 ± 0.094	93.737 ± 2.521	89.741 ± 2.162	82.060 ± 1.931
His	4.090 ± 0.052	4.099 ± 0.053	4.039 ± 0.042	< ± <	3.947 ± 0.139	< ± <	103.629 ± 3.880	103.857 ± 3.896	102.340 ± 3.756
Ile	0.543 ± 0.015	0.576 ± 0.032	0.503 ± 0.011	0.053 ± 0.013	0.562 ± 0.014	0.509 ± 0.019	106.612 ± 4.918	113.104 ± 7.504	98.716 ± 4.267
Leu	0.926 ± 0.016	0.965 ± 0.057	0.894 ± 0.020	0.098 ± 0.023	0.947 ± 0.021	0.849 ± 0.031	109.007 ± 4.357	113.585 ± 7.814	105.196 ± 4.475
Lys	2.468 ± 0.079	2.375 ± 0.078	2.294 ± 0.055	< ± <	2.281 ± 0.115	< ± <	108.193 ± 6.488	104.156 ± 6.280	100.595 ± 5.626
Meth	0.692 ± 0.016	0.663 ± 0.019	0.611 ± 0.025	0.184 ± 0.035	> ± >	> ± >	> ± >	> ± >	> ± >
Phe	0.342 ± 0.010	0.392 ± 0.038	0.351 ± 0.008	0.063 ± 0.014	0.331 ± 0.010	0.269 ± 0.017	127.355 ± 9.010	145.887 ± 16.789	130.535 ± 8.874
Thr	4.814 ± 0.078	4.458 ± 0.072	4.164 ± 0.068	0.401 ± 0.047	> ± >	> ± >	> ± >	> ± >	> ± >
Trp	0.123 ± 0.004	0.138 ± 0.007	0.129 ± 0.003	< ± <	0.123 ± 0.003	> ± >	100.718 ± 4.454	112.464 ± 6.702	105.547 ± 3.931
Val	1.569 ± 0.028	1.523 ± 0.046	1.370 ± 0.023	0.189 ± 0.054	1.733 ± 0.035	1.544 ± 0.064	101.599 ± 4.602	98.649 ± 5.083	88.728 ± 3.980
Ala	23.343 ± 0.620	21.152 ± 0.177	19.074 ± 0.591	1.646 ± 0.221	28.767 ± 0.823	27.121 ± 0.852	86.070 ± 3.542	77.990 ± 2.535	70.328 ± 3.103
Asn	2.985 ± 0.079	2.729 ± 0.073	2.570 ± 0.057	0.197 ± 0.023	3.389 ± 0.051	3.192 ± 0.056	93.525 ± 2.969	85.494 ± 2.744	80.510 ± 2.265
Asp	19.937 ± 0.725	17.965 ± 0.412	17.199 ± 0.605	0.754 ± 0.081	22.729 ± 0.556	21.975 ± 0.562	90.726 ± 4.033	81.752 ± 2.808	78.267 ± 3.404
Cys	0.195 ± 0.010	0.184 ± 0.004	0.170 ± 0.005	0.025 ± 0.003	0.124 ± 0.006	0.099 ± 0.006	196.338 ± 16.445	185.142 ± 12.605	171.655 ± 12.416
Gln	79.952 ± 2.407	74.322 ± 1.429	71.902 ± 2.218	< ± <	88.295 ± 1.277	> ± >	90.551 ± 3.025	84.175 ± 2.026	81.434 ± 2.775
Glu	124.798 ± 2.297	116.271 ± 1.874	107.505 ± 2.757	3.189 ± 0.348	137.528 ± 2.330	134.339 ± 2.356	92.898 ± 2.362	86.550 ± 2.062	80.025 ± 2.486
Gly	3.604 ± 0.077	3.512 ± 0.057	3.103 ± 0.021	0.797 ± 0.258	4.416 ± 0.100	3.619 ± 0.277	99.568 ± 7.902	97.020 ± 7.580	85.744 ± 6.580
Pro	1.418 ± 0.033	1.328 ± 0.010	1.181 ± 0.025	0.159 ± 0.023	1.705 ± 0.039	1.546 ± 0.046	91.700 ± 3.433	85.916 ± 2.617	76.388 ± 2.774
Ser	7.935 ± 0.171	7.670 ± 0.056	6.973 ± 0.128	< ± <	> ± >	> ± >	> ± >	> ± >	> ± >
Tyr	0.329 ± 0.007	0.371 ± 0.021	0.334 ± 0.008	0.060 ± 0.016	0.323 ± 0.017	0.263 ± 0.023	124.909 ± 11.430	140.759 ± 14.746	126.707 ± 11.604
Total							95 ± 4	93 ± 5	89 ± 4

Appendix Chapter 3

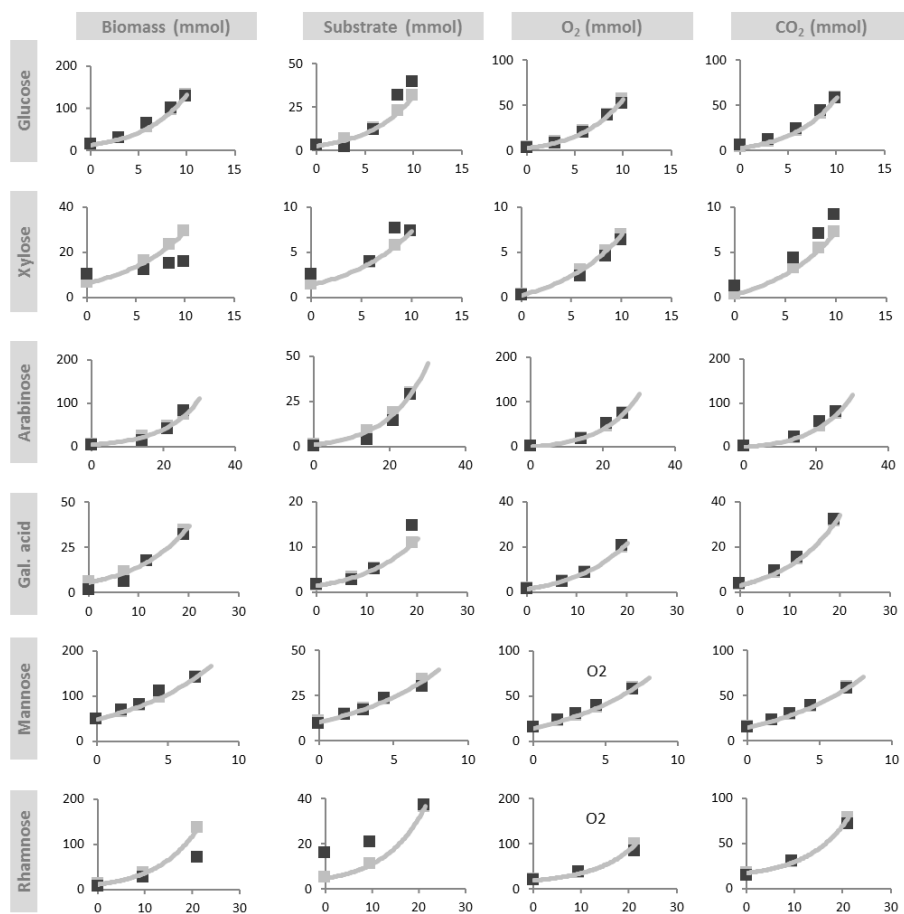


Fig. S3.1. Biomass and CO₂ formation and oxygen and substrate consumption profiles for maximum biomass specific conversion rates estimation during exponential batch phase in different carbon sources.

Unreconciled cumulative amounts (■), reconciled rates (—).

Table S3.1. Biomass elemental composition, molecular weight and degree of reduction for growth in six different carbon sources.

	Elemental composition	Cmol weight (g/Cmol)	Degree of reduction
Glucose	$C_1 H_{1.79} N_{0.14} O_{0.66} P_{0.015} S_{0.004}$	27.93 ± 0.06	4.149
Xylose	$C_1 H_{1.77} N_{0.13} O_{0.68} P_{0.014} S_{0.003}$	27.80 ± 0.19	4.108
Arabinose	$C_1 H_{1.75} N_{0.14} O_{0.66} P_{0.011} S_{0.003}$	27.80 ± 0.06	4.083
Galacturonic acid	$C_1 H_{1.72} N_{0.14} O_{0.63} P_{0.011} S_{0.003}$	27.17 ± 0.12	4.113
Mannose	$C_1 H_{1.75} N_{0.15} O_{0.65} P_{0.018} S_{0.004}$	28.00 ± 0.00	4.114
Rhamnose	$C_1 H_{1.67} N_{0.12} O_{0.67} P_{0.009} S_{0.003}$	27.64 ± 0.10	4.033

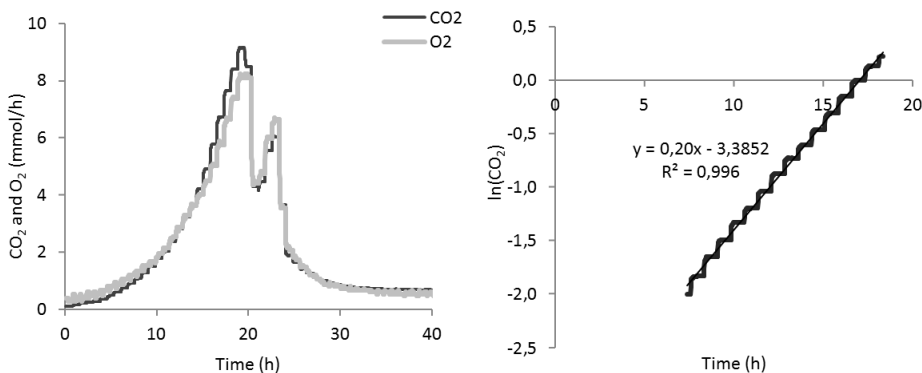
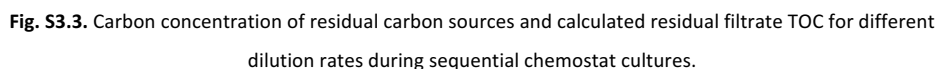


Fig. S3.2. Carbon dioxide production rate and oxygen consumption rate during batch phase in a mixture of six carbon sources (left) and maximum growth rate determination (right).



	0.043	0.059	0.077	0.093	0.110	0.127	0.144	0.160	0.177	0.194	0.209											
Fou(Lin)	0.151	0.000	0.266	0.000	0.345	0.000	0.421	0.000	0.494	0.000	0.573	0.000	0.649	0.000	0.719	0.000	0.774	0.000	0.872	0.000	0.941	0.000
Fin(Lin)	0.190	0.000	0.221	0.000	0.342	0.000	0.419	0.000	0.490	0.000	0.569	0.000	0.643	0.000	0.714	0.000	0.770	0.000	0.865	0.000	0.939	0.000
Fog ₃ (mmol/h)	2678.6	26.8	2678.6	26.8	2678.6	26.8	2678.6	26.8	2678.6	26.8	2678.6	26.8	2678.6	26.8	2678.6	26.8	2678.6	26.8	2678.6	26.8	2678.6	26.8
Fog ₂ (mmol/h)	2678.6	27.6	2680.8	27.6	2683.1	28.3	2685.4	27.6	2686.3	27.6	2687.9	27.6	2689.8	27.7	2692.3	27.7	2693.2	27.7	2693.2	27.7	2695.5	27.7
O ₂ _in (%)	20.350	0.000	20.350	0.000	20.350	0.000	20.350	0.000	20.350	0.000	20.350	0.000	20.350	0.000	20.350	0.000	20.350	0.000	20.350	0.000	20.350	0.000
O ₂ _out (%)	19.367	0.194	18.817	0.188	18.353	0.184	18.034	0.180	17.895	0.179	17.783	0.002	17.800	0.178	17.398	0.179	18.203	0.182	18.814	0.188	19.364	0.193
O ₂ _in (L)	0.048	0.000	0.049	0.000	0.051	0.084	0.054	0.001	0.052	0.001	0.054	0.000	0.052	0.001	0.051	0.001	0.050	0.000	0.050	0.000	0.047	0.000
O ₂ _out (L)	0.1667	0.033	2.247	0.045	2.781	0.056	3.170	0.063	3.394	0.067	3.495	0.001	3.531	0.071	3.657	0.069	3.599	0.064	2.506	0.050	1.682	0.037
Galact (mmol/L)	12.015	0.000	0.000	0.000	0.000	0.000	0.045	0.000	0.045	0.000	0.045	0.000	0.045	0.000	0.045	0.000	0.045	0.000	0.045	0.000	0.045	0.000
Cyloin (mmol/L)	15.187	0.152	15.187	0.152	15.187	0.152	15.187	0.152	15.187	0.152	15.187	0.152	15.187	0.152	15.187	0.152	15.187	0.152	15.187	0.152	15.187	0.152
Caylin (mmol/L)	15.107	0.152	15.187	0.152	15.187	0.152	15.187	0.152	15.187	0.152	15.187	0.152	15.187	0.152	15.187	0.152	15.187	0.152	15.187	0.152	15.187	0.152
Cagin (mmol/L)	11.620	0.116	11.620	0.116	11.620	0.116	11.620	0.116	11.620	0.116	11.620	0.116	11.620	0.116	11.620	0.116	11.620	0.116	11.620	0.116	11.620	0.116
Cmanin (mmol/L)	13.723	0.137	13.723	0.137	13.723	0.137	13.723	0.137	13.723	0.137	13.723	0.137	13.723	0.137	13.723	0.137	13.723	0.137	13.723	0.137	13.723	0.137
Choc (mmol/L)	13.877	0.139	13.877	0.139	13.877	0.139	13.877	0.139	13.877	0.139	13.877	0.139	13.877	0.139	13.877	0.139	13.877	0.139	13.877	0.139	13.877	0.139
Thi (mMol/L)	36.250	0.372	34.542	0.362	31.266	0.343	33.984	0.357	33.674	0.373	23.832	0.423	31.869	0.463	37.029	0.460	34.114	0.352	36.304	0.401	46.028	0.320
Cyloin (mmol/L)	0.004	0.000	0.000	0.000	0.000	0.000	0.000	0.000	0.000	0.000	0.000	0.000	0.000	0.000	0.000	0.000	0.000	0.000	0.000	0.000	0.000	
Cyloin (mmol/L)	0.004	0.000	0.000	0.000	0.000																	

Table S3.3. Residual substrate concentration for six carbon sources at different dilution rates in the sequential chemostat cultivation.

Dilution rate (h ⁻¹)	Glucose (mM)	Xylose (mM)	Arabinose (mM)	Gal acid (mM)	Mannose (mM)	Rhamnose (mM)
0.043	0.012 ± 0.002	0.004 ± 0.000	0.024 ± 0.001	0.050 ± 0.002	0.030 ± 0.002	0.028 ± 0.001
0.059	0.015 ± 0.002	0.005 ± 0.001	0.039 ± 0.001	0.066 ± 0.002	0.033 ± 0.006	0.069 ± 0.004
0.077	0.025 ± 0.004	0.013 ± 0.000	0.095 ± 0.000	0.111 ± 0.004	0.056 ± 0.005	0.173 ± 0.002
0.093	0.043 ± 0.004	0.084 ± 0.009	0.231 ± 0.003	0.291 ± 0.010	0.107 ± 0.015	0.455 ± 0.013
0.110	0.085 ± 0.003	0.206 ± 0.017	0.870 ± 0.013	0.582 ± 0.022	0.138 ± 0.015	2.310 ± 0.067
0.127	0.054 ± 0.004	0.584 ± 0.045	1.795 ± 0.052	0.785 ± 0.026	0.131 ± 0.010	6.289 ± 0.143
0.144	0.053 ± 0.004	0.728 ± 0.089	1.926 ± 0.033	0.942 ± 0.002	0.126 ± 0.012	9.120 ± 0.137
0.160	0.079 ± 0.008	1.402 ± 0.153	3.764 ± 0.014	1.569 ± 0.103	0.293 ± 0.032	10.332 ± 0.100
0.172	0.152 ± 0.012	3.821 ± 0.332	6.761 ± 0.101	3.157 ± 0.111	0.448 ± 0.052	11.911 ± 0.345
0.194	0.547 ± 0.022	8.218 ± 0.715	11.950 ± 0.179	7.366 ± 0.258	2.160 ± 0.269	12.594 ± 0.365
0.209	1.393 ± 0.054	9.445 ± 0.822	13.032 ± 0.195	10.784 ± 0.377	4.529 ± 0.439	12.393 ± 0.359

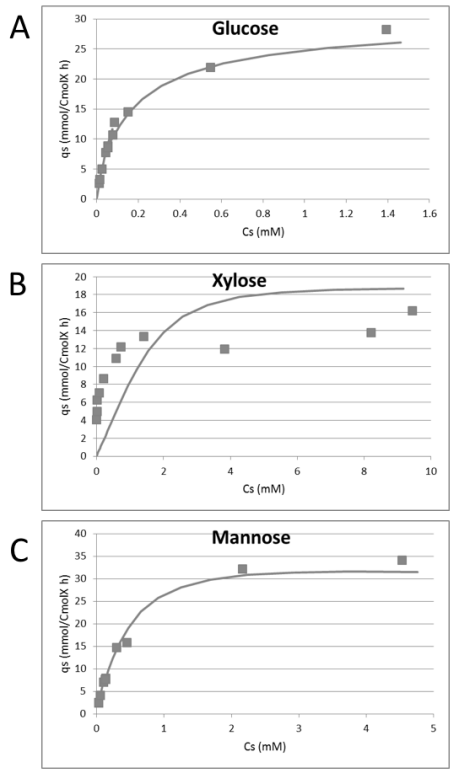


Fig. S3.4. Biomass specific uptake rates of glucose (A), mannose (B) and xylose (C) in the multi substrate sequential chemostat cultivation, plotted against their respective residual concentrations. The solid lines represents the modelling of the uptake rates of the three substrates according to competition for the same transport system.

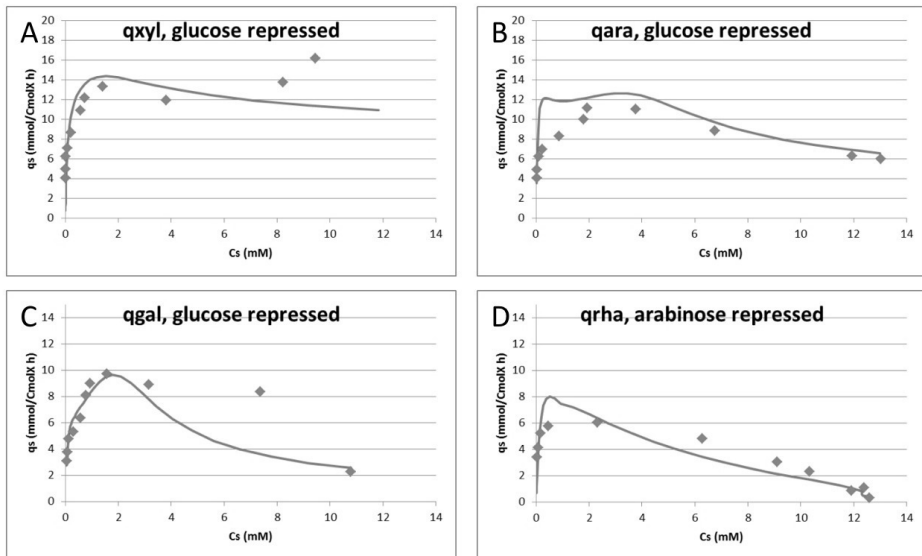


Fig. S3.5. The biomass specific uptake rates of xylose (A), arabinose (B) galacturonic acid (C) and rhamnose (D) in the multi substrate sequential chemostat cultivation, plotted against their respective residual concentrations. The solid lines represent the modelling of the uptake rates according to catabolite repression by glucose (in case of xylose, arabinose and galacturonic acid) and arabinose (in case of rhamnose).

Appendix Chapter 4

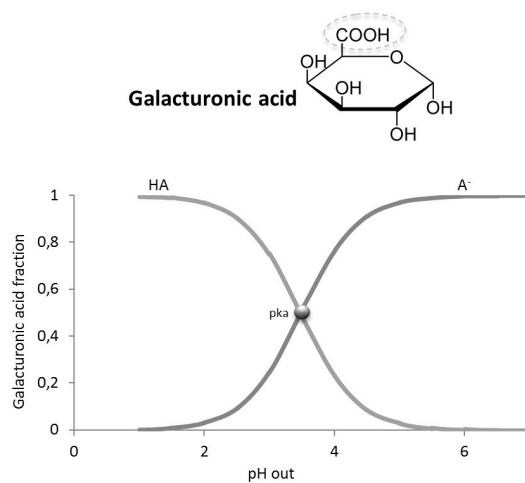


Fig. S4.1. Galacturonic acid fraction of different species depending on extracellular pH.

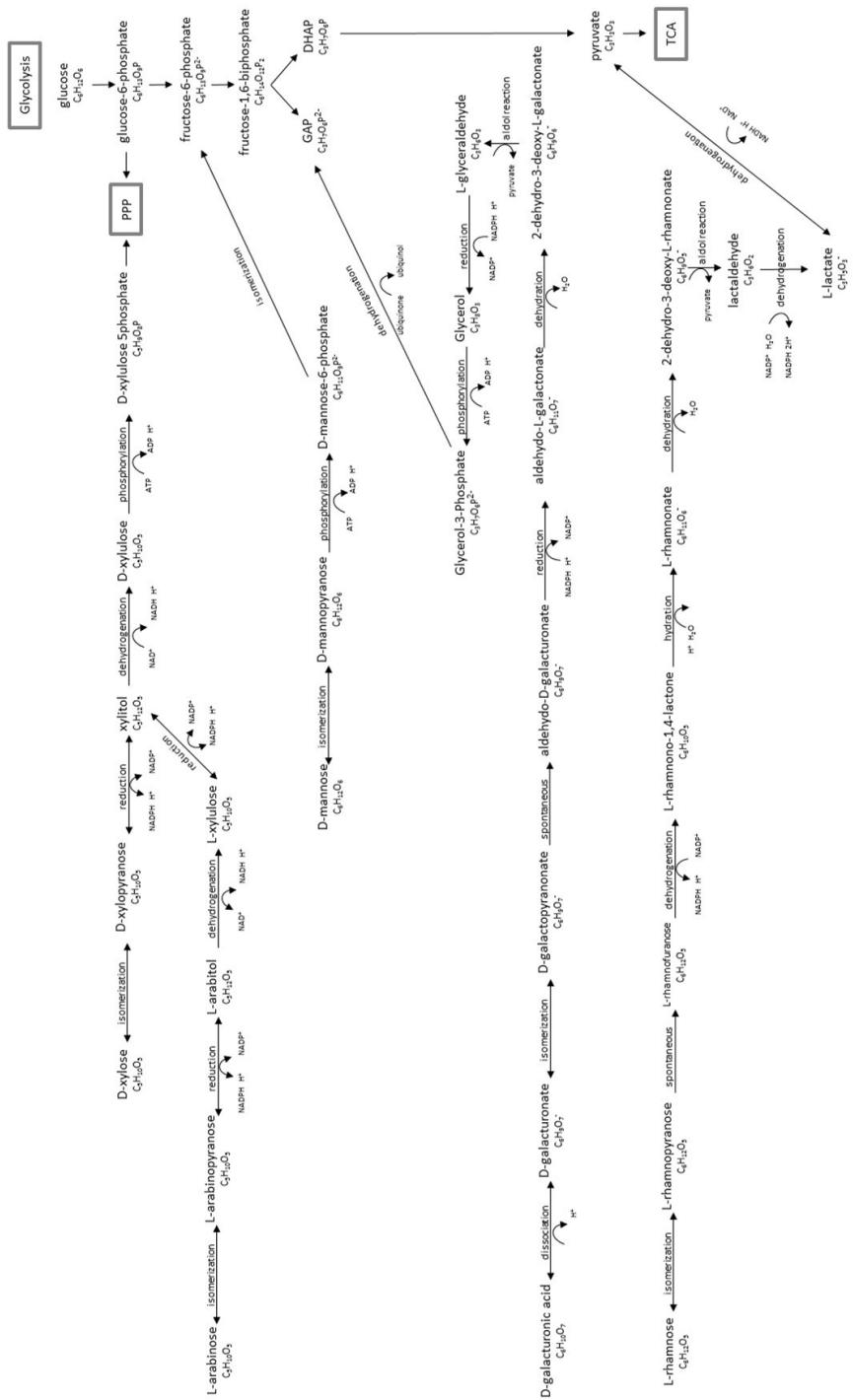


Fig. S4.2. Fungal catabolic pathway of glucose, xylose, arabinose, galacturonic acid, mannose and rhamnose.

Table S4.1. Input data and flux analysis results for dilution rate $D = 0.043\text{h}^{-1}$.

Best estimate of the fluxes (mmol/h)				Input rates (mmol/h)		Corresponding covariance matrix									
vest 1	Values	Variances	Serr	r_m 1	Values	Pr_m 1	ara:ext	BIOMasp:	CO2:ext	D-galac:ext	glc:ext	Ura:ext	mann:ext	O2:ext	xy:ext
ATP GTP Prans	6.21E-02	4.87E-06	0.002027	ara:ext	-2.868	ara:ext	0.011	-0.0673	0	0.00401	0.00437	0.00482	0.00475	0	0.00528
C120psyn	2.77E-03	9.69E-09	9.84E-05	BIOMasp:cyt	37.01	BIOMasp:cyt	-0.0673	1.71	0	-0.0512	-0.0558	-0.0615	-0.0606	0	-0.0674
C140psyn	3.22E-03	1.31E-08	0.000114	CO2:ext	43.4	CO2:ext	0	0	2.02	0	0	0	0	-0.235	0
C141syn	1.39E-03	2.42E-09	4.92E-05	D-galac:ext	-2.183	D-galac:ext	0.00401	-0.0512	0	0.00627	0.00333	0.00367	0.00362	0	0.00402
C160syn	2.27E-02	6.50E-07	0.000806	glc:ext	-2.379	glc:ext	0.00437	-0.0558	0	0.00333	0.00684	0.004	0.00394	0	0.00438
C161syn	3.23E-03	1.32E-08	0.000115	Ura:ext	-2.622	Ura:ext	0.00482	-0.0615	0	0.00367	0.000762	0.00434	0	0.00483	0
C162syn	9.24E-04	1.08E-09	3.28E-05	mann:ext	-2.584	mann:ext	0.00475	-0.0606	0	0.00362	0.00394	0.00434	0.00749	0	0.00476
C180syn	1.04E-01	1.35E-05	0.003678	O2:ext	-42.16	O2:ext	0	0	-0.235	0	0	0	0	42.9	0
C181CoA syn	1.22E-02	1.88E-07	0.000434	xy:ext	-2.872	xy:ext	0.00528	-0.0674	0	0.00402	0.00438	0.00483	0.00476	0	0.011
C181syn	0.1002	1.27E-05	0.003558												
C182syn	4.31E-02	2.35E-06	0.001532	Reconciled rates (mmol/h)		Corresponding covariance matrix									
C183syn	3.74E-03	1.77E-08	0.000133												
C200syn	6.93E-04	6.06E-10	2.46E-05	r_m est 1	Values	Pr_m 1	ara:ext	BIOMasp:	CO2:ext	D-galac:ext	glc:ext	Ura:ext	mann:ext	O2:ext	xy:ext
CLsyn	1.72E-03	3.75E-09	6.12E-05	ara:ext	-2.713	ara:ext	0.008166	-0.05968	-0.04575	0.001912	0.002123	0.002387	0.002347	0.0401	0.002443
DAGLYsyn	4.84E-02	2.95E-06	0.001718	BIOMasp:cyt	36.58	BIOMasp:cyt	-0.05968	1.689	0.1283	-0.04555	-0.04976	-0.05497	-0.05414	0.02938	-0.05978
DGOG syn	7.75E-03	7.59E-08	0.000275	CO2:ext	46	CO2:ext	0	-0.04575	0.1283	1.219	-0.03399	-0.0629	-0.03923	-0.0388	-1.194
GDPMANsyn	6.21E-02	4.87E-06	0.002027	D-galac:ext	-2.067	D-galac:ext	0.001912	-0.04555	-0.03399	0.004717	0.001666	0.001869	0.001841	0.02645	0.00192
MAGLYsyn	5.71E-02	6.12E-06	0.002023	glc:ext	-2.256	glc:ext	0.002123	-0.04976	-0.03629	0.001666	0.005058	0.002071	0.002035	0.03155	0.00213
MGC181 syn	1.22E-02	1.88E-07	0.000434	Ura:ext	-2.488	Ura:ext	0.002387	-0.05497	-0.03923	0.001869	0.002071	0.005532	0.002277	0.03558	0.002394
MGOG syn	3.74E-02	1.77E-06	0.001329	mann:ext	-2.452	mann:ext	0.002347	-0.05414	-0.0388	0.001841	0.002035	0.002277	0.005453	0.03362	0.002355
r1.1	2.256	0.005058	0.07112	O2:ext	-42.15	O2:ext	0.0401	0.02938	-1.194	0.02645	0.03155	0.03558	0.03362	1.188	0.04014
r1.2	-7.048	0.06697	0.258786	xy:ext	-2.716	xy:ext	0.002443	-0.05978	-0.0458	0.00192	0.00213	0.002394	0.002355	0.04014	0.00816
r1.3	3.041	0.01336	0.115585												
r1.4	3.041	0.01336	0.115585	Calculated rates (mmol/h)		Corresponding covariance matrix									
r1.5	11.63	0.07783	0.27898												
r1.6	11.63	0.07783	0.27898	r_c est 1	Values	Pr_c 1	H:ext	H2O:ext	NH4:ext	Pi:ext	SO4:ext				
r1.7	11.21	0.07642	0.276442	H:ext	1.672	H:ext	0.01765	0.06171	-0.01918	-0.00055	-0.00023				
r1.8	11.21	0.07642	0.276442	H2O:ext	55.21	H2O:ext	0.06171	1.367	-0.06707	-0.00192	-0.00079				
r1.9	10.87	0.07562	0.274991	NH4:ext	-4.064	NH4:ext	-0.01918	-0.06707	0.02085	0.000595	0.000245				
r10.1	192.1	26.39	5.13712	Pi:ext	-0.116	Pi:ext	-0.00055	-0.00192	0.000595	1.70E-05	6.99E-06				
r10.10	0.1028	1.33E-05	0.003651	SO4:ext	-0.04774	SO4:ext	-0.00023	-0.00079	0.000245	6.99E-06	2.88E-06				
r10.11	16.47	0.1324	0.363868												
r10.12	37.83	1.124	1.06189												
r10.13	0.1575	1.33E-05	0.005594	Best estimate of the fluxes (mmol/h) continued											
r10.14	4.821	0.02934	0.171289	vest 1	Values	Variances	Serr	vest 1	Values	Variances	Serr				
r10.15	0.1028	1.33E-05	0.003651	r16.13	2.61E-01	8.60E-05	0.009274	r4.7	11.07	0.1323	0.363731				
r10.16	0.349	0.000154	0.012398	r16.14	4.35E-02	2.39E-06	0.001546	r4.8	11.07	0.1323	0.363731				
r10.17	0.1391	2.44E-05	0.004941	r16.15	4.35E-02	2.39E-06	0.001546	r4.9	11.07	0.1323	0.363731				
r10.18	0.1072	1.45E-05	0.003807	r16.16	9.90E-03	1.24E-07	0.000352	r5.1	1.21	0.001846	0.042965				
r10.19	0.1827	4.21E-05	0.00649	r16.2	1.10E-01	1.54E-05	0.003922	r5.2	3.77	0.01794	0.13394				
r10.3	154.6	16.65	0.480441	r16.3	0.1164	1.71E-05	0.004135	r5.3	4.317	0.02352	0.153362				
r10.5	191.5	26.4	5.138093	r16.4	0.1164	1.71E-05	0.004135	r6.1	52.53	1.979	1.406769				
r10.6	1.051	0.001393	0.037323	r16.5	5.33E-02	3.58E-06	0.001892	r6.2	19.97	0.2161	0.464866				
r10.7	0.1072	1.45E-05	0.003807	r16.6	5.33E-02	3.58E-06	0.001892	r6.3	11.07	0.1323	0.363731				
r10.8	0.5045	0.000321	0.017922	r16.7	5.33E-02	3.58E-06	0.001892	r6.4	181.3	22.86	4.781213				
r10.9	0.1028	1.33E-05	0.003651	r16.8	4.98E-02	3.31E-06	0.001769	r7.12	2.713	0.008166	0.093066				
r11.1	2.943	0.01093	0.104547	r16.9	4.95E-02	3.09E-06	0.001757	r7.13	2.713	0.008166	0.093066				
r11.10	0.1565	3.09E-05	0.002556	r17.2	6.11E-01	0.00472	0.021721	r7.14	2.713	0.008166	0.093066				
r11.11	4.77E-02	2.88E-06	0.001696	r17.3	0.1776	3.98E-05	0.006309	r7.16	2.452	0.005453	0.073844				
r11.12	4.77E-02	2.88E-06	0.001696	r17.4	0.1776	3.98E-05	0.006309	r7.17	2.452	0.005453	0.073844				
r11.13	2.73E-02	9.37E-07	0.000968	r17.5	1.58	0.003151	0.056134	r7.18	2.067	0.004717	0.06868				
r11.14	2.73E-02	9.37E-07	0.000968	r17.6	3.95E-02	1.97E-06	0.001402	r7.19	2.067	0.004717	0.06868				
r11.15	2.05E-02	5.30E-07	0.000728	r17.7	3.95E-02	1.97E-06	0.001402	r7.2	5.07E-02	3.24E-06	0.0018				
r11.16	6.63E-01	0.000555	0.023567	r17.8	2.96E-01	0.000111	0.010517	r7.20	2.07E+00	0.004717	0.06868				
r11.17	5.42E-02	3.71E-06	0.001927	r2.1	7.684	0.05595	0.236538	r7.21	2.067	0.004717	0.06868				
r11.18	2.61E-01	8.57E-05	0.009255	r2.2	7.684	0.05595	0.236538	r7.22	2.067	0.004717	0.06868				
r11.19	0.2333	6.87E-05	0.008287	r2.3	4.476	0.01558	0.12482	r7.23	1.615	0.003849	0.06204				
r11.2	1.014	0.001298	0.036028	r2.4	3.06	0.01289	0.113534	r7.24	1.612	0.003844	0.062				
r11.20	0.07257	6.65E-06	0.002578	r2.5	4.476	0.01558	0.12482	r7.25	2.488	0.005532	0.074377				
r11.21	0.1028	1.33E-05	0.003651	r2.6	4.476	0.01558	0.12482	r7.26	2.488	0.005532	0.074377				
r11.22	0.268	9.07E-05	0.009523	r2.7	4.013	0.01247	0.11669	r7.27	2.488	0.005532	0.074377				
r11.23	0.3218	0.000131	0.011432	r23.1	1.022	0.001318	0.036304	r7.28	2.488	0.005532	0.074377				
r11.24	0.1391	2.44E-05	0.004941	r23.10	2.92E-03	1.08E-08	0.000104	r7.29	2.488	0.005532	0.074377				
r11.25	0.1827	4.21E-05	0.00649	r23.11	2.92E-03	1.08E-08	0.000104	r7.30	2.488	0.005532	0.074377				
r11.26	0.1827	4.21E-05	0.00649	r23.12	2.92E-03	1.08E-08	0.000104	r7.6	2.716	0.008166	0.093033				
r11.27	0.1668	3.51E-05	0.005927	r23.14	2.92E-03	1.08E-08	0.000104	r7.7	5.429	0.02121	0.145637				
r11.28	0.08096	8.27E-06	0.002876	r23.15	1.61E-02	3.28E-07	0.000573	r7.8	5.429	0.02121	0.145637				
r11.29	5.32E-02	3.57E-06	0.00189	r23.16	1.43E-01	2.58E-05	0.005074	r8.1	-0.1018	1.31E-05	0.003615				
r11.3	1.14E-01	1.65E-05	0.004066	r23.17	0.3749	0.000177	0.013319	r8.2	-1.45E-02	2.64E-07	0.000513				
r11.30	3.27E-02	1.35E-06	0.001161	r23.18	0.2595	8.50E-05	0.009218	r8.3	6.92E-02	6.04E-06	0.002458				
r11.31	1.49E-01	2.79E-05	0.005282	r23.19	2.03E-02	5.20E-07	0.000721	r8.4	4.53E-02	2.59E-06	0.00161				
r11.32	5.32E-02	3.57E-06	0.00189	r23.2	1.46E-01	2.68E-05	0.005181	r8.5	4.53E-02	2.59E-06	0.00161				
r11.4	1.07E-01	1.45E-05	0.003807	r23.21	0.9866	0.									

Table S4.2. Input data and flux analysis results for dilution rate $D = 0.059\text{h}^{-1}$.

Best estimate of the fluxes (mmol/h)				Input rates (mmol/h)		Corresponding covariance matrix																
vest 1	Values	Variances	Serr	r_m 1	Values	Pr_m 1	ara-ext	BIOMasp:CO2-ext	D-galac-ext	glc-ext	Lrha-ext	mann-ext	O2-ext	xyL-ext								
ATP GTP Ptrans	9.42E-02	6.17E-06	0.002483	ara-ext	-4	ara-ext	0.0224	-0.159	0	0.00857	0.00935	0.0103	0.0102	0	0.0113							
C120syn	4.20E-03	1.23E-08	0.000111	BIOMasp:pyr	57.1	BIOMasp:	-0.159	2.77	0	-0.121	-0.132	-0.145	-0.144	0	-0.16							
C140syn	4.88E-03	1.66E-08	0.000129	CO2-ext	58.93	CO2-ext	0	0	1.9	0	0	0	0	0.918	0							
C141syn	2.10E-03	3.07E-09	5.54E-05	D-galac-ext	-3.04	D-galac-ext	0.00857	-0.121	0	0.0128	0.00711	0.00782	0.00772	0	0.00859							
C160syn	3.44E-02	8.23E-07	0.000907	glc-ext	-3.32	glc-ext	0.00935	-0.132	0	0.00711	0.014	0.00853	0.00843	0	0.00937							
C161syn	4.90E-03	1.67E-08	0.000129	Lrha-ext	-3.65	Lrha-ext	0.0103	-0.145	0	0.00782	0.00853	0.0156	0.00926	0	0.0103							
C162syn	1.40E-03	1.36E-09	3.69E-05	mann-ext	-3.61	mann-ext	0.0102	-0.144	0	0.00772	0.00843	0.00926	0.0154	0	0.0102							
C180syn	1.57E-01	1.71E-05	0.004138	O2-ext	-56.72	O2-ext	0	0	0.918	0	0	0	0	39.4	0							
C181CoA syn	1.85E-02	2.38E-07	0.000488	xyL-ext	-4.01	xyL-ext	0.0113	-0.16	0	0.00859	0.00937	0.0103	0.0102	0	0.0225							
C181syn	0.1518	1.60E-05	0.004004																			
C182syn	6.54E-02	2.97E-06	0.001724	Reconciled rates (mmol/h)					Corresponding covariance matrix													
C183syn	5.67E-03	2.24E-08	0.000149	r_m est 1	Values	Pr_m 1	ara-ext	BIOMasp:CO2-ext	D-galac-ext <td>glc-ext</td> <td>Lrha-ext</td> <td>mann-ext</td> <td>O2-ext</td> <td>xyL-ext</td> <td></td> <td></td> <td></td> <td></td>	glc-ext	Lrha-ext	mann-ext	O2-ext	xyL-ext								
C200syn	1.05E-03	7.66E-10	2.77E-05	ara-ext	-3.81	ara-ext	0.01385	-0.08549	-0.06205	0.002261	0.002583	0.002984	0.002976	0.05422	0.002759							
CLsyn	2.61E-03	4.74E-09	6.88E-05	BIOMasp:pyr	55.45	BIOMasp:	-0.08549	2.138	0.5419	-0.06674	-0.07382	-0.08211	-0.08189	-0.3396	-0.08657							
DAGLYsyn	7.33E-02	3.73E-06	0.001932	CO2-ext	60.52	CO2-ext	-0.06205	0.5419	1.281	-0.0462	-0.04915	-0.05296	-0.05248	-1.216	-0.06199							
DGDG syn	1.18E-02	9.60E-08	0.00031	D-galac-ext	-2.899	D-galac-ext	0.002261	-0.06674	-0.0462	0.008144	0.002117	0.002423	0.00239	0.03375	0.002288							
GDPMANsyn	9.42E-02	6.17E-06	0.000483	glc-ext	-3.169	glc-ext	0.002583	-0.07382	-0.04915	0.002117	0.008644	0.00274	0.002713	0.0423	0.00261							
MAGL181 syn	8.66E-02	5.22E-06	0.002284	Lrha-ext	-3.488	Lrha-ext	0.002984	-0.08211	-0.05296	0.002423	0.00274	0.00934	0.00308	0.04842	0.002992							
MGDC181 syn	1.85E-02	2.38E-07	0.000488	mann-ext	-3.449	mann-ext	0.002976	-0.08189	-0.05248	0.00239	0.002713	0.00308	0.009298	0.04486	0.002985							
MGDG syn	5.67E-02	2.24E-06	0.001495	O2-ext	-54.78	O2-ext	0.05422	-0.3396	-1.216	0.03375	0.0423	0.04842	0.04486	1.179	0.05404							
r1.1	3.169	0.008644	0.092973	xyL-ext	-3.82	xyL-ext	0.002759	-0.08657	-0.06199	0.002288	0.00261	0.002992	0.002985	0.05404	0.01397							
r1.2	-10.53	0.096	0.309839																			
r1.3	3.827	0.01599	0.126452	Calculated rates (mmol/h)					Corresponding covariance matrix													
r1.4	3.827	0.01599	0.126452	r_c est 1	Values	Pr_c 1	H-ext	H2O-ext	NH4-ext	Pi-ext	SO4-ext											
r1.5	15.49	0.09439	0.30723	H-ext	2.769	H-ext	0.02233	0.116	-0.02427	-0.00069	-0.00029											
r1.6	15.49	0.09439	0.30723	H2O-ext	74.72	H2O-ext	0.116	1.693	-0.126	-0.0036	-0.00148											
r1.7	14.85	0.09056	0.300932	NH4-ext	-6.16	NH4-ext	-0.02427	-0.126	0.02638	0.000753	0.00031											
r1.8	14.85	0.09056	0.300932	Pi-ext	-0.1759	Pi-ext	-0.00069	-0.0036	0.000753	2.15E-05	8.85E-06											
r1.9	14.35	0.08794	0.296547	SO4-ext	-0.07237	SO4-ext	-0.00029	-0.00148	0.00031	8.85E-06	3.64E-06											
r10.1	248.2	25.6	5.059644	Best estimate of the fluxes (mmol/h) continued																		
r10.10	0.1558	1.69E-05	0.004106	vest 1	Values	Variances	Serr	vest 1	Values	Variances	Serr											
r10.11	22.03	0.1538	0.392173	r16.13	3.96E-01	1.09E-04	0.010436	r4.7	13.85	0.1176	0.342929											
r10.12	48.54	1.066	1.032473	r16.14	6.60E-02	3.02E-06	0.001739	r4.8	13.85	0.1176	0.342929											
r10.13	0.2387	3.96E-05	0.006293	r16.15	6.60E-02	3.02E-06	0.001739	r4.9	13.84	0.1176	0.342929											
r10.14	7.308	0.03712	0.192666	r16.16	1.50E-02	1.57E-07	0.000396	r5.1	1.833	0.002337	0.048343											
r10.15	0.1558	1.69E-05	0.004106	r16.17	1.67E-01	1.95E-05	0.004411	r5.2	5.715	0.02271	0.150698											
r10.16	0.529	0.000195	0.013946	r16.3	0.1764	2.16E-05	0.004652	r5.3	6.543	0.02976	0.172511											
r10.17	0.2108	3.09E-05	0.005559	r16.4	0.1764	2.16E-05	0.004652	r6.1	67.88	1.927	1.388164											
r10.18	0.1624	1.83E-05	0.004283	r16.5	8.07E-02	4.53E-06	0.002128	r6.2	26.73	0.2638	0.513615											
r10.19	0.2769	5.33E-05	0.007301	r16.6	8.07E-02	4.53E-06	0.002128	r6.3	13.84	0.1176	0.342929											
r10.3	200.2	16.29	4.036087	r16.7	8.07E-02	4.53E-06	0.002128	r6.4	234.9	22.38	4.73075											
r10.5	247.5	25.57	5.066679	r16.8	7.55E-02	3.96E-06	0.00199	r7.12	3.81	0.01385	0.117686											
r10.6	1.593	0.001763	0.041988	r16.9	7.50E-02	3.91E-06	0.001976	r7.13	3.81	0.01385	0.117686											
r10.7	0.1624	1.83E-05	0.004283	r17.2	9.27E-01	0.000597	0.024436	r7.14	3.81	0.01385	0.117686											
r10.8	0.7647	0.000407	0.020162	r17.3	0.2692	5.04E-05	0.007097	r7.16	3.449	0.009298	0.096426											
r10.9	0.1558	1.69E-05	0.004106	r17.4	0.2692	5.04E-05	0.007097	r7.17	3.449	0.009298	0.096426											
r11.1	4.462	0.01384	0.117644	r17.5	2.395	0.003988	0.063151	r7.18	2.899	0.008144	0.090244											
r11.10	0.2372	3.91E-05	0.006255	r17.6	5.98E-02	2.49E-06	0.001577	r7.19	2.899	0.008144	0.090244											
r11.11	7.24E-02	3.64E-06	0.001908	r17.7	5.98E-02	2.49E-06	0.001577	r7.2	7.68E-02	4.10E-06	0.002025											
r11.12	7.24E-02	3.64E-06	0.001908	r17.8	4.49E-01	0.00014	0.011828	r7.20	2.90E+00	0.008144	0.090244											
r11.13	4.13E-02	1.19E-06	0.001089	r2.1	11.25	0.0816	0.285657	r7.21	2.899	0.008144	0.090244											
r11.14	4.13E-02	1.19E-06	0.001089	r2.2	11.25	0.0816	0.285657	r7.22	2.899	0.008144	0.090244											
r11.15	3.11E-02	6.71E-07	0.000819	r2.3	6.451	0.02323	0.152414	r7.23	2.214	0.006821	0.082589											
r11.16	1.01E+00	0.000703	0.02651	r2.4	4.57	0.01874	0.136894	r7.24	2.209	0.006814	0.082547											
r11.17	8.22E-02	4.70E-06	0.002167	r2.5	6.451	0.02323	0.152414	r7.25	3.488	0.00934	0.096644											
r11.18	3.95E-01	1.08E-04	0.010412	r2.6	6.451	0.02323	0.152414	r7.26	3.488	0.00934	0.096644											
r11.19	0.3536	8.69E-05	0.009323	r2.7	5.749	0.01902	0.137913	r7.27	3.488	0.00934	0.096644											
r11.2	1.537	0.001643	0.040534	r23.1	1.549	0.001668	0.040841	r7.28	3.488	0.00934	0.096644											
r11.20	0.11	8.41E-06	0.0029	r23.10	4.42E-03	1.36E-08	0.000117	r7.29	3.488	0.00934	0.096644											
r11.21	0.1558	1.69E-05	0.004106	r23.11	4.42E-03	1.36E-08	0.000117	r7.30	3.488	0.00934	0.096644											
r11.22	0.4063	1.15E-04	0.010714	r23.12	4.42E-03	1.36E-08	0.000117	r7.6	3.82	0.01397	0.118195											
r11.23	0.4877	0.000165	0.012861	r23.14	4.42E-03	1.36E-08	0.000117	r7.7	7.63	0.03334	0.182592											
r11.24	0.2108	3.09E-05	0.005559	r23.15	2.44E-02	4.15E-07	0.000644	r7.8	7.63	0.03334	0.182592											
r11.25	0.2769	5.33E-05	0.007301	r23.16	2.17E-01	3.26E-05	0.005709	r8.1	-0.1543	1.65E-05	0.004067											
r11.26	0.2769	5.33E-05	0.007301	r23.17	0.5683	0.000225	0.014983	r8.2	-2.19E-02	3.34E-07	0.000578											
r11.27	0.2529	4.45E-05	0.006668	r23.18	0.3933	1.08E-04	0.010368	r8.3	1.05E-01	7.65E-06	0.002766											
r11.28	0.1227	1.05E-05	0.003236	r23.19	3.08E-02	6.59E-07	0.000811	r8.4	6.87E-02	3.28E-06	0.001811											
r11.29	8.06E-02	4.52E-06	0.002126	r23.2	2.21E-01	3.3																

Table S4.3. Input data and flux analysis results for dilution rate $D = 0.077\text{h}^{-1}$.

Best estimate of the fluxes (mmol/h)				Input rates (mmol/h)		Corresponding covariance matrix									
vest 1	Values	Variances	Serr	r_m 1	Values	Pr_m 1	ara:ext	BIOMasp:	CO2:ext	D-galac:ext	glc:ext	lra:ext	mann:ext	O2:ext	xy:l:ext
ATP GTP Ptrans	1.23E-01	1.10E-05	0.00032	ara:ext	-5.17	ara:ext	0.0338	-0.242	0	0.0129	0.0141	0.0154	0.0153	0	0.017
C120syn	5.47E-03	2.19E-08	0.000148	BIOMasp:cyt	74.26	BIOMasp:cyt	-0.242	4.44	0	-0.184	-0.202	-0.219	-0.219	0	-0.243
C140syn	6.36E-03	2.96E-08	0.000172	CO2:ext	73.25	CO2:ext	0	0	5.77	0	0	0	0	-1.56	0
C141syn	2.73E-03	5.48E-09	0.000074	D-galac:ext	-3.94	D-galac:ext	0.0129	-0.184	0	0.0197	0.0108	0.0117	0.0117	0	0.013
C160syn	4.48E-02	1.47E-06	0.001213	glc:ext	-4.31	glc:ext	0.0141	-0.202	0	0.0108	0.0234	0.0128	0.0128	0	0.0142
C161syn	6.38E-03	2.98E-08	0.000173	lra:ext	-4.69	lra:ext	0.0154	-0.219	0	0.0117	0.0128	0.0281	0.0139	0	0.0155
C162syn	1.82E-03	2.43E-09	4.93E-05	mann:ext	-4.68	mann:ext	0.0153	-0.219	0	0.0117	0.0128	0.0139	0.0277	0	0.0154
C180syn	2.04E-01	3.06E-05	0.005531	O2:ext	-68.85	O2:ext	0	0	-1.56	0	0	0	0	39.9	0
C181CoA syn	2.41E-02	4.25E-07	0.000652	xy:l:ext	-5.2	xy:l:ext	0.017	-0.243	0	0.013	0.0142	0.0155	0.0154	0	0.034
C181syn	0.1977	2.86E-05	0.005351												
C182syn	8.51E-02	5.31E-06	0.002304												
C183syn	7.38E-03	3.99E-08	0.0002												
C200syn	1.37E-03	1.37E-09	0.000037												
Clsyn	3.40E-03	8.47E-09	9.2E-05												
DAGLysyn	9.54E-02	6.67E-06	0.002583												
DGDsyn	1.53E-02	1.72E-07	0.000414												
GDPMANsyn	1.23E-01	1.10E-05	0.00332												
MAGLysyn	1.13E-01	9.32E-06	0.003053												
MGC181 syn	2.41E-02	4.25E-07	0.000652												
MDGD syn	7.38E-02	3.99E-06	0.001998												
r1	4.1	0.01685	0.129808												
r1.2	-13.75	0.1779	0.421782												
r1.3	4.862	0.03526	0.187776												
r1.4	4.862	0.03526	0.187776												
r1.5	19.89	0.2252	0.474552												
r1.6	19.89	0.2252	0.474552												
r1.7	19.05	0.2171	0.46594												
r1.8	19.05	0.2171	0.46594												
r1.9	18.39	0.2114	0.459783												
r10.1	316.2	65.32	0.802079												
r10.10	0.2028	3.01E-05	0.005489												
r10.11	28.2	0.38	0.616441												
r10.12	61.74	2.728	1.651666												
r10.13	0.3108	7.08E-05	0.008412												
r10.14	9.515	0.06633	0.257546												
r10.15	0.2028	3.01E-05	0.005489												
r10.16	0.6888	0.00348	0.018644												
r10.17	0.2745	5.52E-05	0.00743												
r10.18	0.2115	3.28E-05	0.005725												
r10.19	0.3605	9.52E-05	0.009759												
r10.3	255.1	41.49	6.441273												
r10.5	315.2	65.23	8.076509												
r10.6	2.074	0.00315	0.056125												
r10.7	0.2115	3.28E-05	0.005725												
r10.8	0.9957	0.000726	0.02695												
r10.9	0.2028	3.01E-05	0.005489												
r11.1	5.809	0.02473	0.157258												
r11.10	0.3089	6.99E-05	0.008361												
r11.11	9.42E-02	6.51E-06	0.00255												
r11.12	9.42E-02	6.51E-06	0.00255												
r11.13	5.38E-02	1.12E-06	0.001455												
r11.14	5.38E-02	1.12E-06	0.001455												
r11.15	4.05E-02	1.20E-06	0.001095												
r11.16	1.31E+00	0.001256	0.03544												
r11.17	1.07E-01	8.39E-06	0.002897												
r11.18	5.14E-01	0.001994	0.013918												
r11.19	0.4604	0.000155	0.012462												
r12	2.002	0.002936	0.054185												
r12.10	0.1432	1.50E-05	0.003877												
r12.11	0.2028	3.01E-05	0.005489												
r12.12	0.529	0.000205	0.014318												
r12.13	0.635	0.000295	0.017187												
r12.14	0.2745	5.52E-05	0.00743												
r12.15	0.3605	9.52E-05	0.009759												
r12.16	0.3605	9.52E-05	0.009759												
r12.17	0.3293	7.94E-05	0.008913												
r12.18	0.1598	1.87E-05	0.004324												
r12.19	1.05E-01	8.08E-06	0.002842												
r13	2.26E-01	3.74E-05	0.006113												
r13.10	6.45E-02	3.05E-06	0.001747												
r13.11	2.94E-01	6.31E-05	0.007943												
r13.12	1.05E-01	8.08E-06	0.002842												
r14	2.12E-01	3.28E-05	0.005725												
r15	0.2115	3.28E-05	0.005725												
r16	0.2115	3.28E-05	0.005725												
r17	0.3334	8.14E-05	0.009024												
r18	0.3334	8.14E-05	0.009024												
r19	0.8338	0.000509	0.022568												
r21.1	6.83E-02	3.42E-06	0.001848												
r21.2	3.10E-02	7.03E-07	0.000838												
r21.3	3.73E-02	1.02E-06	0.00101												
r21.4	5.57E-02	2.27E-06	0.001507												
r21.5	3.10E-02	7.03E-07	0.000838												
r21.6	3.10E-02	7.03E-07	0.000838												
r21.7	-7.41E-02	4.02E-06	0.002006												
r21.8	8.95E-02	5.86E-06	0.002421												
r21.9	3.13E+00	0.007152	0.084569												
r25.1	254.8	64.79	0.849224												
r26.10	2.98E-02	6.51E-07	0.000807												
Best estimate of the fluxes (mmol/h) continued				Corresponding covariance matrix											
vest 1	Values	Variances	Serr	vest 1	Values	Variances	Serr								
r16.13	5.15E-01	0.0001945	0.013946	r4.7	17.54	0.2962	0.544243								
r16.14	8.59E-02	5.40E-06	0.002324	r4.8	17.54	0.2962	0.544243								
r16.15	8.59E-02	5.40E-06	0.002324	r4.9	17.54	0.2962	0.544243								
r16.16	1.96E-02	2.80E-07	0.000529	r5.1	2.387	0.004175	0.064614								
r16.2	2.18E-01	3.48E-05	0.005897	r5.2	7.442	0.04057	0.20142								
r16.3	0.2297	3.87E-05	0.006219	r5.3	8.52	0.05318	0.236608								
r16.4	0.2297	3.87E-05	0.006219	r6.1	86.44	4.937	2.221936								
r16.5	1.05E-01	8.09E-06	0.002845	r6.2	34.28	6.098	0.780897								
r16.6	1.05E-01	8.09E-06	0.002845	r6.3	17.54	0.2962	0.544243								
r16.7	1.05E-01	8.09E-06	0.002845	r6.4	299.3	57.07	7.554469								
r16.8	9.83E-02	7.08E-06	0.00266	r7.12	4.917	0.2435	0.156045								
r16.9	9.76E-02	6.98E-06	0.002642	r7.13	4.917	0.2435	0.156045								
r17	0.001067	0.032665	0.001067	r7.14	4.917	0.2435	0.156045								
r17.3	0.3505	9.00E-05	0.009487	r7.16	4.447	0.1962	0.140071								
r17.4	9.00E-05	0.009487	0.009487	r7.17	4.447	0.1962	0.140071	</							

Table S4.4. Input data and flux analysis results for dilution rate $D = 0.093\text{h}^{-1}$.

Best estimate of the fluxes (mmol/h)				Input rates (mmol/h)		Corresponding covariance matrix										
vest 1	Values	Variances	Serr	r_m 1	Values	Pr_m 1	ara-ext	BIOMasp	CO2-ext	D-galacex	glc-ext	Lrha-ext	mann-ext	O2-ext	xyI-ext	
ATP GTP Ptrans	0.1511	2.94E-05	0.005418	ara-ext	-6.25	ara-ext	0.0288	-0.352	0	0.0188	0.0208	0.0222	0.0225	0	0.025	
C120syn	0.006735	5.83E-08	0.000242	BIOMasp:cyt	89.3	BIOMasp:cyt	-0.352	10.2	0	-0.266	-0.296	-0.315	-0.32	0	-0.355	
C140syn	0.007831	7.89E-08	0.000281	CO2-ext	83.7	CO2-ext	0	0	7.55	0	0	0	0	-2.18	0	
C141syn	0.003368	1.46E-08	0.000121	D-galac-ext	-4.73	D-galac-ext	0.0188	-0.266	0	0.0166	0.0158	0.0168	0.0171	0	0.0189	
C160syn	0.05519	3.92E-06	0.001979	glc-ext	-5.25	glc-ext	0.0208	-0.296	0	0.0158	0.0203	0.0187	0.0189	0	0.021	
C161syn	0.007858	7.94E-08	0.000282	Lrha-ext	-5.6	Lrha-ext	0.0222	-0.315	0	0.0168	0.0187	0.0233	0.0202	0	0.0224	
C162syn	0.002245	6.48E-09	8.05E-05	mann-ext	-5.68	mann-ext	0.0225	-0.32	0	0.0171	0.0189	0.0202	0.0238	0	0.0228	
C180syn	0.2517	8.15E-05	0.009026	O2-ext	-77	O2-ext	0	0	-2.18	0	0	0	0	39.3	0	
C181CoA syn	0.02968	1.13E-06	0.001064	xyI-ext	-6.31	xyI-ext	0.025	-0.355	0	0.0189	0.021	0.0224	0.0228	0	0.0293	
C181syn	0.2435	7.63E-05	0.008733	Reconciled rates (mmol/h)												
C182syn	0.1048	1.41E-05	0.00376	Corresponding covariance matrix												
C183syn	0.009093	1.06E-07	0.000326	r_m est 1	Values	Pr_m 1	ara-ext	BIOMasp	CO2-ext	D-galacex	glc-ext	Lrha-ext	mann-ext	O2-ext	xyI-ext	
C200syn	0.001684	3.65E-09	6.04E-05	ara-ext	-5.886	ara-ext	0.01974	-0.3435	-0.1532	0.01194	0.01319	0.01401	0.01421	0.1198	0.01584	
DAGLYsyn	0.1175	1.78E-05	0.004215	BIOMasp:cyt	88.93	BIOMasp:cyt	-0.3435	10.17	0.2463	-0.2595	-0.2889	-0.3074	-0.3122	0.7003	-0.3464	
DGDGsyn	0.01885	4.57E-07	0.000676	CO2-ext	89.97	CO2-ext	-0.1532	0.2463	4.431	-0.1162	-0.1287	-0.1382	-0.14	-4.363	-0.1547	
GDPMANsyn	0.1511	2.94E-05	0.005418	D-galac-ext	-4.455	D-galac-ext	0.01194	-0.2595	-0.1162	0.0114	0.0104	0.0106	0.01083	0.08866	0.01197	
MAGLYsyn	0.1389	2.48E-05	0.004982	glc-ext	-4.944	glc-ext	0.01319	-0.2889	-0.1287	0.01004	0.0139	0.0182	0.0194	0.1007	0.01331	
MGC181 syn	0.02968	1.13E-06	0.001064	Lrha-ext	-5.271	Lrha-ext	0.01401	-0.3074	-0.1382	0.0106	0.0182	0.01589	0.01271	0.1102	0.01412	
MGDG syn	0.09093	1.06E-05	0.00326	mann-ext	-5.347	mann-ext	0.01421	-0.3122	-0.14	0.01083	0.0194	0.01271	0.01622	0.1097	0.01443	
r1.1	4.944	0.0139	0.117898	O2-ext	-80.8	O2-ext	0.1198	0.7003	-4.363	0.08866	0.1007	0.1102	0.1097	4.388	0.1212	
r1.2	-16.84	0.3168	0.56285	xyI-ext	-5.942	xyI-ext	0.01584	-0.3464	-0.1547	0.01197	0.01331	0.01412	0.01443	0.1212	0.02005	
r1.3	5.606	0.04138	0.203421	Calculated rates (mmol/h)												
r1.4	5.606	0.04138	0.203421	Corresponding covariance matrix												
r1.5	23.39	0.2611	0.510979	r_c est 1	Values	Pr_c 1	Hext	H2O-ext	NH4-ext	Pi-ext	SO4-ext					
r1.6	23.39	0.2611	0.510979	Hext	4.636	Hext	0.1063	0.3194	-0.1155	-0.0033	-0.00136					
r1.7	22.36	0.2551	0.505074	H2O-ext	113	H2O-ext	0.3194	5.169	-0.3471	-0.00991	-0.00408					
r1.8	22.36	0.2551	0.505074	NH4-ext	-9.88	NH4-ext	-0.1155	-0.3471	0.1255	0.003585	0.001475					
r10.1	364.8	98.66	9.932774	Pi-ext	-0.2821	Pi-ext	-0.0033	-0.00991	0.003585	1.02E-04	4.21E-05					
r10.10	0.2498	8.03E-05	0.008958	SO4-ext	-0.1161	SO4-ext	-0.00136	-0.00408	0.001475	4.21E-05	1.73E-05					
r10.11	33.04	0.4831	0.695054	Best estimate of the fluxes (mmol/h) continued												
r10.12	70.96	4.264	0.264946	vest 1	Values	Variances	Serr	vest 1	Values	Variances	Serr					
r10.13	0.3828	0.000188	0.013726	r16.13	0.6346	0.000518	0.02276	r4.7	19.91	0.5333	0.730274					
r10.14	11.72	0.1767	0.420357	r16.14	0.1058	1.44E-05	0.003793	r4.8	19.91	0.5333	0.730274					
r10.15	0.2498	8.03E-05	0.008958	r16.15	0.1058	1.44E-05	0.003793	r4.9	19.9	0.5334	0.730342					
r10.16	0.8484	0.000926	0.030427	r16.16	0.02408	7.46E-07	0.000863	r5.1	2.94	0.01112	0.105451					
r10.17	0.3381	0.000147	0.012124	r16.17	0.2684	9.26E-05	0.009624	r5.2	9.166	0.1081	0.328786					
r10.18	0.2605	8.73E-05	0.009343	r16.2	0.283	0.000103	0.010149	r5.3	10.49	0.1416	0.376298					
r10.19	0.4441	0.000254	0.015925	r16.3	0.283	0.000103	0.010149	r6.1	99.67	7.389	2.718272					
r10.3	294.7	61.94	7.870197	r16.4	0.1294	2.16E-05	0.004642	r6.2	40.25	0.7279	0.853171					
r10.5	363.6	98.8	9.938199	r16.5	0.1294	2.16E-05	0.004642	r6.3	19.9	0.5334	0.730342					
r10.6	2.554	0.00839	0.091597	r16.6	0.1294	2.16E-05	0.004642	r6.4	345.7	85.06	9.222798					
r10.7	0.2605	8.73E-05	0.009343	r16.7	0.1211	1.89E-05	0.004342	r7.12	5.886	0.01974	0.140499					
r10.8	1.226	0.001934	0.043977	r16.8	0.1211	1.89E-05	0.004342	r7.13	5.886	0.01974	0.140499					
r10.9	0.2498	8.03E-05	0.008958	r16.9	0.1202	1.86E-05	0.00431	r7.16	5.886	0.01974	0.140499					
r11.1	7.156	0.06585	0.256613	r17.2	1.486	0.002841	0.053301	r7.17	5.347	0.01622	0.127358					
r11.10	0.3805	0.000186	0.013646	r17.3	0.4317	0.0002397	0.015482	r7.18	5.347	0.01622	0.127358					
r11.11	0.1161	1.73E-05	0.004163	r17.4	0.4317	0.0002397	0.015482	r7.19	4.455	0.0114	0.106771					
r11.12	0.1161	1.73E-05	0.004163	r17.5	3.841	0.01898	0.137768	r7.2	4.455	0.0114	0.106771					
r11.13	0.06623	5.64E-06	0.002375	r17.6	0.09594	1.18E-05	0.003441	r7.20	4.455	0.0114	0.106771					
r11.14	0.06623	5.64E-06	0.002375	r17.7	0.09594	1.18E-05	0.003441	r7.21	0.1232	1.95E-05	0.004417					
r11.15	0.04983	3.19E-06	0.001787	r17.8	0.7195	0.0006659	0.025805	r7.22	4.455	0.0114	0.106771					
r11.16	1.613	0.003345	0.057836	r17.9	0.1294	2.16E-05	0.004642	r7.23	4.455	0.0114	0.106771					
r11.17	0.1318	2.24E-05	0.004728	r18.1	17.85	0.2675	0.517204	r7.24	4.455	0.0114	0.106771					
r11.18	0.6333	0.000516	0.022713	r18.2	17.85	0.2675	0.517204	r7.25	4.455	0.0114	0.106771					
r11.19	0.5671	0.000414	0.020337	r18.3	10.15	0.06997	0.264518	r7.26	3.355	0.006544	0.080895					
r11.2	2.466	0.00782	0.088431	r18.4	7.34	0.0601	0.245153	r7.27	3.347	0.006519	0.080704					
r11.20	0.1764	4.00E-05	0.006326	r18.5	10.15	0.06997	0.264518	r7.28	5.271	0.01589	0.126056					
r11.21	0.2498	8.03E-05	0.008958	r18.6	10.15	0.06997	0.264518	r7.29	5.271	0.01589	0.126056					
r11.22	0.6516	0.000546	0.023369	r18.7	10.15	0.06997	0.264518	r7.30	5.271	0.01589	0.126056					
r11.23	0.7822	0.000787	0.028052	r18.8	9.022	0.05162	0.2272	r7.31	5.271	0.01589	0.126056					
r11.24	0.3381	0.000147	0.012124	r18.9	2.485	0.007939	0.089101	r7.32	5.271	0.01589	0.126056					
r11.25	0.4441	0.000254	0.015925	r19.1	0.007094	6.47E-08	0.000254	r7.33	5.271	0.01589	0.126056					
r11.26	0.4441	0.000254	0.015925	r19.2	0.007094	6.47E-08	0.000254	r7.34	5.271	0.01589	0.126056					
r11.27	0.4056	0.000212	0.014546	r19.3	0.007094	6.47E-08	0.000254	r7.35	5.942	0.02005	0.141598					
r11.28	0.1968	4.98E-05	0.007058	r19.4	0.007094	6.47E-08	0.000254	r7.36	11.83	0.07147	0.267339					
r11.29	0.1293	2.15E-05	0.004638	r19.5	0.03919	1.98E-06	0.001405	r7.37	11.83	0.07147	0.267339					
r11.3	0.2782	9.95E-05	0.009976	r19.6	0.3473	0.0001551	0.012454	r7.38	-0.2474	1.78E-05	0.008872					
r11.30	0.07948	8.13E-06	0.00285	r19.7	0.9114	0.001068	0.03268	r7.39	-0.03514	1.59E-06	0.00126					
r11.31	0.3615	0.000168	0.012961	r19.8	0.6308	0.0005118	0.022623	r8.1	0.1682	1.64E-05	0.006032					
r11.32	0.1293	2.15E-05	0.004638	r19.9	0.4936	3.13E-06	0.00177	r8.2	0.1102	3.56E-05	0.003951					
r11.4	0.2605	8.73E-05	0.009343	r2.1	0.3545	0.0001617	0.012716	r8.3	0.1102	1.56E-05	0.003951					
r11.5	0.2605	8.73E-05	0.009343	r2.2	2.398	0.007399	0.086017	r8.4	32.82	0.838	0.915423					
r11.6	0.2605	8.73E-05	0.009343	r2.3	2.398	0.007399	0.086017	r8.5	113	5.169	2.735443					
r11.7	0.4107	0.000217	0.014728	r2.4	2.398	0.007399	0.086017	r9.1	5.942	0.02005	0.141598					
r11.8	0.4107	0.000217	0.014728	r2.5	3.071	0.0001213	0.011014	r9.2	0.2821	0.000102	0.010119					
r11.9	1.027	0.001356	0.036824	r2.6	0.2315	6.89E-05	0.008302	r9.3	4.944	0.01399	0.117898					
r13.1	0.08411	9.10E-06	0.003016	r2.7	0.007094	6.47E-08	0.000254	r9.4	3.2	4.455	0.0114	0.106771				
r13.2	0.1876	0.00108	0.004854	r2.8	0.007094	6.47E-08	0.000254	r9.5	9.38	0.125	0.354266					
r13.3	0.04495	2.72E-06	0.001648	r2.9	0.007094	6.47E-08	0.000254	r9.6	5.886	0.01974	0.140499					
r13.4	0.06856	6.05E-06	0.002459	r3.1	20.22	0.4636	0.680882	r9.7	5.347	0.01622	0.127358					
r13.5	0.08616	1.87E-06	0.001368	r4.10	31.29	0.5256	0.724983	r9.8	5.271	0.01589	0.126056					
r13.6	0.08616	1.87E-06	0.001368	r4.11	30.78	0.4601	0.678307	r9.9	0.1161	1.73E-05	0.004163					
r13.7	-0.09129	1.07E-05	0.003274	r4.2	30.78	0.4601	0.678307	r10.6	80.8	4.388	0.294755					
r13.8	0.1102	1.56E-05	0.003951	r4.3	21.61	0.5017	0.708308	r10.7	89.97	4.341	2.019494					
r13.9	3.849	0.01905	0.138022	r4.4	17.77	0.5836	0.763937									

Table S4.5. Input data and flux analysis results for dilution rate $D = 0.110\text{h}^{-1}$.

Best estimate of the fluxes (mmol/					Corresponding covariance matrix													
v est 1	Values	Variances	S err	r_m		Pm 1	ara:ext	BIOMasp:	CO2:ext	D-galac:ext	glc:ext	Lrha:ext	mann:ext	O2:ext	xyL:ext			
ATP GTP P	1.83E-01	3.20E-05	0.005653	ara:ext	-7.02	ara:ext	0.03687	-0.4853	0	0.02411	0.02738	0.02527	0.02967	0	0.03273			
C120syn	8.13E-03	6.35E-08	0.000252	BIOMasp:cyt	110	BIOMasp:	-0.4853	11.59	0	-0.3741	-0.4248	-0.3921	-0.4603	0	-0.5078			
C140syn	9.46E-03	8.59E-08	0.000293	CO2:ext	88.2	CO2:ext	0	0	8.386	0	0	0	0	-2.461	0			
C141syn	4.07E-03	1.59E-08	0.000126	D-galac:ext	-5.41	D-galac:ext	0.02411	-0.3741	0	0.02195	0.02211	0.01948	0.02287	0	0.02523			
C160syn	6.66E-02	4.27E-06	0.002065	glc:ext	-6.15	glc:ext	0.02738	-0.4248	0	0.0211	0.0278	0.02212	0.02597	0	0.02865			
C161syn	9.49E-03	8.65E-08	0.000294	Lrha:ext	-5.66	Lrha:ext	0.02527	-0.3921	0	0.01948	0.02212	0.02614	0.02397	0	0.02644			
C162syn	2.71E-03	7.06E-09	8.4E-05	mann:ext	-6.66	mann:ext	0.02967	-0.4603	0	0.02287	0.02597	0.02397	0.03272	0	0.03104			
C180syn	3.04E-01	8.87E-05	0.009419	O2:ext	-80.3	O2:ext	0	0	-2.461	0	0	0	0	39.03	0			
C181CoA c	3.58E-02	1.23E-06	0.001111	xyL:ext	-7.35	xyL:ext	0.03273	-0.5078	0	0.02523	0.02865	0.02644	0.03104	0	0.03986			
C181syn	0.2941	8.31E-05	0.009114															
C182syn	1.27E-01	1.54E-05	0.003924	Reconciled rates (mmol/h)					Corresponding covariance matrix									
C183syn	1.10E-02	1.16E-07	0.00034															
C200syn	2.03E-03	3.97E-09	6.3E-05	r_m est 1	Values	Pr_m 1	ara:ext	BIOMasp:	CO2:ext	D-galac:ext	glc:ext	Lrha:ext	mann:ext	O2:ext	xyL:ext			
CLsyn	5.06E-03	2.46E-08	0.000157	ara:ext	-6.14	ara:ext	0.02443	-0.4067	-0.1959	0.01457	0.01653	0.01492	0.01785	0.1552	0.01975			
DAGLYSyn	1.42E-01	1.94E-05	0.004399	BIOMasp:cyt	107.4	BIOMasp:	-0.4067	11.08	1.336	-0.3137	-0.3563	-0.3268	-0.3856	-0.2698	-0.4258			
DGDSyn	2.28E-02	4.98E-07	0.000705	CO2:ext	94.85	CO2:ext	-0.1959	1.336	4.683	-0.1508	-0.1709	-0.1626	-0.1862	-4.504	-0.2045			
GDPMAN	1.82E-01	3.20E-05	0.005653	D-galac:ext	-5.098	D-galac:ext	0.01457	-0.3137	-0.1508	0.01463	0.01278	0.01154	0.0138	0.116	0.01527			
MAGLYSyn	1.68E-01	2.70E-05	0.005199	glc:ext	-5.796	glc:ext	0.01653	-0.3563	-0.1709	0.01278	0.01834	0.01309	0.01566	0.1352	0.01732			
MGCD181 s	3.58E-02	1.23E-06	0.001111	Lrha:ext	-5.322	Lrha:ext	0.01492	-0.3268	-0.1626	0.01154	0.01309	0.01753	0.01413	0.1328	0.01564			
MGDG syri	1.10E-01	1.16E-05	0.003403	mann:ext	-6.274	mann:ext	0.01785	-0.3856	-0.1862	0.0138	0.01566	0.01413	0.02149	0.1476	0.01871			
r1.1	5.796	0.01834	0.135425	O2:ext	-83.53	O2:ext	0.1552	-0.2698	-4.504	0.116	0.1352	0.1328	0.1476	4.432	0.1619			
r1.2	-20.66	0.3693	0.607701	xyL:ext	-6.926	xyL:ext	0.01975	-0.4258	-0.2045	0.01527	0.01732	0.01564	0.01871	0.1619	0.02631			
r1.3	5.868	0.04115	0.202855															
r1.4	5.868	0.04115	0.202855	Calculated rates (mmol/h)					Corresponding covariance matrix									
r1.5	25.96	0.3076	0.554617															
r1.6	25.96	0.3076	0.554617	r_c est 1	Values	Pr_c 1	H:ext	H2O:ext	NH4:ext	Pi:ext	SO4:ext							
r1.7	24.72	0.2939	0.542125	H:ext	5.879	H:ext	0.1157	0.4538	-0.1258	-0.00359	-0.00148							
r1.8	24.72	0.2939	0.542125	H2O:ext	122.9	H2O:ext	0.4538	6.081	-0.4932	-0.01408	-0.00579							
r1.9	23.74	0.2852	0.534041	NH4:ext	-11.93	NH4:ext	-0.1258	-0.4932	0.1367	0.003904	0.001606							
r10.1	373.9	98.02	9.900505	Pi:ext	-0.3407	Pi:ext	-0.00359	-0.01408	0.003904	1.12E-04	4.59E-05							
r10.10	0.3016	8.74E-05	0.009349	SO4:ext	-0.1402	SO4:ext	-0.00148	-0.00579	0.001606	4.59E-05	1.89E-05							
r10.11	35.25	0.5405	0.735187															
r10.12	71.74	4.158	2.039117															
r10.13	0.4622	0.000205	0.014325	Best estimate of the fluxes (mmol/h) continued														
r10.14	14.15	0.1924	0.438634															
r10.15	0.3016	8.74E-05	0.009349	v est 1	Values	Variances	S err		v est 1	Values	Variances	S err						
r10.16	1.025	0.001008	0.031749	r16.13	0.7664	0.0005642	0.023753		r4.7	19.39	0.4996	0.706824						
r10.17	0.4083	0.00016	0.012653	r16.14	0.1277	1.57E-05	0.003959		r4.8	19.39	0.4996	0.706824						
r10.18	0.3146	9.51E-05	0.00975	r16.15	0.1277	1.57E-05	0.003959		r4.9	19.39	0.4996	0.706824						
r10.19	0.5363	0.000276	0.016619	r16.16	0.02907	8.12E-07	0.000901		r5.1	3.551	0.01211	0.110045						
r10.3	303.2	61.93	7.869562	r16.2	0.3241	0.0001009	0.010045		r5.2	11.07	0.1177	0.343074						
r10.5	372.4	98.04	9.901515	r16.3	0.3417	0.0001122	0.010592		r5.3	12.67	0.1543	0.39281						
r10.6	3.084	0.009138	0.059593	r16.4	0.3417	0.0001122	0.010592		r6.1	101.8	7.331	2.707582						
r10.7	0.3146	9.51E-05	0.00975	r16.5	0.1563	2.35E-05	0.004845		r6.2	43.77	0.8396	0.916297						
r10.8	1.481	0.002107	0.045902	r16.6	0.1563	2.35E-05	0.004845		r6.3	19.39	0.4996	0.706824						
r10.9	0.3016	8.74E-05	0.009349	r16.7	0.1563	2.35E-05	0.004845		r6.4	355.5	85.05	9.222256						
r11.1	8.641	0.07172	0.267806	r16.8	0.1462	2.05E-05	0.004531		r7.12	6.614	0.02443	0.156301						
r11.10	0.4955	0.000203	0.014241	r16.9	0.1452	2.02E-05	0.004499		r7.13	6.614	0.02443	0.156301						
r11.11	1.40E-01	1.89E-05	0.004344	r17.2	1.795	0.003095	0.055633		r7.14	6.614	0.02443	0.156301						
r11.12	1.40E-01	1.89E-05	0.004344	r17.3	0.5213	0.0002611	0.016159		r7.16	6.274	0.02149	0.146595						
r11.13	8.00E-02	6.15E-06	0.002479	r17.4	0.5213	0.0002611	0.016159		r7.17	6.274	0.02149	0.146595						
r11.14	8.00E-02	6.15E-06	0.002479	r17.5	4.639	0.02067	0.143771		r7.18	5.098	0.01463	0.120955						
r11.15	6.02E-02	3.48E-06	0.001865	r17.6	0.1159	1.29E-05	0.00359		r7.19	5.098	0.01463	0.120955						
r11.16	1.95E+00	0.003643	0.060357	r17.7	0.1159	1.29E-05	0.00359		r7.2	0.1487	2.13E-05	0.00461						
r11.17	1.59E-01	2.44E-05	0.004935	r17.8	0.8689	0.0007252	0.02693		r7.20	5.098	0.01463	0.120955						
r11.18	7.65E-01	0.005062	0.023702	r2.1	21.7	0.3273	0.572101		r7.21	5.098	0.01463	0.120955						
r11.19	0.6848	0.000451	0.021225	r2.2	21.7	0.3273	0.572101		r7.22	5.098	0.01463	0.120955						
r11.2	2.978	0.008517	0.092288	r2.3	12.05	0.08674	0.294517		r7.23	3.771	0.008568	0.092563						
r11.20	0.213	4.36E-05	0.006602	r2.4	9.207	0.07262	0.269481		r7.24	3.761	0.008535	0.092385						
r11.21	0.3016	8.74E-05	0.009349	r2.5	12.05	0.08674	0.294517		r7.25	5.322	0.01753	0.132401						
r11.22	0.7869	0.000595	0.024389	r2.6	12.05	0.08674	0.294517		r7.26	5.322	0.01753	0.132401						
r11.23	0.9446	0.000857	0.029275	r2.7	10.69	0.06526	0.25546		r7.27	5.322	0.01753	0.132401						
r11.24	0.4083	0.00016	0.012653	r23.1	3	0.008647	0.092989		r7.28	5.322	0.01753	0.132401						
r11.25	0.5363	0.000276	0.016619	r23.10	0.008566	7.05E-08	0.000265		r7.29	5.322	0.01753	0.132401						
r11.26	0.5363	0.000276	0.016619	r23.11	0.008566	7.05E-08	0.000265		r7.30	5.322	0.01753	0.132401						
r11.27	0.4898	0.00023	0.015179	r23.12	0.008566	7.05E-08	0.000265		r7.6	6.926	0.02631	0.162204						
r11.28	0.2377	5.43E-05	0.007366	r23.14	0.008566	7.05E-08	0.000265		r7.7	13.54	0.09024	0.3004						
r11.29	0.1562	2.34E-05	0.004839	r23.15	0.04733	2.15E-06	0.001467		r7.8	13.54	0.09024	0.3004						
r11.3	0.3359	0.000108	0.010412	r23.16	0.4193	0.0001689	0.012996		r8.1	-0.2987	8.57E-05	0.009259						
r11.30	0.09598	8.85E-06	0.002975	r23.17	1.101	0.001164	0.034117		r8.2	-0.04243	1.73E-06	0.001315						
r11.31	0.4365	0.000183	0.013528	r23.18	0.7617	0.0005574	0.023609		r8.3	0.2031	3.96E-05	0.006296						
r11.32	0.1562	2.34E-05	0.004839	r23.19	0.05961	3.41E-06	0.001847		r8.4	0.133	1.70E-05	0.004123						
r11.4	0.3146	9.51E-05	0.00975	r23.2	0.4281	0.0001761	0.01327		r8.5	0.133	1.70E-05	0.004123						
r11.5	0.3146	9.51E-05	0.00975	r23.21	2.896	0.008058	0.089766		r9.1	37.77	0.9949	0.997447						
r11.6	0.3146	9.51E-05	0.00975	r23.22	2.896	0.008058	0.089766		r9.15	122.9	6.081	2.465988						
r11.7	0.4959	0.000236																

Table S4.6. Input data and flux analysis results for dilution rate $D = 0.127\text{h}^{-1}$.

Best estimate of the fluxes (mmol/ input rates (mmol/h)							Corresponding covariance matrix													
vest 1	Values	Variances	Serr	r_m 1	Values		Pr_m 1	ara:ext	BIOMasp:	CO2:ext	D-galace:	glc:ext	Lrha:ext	mann:ext	O2:ext	xyf:ext				
ATP GTP P	1.92E-01	5.43E-05	0.007367	ara:ext	-7.62		ara:ext	0.0453	-0.53	0	0.0298	0.0346	0.0209	0.0374	0	0.0402				
C120syn	8.56E-03	1.08E-07	0.000328	BIOMasp:	110		BIOMasp:	-0.53	19.3	0	-0.429	-0.497	-0.3	-0.538	0	-0.578				
C140syn	9.96E-03	1.46E-07	0.000382	CO2:ext	92.5		CO2:ext	0	0	9.24	0	0	0	0	-2.74	0				
C141syn	4.28E-03	2.70E-08	0.000164	D-galace:	-6.17		D-galace:	0.0298	-0.429	0	0.0287	0.028	0.0169	0.0303	0	0.0325				
C160syn	7.02E-02	7.24E-06	0.002691	glc:ext	-7.15		glc:ext	0.0346	-0.497	0	0.028	0.0376	0.0196	0.0351	0	0.0377				
C161syn	9.99E-03	1.47E-07	0.000383	Lrha:ext	-4.3		Lrha:ext	0.0209	-0.3	0	0.0169	0.0196	0.0248	0.0212	0	0.0228				
C162syn	2.85E-03	1.20E-08	0.000109	mann:ext	-7.74		mann:ext	0.0374	-0.538	0	0.0303	0.0351	0.0212	0.0441	0	0.0408				
C180syn	3.20E-01	0.000151	0.012276	O2:ext	-83.3		O2:ext	0	0	-2.74	0	0	0	0	38.8	0				
C181CoA	3.77E-02	2.10E-06	0.001447	xyf:ext	-8.31		xyf:ext	0.0402	-0.578	0	0.0325	0.0377	0.0228	0.0408	0	0.052				
C181syn	0.3096	0.000141	0.011874																	
C182syn	1.33E-01	2.62E-05	0.005114	Reconciled rates (mmol/h)																
C183syn	1.16E-02	1.97E-07	0.000044																	
C200syn	2.14E-03	6.74E-09	8.21E-05	r_m est 1	Values		Pr_m 1	ara:ext	BIOMasp:	CO2:ext	D-galace:	glc:ext	Lrha:ext	mann:ext	O2:ext	xyf:ext				
CLyn	5.32E-03	4.17E-08	0.000204	ara:ext	-7.045		ara:ext	0.03268	-0.5984	-0.1756	0.01974	0.02293	0.01265	0.02472	0.1128	0.02655				
DAGLysyn	1.49E-01	3.29E-05	0.005732	BIOMasp:	113.1		BIOMasp:	-0.5984	18.81	-0.6589	-0.4833	-0.5602	-0.3454	-0.6067	2.524	-0.652				
DGDG syn	2.40E-02	8.45E-07	0.000919	CO2:ext	100.6		CO2:ext	-0.1756	-0.6589	6.05	-0.1408	-0.1626	-0.1133	-0.1767	-6.021	-0.1901				
GDPMAN:	1.92E-01	5.43E-05	0.007367	D-galace:	-5.711		D-galace:	0.01974	-0.4833	-0.1408	0.02697	0.01869	0.01032	0.02018	0.08534	0.02161				
MAGLysyn	1.77E-01	4.59E-05	0.006775	glc:ext	-6.618		glc:ext	0.02293	-0.5602	-0.1626	0.01869	0.0268	0.01196	0.02337	0.1036	0.02507				
MGC181 s	3.77E-02	2.10E-06	0.001447	Lrha:ext	-3.924		Lrha:ext	0.01265	-0.3454	-0.1133	0.01032	0.01196	0.0194	0.0129	0.08416	0.01387				
MGDG syn	1.16E-01	1.97E-05	0.004435	mann:ext	-7.162		mann:ext	0.02472	-0.6067	-0.1767	0.02018	0.02337	0.0129	0.0135	0.1128	0.02707				
r1.1	6.618	0.0268	0.163707	O2:ext	-87.55		O2:ext	0.1128	2.524	-6.021	0.08534	0.1036	0.08416	0.1128	6.186	0.1216				
r1.2	-23.53	0.6569	0.810494	xyf:ext	-7.687		xyf:ext	0.02655	-0.652	-0.1901	0.02161	0.02507	0.01387	0.02707	0.1216	0.03723				
r1.3	6.8	0.06572	0.256359	Calculated rates (mmol/h)																
r1.4	6.8	0.06572	0.256359																	
r1.5	29.85	0.4105	0.640703	r_c est 1	Values		Pr_c 1	H:ext	H2O:ext	NH4:ext	Pi:ext	SO4:ext								
r1.6	29.85	0.4105	0.640703	H:ext	5.846		H:ext	0.1965	0.4764	-0.2136	-0.0061	-0.00251								
r1.7	28.54	0.3993	0.631902	H2O:ext	129.8		H2O:ext	0.4764	6.875	-0.5178	-0.01479	-0.00608								
r1.8	28.54	0.3993	0.631902	NH4:ext	-12.56		NH4:ext	-0.2136	-0.5178	0.2322	0.00663	0.002728								
r1.9	390.4	141.7	11.90378	Pi:ext	-0.3587		Pi:ext	-0.0061	-0.01479	0.00663	1.89E-04	7.79E-05								
r10.1	0.3176	0.000148	0.012182	SO4:ext	-0.1476		SO4:ext	-0.00251	-0.00608	0.002728	7.79E-05	3.20E-05								
r10.11	36.6	0.6223	0.78886																	
r10.12	74.02	6.275	2.504995																	
r10.13	0.4867	0.000349	0.018668	Best estimate of the fluxes (mmol/h) continued																
r10.14	14.9	0.3267	0.571577	vest 1	Values	Variances	Serr	vest 1	Values	Variances	Serr									
r10.15	0.3176	0.000148	0.012182	r16.13	0.8068	0.000958	0.030952	r4.7	19.91	0.8442	0.918804									
r10.16	1.079	0.001712	0.041376	r16.14	0.1345	2.66E-05	0.005158	r4.8	19.91	0.8442	0.918804									
r10.17	0.4299	0.000272	0.016489	r16.15	0.1345	2.66E-05	0.005158	r4.9	19.91	0.8443	0.918858									
r10.18	0.3312	0.000161	0.012704	r16.16	0.03061	1.38E-06	0.001174	r5.1	3.738	0.02057	0.143422									
r10.19	0.5646	0.000469	0.021659	r16.16	0.03061	1.38E-06	0.001174	r5.2	11.65	0.1999	0.447102									
r10.3	317.4	88.34	9.398936	r16.2	0.3412	0.0001713	0.013088	r5.3	13.34	0.2619	0.511762									
r10.5	388.8	142.1	11.92057	r16.3	0.3598	0.0001905	0.013802	r6.1	105.1	10.6	3.255764									
r10.6	3.247	0.01552	0.124579	r16.4	0.3598	0.0001905	0.013802	r6.2	47.81	1.031	0.105382									
r10.7	0.3312	0.000161	0.012704	r16.5	0.1646	3.99E-05	0.006313	r6.3	19.91	0.8443	0.918858									
r10.8	1.559	0.003577	0.059808	r16.6	0.1646	3.99E-05	0.006313	r6.4	371.5	121.2	11.0909									
r10.9	0.3176	0.000148	0.012182	r16.7	0.1646	3.99E-05	0.006313	r7.12	7.045	0.03268	0.180776									
r11.1	9.097	0.1218	0.348999	r16.8	0.1539	3.49E-05	0.005905	r7.13	7.045	0.03268	0.180776									
r11.10	0.4867	0.000349	0.018668	r16.9	0.1528	3.44E-05	0.005863	r7.14	7.045	0.03268	0.180776									
r11.11	1.48E-01	3.20E-05	0.00566	r17.2	1.89	0.005255	0.072491	r7.15	7.045	0.03268	0.180776									
r11.12	1.48E-01	3.20E-05	0.00566	r17.3	0.5489	0.0004433	0.021055	r7.16	7.162	0.03135	0.177059									
r11.13	8.42E-02	1.04E-05	0.00323	r17.4	0.5489	0.0004433	0.021055	r7.17	7.162	0.03135	0.177059									
r11.14	8.42E-02	1.04E-05	0.00323	r17.5	4.884	0.0351	0.18735	r7.18	5.711	0.02067	0.143771									
r11.15	6.34E-02	5.91E-06	0.00243	r17.6	0.122	2.19E-05	0.004679	r7.19	5.711	0.02067	0.143771									
r11.16	2.05E+00	0.006186	0.078651	r17.7	0.122	2.19E-05	0.004679	r7.2	0.1566	3.61E-05	0.006007									
r11.17	1.68E-01	4.13E-05	0.00643	r17.8	0.9148	0.001232	0.0351	r7.20	5.711	0.02067	0.143771									
r11.18	8.05E-01	0.000954	0.030889	r2.1	25.14	0.573	0.756968	r7.21	5.711	0.02067	0.143771									
r11.19	0.721	0.000765	0.027657	r2.2	25.14	0.573	0.756968	r7.22	5.711	0.02067	0.143771									
r11.2	3.135	0.04465	0.12025	r2.3	13.62	0.14	0.374166	r7.23	4.314	0.0116	0.107703									
r11.20	0.2243	7.40E-05	0.008603	r2.4	11.07	0.1377	0.37108	r7.24	4.303	0.0155	0.107471									
r11.21	0.3176	0.000148	0.012182	r2.5	13.62	0.14	0.374166	r7.25	3.924	0.0194	0.139284									
r11.22	0.8284	0.00101	0.03178	r2.6	13.62	0.14	0.374166	r7.26	3.924	0.0194	0.139284									
r11.23	0.9944	0.001455	0.038144	r2.7	12.19	0.1047	0.323574	r7.27	3.924	0.0194	0.139284									
r11.24	0.4299	0.000272	0.016489	r2.8	3.159	0.01468	0.121161	r7.28	3.924	0.0194	0.139284									
r11.25	0.5646	0.000469	0.021659	r2.9	0.009018	1.20E-07	0.000346	r7.29	3.924	0.0194	0.139284									
r11.26	0.5646	0.000469	0.021659	r2.11	0.009018	1.20E-07	0.000346	r7.30	3.924	0.0194	0.139284									
r11.27	0.5157	0.000391	0.019781	r2.12	0.009018	1.20E-07	0.000346	r7.6	7.687	0.03723	0.192951									
r11.28	0.2502	9.21E-05	0.009598	r2.13	0.009018	1.20E-07	0.000346	r7.7	14.73	0.123	0.350714									
r11.29	0.1644	3.98E-05	0.006307	r2.15	0.04983	3.65E-06	0.001911	r7.8	14.73	0.123	0.350714									
r11.3	0.3537	0.000184	0.013568	r2.16	0.4415	0.0002868	0.016935	r8.1	-0.3145	0.000146	0.012066									
r11.30	0.101	1.50E-05	0.003877	r2.17	1.159	0.001976	0.044452	r8.2	-0.04467	2.94E-06	0.001713									
r11.31	0.4596	0.000311	0.01763	r2.18	0.802	0.0009465	0.030765	r8.3	0.2139	6.73E-05	0.008204									
r11.32	0.1644	3.98E-05	0.006307	r2.19	0.12375	5.80E-06	0.002407	r8.4	0.1401	2.89E-05	0.005373									
r11.4	0.3312	0.000161	0.012704	r2.20	0.4507	0.000299	0.017292	r8.5	0.1401	2.89E-05	0.005373									
r11.5	0.3312	0.000161	0.012704	r2.21	3.049	0.01368	0.116962	r9.1	39.29	1.396	1.181524									
r11.6	0.3312	0.000161	0.012704																	

Table S4.7. Input data and flux analysis results for dilution rate $D = 0.144\text{h}^{-1}$.

Best estimate of the fluxes (mmol/ Input rates (mmol/h)							Corresponding covariance matrix											
vest 1	Values	Variances	Serr	r_m 1	Values		Pm 1	ara:ext	BIOMasp:	CO2:ext	D-galac:ext	glc:ext	Lrha:ext	mann:ext	O2:ext	xyf:ext		
ATP GTP P	2.44E-01	0.000104	0.010183	ara:ext	-8.52		ara:ext	0.0561	-0.7	0	0.0371	0.0437	0.0166	0.0473	0	0.0503		
C120syn	1.09E-02	2.06E-07	0.000454	BIOMasp:	130		BIOMasp:	-0.7	58.7	0	-0.563	-0.663	-0.251	-0.717	0	-0.763		
C140syn	1.26E-02	2.79E-07	0.000528	CO2:ext	93.6		CO2:ext	0	0	9.46	0	0	0	0	-2.7	0		
C141syn	5.43E-03	5.15E-08	0.000227	D-galac:ext	-6.86		D-galac:ext	0.0371	-0.563	0	0.0355	0.0352	0.0133	0.0381	0	0.0405		
C160syn	8.90E-02	1.38E-05	0.00372	glc:ext	-8.08		glc:ext	0.0437	-0.663	0	0.0352	0.048	0.0157	0.0448	0	0.0476		
C161syn	1.27E-02	2.81E-07	0.00053	Lrha:ext	-3.02		Lrha:ext	0.0166	-0.251	0	0.0133	0.0157	0.0217	0.017	0	0.018		
C162syn	3.62E-03	2.29E-08	0.000151	mann:ext	-8.74		mann:ext	0.0473	-0.717	0	0.0381	0.0448	0.017	0.0563	0	0.0515		
C180syn	4.06E-01	0.000288	0.016965	O2:ext	-82.4		O2:ext	0	0	-2.7	0	0	0	0	38.9	0		
C181CoA	4.79E-02	4.00E-06	0.002	xyf:ext	-9.3		xyf:ext	0.0503	-0.763	0	0.0405	0.0476	0.018	0.0515	0	0.0677		
C181syn	0.3928	0.000269	0.016413															
C182syn	1.69E-01	5.00E-05	0.007068	Reconciled rates (mmol/h) Corresponding covariance matrix														
C183syn	1.47E-02	3.76E-07	0.000613															
C200syn	2.72E-03	1.29E-08	0.000113	r_m est 1	Values		Pr_m 1	ara:ext	BIOMasp:	CO2:ext	D-galac:ext	glc:ext	Lrha:ext	mann:ext	O2:ext	xyf:ext		
CLsyn	6.76E-03	7.97E-08	0.000282	ara:ext	-8.261		ara:ext	0.04899	-1.081	-0.1025	0.03143	0.03704	0.01328	0.04004	-0.0168	0.04245		
DAGLYsyn	1.90E-01	6.28E-05	0.007923	BIOMasp:	143.5		BIOMasp:	-1.081	35.94	-4.202	-0.8655	-1.02	-0.4329	-1.106	7.821	-1.184		
DGOG syn	3.04E-02	1.61E-06	0.00127	CO2:ext	97.56		CO2:ext	-0.1025	-4.202	7.267	-0.08252	-0.09611	-0.04557	-0.1046	-7.555	-0.1129		
GDPMAN:	2.44E-01	0.000104	0.010183	D-galac:ext	-6.653		D-galac:ext	0.03143	-0.8655	-0.08252	0.03098	0.02989	0.01066	0.03231	-0.01466	0.03244		
MAGLYsyn	2.24E-01	8.77E-05	0.009363	glc:ext	-7.837		glc:ext	0.03704	-1.02	-0.09611	0.02989	0.04176	0.01259	0.038	-0.01178	0.04025		
MGC181 s	4.79E-02	4.00E-06	0.002	Lrha:ext	-2.9		Lrha:ext	0.01328	-0.4329	-0.04557	0.01066	0.01259	0.02014	0.01361	0.009202	0.01434		
MGDG syri	1.47E-01	3.76E-05	0.006129	mann:ext	-8.476		mann:ext	0.04004	-1.106	-0.1046	0.03231	0.038	0.01361	0.0489	-0.01231	0.04349		
r1.1	7.837	0.04176	0.204353	O2:ext	-80.49		O2:ext	-0.01168	7.821	-7.555	-0.01466	-0.01178	0.009202	-0.01231	8.221	-0.012		
r1.2	-30.86	1.279	1.130929	xyf:ext	-9.014		xyf:ext	0.04245	-1.184	-0.1129	0.03424	0.04025	0.01434	0.04349	-0.012	0.05904		
r1.3	6.365	0.0967	0.310966															
r1.4	6.365	0.0967	0.310966	Calculated rates (mmol/h) Corresponding covariance matrix														
r1.5	32.43	0.4867	0.697639															
r1.6	32.43	0.4867	0.697639	r_c est 1	Values		Pr_c 1	H:ext	H2O:ext	NH4:ext	Pi:ext	SO4:ext						
r1.7	30.77	0.4767	0.690435	H:ext	8.011		H:ext	0.3754	0.615	-0.4081	-0.01165	-0.00479						
r1.8	30.77	0.4767	0.690435	H2O:ext	135.2		H2O:ext	0.615	7.426	-0.6685	-0.01909	-0.00785						
r1.9	29.46	0.4755	0.689565	NH4:ext	-15.94		NH4:ext	-0.4081	-0.6685	0.4435	0.01266	0.00521						
r1.0.1	350	196.3	14.01071	Pi:ext	-0.4551		Pi:ext	-0.01165	-0.01909	0.01266	3.62E-04	1.49E-04						
r1.0.10	0.403	0.000284	0.016837	SO4:ext	-0.1872		SO4:ext	-0.00479	-0.00785	0.00521	1.49E-04	6.12E-05						
r1.0.11	36.25	0.6635	0.814555															
r1.0.12	63.33	9.172	3.028531															
r1.0.13	0.6175	0.000666	0.025801	Best estimate of the fluxes (mmol/h) continued														
r1.0.14	18.91	0.6241	0.79	vest 1	Values	Variances	Serr		vest 1	Values	Variances	Serr						
r1.0.15	0.403	0.000284	0.016837	r16.13	1.024	0.00183	0.042778		r4.7	15.07	1.385	1.17686						
r1.0.16	1.369	0.003271	0.057193	r16.14	0.1706	5.08E-05	0.00713		r4.8	15.07	1.385	1.17686						
r1.0.17	0.5454	0.000519	0.02279	r16.15	0.1706	5.08E-05	0.00713		r4.9	15.06	1.385	1.17686						
r1.0.18	0.4203	0.000308	0.017561	r16.16	0.03884	2.63E-06	0.001623		r5.1	4.744	0.03928	0.198192						
r1.0.19	0.7164	0.000896	0.029933	r16.2	0.4329	0.0003272	0.018089		r5.2	14.79	0.03817	0.617819						
r1.0.3	288.1	120.4	10.97269	r16.3	0.4565	0.0003638	0.019074		r5.3	16.93	0.5003	0.707319						
r1.0.5	348.1	197.5	14.05347	r16.4	0.4565	0.0003638	0.019074		r6.1	92.6	14.79	3.845777						
r1.0.6	4.12	0.02964	0.172163	r16.5	0.2088	7.61E-05	0.008725		r6.2	50.45	1.168	1.08074						
r1.0.7	0.4203	0.000308	0.017561	r16.6	0.2088	7.61E-05	0.008725		r6.3	15.06	1.385	1.17686						
r1.0.8	1.978	0.006833	0.082662	r16.7	0.2088	7.61E-05	0.008725		r6.4	336.2	165.2	12.85302						
r1.0.9	0.403	0.000284	0.016837	r16.8	0.1953	6.66E-05	0.008161		r7.12	8.261	0.04899	0.221337						
r1.1	11.54	0.2326	0.482286	r16.9	0.1939	6.57E-05	0.008102		r7.13	8.261	0.04899	0.221337						
r1.1.10	0.6138	0.000658	0.025646	r17.2	2.398	0.01004	0.1002		r7.14	8.261	0.04899	0.221337						
r1.1.11	1.87E-01	6.12E-05	0.007824	r17.3	0.6965	0.0008469	0.029102		r7.16	8.476	0.0489	0.221133						
r1.1.12	1.87E-01	6.12E-05	0.007824	r17.4	0.6965	0.0008469	0.029102		r7.17	8.476	0.0489	0.221133						
r1.1.13	1.07E-01	1.99E-05	0.004464	r17.5	6.197	0.06705	0.25894		r7.18	6.653	0.03908	0.176011						
r1.1.14	1.07E-01	1.99E-05	0.004464	r17.6	0.1548	4.18E-05	0.006467		r7.19	6.653	0.03908	0.176011						
r1.1.15	8.04E-02	1.13E-05	0.003359	r17.7	0.1548	4.18E-05	0.006467		r7.2	0.1987	6.89E-05	0.008302						
r1.1.16	2.60E+00	0.01182	0.10872	r17.8	1.161	0.002352	0.048497		r7.20	6.653	0.03908	0.176011						
r1.1.17	2.13E-01	7.90E-05	0.008887	r17.8	1.161	0.002352	0.048497		r7.20	6.653	0.03908	0.176011						
r1.1.18	1.02E+00	0.001822	0.042685	r2.1	32.34	1.094	1.045945		r7.21	6.653	0.03908	0.176011						
r1.1.19	0.9148	0.001461	0.038223	r2.2	32.34	1.094	1.045945		r7.22	6.653	0.03908	0.176011						
r1.1.2	3.978	0.02762	0.166193	r2.3	16.95	0.2547	0.504678		r7.23	4.88	0.01507	0.12276						
r1.1.20	0.2846	0.000141	0.011891	r2.4	14.81	0.2725	0.522015		r7.24	4.867	0.01499	0.122434						
r1.1.21	0.403	0.000284	0.016837	r2.5	16.95	0.2547	0.504678		r7.25	2.9	0.02014	0.141915						
r1.1.22	1.051	0.001929	0.04392	r2.6	16.95	0.2547	0.504678		r7.26	2.9	0.02014	0.141915						
r1.1.23	1.262	0.00278	0.052726	r2.7	15.14	0.1876	0.433128		r7.27	2.9	0.02014	0.141915						
r1.1.24	0.5454	0.000519	0.02279	r2.8	0.008	0.02805	0.167481		r7.28	2.9	0.02014	0.141915						
r1.1.25	0.7164	0.000896	0.029933	r2.9	0.01144	2.29E-07	0.000478		r7.29	2.9	0.02014	0.141915						
r1.1.26	0.7164	0.000896	0.029933	r2.10	0.01144	2.29E-07	0.000478		r7.30	2.9	0.02014	0.141915						
r1.1.27	0.6543	0.000748	0.02734	r2.11	0.01144	2.29E-07	0.000478		r7.6	9.014	0.05904	0.242981						
r1.1.28	0.3175	0.000176	0.013266	r2.12	0.01144	2.29E-07	0.000478		r7.7	17.28	0.1929	0.439204						
r1.1.29	0.2086	7.60E-05	0.008717	r2.13	0.01144	2.29E-07	0.000478		r7.8	17.28	0.1929	0.439204						
r1.1.3	0.4488	0.000352	0.018751	r2.14	0.5602	0.0005479	0.023407		r8.1	-0.3991	0.000278	0.016676						
r1.1.30	0.1282	2.87E-05	0.005357	r2.15	1.47	0.003774	0.061433		r8.2	-0.05668	5.61E-06	0.002368						
r1.1.31	0.5831	0.000594	0.024364	r2.16	1.018	0.001808	0.042521		r8.3	0.2714	0.000129	0.01134						
r1.1.32	0.2086	7.60E-05	0.008717	r2.17	0.07963	1.11E-05	0.003327		r8.4	0.1777	5.52E-05	0.007426						
r1.1.4	0.4203	0.000308	0.017561	r2.2	0.572	0.0005711	0.023898		r8.5	0.1777	5.52E-05	0.007426						
r1.1.5	0.4203	0.000308	0.017561	r2.21	3.869	0.02614	0.161679		r9.1	45.78								

Table S4.8. Input data and flux analysis results for dilution rate $D = 0.160\text{h}^{-1}$.

Best estimate of the fluxes (mmol/ Input rates (mmol/h)					Corresponding covariance matrix									
vest 1	Values	Variances	Serr	r_m		Pm 1	ara:ext	BIOMasp:CO2:ext	D-galac:ex	glc:ext	Urha:ext	mann:ext	O2:ext	xyL:ext
ATP GTP P	2.69E-01	0.000119	0.010927	ara:ext	-8.14	ara:ext	0.05402	-0.7421	0	0.03709	0.04628	0.0131	0.04954	0 0.05088
C120syn	1.20E-02	2.37E-07	0.000487	BIOMasp:	145	BIOMasp:	-0.7421	78.49	0	-0.6528	-0.8145	-0.2306	-0.8721	0 -0.8955
C140syn	1.39E-02	3.21E-07	0.000566	CO2:ext	92	CO2:ext	0	0	9.132	0	0	0	0	0 -2.396
C141syn	5.99E-03	5.93E-08	0.000244	D-galac:ex	-7.17	D-galac:ex	0.03709	-0.6528	0	0.04502	0.04071	0.01152	0.04358	0 0.04475
C160syn	9.81E-02	1.59E-05	0.003991	glc:ext	-8.95	glc:ext	0.04628	-0.8145	0	0.04071	0.05894	0.01438	0.05438	0 0.05584
C161syn	1.40E-02	3.23E-07	0.000568	Lrha:ext	-2.49	Lrha:ext	0.0131	-0.2306	0	0.01152	0.01438	0.01905	0.01539	0 0.01581
C162syn	3.99E-03	2.64E-08	0.000162	mann:ext	-9.59	mann:ext	0.04954	-0.8721	0	0.04358	0.05438	0.01539	0.06835	0 0.05979
C180syn	4.48E-01	0.000331	0.018202	O2:ext	-78.2	O2:ext	0	0	-2.396	0	0	0	0	39.21 0
C181CoA	5.28E-02	4.61E-06	0.002147	xyL:ext	-9.84	xyL:ext	0.05088	-0.8955	0	0.04475	0.05584	0.01581	0.05979	0 0.08526
C181syn	0.433	0.00031	0.017612											
C182syn	1.86E-01	5.75E-05	0.007584											
C183syn	1.62E-02	4.33E-07	0.000658											
C200syn	2.99E-03	1.48E-08	0.000122											
C1syn	7.45E-03	9.17E-08	0.001363	r_m est 1	Values	Pr_m 1	ara:ext	BIOMasp:CO2:ext	D-galac:ex	glc:ext	Urha:ext	mann:ext	O2:ext	xyL:ext
DAGLysyn	2.09E-01	7.23E-05	0.008501	BIOMasp:	158.1	BIOMasp:	-1.148	41.37	-4.582	-1.022	-1.25	-0.4046	-1.344	8.822 -1.417
DGDG syn	3.35E-02	1.86E-06	0.001363	CO2:ext	94.79	CO2:ext	-0.08009	-4.582	7.218	-0.07453	-0.08626	-0.03106	-0.09321	-7.538 -0.1015
GDPMAN	2.69E-01	0.000119	0.010927	D-galac:ex	-7.014	D-galac:ex	0.0324	-1.022	-0.07453	0.04072	0.03568	0.009587	0.03814	-0.04589 0.03877
MAGLysyn	2.47E-01	0.000101	0.010045	glc:ext	-8.768	glc:ext	0.04079	-1.25	-0.08626	0.03568	0.05305	0.01211	0.048	-0.04668 0.04883
MGC181 s	5.28E-02	4.61E-06	0.002147	Lrha:ext	-2.42	Lrha:ext	0.01098	-0.4046	-0.03106	0.009587	0.01211	0.01816	0.01293	-0.00289 0.0131
MGDG syri	1.62E-01	4.33E-05	0.006576	mann:ext	-9.393	mann:ext	0.0436	-1.344	-0.09321	0.03814	0.048	0.01293	0.06145	-0.04953 0.0522
r1.1	8.768	0.05305	2.230326	O2:ext	-75.92	O2:ext	-0.04174	8.822	-7.538	-0.04589	-0.04668	-0.00289	-0.04953	8.312 -0.04781
r1.2	-33.05	1.463	1.209545	xyL:ext	-9.623	xyL:ext	0.04435	-1.417	-0.1015	0.03877	0.04883	0.0131	0.0522	-0.04781 0.07692
r1.3	6.508	0.1037	0.322025											
r1.4	6.508	0.1037	0.322025											
r1.5	33.65	0.5154	0.717914											
r1.6	33.65	0.5154	0.717914	r_c est 1	Values	Pr_c 1	H:ext	H2O:ext	NH4:ext	Pi:ext	SO4:ext			
r1.7	31.82	0.4985	0.706045	H:ext	16.16	H:ext	0.4323	0.7316	-0.4698	-0.01342	-0.00552			
r1.8	31.82	0.4985	0.706045	H2O:ext	136.6	H2O:ext	0.7316	7.589	-0.7951	-0.0227	-0.00934			
r1.9	30.38	0.493	0.70214	NH4:ext	-17.57	NH4:ext	-0.4698	-0.7951	0.5106	0.01458	0.005999			
r10.1	326.1	200.2	14.1492	Pi:ext	-0.5017	Pi:ext	-0.01342	-0.0227	0.01458	4.16E-04	1.71E-04			
r10.10	0.4442	0.000326	0.018067	SO4:ext	-0.2064	SO4:ext	-0.00552	-0.00934	0.005999	1.71E-04	7.05E-05			
r10.11	35.99	0.6564	0.810185											
r10.12	57.9	9.462	3.076036											
r10.13	0.6807	0.000767	0.027686											
r10.14	20.84	0.7186	0.847703											
r10.15	0.4442	0.000326	0.018067											
r10.16	1.509	0.03766	0.061368	r16.13	1.128	0.002107	0.045902	r4.7	12.64	1.466	1.210785			
r10.17	0.6012	0.000598	0.024454	r16.14	0.1881	5.85E-05	0.00765	r4.8	12.64	1.466	1.210785			
r10.18	0.4632	0.000355	0.018841	r16.15	0.1881	5.85E-05	0.00765	r4.9	12.63	1.467	1.211198			
r10.19	0.7897	0.001032	0.032125	r16.16	0.04281	3.03E-06	0.001741	r5.1	5.229	0.04523	0.212673			
r10.3	269.7	122.4	11.06345	r16.2	0.4772	0.0003767	0.019409	r5.2	16.3	0.4395	0.662948			
r10.5	323.9	201.6	14.19859	r16.3	0.5032	0.0004189	0.020467	r5.3	18.66	0.5761	0.759013			
r10.6	4.542	0.03413	0.184743	r16.4	0.5032	0.0004189	0.020467	r6.1	86.2	15.11	3.887158			
r10.7	0.4632	0.000355	0.018841	r16.5	0.2302	8.77E-05	0.009362	r6.2	49.84	1.162	1.077961			
r10.8	2.181	0.007868	0.088702	r16.6	0.2302	8.77E-05	0.009362	r6.3	12.63	1.467	1.211198			
r10.9	0.4442	0.000326	0.018067	r16.7	0.2302	8.77E-05	0.009362	r6.4	314.9	167.9	12.95762			
r11.1	12.72	0.2678	0.517494	r16.8	0.2153	7.67E-05	0.008757	r7.12	7.97	0.04891	0.221156			
r11.10	0.6765	0.000757	0.027519	r16.9	0.2138	7.56E-05	0.008694	r7.13	7.97	0.04891	0.221156			
r11.11	2.06E-01	7.05E-05	0.008395	r17.2	2.643	0.01156	0.107517	r7.14	7.97	0.04891	0.221156			
r11.12	2.06E-01	7.05E-05	0.008395	r17.3	0.7677	0.000975	0.031225	r7.16	9.393	0.06145	0.247891			
r11.13	1.18E-01	2.30E-05	0.004791	r17.4	0.7677	0.000975	0.031225	r7.17	9.393	0.06145	0.247891			
r11.14	1.18E-01	2.30E-05	0.004791	r17.5	6.831	0.07719	0.277831	r7.18	7.014	0.04072	0.201792			
r11.15	8.86E-02	1.30E-05	0.003604	r17.6	0.1706	4.82E-05	0.006939	r7.19	7.014	0.04072	0.201792			
r11.16	2.87E+00	0.0136	0.116619	r17.7	0.1706	4.82E-05	0.006939	r7.2	0.219	7.94E-05	0.008908			
r11.17	2.34E-01	9.09E-05	0.009535	r17.8	1.279	0.002708	0.052038	r7.20	7.014	0.04072	0.201792			
r11.18	1.13E+00	0.002098	0.045804	r2.1	34.82	1.27	1.126943	r7.21	7.014	0.04072	0.201792			
r11.19	1.008	0.01682	0.041012	r2.2	34.82	1.27	1.126943	r7.22	7.014	0.04072	0.201792			
r11.2	4.385	0.03181	0.178354	r2.3	17.92	0.2911	0.539537	r7.23	5.06	0.02178	0.147558			
r11.20	0.3137	0.000163	0.012759	r2.4	16.25	0.3219	0.567362	r7.24	5.045	0.02168	0.147241			
r11.21	0.4442	0.000326	0.018067	r2.5	17.92	0.2911	0.539537	r7.25	2.42	0.01816	0.134759			
r11.22	1.159	0.002221	0.047127	r2.6	17.92	0.2911	0.539537	r7.26	2.42	0.01816	0.134759			
r11.23	1.391	0.003201	0.056577	r2.7	15.92	0.2137	0.462277	r7.27	2.42	0.01816	0.134759			
r11.24	0.6012	0.000598	0.024454	r23.1	4.418	0.03229	0.179694	r7.28	2.42	0.01816	0.134759			
r11.25	0.7897	0.001032	0.032125	r23.10	0.01261	2.63E-07	0.000513	r7.29	2.42	0.01816	0.134759			
r11.26	0.7897	0.001032	0.032125	r23.11	0.01261	2.63E-07	0.000513	r7.30	2.42	0.01816	0.134759			
r11.27	0.7212	0.000861	0.029336	r23.12	0.01261	2.63E-07	0.000513	r7.6	9.623	0.07692	0.277345			
r11.28	0.35	0.000203	0.014234	r23.14	0.01261	2.63E-07	0.000513	r7.7	17.59	0.2145	0.463141			
r11.29	0.2299	8.75E-05	0.009353	r23.15	0.06969	8.04E-06	0.002835	r7.8	17.59	0.2145	0.463141			
r11.3	0.4947	0.000405	0.02012	r23.16	0.6175	0.0006308	0.025116	r8.1	-0.4399	0.00032	0.017891			
r11.30	0.1413	3.31E-05	0.005749	r23.17	1.621	0.004345	0.065917	r8.2	-0.06248	6.46E-06	0.002541			
r11.31	0.6427	0.000684	0.026144	r23.18	1.122	0.002082	0.045629	r8.3	0.2991	0.000148	0.012166			
r11.32	0.2299	8.75E-05	0.009353	r23.19	0.08777	1.28E-05	0.003571	r8.4	0.1959	6.35E-05	0.007969			
r11.4	0.4632	0.000355	0.018841	r23.2	0.6304	0.0006576	0.025644	r8.5	0.1959	6.35E-05	0.007969			
r11.5	0.4632	0.000355	0.018841	r23.21	4.265	0.03009	0.173465	r9.1	55.75	2.661	1.631257			
r11.6	0.4632	0.000355	0.018841	r23.22	4.265	0.03009	0.173465	r9.15	136.6	7.589	2.754814			
r11.7	0.7302	0.000882	0.0297	r23.23	4.265	0.03009	0.173465	r9.19	9.623	0.07692	0.277345			
r11.8	0.7302	0.000882	0.0297	r23.3	0.5462	0.0004935	0.022215	r9.2	0.5017	0.000416	0.020406			
r11.9	1.826	0.005517	0.047277	r23.4	0.4116	0.0002804	0.016745	r9.3	8.768	0.05305	0.230326			
r13.1	0.1496	3.70E-05	0.006684	r23.6	0.01261	2.63E-07	0.000513	r9.32	7.014	0.04072	0.201792			
r13.2	0.06785	7.62E-06	0.00276	r23.7	0.01261	2.63E-07	0.000513	r9.35	12.57	0.5106	0.714563			
r13.3	0.08172	1.11E-05	0.003324	r23.8	0.01261	2.63E-07	0.000513	r9.36	7.97	0.04891	0.211156			
r13.4	0.1219													

Table S4.9. Input data and flux analysis results for dilution rate $D = 0.172\text{h}^{-1}$.

Best estimate of the fluxes (mmol/ input rates (mmol/h)					Corresponding covariance matrix											
vest 1	Values	Variances	Serr	r_m		Pr_m 1	ara:ext	BIOMasp:	CO2:ext	D-galac:ext	glc:ext	Lrha:ext	mann:ext	O2:ext	xy:ext	
ATP GTP P	2.57E-01	9.24E-05	0.009612	ara:ext	-6.46	ara:ext	0.0464	-0.609	0	0.0267	0.0394	0.00622	0.0419	0	0.0359	
C120syn	1.15E-02	1.84E-07	0.000429	BIOMasp:cyt	149	BIOMasp:	-0.609	37.9	0	-0.611	-0.901	-0.142	-0.959	0	-0.821	
C140syn	1.13E-02	2.48E-07	0.000498	CO2:ext	84.8	CO2:ext	0	0	7.74	0	0	0	0	-1.85	0	
C141syn	5.73E-03	4.59E-08	0.000214	D-galac:ext	-6.5	D-galac:ext	0.0267	-0.611	0	0.0421	0.0395	0.00624	0.0421	0	0.036	
C160syn	9.39E-02	1.23E-05	0.003511	glc:ext	-9.59	glc:ext	0.0394	-0.901	0	0.0395	0.0677	0.0092	0.062	0	0.0531	
C161syn	1.34E-02	2.50E-07	0.0005	Lrha:ext	-1.46	Lrha:ext	0.00622	-0.142	0	0.00624	0.0092	0.0844	0.00979	0	0.00839	
C162syn	3.82E-03	2.04E-08	0.000143	mann:ext	-10.2	mann:ext	0.0419	-0.959	0	0.0421	0.062	0.00979	0.0787	0	0.0565	
C180syn	4.28E-01	0.000257	0.016016	O2:ext	-71.2	O2:ext	0	0	-1.85	0	0	0	0	39.7	0	
C181CoA	5.05E-02	3.57E-06	0.001889	xy:ext	-8.73	xy:ext	0.0359	-0.821	0	0.036	0.0531	0.00839	0.0565	0	0.128	
C181syn	0.4144	0.00024	0.015495													
C182syn	1.78E-01	4.45E-05	0.006672	Reconciled rates (mmol/h)												
C183syn	1.55E-02	3.35E-07	0.000579													
C200syn	2.87E-03	1.15E-08	0.000107	r_m est 1	Values	Pr_m 1	ara:ext	BIOMasp:	CO2:ext	D-galac:ext	glc:ext	Lrha:ext	mann:ext	O2:ext	xy:ext	
CLsyn	7.13E-03	7.10E-08	0.000266	ara:ext	-6.37	ara:ext	0.04107	-0.7731	-0.08722	0.02143	0.0325	-0.00018	0.03438	0.001807	0.02583	
DAGLYsyn	2.00E-01	5.59E-05	0.007479	BIOMasp:cyt	151.3	BIOMasp:	-0.7731	32.03	-2.04	-0.7711	-1.112	-0.3547	-1.189	5.281	-1.137	
DGLGsyn	3.21E-02	1.44E-06	0.0012	CO2:ext	86.63	CO2:ext	-0.08722	-2.04	5.804	-0.0881	-0.1145	-0.09252	-0.1245	-5.931	-0.1605	
GDPMAN:	2.57E-01	9.24E-05	0.009612	D-galac:ext	-6.409	D-galac:ext	0.02143	-0.7711	-0.0881	0.03687	0.03266	-5.23E-05	0.03465	-0.01254	0.02605	
MGCL181	5.05E-02	3.57E-06	0.001889	glc:ext	-9.472	glc:ext	0.0325	-1.112	-0.1145	0.03266	0.05875	0.000942	0.05225	-0.00959	0.04007	
MAGLYsyn	2.36E-01	7.81E-05	0.008839	Lrha:ext	-1.36	Lrha:ext	-0.00018	-0.3547	-0.09252	-5.23E-05	0.000942	0.07641	0.000786	0.1015	-0.00381	
MGDGsyn	1.55E-01	3.35E-05	0.005786	mann:ext	-10.07	mann:ext	0.03438	-1.189	-0.1245	0.03465	0.05225	0.000786	0.06808	-0.00808	0.0423	
r1.1	9.472	0.05875	0.242384	O2:ext	-68.39	O2:ext	0.001807	5.281	-5.931	-0.01254	-0.00959	0.1015	-0.00808	6.431	0.03859	
r1.2	-29.62	1.136	1.05833	xy:ext	-8.562	xy:ext	0.02583	-1.137	-0.1605	0.02605	0.04007	-0.00381	0.0423	0.03859	0.1089	
r1.3	7.433	0.08435	0.290431													
r1.4	7.433	0.08435	0.290431	Calculated rates (mmol/h)												
r1.5	33.36	0.5555	0.745319													
r1.6	33.36	0.5555	0.745319	r_c est 1	Values	Pr_c 1	H:ext	H2O:ext	NH4:ext	Pi:ext	SO4:ext					
r1.7	31.61	0.5311	0.728766	H:ext	15.47	H:ext	0.3346	0.7223	-0.3637	-0.01038	-0.00427					
r1.8	31.61	0.5311	0.728766	H2O:ext	126.9	H2O:ext	0.7223	6.977	-0.7851	-0.02242	-0.00922					
r1.9	30.23	0.5179	0.719653	NH4:ext	-16.81	NH4:ext	-0.3637	-0.7851	0.3953	0.01129	0.004643					
r1.10	293.2	152.9	12.36527	Pi:ext	-0.4801	Pi:ext	-0.01038	-0.02242	0.01129	3.22E-04	1.33E-04					
r1.10	0.4251	0.000253	0.015897	SO4:ext	-0.1975	SO4:ext	-0.00427	-0.00922	0.004643	1.33E-04	5.46E-05					
r1.11	33.39	0.6096	0.780769													
r1.12	52.25	7.184	2.680298													
r1.13	0.6514	0.000593	0.024358	Best estimate of the fluxes (mmol/h) continued												
r1.14	19.94	0.5562	0.745788	vest 1	Values	Variances	Serr	vest 1	Values	Variances	Serr					
r1.15	0.4251	0.000253	0.015897	r16.13	1.08	0.001631	0.040386	r4.7	11.04	1.073	1.035857					
r1.16	1.444	0.002915	0.053991	r16.14	0.18	4.53E-05	0.006731	r4.8	11.04	1.073	1.035857					
r1.17	0.5753	0.000463	0.021515	r16.15	0.18	4.53E-05	0.006731	r4.9	11.04	1.073	1.035857					
r1.18	0.4433	0.000275	0.016577	r16.16	0.04097	2.35E-06	0.001532	r5.1	5.003	0.03501	0.18711					
r1.19	0.7557	0.000799	0.028258	r16.2	0.4566	0.0002916	0.017076	r5.2	15.6	0.3402	0.583267					
r1.20	242.4	93.75	9.682458	r16.3	0.4815	0.0003242	0.018006	r5.3	17.86	0.4459	0.667757					
r1.21	291.2	153.7	12.39758	r16.4	0.4815	0.0003242	0.018006	r6.1	78.28	11.7	3.420526					
r1.22	4.346	0.02641	0.162512	r16.5	0.2203	6.79E-05	0.008237	r6.2	44.43	1.049	1.024207					
r1.23	0.4433	0.000275	0.016577	r16.6	0.2203	6.79E-05	0.008237	r6.3	11.04	1.073	1.035857					
r1.24	2.087	0.00609	0.078038	r16.7	0.2203	6.79E-05	0.008237	r6.4	283.5	128.9	11.35341					
r1.25	0.4251	0.000253	0.015897	r16.8	0.206	5.94E-05	0.007704	r7.12	6.37	0.04107	0.202657					
r1.26	12.18	0.2073	0.455302	r16.9	0.2046	5.85E-05	0.007649	r7.13	6.37	0.04107	0.202657					
r1.27	0.6474	0.000586	0.024212	r17.2	2.529	0.000845	0.094578	r7.14	6.37	0.04107	0.202657					
r1.28	1.39E-01	5.46E-05	0.007386	r17.3	0.7346	0.0007547	0.027472	r7.16	10.07	0.6808	0.260921					
r1.29	1.39E-01	5.46E-05	0.007386	r17.4	0.7346	0.0007547	0.027472	r7.17	10.07	0.6808	0.260921					
r1.30	1.13E-01	1.78E-05	0.004214	r17.5	6.537	0.05975	0.244438	r7.18	6.409	0.3687	0.192016					
r1.31	1.13E-01	1.78E-05	0.004214	r17.6	0.1633	3.73E-05	0.006105	r7.19	6.409	0.3687	0.192016					
r1.32	8.48E-02	0.101E-05	0.003172	r17.7	0.1633	3.73E-05	0.006105	r7.2	0.2096	6.14E-05	0.007837					
r1.33	2.74E-01	0.01053	0.102616	r17.8	1.224	0.002096	0.045782	r7.20	6.409	0.3687	0.192016					
r1.34	2.24E-01	7.04E-05	0.008389	r2.1	32.39	1.058	0.128591	r7.21	6.409	0.3687	0.192016					
r1.35	1.08E-01	0.001624	0.040299	r2.2	32.39	1.058	0.128591	r7.22	6.409	0.3687	0.192016					
r1.36	0.965	0.001302	0.036083	r2.3	16.21	0.242	0.491935	r7.23	4.539	0.02271	0.150698					
r1.37	4.196	0.02462	0.156908	r2.4	15.57	0.2779	0.527162	r7.24	4.525	0.02263	0.150433					
r1.38	0.3002	0.000126	0.011225	r2.5	16.21	0.242	0.491935	r7.25	1.36	0.07641	0.276424					
r1.39	0.4251	0.000253	0.015897	r2.6	16.21	0.242	0.491935	r7.26	1.36	0.07641	0.276424					
r1.40	1.109	0.001719	0.041461	r2.7	14.29	0.1841	0.429069	r7.27	1.36	0.07641	0.276424					
r1.41	1.331	0.002477	0.049769	r2.8	4.228	0.025	0.158114	r7.28	1.36	0.07641	0.276424					
r1.42	0.5753	0.000463	0.021515	r2.9	0.01207	2.04E-07	0.000451	r7.29	1.36	0.07641	0.276424					
r1.43	0.7557	0.000799	0.028258	r2.10	0.01207	2.04E-07	0.000451	r7.30	1.36	0.07641	0.276424					
r1.44	0.7557	0.000799	0.028258	r2.11	0.01207	2.04E-07	0.000451	r7.31	8.562	0.1089	0.33					
r1.45	0.6902	0.000666	0.025811	r2.12	0.01207	2.04E-07	0.000451	r7.32	14.93	0.2017	0.44911					
r1.46	0.3349	0.000157	0.012522	r2.13	0.01207	2.04E-07	0.000451	r7.7	14.93	0.2017	0.44911					
r1.47	0.22	6.77E-05	0.008229	r2.14	0.06669	6.22E-06	0.002494	r7.8	14.93	0.2017	0.44911					
r1.48	0.4734	0.000313	0.0177	r2.15	0.5909	0.0004883	0.022098	r8.1	-0.421	0.000248	0.015742					
r1.49	0.1352	2.56E-05	0.005058	r2.16	1.551	0.003364	0.058	r8.2	0.05979	5.00E-06	0.002236					
r1.50	0.6151	0.000529	0.023002	r2.17	1.073	0.001611	0.040137	r8.3	0.2863	0.000115	0.010705					
r1.51	0.1132	0.22	6.77E-05	r2.18	0.08399	9.87E-06	0.003141	r8.4	0.1875	4.92E-05	0.007011					
r1.52	0.4433	0.000275	0.016577	r2.19	0.6033	0.000509	0.022561	r8.5	0.1875	4.92E-05	0.007011					
r1.53	0.4433	0.000275	0.016577	r2.20	4.081	0.02329	0.152611	r9.1	52.66	2.214	1.487952					
r1.54	0.4433	0.000275	0.016577	r2.21	4.081	0.02329	0.152611	r9.15	126.9	6.977	2.641401					
r1.55	0.6908	0.000683	0.02613	r2.22	4.081	0.02329	0.152611	r9.19	8.562	0.1089						

Table S4.10. Input data and flux analysis results for dilution rate $D = 0.194\text{h}^{-1}$.

Best estimate of the fluxes (mmol/ Input rates (mmol/h)							Corresponding covariance matrix									
vest 1	Values	Variances	Serr	r_m 1	Values	Pr_m 1	ara:ext	BIOMasp:	CO2:ext	D-galac:ex	glc:ext	Ura:ext	mann:ext	O2:ext	xyL:ext	
ATP_GTP_P	2.12E-01	9.98E-05	0.009897	ara:ext	-2.77	ara:ext	0.0468	-0.21	0	0.00655	0.0186	0.00139	0.0178	0	0.0107	
C120syn	9.44E-03	1.98E-07	0.000445	BIOMasp:	119	BIOMasp:	-0.21	66.1	0	-0.275	-0.782	-0.0835	-0.749	0	-0.451	
C140syn	1.10E-02	2.68E-07	0.000518	CO2:ext	66.1	CO2:ext	0	0	4.69	0	0	0	0	0	-0.824	
C141syn	4.72E-03	4.96E-08	0.000223	D-galac:ex	-3.67	D-galac:ex	0.00655	-0.275	0	0.0693	0.0244	0.00261	0.0234	0	0.0141	
C160syn	7.74E-02	1.33E-05	0.003648	glc:ext	-10.5	glc:ext	0.0186	-0.782	0	0.0244	0.0817	0.0074	0.0663	0	0.04	
C161syn	1.10E-02	2.70E-07	0.00052	Ura:ext	-1.08	Ura:ext	0.00199	-0.0835	0	0.00261	0.0074	0.117	0.00709	0	0.00428	
C162syn	3.15E-03	2.20E-08	0.000148	mann:ext	-10	mann:ext	0.0178	-0.749	0	0.0234	0.0663	0.00709	0.133	0	0.0383	
C180syn	3.53E-01	0.000277	0.01664	O2:ext	-55.3	O2:ext	0	0	-0.824	0	0	0	0	0	41.3	
C181CoA	4.16E-02	3.85E-06	0.001962	xyL:ext	-6.03	xyL:ext	0.0107	-0.451	0	0.0141	0.04	0.00428	0.0383	0	0.429	
C181syn	0.3413	0.000259	0.0161													
C182syn	1.47E-01	4.81E-05	0.006933	Reconciled rates (mmol/h)												
C183syn	1.28E-02	3.61E-07	0.000601	Corresponding covariance matrix												
C200syn	2.36E-03	1.24E-08	0.000111	r_m est 1	Values	Pr_m 1	ara:ext	BIOMasp:	CO2:ext	D-galac:ex	glc:ext	Ura:ext	mann:ext	O2:ext	xyL:ext	
CLsyn	5.87E-03	7.67E-08	0.000277	ara:ext	-2.729	ara:ext	0.0454	-0.4136	-0.02079	0.004322	0.01621	-0.00099	0.01413	-0.01821	0.00138	
DAGLYsyn	1.65E-01	6.04E-05	0.000771	BIOMasp:	124.7	BIOMasp:	-0.4136	34.58	-2.317	-0.5889	-1.121	-0.5378	-1.28	5.495	-1.831	
DGDG syn	2.64E-02	1.55E-06	0.001246	CO2:ext	66.83	CO2:ext	-0.02079	-2.317	4.101	-0.03747	-0.03925	-0.03663	-0.05635	-4.274	-0.1306	
GDPMAN	1.12E-01	9.98E-05	0.009897	D-galac:ex	-3.603	D-galac:ex	0.004322	-0.5889	-0.03747	0.06568	0.02053	-0.00203	0.01752	-0.0779	-0.00065	
MAGLYsyn	1.95E-01	8.44E-05	0.009184	glc:ext	-10.43	glc:ext	0.01621	-1.121	-0.03925	0.02053	0.07756	0.002401	0.06	-0.07275	0.02415	
MGC181 s	4.16E-02	3.85E-06	0.001962	Ura:ext	-0.996	Ura:ext	-0.00099	-0.5378	-0.03663	-0.00203	0.002401	0.1104	-0.00069	0.04941	-0.01584	
MGDG syn	1.28E-01	3.62E-05	0.006012	mann:ext	-9.892	mann:ext	0.01413	-1.28	-0.05635	0.01752	0.06	-0.00069	0.1233	-0.06728	0.01386	
r1.1	10.43	0.07756	0.278496	O2:ext	-53.42	O2:ext	-0.01821	5.495	-4.274	-0.0779	-0.07275	0.04941	-0.06728	4.831	-0.02802	
r1.2	-17.05	1.235	1.11306	xyL:ext	-5.76	xyL:ext	0.00138	-1.831	-0.1306	-0.00065	0.02415	-0.01584	0.01386	-0.02802	0.3665	
r1.3	9.376	0.1289	0.359026													
r1.4	9.376	0.1289	0.359026	Calculated rates (mmol/h)												
r1.5	29.47	0.6008	0.775113	r_c est 1	Values	Pr_c 1	H:ext	H2O:ext	NH4:ext	Pi:ext	SO4:ext					
r1.6	29.47	0.6008	0.775113													
r1.7	28.03	0.5729	0.756902	H:ext	12.74	H:ext	0.3612	0.793	-0.3926	-0.01121	-0.00461					
r1.8	28.03	0.5729	0.756902	H2O:ext	101.7	H2O:ext	0.793	5.589	-0.8619	-0.02461	-0.01013					
r1.9	26.89	0.5573	0.746525	NH4:ext	-13.85	NH4:ext	-0.3926	-0.8619	0.4267	0.01218	0.005013					
r10.1	231.6	117.4	10.83513	Pi:ext	-0.3954	Pi:ext	-0.01121	-0.02461	0.01218	3.48E-04	1.43E-04					
r10.10	0.3501	0.000273	0.016517	SO4:ext	-0.1627	SO4:ext	-0.00461	-0.01013	0.005013	1.43E-04	5.89E-05					
r10.11	27.56	0.4593	0.677717													
r10.12	43.23	5.711	2.38977													
r10.13	0.5366	0.000641	0.025308	Best estimate of the fluxes (mmol/h) continued												
r10.14	16.43	0.6005	0.774919	vest 1	Values	Variances	Serr	vest 1	Values	Variances	Serr					
r10.15	0.3501	0.000273	0.016517	r16.13	0.8896	0.001761	0.041964	r4.7	9.157	0.9196	0.958958					
r10.16	1.189	0.003147	0.056098	r16.14	0.1483	4.89E-05	0.006994	r4.8	9.157	0.9196	0.958958					
r10.17	0.4739	0.0005	0.022354	r16.15	0.1483	4.89E-05	0.006994	r4.9	9.154	0.9198	0.959062					
r10.18	0.3652	0.000297	0.017225	r16.16	0.03375	2.53E-06	0.001592	r5.1	4.122	0.0378	0.194422					
r10.19	0.6225	0.000862	0.029362	r16.2	0.3762	0.0003148	0.017743	r5.2	12.85	0.3673	0.606053					
r10.3	189.5	71.44	8.452219	r16.3	0.3966	0.00035	0.018708	r5.3	14.71	0.4814	0.69383					
r10.5	229.9	118.3	10.87658	r16.4	0.3966	0.00035	0.018708	r6.1	64.73	9.056	3.009319					
r10.6	3.58	0.02852	0.168879	r16.5	0.1814	7.33E-05	0.008559	r6.2	30.46	9932	9.96594					
r10.7	0.3652	0.000297	0.017225	r16.6	0.1814	7.33E-05	0.008559	r6.3	9.154	0.9198	0.959062					
r10.8	1.719	0.006575	0.081086	r16.7	0.1814	7.33E-05	0.008559	r6.4	223.5	98.11	9.905049					
r10.9	0.3501	0.000273	0.016517	r16.8	0.1697	6.41E-05	0.008005	r7.12	2.729	0.0454	0.213073					
r11.1	10.03	0.2238	0.473075	r16.9	0.1685	6.32E-05	0.007948	r7.13	2.729	0.0454	0.213073					
r11.10	0.5333	0.000633	0.025156	r17.2	2.083	0.009657	0.09827	r7.14	2.729	0.0454	0.213073					
r11.11	1.63E-01	5.89E-05	0.007674	r17.3	0.6052	0.0008148	0.028545	r7.16	9.892	0.1233	0.351141					
r11.12	1.63E-01	5.89E-05	0.007674	r17.4	0.6052	0.0008148	0.028545	r7.17	9.892	0.1233	0.351141					
r11.13	9.28E-02	1.93E-05	0.004379	r17.5	5.385	0.006451	0.253988	r7.18	3.603	0.06568	0.256281					
r11.14	9.28E-02	1.93E-05	0.004379	r17.6	0.1345	4.02E-05	0.006344	r7.19	3.603	0.06568	0.256281					
r11.15	6.99E-02	1.09E-05	0.003295	r17.7	0.1345	4.02E-05	0.006344	r7.2	0.1726	6.63E-05	0.008143					
r11.16	2.26E-00	0.01137	0.10663	r17.8	1.009	0.002263	0.047571	r7.20	3.603	0.06568	0.256281					
r11.17	1.85E-01	7.60E-05	0.008717	r18.1	21.96	1.069	0.103925	r7.21	3.603	0.06568	0.256281					
r11.18	8.88E-01	0.001753	0.041869	r2.1	21.96	1.069	0.103925	r7.22	3.603	0.06568	0.256281					
r11.19	0.7949	0.001406	0.037497	r2.2	21.96	1.069	0.103925	r7.23	3.603	0.06568	0.256281					
r11.2	3.456	0.02658	0.163034	r2.3	10.51	0.2902	0.538702	r7.24	2.062	0.0564	0.237487					
r11.20	0.2473	0.000136	0.011662	r2.4	10.95	0.2637	0.513517	r7.25	2.051	0.05637	0.237424					
r11.21	0.3501	0.000273	0.016517	r2.5	10.51	0.2902	0.538702	r7.26	0.996	0.1104	0.332265					
r11.22	0.9134	0.001856	0.043081	r2.6	10.51	0.2902	0.538702	r7.27	0.996	0.1104	0.332265					
r11.23	1.096	0.002675	0.05172	r2.7	8.931	0.2305	0.480104	r7.28	0.996	0.1104	0.332265					
r11.24	0.4739	0.0005	0.022354	r23.1	3.483	0.02698	0.164256	r7.29	0.996	0.1104	0.332265					
r11.25	0.6225	0.000862	0.029362	r23.10	0.009943	2.20E-07	0.000469	r7.30	0.996	0.1104	0.332265					
r11.26	0.6225	0.000862	0.029362	r23.11	0.009943	2.20E-07	0.000469	r7.6	5.76	0.3665	0.605392					
r11.27	0.5685	0.000719	0.026818	r23.12	0.009943	2.20E-07	0.000469	r7.7	8.49	0.4147	0.643972					
r11.28	0.2759	0.000169	0.013012	r23.14	0.009943	2.20E-07	0.000469	r7.8	8.49	0.4147	0.643972					
r11.29	0.1813	7.31E-05	0.00885	r23.15	0.05493	6.71E-06	0.002591	r8.1	8.49	0.4147	0.643972					
r11.3	0.3899	0.000338	0.018393	r23.16	0.4867	0.0005271	0.022959	r8.2	-0.3468	0.000268	0.016355					
r11.30	0.1114	2.76E-05	0.005255	r23.17	1.278	0.003631	0.060258	r8.3	-0.04925	5.40E-06	0.002323					
r11.31	0.5067	0.000571	0.0239	r23.18	0.8842	0.01079	0.041701	r8.4	0.2358	0.000124	0.011224					
r11.32	0.1813	7.31E-05	0.00885	r23.19	0.06919	0.0173E-05	0.003263	r8.5	0.1544	5.31E-05	0.007784					
r11.4	0.3652	0.000297	0.017225	r23.2	0.497	0.0005495	0.023441	r8.5	0.1544	5.31E-05	0.007784					
r11.5	0.3652	0.000297	0.017225	r23.21	3.362	0.02515	0.158588	r9.1	43.66	2.532	1.591226					
r11.6	0.3652	0.000297	0.017225	r23.22	3.362	0.02515	0.158588	r9.15	101.7	5.589	2.364107					
r11.7	0.5756	0.000737	0.027151	r23.23	3.362	0.02515	0.158588	r9.19	5.76	0.3665	0.605392					
r11.8	0.5756	0.000737	0.027151	r23.3	0.4305	0.0004124	0.020308	r9.2	0.3954	0.000348	0					

Table S4.11. Input data and flux analysis results for dilution rate $D = 0.209\text{h}^{-1}$.

Best estimate of the fluxes (mmol/ input rates (mmol/h)					Corresponding covariance matrix											
vest 1	Values	Variances	Serr	r_m 1	Values	Pr_m 1	ara:ext	BIOMasp:ext	CO2:ext	D-galac:ext	glc:ext	Lrha:ext	mann:ext	O2:ext	xyL:ext	
ATP GTP P	1.94E-01	0.001016	0.010296	ara:ext	-1.99	ara:ext	0.0568	-0.143	0	0.00101	0.0134	0.00178	0.011	0	0.00688	
C120yn	8.65E-03	2.11E-07	0.000459	BIOMasp:cyt	113	BIOMasp:ext	-0.143	78.4	0	-0.0557	-0.745	-0.0989	-0.61	0	-0.381	
C140yn	1.01E-02	2.85E-07	0.000534	CO2:ext	48.5	CO2:ext	0	0	2.52	0	0	0	0	-0.229	0	
C141yn	4.32E-03	5.27E-08	0.00023	D-galac:ext	-0.759	D-galac:ext	0.00101	-0.0557	0	0.139	0.00523	0.000694	0.00428	0	0.00267	
C160yn	7.08E-02	1.42E-05	0.003762	glc:ext	-10.5	glc:ext	0.0134	-0.745	0	0.00523	0.0865	0.00927	0.0572	0	0.0357	
C161yn	1.01E-02	2.87E-07	0.000536	Lrha:ext	-1.37	Lrha:ext	0.00178	-0.0989	0	0.000694	0.00927	0.133	0.00759	0	0.00474	
C162yn	2.88E-03	2.34E-08	0.000153	mann:ext	-8.62	mann:ext	0.011	-0.61	0	0.00428	0.0572	0.00759	0.234	0	0.0293	
C180yn	3.23E-01	0.000294	0.017155	O2:ext	-41.9	O2:ext	0	0	-0.229	0	0	0	0	43	0	
C181CoA	3.81E-02	4.09E-06	0.002023	xyL:ext	-5.37	xyL:ext	0.00688	-0.381	0	0.00267	0.0357	0.00474	0.0293	0	0.637	
C181syn	0.3126	0.000276	0.016598													
C182syn	1.35E-01	5.11E-05	0.007146	Reconciled rates (mmol/h)					Corresponding covariance matrix							
C183syn	1.17E-02	3.84E-07	0.00062													
C200syn	2.16E-03	1.32E-08	0.000115	r_m est 1	Values	Pr_m 1	ara:ext	BIOMasp:ext	CO2:ext	D-galac:ext	glc:ext	Lrha:ext	mann:ext	O2:ext	xyL:ext	
Cloyn	5.38E-03	8.15E-08	0.000285	ara:ext	-1.981	ara:ext	0.05574	-0.3484	-0.00887	-0.00172	0.01198	-0.00079	0.006601	-0.01861	-0.0033	
DAGLYsyn	1.51E-01	6.42E-05	0.008011	BIOMasp:cyt	114.2	BIOMasp:ext	-0.3484	36.75	-1.302	-0.5652	-1.012	-0.6164	-1.465	4.596	-2.378	
DGDGsyn	2.42E-02	1.65E-06	0.001285	CO2:ext	48.7	CO2:ext	-0.00887	-1.302	2.34	-0.02833	-0.01412	-0.01746	-0.03699	-2.428	-0.08152	
DGPMAN	1.94E-01	0.001016	0.010296	D-galac:ext	-0.73	D-galac:ext	-0.00172	-0.5652	-0.02833	0.1317	0.001452	-0.00575	-0.0071	-0.1529	-0.02346	
MAGLYsyn	1.78E-01	8.97E-05	0.009468	glc:ext	-10.49	glc:ext	0.01198	-1.012	-0.01412	0.001452	0.008455	0.005903	0.0513	-0.06801	0.02212	
MGCL181 s	3.81E-02	4.09E-06	0.002023	Lrha:ext	-1.354	Lrha:ext	-0.00079	-0.6164	-0.01746	-0.00575	0.005903	0.1266	-0.00313	0.03554	-0.02025	
MGDGsyn	1.17E-01	3.84E-05	0.006198	mann:ext	-8.584	mann:ext	0.006601	-1.465	-0.03699	-0.0071	0.0513	-0.00313	0.2157	-0.07859	-0.01311	
r.1	10.49	0.08455	0.290775	O2:ext	-39.21	O2:ext	-0.01861	4.596	-2.428	-0.1529	-0.06801	0.03554	-0.07859	2.979	-0.1017	
r.2	-11.16	1.523	1.234093	xyL:ext	-5.292	xyL:ext	-0.0033	-2.378	-0.08152	-0.02346	0.02212	-0.02025	-0.01311	-0.1017	0.5386	
r.3	9.888	0.2103	0.458585													
r.4	9.888	0.2103	0.458585	Calculated rates (mmol/h)					Corresponding covariance matrix							
r.5	25.68	0.6518	0.807341													
r.6	25.68	0.6518	0.807341	r_c est 1	Values	Pr_c 1	H:ext	H2O:ext	NH4:ext	Pi:ext	SO4:ext					
r.7	24.36	0.614	0.783582	H:ext	11.67	H:ext	0.3839	0.9676	-0.4173	-0.01191	-0.0049					
r.8	24.36	0.614	0.783582	H2O:ext	83.18	H2O:ext	0.9676	4.759	-1.052	-0.03003	-0.01236					
r.9	23.32	0.591	0.768765	NH4:ext	-12.68	NH4:ext	-0.4173	-1.052	0.4535	0.01295	0.005328					
r.10.1	166.9	75.11	8.666003	Pi:ext	-0.3621	Pi:ext	-0.01191	-0.03003	0.01295	3.70E-04	1.52E-04					
r.10.10	0.3206	0.00029	0.017026	SO4:ext	-0.149	SO4:ext	-0.0049	-0.01236	0.005328	1.52E-04	6.26E-05					
r.10.11	22.25	0.3294	0.573934													
r.10.12	30.61	3.919	1.979646													
r.10.13	0.4913	0.000681	0.02609	Best estimate of the fluxes (mmol/h) continued												
r.10.14	15.04	0.6382	0.798874	v est 1	Values	Variances	Serr	v est 1	Values	Variances	Serr					
r.10.15	0.3206	0.00029	0.017026	r.16.13	0.8146	0.001871	0.043255	r.4.7	5.395	0.7063	0.840417					
r.10.16	1.089	0.003344	0.057827	r.16.14	0.1358	5.20E-05	0.00721	r.4.8	5.395	0.7063	0.840417					
r.10.17	0.434	0.000531	0.023046	r.16.15	0.1358	5.20E-05	0.00721	r.4.9	5.392	0.7065	0.840536					
r.10.18	0.3344	0.000315	0.017757	r.16.16	0.0309	2.69E-06	0.001641	r.5.1	3.774	0.04017	0.200425					
r.10.19	0.57	0.000916	0.030269	r.16.17	0.3444	0.0003346	0.018292	r.5.2	11.77	0.3903	0.62474					
r.10.3	137.3	44.97	6.705967	r.16.3	0.3632	0.000372	0.019287	r.5.3	13.47	0.5116	0.715262					
r.10.5	165.3	75.89	8.711487	r.16.4	0.3632	0.000372	0.019287	r.6.1	47.31	5.975	2.444381					
r.10.6	3.278	0.03031	0.174098	r.16.5	0.1662	7.79E-05	0.008823	r.6.2	23.44	0.9467	0.972985					
r.10.7	0.3344	0.000315	0.017757	r.16.6	0.1662	7.79E-05	0.008823	r.6.3	5.392	0.7065	0.840536					
r.10.8	1.574	0.006987	0.083588	r.16.7	0.1662	7.79E-05	0.008823	r.6.4	162.5	61.81	7.861934					
r.10.9	0.3206	0.00029	0.017026	r.16.8	0.1554	6.81E-05	0.008252	r.7.12	1.981	0.05574	0.236093					
r.11.1	9.185	0.2379	0.48775	r.16.9	0.1543	6.71E-05	0.008193	r.7.13	1.981	0.05574	0.236093					
r.11.10	0.4884	0.006073	0.025933	r.17.2	1.908	0.01026	0.101292	r.7.14	1.981	0.05574	0.236093					
r.11.11	1.49E-01	6.26E-05	0.007911	r.17.3	0.5541	0.0008659	0.029426	r.7.16	8.584	0.2157	0.464435					
r.11.12	1.49E-01	6.26E-05	0.007911	r.17.4	0.5541	0.0008659	0.029426	r.7.17	8.584	0.2157	0.464435					
r.11.13	8.50E-02	2.04E-05	0.004514	r.17.5	4.931	0.06856	0.26184	r.7.18	0.73	0.1317	0.362905					
r.11.14	8.50E-02	2.04E-05	0.004514	r.17.6	0.1231	4.28E-05	0.006539	r.7.19	0.73	0.1317	0.362905					
r.11.15	6.40E-02	1.15E-05	0.003397	r.17.7	0.1231	4.28E-05	0.006539	r.7.2	0.1581	7.05E-05	0.008395					
r.11.16	2.07E+00	0.01208	0.109909	r.17.8	0.9236	0.002405	0.049041	r.7.20	0.73	0.1317	0.362905					
r.11.17	1.69E-01	8.08E-05	0.008986	r.2.1	16.59	1.226	1.107249	r.7.21	0.73	0.1317	0.362905					
r.11.18	8.13E-01	0.001863	0.043162	r.2.2	16.59	1.226	1.107249	r.7.22	0.73	0.1317	0.362905					
r.11.19	0.7279	0.001494	0.038652	r.2.3	8.282	0.3547	0.595567	r.7.23	-0.6807	0.1233	0.351141					
r.11.2	3.165	0.02825	0.168077	r.2.4	7.846	0.2995	0.547266	r.7.24	-0.6915	0.1233	0.351141					
r.11.20	0.2264	0.000145	0.012025	r.2.5	8.282	0.3547	0.595567	r.7.25	1.354	0.1266	0.355809					
r.11.21	0.3206	0.00029	0.017026	r.2.6	8.282	0.3547	0.595567	r.7.26	1.354	0.1266	0.355809					
r.11.22	0.8364	0.001973	0.044418	r.2.7	6.838	0.2882	0.536843	r.7.27	1.354	0.1266	0.355809					
r.11.23	1.004	0.002842	0.05331	r.2.1	3.189	0.02868	0.169352	r.7.28	1.354	0.1266	0.355809					
r.11.24	0.434	0.000531	0.023046	r.23.10	0.009105	2.34E-07	0.000484	r.7.29	1.354	0.1266	0.355809					
r.11.25	0.57	0.000916	0.030269	r.23.11	0.009105	2.34E-07	0.000484	r.7.30	1.354	0.1266	0.355809					
r.11.26	0.57	0.000916	0.030269	r.23.12	0.009105	2.34E-07	0.000484	r.7.6	5.292	0.5386	0.733894					
r.11.27	0.5206	0.000764	0.027646	r.23.14	0.009105	2.34E-07	0.000484	r.7.7	7.273	0.5878	0.766681					
r.11.28	0.2526	0.00018	0.013416	r.23.15	0.009105	2.34E-07	0.000484	r.7.8	7.273	0.5878	0.766681					
r.11.29	0.166	7.77E-05	0.008814	r.23.16	0.0503	7.14E-06	0.002671	r.8.1	-0.3175	0.000284	0.016861					
r.11.3	0.3571	0.00036	0.01896	r.23.17	0.4457	0.0005602	0.023669	r.8.2	-0.0451	5.74E-06	0.002395					
r.11.30	0.102	2.94E-05	0.005418	r.23.18	1.17	0.003859	0.062121	r.8.3	0.2159	0.000132	0.011467					
r.11.31	0.464	0.000607	0.024637	r.23.19	0.8097	0.001849	0.043	r.8.4	0.1414	5.64E-05	0.00751					
r.11.32	0.166	7.77E-05	0.008814	r.23.19	0.06336	1.13E-05	0.003365	r.8.5	0.1414	5.64E-05	0.00751					
r.11.4	0.3344	0.000315	0.017757	r.23.2	0.4551	0.000584	0.024166	r.9.1	40.39	2.884	1.698234					
r.11.5	0.3344	0.000315	0.017757	r.23.21	3.079	0.02673	0.163493	r.9.15	83.18	4.759	2.181513					
r.11.6	0.3344	0.000315	0													

List of reactions

Glycolysis

r1.1 1 ATP:cyt + 1 glc:cyt => 1 ADP:cyt + 1 g6P:cyt + 1 H:cyt
 r1.2 1 g6P:cyt => 1 f6P:cyt
 r1.3 1 ATP:cyt + 1 f6P:cyt => 1 ADP:cyt + 1 f16P:cyt + 1 H:cyt
 r1.4 1 f16P:cyt => 2 GAP:cyt
 r1.5 1 GAP:cyt + 1 NAD:cyt + 1 Pi:cyt => 1 l3PG:cyt + 1 H:cyt + 1 NADH:cyt
 r1.6 1 l3PG:cyt + 1 ADP:cyt => 1 3PG:cyt + 1 ATP:cyt
 r1.7 1 3PG:cyt => 1 2PG:cyt
 r1.8 1 2PG:cyt => 1 H2O:cyt + 1 PEP:cyt
 r1.9 1 ADP:cyt + 1 H:cyt + 1 PEP:cyt => 1 ATP:cyt + 1 pyr:cyt

Pentose phosphate pathway

r2.1 1 g6P:cyt + 1 H2O:cyt + 1 NADP:cyt => 1 6Pgluct:cyt + 2 H:cyt + 1 NADPH:cyt
 r2.2 1 6Pgluct:cyt + 1 NADP:cyt => 1 CO2:cyt + 1 NADPH:cyt + 1 Rib5P:cyt
 r2.3 1 Rib5P:cyt => 1 Rib5P:cyt
 r2.4 1 Rib5P:cyt => 1 Xyl5P:cyt
 r2.5 1 Rib5P:cyt + 1 Xyl5P:cyt => 1 GAP:cyt + 1 sed7P:cyt
 r2.6 1 GAP:cyt + 1 sed7P:cyt => 1 E4P:cyt + 1 f6P:cyt
 r2.7 1 E4P:cyt + 1 Xyl5P:cyt => 1 f6P:cyt + 1 GAP:cyt

TCA cycle

r4.1 1 HCoA:mit + 1 NAD:mit + 1 pyr:mit => 1 AcCoA:mit + 1 CO2:mit + 1 NADH:mit
 r4.2 1 AcCoA:mit + 1 H2O:mit + 1 OAA:mit => 1 citr:mit + 1 H:mit + 1 HCoA:mit
 r4.3 1 citr:mit => 1 iCitr:mit
 r4.4 1 iCitr:mit + 1 NAD:mit => 1 aKG:mit + 1 CO2:mit + 1 NADH:mit
 r4.5 1 iCitr:mit + 1 NADP:mit => 1 aKG:mit + 1 CO2:mit + 1 NADPH:mit
 r4.6 1 iCitr:cyt + 1 NADP:cyt => 1 aKG:cyt + 1 CO2:cyt + 1 NADPH:cyt
 r4.7 1 aKG:mit + 1 HCoA:mit + 1 NAD:mit => 1 CO2:mit + 1 NADH:mit + 1 succCoA:mit
 r4.8 1 ADP:mit + 1 Pi:mit + 1 succCoA:mit => 1 ATP:mit + 1 HCoA:mit + 1 succ:mit
 r4.9 1 FAD:mit + 1 succ:mit => 1 FADH2:mit + 1 fum:mit
 r4.10 1 fum:mit + 1 H2O:mit => 1 mal:mit
 r4.11 1 mal:mit + 1 NAD:mit => 1 H:mit + 1 NADH:mit + 1 OAA:mit

Anaplerotic pathways

r5.1 1 ATP:cyt + 1 CO2:cyt + 1 H2O:cyt + 1 pyr:cyt => 1 ADP:cyt + 2 H:cyt + 1 OAA:cyt + 1 Pi:cyt
 r5.2 1 ATP:cyt + 1 citr:cyt + 1 HCoA:cyt => 1 AcCoA:cyt + 1 ADP:cyt + 1 OAA:cyt + 1 Pi:cyt
 r5.3 1 H:cyt + 1 NADH:cyt + 1 OAA:cyt => 1 mal:cyt + 1 NAD:cyt

Oxidative phosphorylation

r6.1 11 H:mit + 1 NADH:mit + 0.5 O2:cyt => 10 H:cyt + 1 H2O:cyt + 1 NAD:mit
 r6.2 7 H:mit + 1 NADH:cyt + 0.5 O2:cyt => 6 H:cyt + 1 H2O:cyt + 1 NAD:cyt
 r6.3 1 FADH2:mit + 6 H:mit + 0.5 O2:cyt => 1 FAD:mit + 6 H:cyt + 1 H2O:cyt
 r6.4 1 ADP:mit + 4 H:cyt + 1 Pi:mit => 1 ATP:mit + 3 H:mit + 1 H2O:mit

Different carbon substrates

r7.2 1 Ac:cyt + 2 ATP:cyt + 1 H2O:cyt + 1 HCoA:cyt => 1 AcCoA:cyt + 2 ADP:cyt + 1 H:cyt + 2 Pi:cyt

```

r7.6      1 H:cyt + 1 NADPH:cyt + 1 xyl:cyt => 1 NADP:cyt + 1 xol:cyt
r7.7      1 NAD:cyt + 1 xol:cyt => 1 H:cyt + 1 NADH:cyt + 1 xylu:cyt
r7.8      1 ATP:cyt + 1 xylu:cyt => 1 ADP:cyt + 1 H:cyt + 1 Xylu5P:cyt
r7.12     1 ara:cyt + 1 H:cyt + 1 NADPH:cyt <=> 1 arab:cyt + 1 NADP:cyt
r7.13     1 arab:cyt + 1 NAD:cyt => 1 H:cyt + 1 L-xylu:cyt + 1 NADH:cyt
r7.14     1 H:cyt + 1 L-xylu:cyt + 1 NADPH:cyt <=> 1 NADP:cyt + 1 xol:cyt
r7.16     1 ATP:cyt + 1 mann:cyt => 1 ADP:cyt + 1 H:cyt + 1 mann6P:cyt
r7.17     1 mann6P:cyt => 1 f6P:cyt
r7.18     1 D-galac:cyt <=> 1 D-galacn:cyt
r7.19     1 D-galacn:cyt + 1 H:cyt + 1 NADPH:cyt => 1 aldeLgal:cyt + 1 NADP:cyt
r7.20     1 aldeLgal:cyt => 1 23gal:cyt + 1 H2O:cyt
r7.21     1 23gal:cyt => 1 glycal:cyt + 1 pyr:cyt
r7.22     1 glycal:cyt + 1 H:cyt + 1 NADPH:cyt => 1 gcl:cyt + 1 NADP:cyt
r7.23     1 ATP:cyt + 1 gcl:cyt => 1 ADP:cyt + 1 g3p:cyt + 1 H:cyt
r7.24     1 g3p:cyt + 1 NAD:cyt => 1 GAP:cyt + 1 H:cyt + 1 NADH:cyt
r7.25     1 Lrha:cyt + 1 NADP:cyt => 1 H:cyt + 1 Lrha14lac:cyt + 1 NADPH:cyt
r7.26     1 H2O:cyt + 1 Lrha14lac:cyt => 1 H:cyt + 1 Lrhant:cyt
r7.27     1 Lrhant:cyt => 1 23rha:cyt + 1 H2O:cyt
r7.28     1 23rha:cyt => 1 lactal:cyt + 1 pyr:cyt
r7.29     1 H2O:cyt + 1 lactal:cyt + 1 NADP:cyt => 2 H:cyt + 1 lact:cyt + 1 NADPH:cyt
r7.30     1 lact:cyt + 1 NAD:cyt <=> 1 H:cyt + 1 NADH:cyt + 1 pyr:cyt

```

Transfer of 1-C compounds

```

r8.1      1 gly:cyt + 1 NAD:cyt + 1 THF:cyt => 1 CO2:cyt + 1 METHF:cyt + 1 NADH:cyt + 1 NH4:cyt
r8.2      1 H:cyt + 1 METHF:cyt + 1 NADH:cyt => 1 MYTHF:cyt + 1 NAD:cyt
r8.3      1 ATP:cyt + 2 H2O:cyt + 1 METHF:cyt + 1 NAD:cyt => 1 ADP:cyt + 1 FTHF:cyt + 2 H:cyt + 1
NADH:cyt + 1 Pi:cyt
r8.4      1 ATP:cyt + 2 H2O:cyt + 1 met:cyt => 1 H:cyt + 3 Pi:cyt + 1 SAM:cyt
r8.5      1 H2O:cyt + 1 SAH:cyt => 1 A:cyt + 1 homcys:cyt

```

Transport across the plasma membrane

```

r9.1      1 ATP:cyt + 1 H2O:cyt => 1 ADP:cyt + 1 H:ext + 1 Pi:cyt
r9.2      2 H:ext + 1 Pi:ext => 2 H:cyt + 1 Pi:cyt
r9.3      1 glc:ext + 1 H:ext => 1 glc:cyt + 1 H:cyt
r9.4      2 H:ext + 1 SO4:ext => 2 H:cyt + 1 SO4:cyt
r9.6      1 O2:ext => 1 O2:cyt
r9.7      1 CO2:cyt => 1 CO2:ext
r9.14     1 psacch:cyt => 1 psacch:ext
r9.15     1 H2O:cyt => 1 H2O:ext
r9.19     1 H:ext + 1 xyl:ext => 1 H:cyt + 1 xyl:cyt
r9.32     1 D-galac:ext => 1 D-galac:cyt
R9.35     1 NH4:ext => 1 NH4:cyt
r9.36     1 ara:ext + 1 H:ext => 1 ara:cyt + 1 H:cyt
r9.37     1 H:ext + 1 mann:ext => 1 H:cyt + 1 mann:cyt
r9.38     1 H:ext + 1 Lrha:ext => 1 H:cyt + 1 Lrha:cyt

```

Transport across the mitochondrial membrane

```

r10.1          1 ADP:cyt + 1 ATP:mit => 1 ADP:mit + 1 ATP:cyt
r10.3          1 H2O:mit => 1 H2O:cyt
r10.5          1 H:cyt + 1 Pi:cyt => 1 H:mit + 1 Pi:mit
r10.6          1 citr:cyt + 1 iCitr:mit => 1 citr:mit + 1 iCitr:cyt
r10.7          1 ctl:mit + 1 H:cyt => 1 ctl:cyt + 1 H:mit
r10.8          1 mal:mit + 1 Pi:cyt => 1 mal:cyt + 1 Pi:mit
r10.9          1 NH4:mit => 1 NH4:cyt
r10.10         1 H:cyt + 1 ile:mit => 1 H:mit + 1 ile:cyt
r10.11         1 H:cyt + 1 pyr:cyt => 1 H:mit + 1 pyr:mit
r10.12         1 CO2:mit => 1 CO2:cyt
r10.13         1 fum:cyt + 1 H:cyt => 1 fum:mit + 1 H:mit
r10.14         1 citr:mit + 1 mal:cyt => 1 citr:cyt + 1 mal:mit
r10.15         1 H:cyt + 1 thr:cyt => 1 H:mit + 1 thr:mit
r10.16         1 glu:cyt + 1 H:cyt => 1 glu:mit + 1 H:mit
r10.17         1 H:cyt + 1 val:mit => 1 H:mit + 1 val:cyt
r10.18         1 gln:cyt + 1 H:cyt => 1 gln:mit + 1 H:mit
r10.19         1 bIM:mit + 1 H:cyt => 1 bIM:cyt + 1 H:mit

```

Amino acid synthesis

```

r11.1          1 aKG:cyt + 1 H:cyt + 1 NADPH:cyt + 1 NH4:cyt => 1 glu:cyt + 1 H2O:cyt + 1 NADP:cyt
r11.2          1 ATP:cyt + 1 glu:cyt + 1 NH4:cyt => 1 ADP:cyt + 1 gln:cyt + 1 H:cyt + 1 Pi:cyt
r11.3          1 ATP:cyt + 1 glu:cyt + 2 H:cyt + 2 NADPH:cyt => 1 ADP:cyt + 1 H2O:cyt + 2 NADP:cyt + 1
Pi:cyt + 1 pro:cyt
r11.4          2 ATP:mit + 1 CO2:mit + 1 gln:mit + 2 H2O:mit => 2 ADP:mit + 1 carbP:mit + 1 glu:mit + 3
H:mit + 1 Pi:mit
r11.5          1 ATP:mit + 1 carbP:mit + 2 glu:mit + 1 NADPH:mit => 1 ADP:mit + 1 aKG:mit + 1 ctl:mit +
1 H:mit + 1 NADP:mit + 2 Pi:mit
r11.6          1 asp:cyt + 2 ATP:cyt + 1 ctl:cyt + 1 H2O:cyt => 2 ADP:cyt + 1 arg:cyt + 1 fum:cyt + 1
H:cyt + 2 Pi:cyt
r11.7          1 AcCoA:cyt + 1 glu:cyt + 1 H2O:cyt + 1 NAD:cyt => 1 aAd:cyt + 1 CO2:cyt + 1 HCoA:cyt + 1
NADH:cyt
r11.8          1 aAd:cyt + 2 ATP:cyt + 1 glu:cyt + 1 H2O:cyt + 1 NAD:cyt + 2 NADPH:cyt => 2 ADP:cyt + 1
aKG:cyt + 1 H:cyt + 1 lys:cyt
+ 1 NADH:cyt + 2 NADP:cyt + 2 Pi:cyt
r11.9          1 3PG:cyt + 1 glu:cyt + 1 H2O:cyt + 1 NAD:cyt => 1 aKG:cyt + 1 H:cyt + 1 NADH:cyt + 1
Pi:cyt + 1 ser:cyt
r11.10         1 ser:cyt + 1 THF:cyt => 1 gly:cyt + 1 H2O:cyt + 1 METHF:cyt
r11.11         2 ATP:cyt + 3 H:cyt + 1 H2O:cyt + 1 SO4:cyt => 1 ADP:cyt + 1 PAPS:cyt + 2 Pi:cyt
r11.12         1 H:cyt + 4 NADPH:cyt + 1 PAPS:cyt => 1 ADP:cyt + 3 H2O:cyt + 1 H2S:cyt + 4 NADP:cyt
r11.13         1 AcCoA:cyt + 1 homser:cyt => 1 AcHomser:cyt + 1 HCoA:cyt
r11.14         1 AcHomser:cyt + 1 H2S:cyt => 1 Ac:cyt + 1 H:cyt + 1 homcys:cyt
r11.15         1 AcCoA:cyt + 1 H2S:cyt + 1 ser:cyt => 1 Ac:cyt + 1 cys:cyt + 1 H:cyt + 1 HCoA:cyt
r11.16         1 glu:cyt + 1 OAA:cyt => 1 aKG:cyt + 1 asp:cyt
r11.17         1 asp:cyt + 2 ATP:cyt + 1 H2O:cyt + 1 NH4:cyt => 2 ADP:cyt + 1 asn:cyt + 2 H:cyt + 2
Pi:cyt
r11.18         1 asp:cyt + 1 ATP:cyt + 2 H:cyt + 2 NADPH:cyt => 1 ADP:cyt + 1 homser:cyt + 2 NADP:cyt +
1 Pi:cyt
r11.19         1 ATP:cyt + 1 H2O:cyt + 1 homser:cyt => 1 ADP:cyt + 1 H:cyt + 1 Pi:cyt + 1 thr:cyt
r11.20         1 homcys:cyt + 1 MYTHF:cyt => 1 met:cyt + 1 THF:cyt
r11.21

```



```

1 glu:mit + 2 H:mit + 1 NADPH:mit + 1 pyr:mit + 1 thr:mit => 1 aKG:mit + 1 CO2:mit + 1
H2O:mit + 1 ile:mit + 1 NADP:mit
+ 1 NH4:mit
r11.22
1 glu:cyt + 1 pyr:cyt => 1 aKG:cyt + 1 ala:cyt
r11.23
2 H:mit + 1 NADPH:mit + 2 pyr:mit => 1 aKI:mit + 1 CO2:mit + 1 H2O:mit + 1 NADP:mit
r11.24
1 aKI:mit + 1 glu:mit => 1 aKG:mit + 1 val:mit
r11.25
1 AcCoA:mit + 1 aKI:mit + 1 H2O:mit => 1 bIM:mit + 1 H:mit + 1 HCoA:mit
r11.26
1 bIM:cyt + 1 glu:cyt + 1 NAD:cyt => 1 aKG:cyt + 1 CO2:cyt + 1 leu:cyt + 1 NADH:cyt
r11.27
1 ATP:cyt + 1 E4P:cyt + 1 NADPH:cyt + 2 PEP:cyt => 1 ADP:cyt + 1 chor:cyt + 1 NADP:cyt +
4 Pi:cyt
r11.28
1 chor:cyt + 1 glu:cyt + 1 H:cyt => 1 aKG:cyt + 1 CO2:cyt + 1 H2O:cyt + 1 phe:cyt
r11.29
1 chor:cyt + 1 glu:cyt + 1 NAD:cyt => 1 aKG:cyt + 1 CO2:cyt + 1 NADH:cyt + 1 tyr:cyt
r11.30
1 chor:cyt + 1 gln:cyt + 1 PRPP:cyt + 1 ser:cyt => 1 CO2:cyt + 1 GAP:cyt + 1 glu:cyt + 1
H:cyt + 1 H2O:cyt + 2 Pi:cyt
+ 1 pyr:cyt + 1 trp:cyt
r11.31
2 ATP:cyt + 1 Ribul5P:cyt => 2 ADP:cyt + 1 H:cyt + 1 PRPP:cyt
r11.32
3 ATP:cyt + 1 CO2:cyt + 1 gln:cyt + 3 H2O:cyt + 2 NAD:cyt + 1 NADPH:cyt + 1 NH4:cyt + 1
PRPP:cyt => 3 ADP:cyt + 1 aKG:cyt
+ 8 H:cyt + 1 his:cyt + 2 NADH:cyt + 1 NADP:cyt + 6 Pi:cyt

```

Nucleotide biosynthesis

```

r13.1
1 asp:cyt + 4 ATP:cyt + 1 CO2:cyt + 2 FTHF:cyt + 2 gln:cyt + 1 gly:cyt + 2 H2O:cyt + 1
PRPP:cyt => 4 ADP:cyt + 1 fum:cyt
+ 2 glu:cyt + 8 H:cyt + 1 IMP:cyt + 6 Pi:cyt + 2 THF:cyt
r13.2
1 asp:cyt + 1 ATP:cyt + 1 IMP:cyt => 1 ADP:cyt + 1 AMP:cyt + 1 fum:cyt + 2 H:cyt + 1
Pi:cyt
r13.3
2 ATP:cyt + 1 gln:cyt + 3 H2O:cyt + 1 IMP:cyt + 1 NAD:cyt => 2 ADP:cyt + 1 glu:cyt + 1
GMP:cyt + 4 H:cyt + 1 NADH:cyt
+ 2 Pi:cyt
r13.4
1 asp:cyt + 2 ATP:cyt + 1 gln:cyt + 2 H2O:cyt + 1 NAD:cyt + 1 PRPP:cyt => 2 ADP:cyt + 1
glu:cyt + 4 H:cyt + 1 NADH:cyt
+ 4 Pi:cyt + 1 UMP:cyt
r13.5
2 ATP:cyt + 1 UMP:cyt => 2 ADP:cyt + 1 UTP:cyt
r13.6
1 ATP:cyt + 1 gln:cyt + 1 H2O:cyt + 1 UTP:cyt => 1 ADP:cyt + 1 CTP:cyt + 1 glu:cyt + 2
H:cyt + 1 Pi:cyt
r13.7
2 ADP:cyt + 1 CTP:cyt => 2 ATP:cyt + 1 CMP:cyt
r13.8
1 A:cyt + 2 ATP:cyt => 3 ADP:cyt + 1 H:cyt
r13.9
1 ATP:cyt + 1 UDP:cyt => 1 ADP:cyt + 1 UTP:cyt
UDPGlc4ep
1 UDPGlc:cyt <=> 1 UDPGAL:cyt
ATP GTP Ptrans
1 ATP:cyt + 1 GDP:cyt <=> 1 ADP:cyt + 1 GTP:cyt

```

ATP-hydrolysis

```

r15.1
1 ATP:cyt + 1 H2O:cyt => 1 ADP:cyt + 1 H:cyt + 1 Pi:cyt

```

Synthesis of fatty acids

```

C120syn
6 AcCoA:cyt + 5 ATP:cyt + 5 H:cyt + 1 H2O:cyt + 10 NADPH:cyt => 5 ADP:cyt + 1 C120:cyt +
6 HCoA:cyt + 10 NADP:cyt + 5 Pi:cyt
C140syn
7 AcCoA:cyt + 6 ATP:cyt + 6 H:cyt + 1 H2O:cyt + 12 NADPH:cyt => 6 ADP:cyt + 1 C140:cyt +
7 HCoA:cyt + 12 NADP:cyt + 6 Pi:cyt
C141syn
1 C140:cyt + 1 H:cyt + 1 NADPH:cyt + 1 O2:cyt => 1 C141:cyt + 2 H2O:cyt + 1 NADP:cyt
C160syn
8 AcCoA:cyt + 7 ATP:cyt + 7 H:cyt + 1 H2O:cyt + 14 NADPH:cyt => 7 ADP:cyt + 1 C160:cyt +
8 HCoA:cyt + 14 NADP:cyt + 7 Pi:cyt
C161syn
1 C160:cyt + 1 H:cyt + 1 NADPH:cyt + 1 O2:cyt => 1 C161:cyt + 2 H2O:cyt + 1 NADP:cyt
C162syn
1 C161:cyt + 1 H:cyt + 1 NADPH:cyt + 1 O2:cyt => 1 C162:cyt + 2 H2O:cyt + 1 NADP:cyt
C180syn
9 AcCoA:cyt + 8 ATP:cyt + 8 H:cyt + 1 H2O:cyt + 16 NADPH:cyt => 8 ADP:cyt + 1 C180:cyt +
9 HCoA:cyt + 16 NADP:cyt + 8 Pi:cyt
C181CoA syn

```

```

2 ATP:cyt + 1 C181:cyt + 2 H2O:cyt + 1 HCoA:cyt => 2 ADP:cyt + 1 C181CoA:cyt + 2 H:cyt +
2 Pi:cyt
C181syn
1 C180:cyt + 1 H:cyt + 1 NADPH:cyt + 1 O2:cyt => 1 C181:cyt + 2 H2O:cyt + 1 NADP:cyt
C182syn
1 C181:cyt + 1 H:cyt + 1 NADPH:cyt + 1 O2:cyt => 1 C182:cyt + 2 H2O:cyt + 1 NADP:cyt
C183syn
1 C182:cyt + 1 H:cyt + 1 NADPH:cyt + 1 O2:cyt => 1 C183:cyt + 2 H2O:cyt + 1 NADP:cyt
C200syn
10 AcCoA:cyt + 9 ATP:cyt + 9 H:cyt + 1 H2O:cyt + 18 NADPH:cyt => 9 ADP:cyt + 1 C200:cyt +
10 HCoA:cyt + 18 NADP:cyt + 9 Pi:cyt
CLsyn
2 CDPDAcgc1:cyt + 2 g3p:cyt + 2 H2O:cyt => 1 CL:cyt + 2 CMP:cyt + 1 gcl:cyt + 2 H:cyt + 2
Pi:cyt
DAGLYsyn
0.024 C120:cyt + 0.014 C140:cyt + 0.012 C141:cyt + 0.156 C160:cyt + 0.02 C161:cyt + 0.008
C162:cyt + 0.027 C180:cyt
+ 0.374 C181:cyt + 0.327 C182:cyt + 0.032 C183:cyt + 0.006 C200:cyt + 1 MAGLY:cyt => 1
DAGLY:cyt + 1 H2O:cyt
DGDG syn
1 MGDG:cyt + 1 UDPGAL:cyt => 1 DGDG:cyt + 1 H:cyt + 1 UDP:cyt
MAGLYsyn
0.024 C120:cyt + 0.014 C140:cyt + 0.012 C141:cyt + 0.156 C160:cyt + 0.02 C161:cyt + 0.008
C162:cyt + 0.027 C180:cyt
+ 0.374 C181:cyt + 0.327 C182:cyt + 0.032 C183:cyt + 0.006 C200:cyt + 1 gcl3P:cyt => 1
MAGLY:cyt + 1 Pi:cyt
MGC181 syn
1 C181CoA:cyt + 1 H2O:cyt + 1 UDPGAL:cyt => 1 H:cyt + 1 HCoA:cyt + 1 MGC181:cyt + 1
UDP:cyt
MGDG syn
1 DAGLY:cyt + 1 UDPGAL:cyt => 1 H:cyt + 1 MGDG:cyt + 1 UDP:cyt
r16.10
1 PHeta:cyt + 3 SAM:cyt => 3 H:cyt + 1 PHchol:cyt + 3 SAH:cyt
r16.13
3 AcCoA:cyt + 1 H:cyt + 1 H2O:cyt + 2 NADPH:cyt => 3 HCoA:cyt + 1 meva:cyt + 2 NADP:cyt
r16.14
18 ATP:cyt + 5 H2O:cyt + 6 meva:cyt + 2 NADPH:cyt + 1 O2:cyt => 18 ADP:cyt + 6 CO2:cyt +
10 H:cyt + 1 lano:cyt + 2 NADP:cyt
+ 18 Pi:cyt
r16.15
1 lano:cyt + 1 NAD:cyt + 2 THF:cyt => 1 ergo:cyt + 1 H:cyt + 2 MYTHF:cyt + 1 NADH:cyt
r16.16
1 ergo:cyt + 1 olCoA:cyt => 1 ESE:cyt + 1 HCoA:cyt
r16.2
1 GAP:cyt + 1 H:cyt + 1 NADH:cyt => 1 gcl3P:cyt + 1 NAD:cyt
r16.3
9 AcCoA:cyt + 8 ATP:cyt + 8 H:cyt + 16 NADPH:cyt => 8 ADP:cyt + 8 HCoA:cyt + 16 NADP:cyt
+ 8 Pi:cyt + 1 steaCoA:cyt
r16.4
1 H:cyt + 1 NADH:cyt + 1 O2:cyt + 1 steaCoA:cyt => 2 H2O:cyt + 1 NAD:cyt + 1 olCoA:cyt
r16.5
1 H:cyt + 1 NADH:cyt + 1 O2:cyt + 1 olCoA:cyt => 2 H2O:cyt + 1 linCoA:cyt + 1 NAD:cyt
r16.6
1 gcl3P:cyt + 1 linCoA:cyt + 1 olCoA:cyt => 2 HCoA:cyt + 1 phospht:cyt
r16.7
1 CTP:cyt + 1 H2O:cyt + 1 phospht:cyt => 1 CDPDAcgc1:cyt + 2 Pi:cyt
r16.8
1 CDPDAcgc1:cyt + 1 ser:cyt => 1 CMP:cyt + 1 H:cyt + 1 PHser:cyt
r16.9
1 H:cyt + 1 PHser:cyt => 1 CO2:cyt + 1 PHeta:cyt
r23.22
0.000223 C140:cyt + 0.00148 C160:cyt + 0.000245 C180:cyt + 0.00168 C181:cyt + 0.00166
C182:cyt + 4.7E-005 C183:cyt
+ 0.00175 CL:cyt + 0.00101 DAGLY:cyt + 0.00786 DGDG:cyt + 0.0341 ergo:cyt + 0.01 ESE:cyt
+ 0.00891 MAGLY:cyt
+ 0.0124 MGC181:cyt + 0.0301 MGDG:cyt + 0.0153 PHchol:cyt + 0.0348 PHeta:cyt + 0.000359
PHser:cyt + 0.0101 TAGLY:cyt
=> 1 lipidsASP:cyt
TAGLYsyn
0.024 C120:cyt + 0.014 C140:cyt + 0.012 C141:cyt + 0.156 C160:cyt + 0.02 C161:cyt + 0.008
C162:cyt + 0.027 C180:cyt
+ 0.374 C181:cyt + 0.327 C182:cyt + 0.032 C183:cyt + 0.006 C200:cyt + 1 DAGLY:cyt => 1
H2O:cyt + 1 TAGLY:cyt

Synthesis of glycogen and polysaccharides
GDPMANsyn
1 f6P:cyt + 1 GTP:cyt + 2 H:cyt + 1 H2O:cyt => 1 GDPMAN:cyt + 2 Pi:cyt
r17.1
0.167 ATP:cyt + 0.167 g6P:cyt + 0.167 H2O:cyt => 0.167 ADP:cyt + 0.167 H:cyt + 0.333
Pi:cyt + 1 psacch:cyt
r17.2
1 AcCoA:cyt + 1 f6P:cyt + 1 gln:cyt => 1 chit:cyt + 1 glu:cyt + 1 H:cyt + 1 HCoA:cyt + 1
Pi:cyt
r17.3
1 f6P:cyt + 1 H:cyt + 1 NADH:cyt => 1 m1P:cyt + 1 NAD:cyt
r17.4
1 H2O:cyt + 1 m1P:cyt => 1 man:cyt + 1 Pi:cyt
r17.5
1 g6P:cyt + 1 H2O:cyt + 1 UTP:cyt => 2 Pi:cyt + 1 UDPg1c:cyt

```

r17.6
1 g6P:cyt + 1 UDPglc:cyt => 1 H:cyt + 1 t6P:cyt + 1 UDP:cyt
r17.7
1 H2O:cyt + 1 t6P:cyt => 1 Pi:cyt + 1 tre:cyt
r17.8
1 E4P:cyt + 1 H:cyt + 1 H2O:cyt + 1 NADH:cyt => 1 ery:cyt + 1 NAD:cyt + 1 Pi:cyt

Cell Wall Components

r23.1
1 UDPglc:cyt => 1 13GLUCAN:cyt + 1 H:cyt + 1 UDP:cyt
r23.2
1 UDPglc:cyt => 1 14GLUCAN:cyt + 1 H:cyt + 1 UDP:cyt
r23.3
1 UDPglc:cyt => 1 H:cyt + 1 PSNIG:cyt + 1 UDP:cyt
r23.4
1 UDPglc:cyt => 1 H:cyt + 1 NIG:cyt + 1 UDP:cyt
r23.6
1 AcCoA:cyt + 1 GA6P:cyt <=> 1 HCoA:cyt + 1 NAGA6P:cyt
r23.7
1 NAGA6P:cyt <=> 1 NAGA1P:cyt
r23.8
1 H2O:cyt + 1 NAGA1P:cyt + 1 UTP:cyt <=> 2 Pi:cyt + 1 UDPNAG:cyt
r23.10
1 chit:cyt + 1 H2O:cyt => 1 NAG:cyt
r23.11
1 H2O:cyt + 1 NAG:cyt => 1 Ac:cyt + 1 GLCN:cyt + 1 H:cyt
r23.12
1 ATP:cyt + 1 GLCN:cyt + 1 H:cyt => 1 ADP:cyt + 1 GA6P:cyt
r23.14
1 UDPNAG:cyt <=> 1 UDPNAGAL:cyt
r23.15
1.51 H:cyt + 0.754 UDPGAL:cyt + 0.065 UDPglc:cyt + 0.181 UDPNAGAL:cyt => 1 GAG:cyt + 1
UDP:cyt
r23.16
0.435 GDPMAN:cyt + 0.435 UDPGAL:cyt + 0.13 UDPglc:cyt => 0.435 GDP:cyt + 1 GGM:cyt +
0.435 H:cyt + 0.565 UDP:cyt
r23.17
2.73 13GLUCAN:cyt + 0.389 14GLUCAN:cyt + 1.62 chit:cyt + 0.043 GAG:cyt + 0.381 GGM:cyt +
0.254 NIG:cyt + 0.337 PSNIG:cyt
=> 1 cellwall:cyt

Protein synthesis

r23.18
1.03 ala:cyt + 0.413 arg:cyt + 0.209 asn:cyt + 0.628 asp:cyt + 39.7 ATP:cyt + 0.079
cys:cyt + 0.3 gln:cyt + 0.899 glu:cyt
+ 0.862 gly:cyt + 30.5 H2O:cyt + 0.205 his:cyt + 0.396 ile:cyt + 0.704 leu:cyt + 0.651
lys:cyt + 0.105 met:cyt + 0.312 phe:cyt
+ 0.441 pro:cyt + 0.628 ser:cyt + 0.503 thr:cyt + 0.126 trp:cyt + 0.205 tyr:cyt + 0.536
val:cyt => 39.7 ADP:cyt + 39.7 H:cyt
+ 39.7 Pi:cyt + 1 PROTASP:cyt

RNA synthesis

r23.19
0.773 AMP:cyt + 7.42 ATP:cyt + 0.773 CMP:cyt + 0.931 GMP:cyt + 4.31 H2O:cyt + 0.616
UMP:cyt => 7.42 ADP:cyt + 7.42 H:cyt
+ 7.42 Pi:cyt + 1 RNAasp:cyt

Miscellaneous

r23.21
0.3 ery:cyt + 7E-005 fum:mit + 0.46 gcl:cyt + 0.00039 iCitr:mit + 0.00065 mal:mit + 0.18
man:cyt + 0.00091 succ:mit
+ 0.04 tre:cyt => 1 poolAsp:cyt

Biomass formation

r23.23
0.38 cellwall:cyt + 1 lipidsASP:cyt + 1 poolAsp:cyt + 0.263 PROTASP:cyt + 0.0206
RNAasp:cyt => 37.1 BIOMasp:cyt

List of compounds

Name	ShortName	Composition
1,3-bisphosphoglycerate	13PG	C3H4O10P2-4
13-b-D-GLUCAN	13GLUCAN	C6H10O5
14alphaaglucan	14GLUCAN	C6H10O5
2-dehydro-3-deoxy-L-galactonate	23gal	C6H9O6-1
2-dehydro-3-deoxy-L-rhamnonate	23rha	C6H9O5-1
2-phosphoglycerate	2PG	C3H4O7P-3
3-phospho-adenosine-5-phosphosulfate	PAPS	C10H15N5O13P2S
3-phospho-glyceraldehyde	GAP	C3H5O6P-2
3-phosphoglycerate	3PG	C3H4O7P-3
3-phospho-glycerol	gcl3P	C3H7O6P-2
6-phosphogluconate	6Pgluct	C6H10O10P-3
a-5-phosphoribosyl-pyrophosphate	PRPP	C5H8O14P3-5

acetate	Ac	C2H3O2-1
acetyl coenzyme A	AcCoA	C23H34N7O17P3S-4
adenosine	A	C10H13N5O4
adenosine-5-diphosphate	ADP	C10H12N5O10P2-3
adenosine-5-monophosphate	AMP	C10H12N5O7P-2
adenosine-5-triphosphate	ATP	C10H12N5O13P3-4
alanine	ala	C3H7NO2
aldehyde-L-galactonate	aldeLgal	C6H11O7-1
α-linolenic acid	C183	C18H30O2
α-aminoadipate	aAd	C6H11NO4
α-ketoglutarate	aKG	C5H4O5-2
α-ketoisovalerate	aKI	C5H7O3-1
ammonia	NH4	H4N+1
arabinose	ara	C5H10O5
Arabitol	arab	C5H12O5
Arachidic acid	C200	C20H40O2
arginine	arg	C6H15N4O2+1
asparagine	asn	C4H8N2O3
aspartate	asp	C4H6NO4-1
β-isopropylmalate	bIM	C7H10O5-2
biomass aspergillus	BIOMasp	CH1.73N0.1110O.547P0.00308S0.00131
C162	C162	C16H28O2
carbamoyl phosphate	carbP	CH2NO5P-2
carbon dioxide	CO2	CO2
Cardiolipin	CL	C81H144O17P2-2
cell wall	cellwall	C37.8H63.1N1.63O28.8+0.67
chitin	chit	C8H13NO5
chorismate	chor	C10H8O6-2
citrate	citr	C6H5O7-3
citrulline	ctl	C6H12N3O3-1
coenzyme A	HCoA	C21H32N7O16P3S-4
cysteine	cys	C3H7NO2S
cytidine diphosphate-diacylglycerol	CDPDAcgcl	C48H81N3O15P2-2
cytidine monophosphate	CMP	C9H12N3O8P-2
cytidine triphosphate	CTP	C9H12N3O14P3-4
D-galacturonate	D-galacn	C6H9O7-1
D-galacturonic acid	D-galac	C6H9O7-1
D-glucosamine	GLCN	C6H13NO5
Diacylglycerol	DAGLY	C37.8H68.9O5
Digalactosyl diglyceride	DGDG	C49.8H92.9O15
ergosterol	ergo	C28H44O
ergosterolester	ESE	C46H76O2
erythritol	ery	C4H10O4
erythrose-4-phosphate	E4P	C4H7O7P-2
flavine adenine dinucleotide (oxidized)	FAD	C27H33N9O15P2
flavine adenine dinucleotide (reduced)	FADH2	C27H35N9O15P2
formyl tetrahydrofolate	FTHF	C20H21N7O7-2
fructose-1,6-bisphosphate	f16P	C6H10O12P2-4
fructose-6-phosphate	f6P	C6H11O9P-2
fumarate	fum	C4H2O4-2
Galactoglucomanan	GGM	C6H11.4O5+1.44
Galactosaminogalactan	GAG	C6.36H13.4N0.181O5+2.87
GDPmannose	GDPMAN	C16H25N5O16P2
Glucosamine6phosphate	GA6P	C6H14NO8P
glucose	glc	C6H12O6
glucose-6-phosphate	g6P	C6H11O9P-2
glutamate	glu	C5H8NO4-1
glutamine	gln	C5H10N2O3
glyceraldehyde	glycal	C3H6O3
glycerol	gcl	C3H8O3
glycerol-3-phosphate	g3p	C3H7O6P-2
glycine	gly	C2H5NO2
guanosine diphosphate	GDP	C10H12N5O11P2-3
guanosine monophosphate	GMP	C10H12N5O8P-2
Guanosine triphosphate	GTP	C10H12N5O14P3-4
histidine	his	C6H9N3O2
homocysteine	homcys	C4H9NO2S
homoserine	homser	C4H9NO3
hydrogen sulphide	H2S	H2S
inosine monophosphate	IMP	C10H11N4O8P-2
isocitrate	iCitr	C6H5O7-3
isoleucine	ile	C6H13NO2
lactaldehyde	lactal	C3H6O2
lactate	lact	C3H5O3-1
lanosterol	lano	C30H50O
Lauric acid	C120	C12H24O2
leucine	leu	C6H13NO2
linoleic acid	C182	C18H32O2
linoleoyl coenzyme A	linCoA	C39H62N7O17P3S-4
LipidsASP	lipidsASP	C6.4H11.5N0.0505O1.09P0.0505-0.000359
L-rhamnonate	Lrhant	C6H11O6-1
L-rhamnono-1-4-lactone	Lrha14lac	C6H10O5
L-rhamnose	Lrha	C6H12O5
L-xylulose	L-xylu	C5H10O5
lysine	lys	C6H15N2O2+1
malate	mal	C4H4O5-2
mannitol	man	C6H14O6
mannitol-1-phosphate	m1P	C6H13O9P-2
mannose	mann	C6H12O6

mannose-6-phosphate	mann6P	C6H11O9P-2
methionine	met	C5H11NO2S
methyl tetrahydrofolate	MYTHF	C20H23N7O6-2
methylene tetrahydrofolate	METHF	C20H21N7O6-2
mevalonate	meva	C6H11O4-1
Monoacylglycerol	MAGLY	C20.4H38.4O4
Monogalactosyl diglyceride	MGDG	C43.8H80.9O10
Monoglucosyloxyoctadecenoic acid	MGC181	C24H48O8
Myristic acid	C140	C14H28O2
Myristoleic acid	C141	C14H26O2
N-acetyl-d-glucosamine	NAG	C8H15NO6
NacetylDglucosamine 1-phosphate	NAGA1P	C8H16NO9P
NacetylDglucosamine 6-phosphate	NAGA6P	C8H16NO9P
nicotinamide adenine dinucleotide (oxidized)	NAD	C21H26N7O14P2-1
nicotinamide adenine dinucleotide (reduced)	NADH	C21H27N7O14P2-2
nicotinamide adenine dinucleotide phosphate (oxidized)	NADP	C21H25N7O17P3-4
nicotinamide adenine dinucleotide phosphate (reduced)	NADPH	C21H26N7O17P3-5
Nigeran	NIG	C6H10O5
o-acetyl homoserine	AcHomser	C6H11NO4
Octadecenoyl-CoA	C181CoA	C39H66N7O18P3S-4
Oleic acid	C181	C18H34O2
oleoyl coenzyme A	olCoA	C39H64N7O17P3S-4
orthophosphate	Pi	HO4P-2
oxaloacetate	OAA	C4H2O5-2
oxygen	O2	O2
Palmitic acid	C160	C16H32O2
Palmitoleic acid	C161	C16H30O2
phenylalanine	phe	C9H11NO2
phosphatidate	phosphpt	C39H69O8P-2
phosphatidyl choline	PHchol	C44H82NO8P
phosphatidyl ethanolamine	PHeta	C41H76NO8P
phosphatidyl serine	PHser	C42H75NO10P-1
phosphoenolpyruvate	PEP	C3H2O6P-3
polysaccharide	psacch	CH1.6700.833
pool of small molecules Asp	poolAsp	C4.15H10.104.11-0.00433
proline	pro	C5H9NO2
proteinASP	PROTASP	C44H68.5N12.2014.1S0.184-0.463
proton	H	H+1
pseudonigeran	PSNIG	C6H10O5
pyruvate	pyr	C3H3O3-1
ribose nucleic acid ASP	RNAasp	C29.5H30.3N12.1021.5P3.09-6.19
ribose-5-phosphate	Rib5P	C5H9O8P-2
ribulose-5-phosphate	Ribu5P	C5H9O8P-2
S-adenosylhomocysteine	SAH	C14H20N6O5S
S-adenosylmethionine	SAM	C15H23N6O5S+1
sedoheptulose-7-phosphate	sed7P	C7H13O10P-2
serine	ser	C3H7NO3
Stearic acid	C180	C18H36O2
stearoyl coenzyme A	steaCoA	C39H66N7O17P3S-4
succinate	succ	C4H4O4-2
succinyl coenzyme A	succCoA	C25H35N7O19P3S-5
sulphate	SO4	O4S-2
tetrahydrofolate	THF	C19H21N7O6-2
threonine	thr	C4H9NO3
trehalose	tre	C12H22O11
trehalose-6-phosphate	t6P	C12H21O14P-2
triacylglycerol_asp	TAGLY	C55.2H99.3O6
tryptophane	trp	C11H12N2O2
tyrosine	tyr	C9H11NO3
UDPGalactose	UDPGAL	C15H22N2O17P2-2
UDP-N-acetyl-D-galactosamine	UDPNAGAL	C17H27N3O17P2
UDP-N-acetyl-D-glucosamine	UDPNAG	C17H27N3O17P2
uridine monophosphate	UMP	C9H11N2O9P-2
uridine triphosphate	UTP	C9H11N2O15P3-4
uridine-5-diphosphate	UDP	C9H11N2O12P2-3
uridine-5-diphosphoglucose	UDPGlc	C15H22N2O17P2-2
valine	val	C5H11NO2
water	H2O	H2O
xylitol	xol	C5H12O5
xylose	xyl	C5H10O5
xylulose	xylu	C5H10O5
xylulose-5-phosphate	Xylu5P	C5H9O8P-2

Fig. S4.3. List of reactions and compounds for the Stoichiometric model for growth of *A. niger* on mixtures of glucose, mannose, arabinose, xylose, galacturonic acid and rhamnose.

Appendix Chapter 5

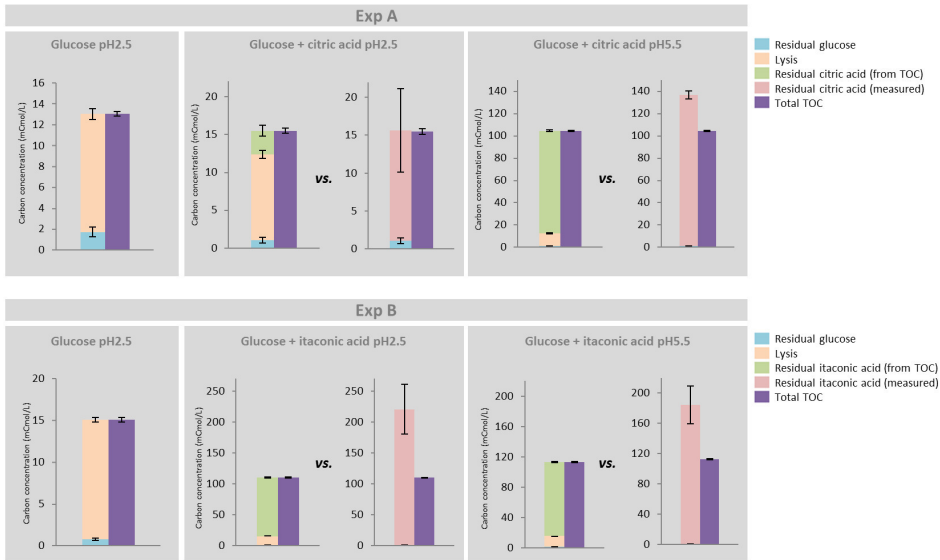


Fig. S5.1. Comparison of measured residual organic acid and estimated organic acid from TOC values (citric acid in experiment A and itaconic acid in experiment B).

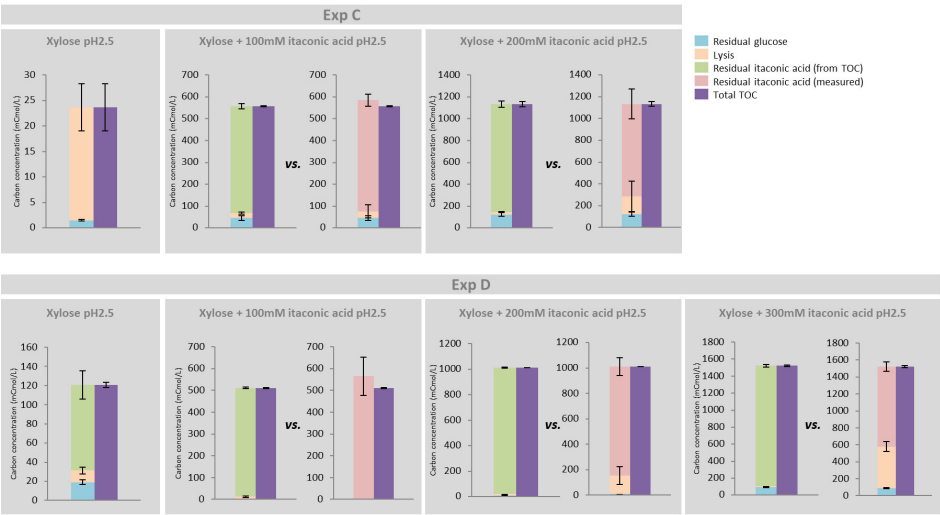


Fig. S5.2. Comparison of measured residual itaconic acid and estimated itaconic acid from TOC values in experiments C and D.

Table S5.1. Unreconciled and reconciled measurements of experiment A
in strain *A. niger* NW185 in presence of citric acid.

Exp A						
	38mM Glucose pH 2.5		19mM Glucose + 19mM citric acid pH 2.5		19mM Glucose + 19mM citric acid pH 5.5	
	Unreconciled	Reconciled	Unreconciled	Reconciled	Unreconciled	Reconciled
F_{out} (L/h)	0.44290 ± 0.00003	0.44290 ± 0.00003	0.44360 ± 0.00033	0.44358 ± 0.00033	0.44350 ± 0.00003	0.44350 ± 0.00003
F_{in} (L/h)	0.44200 ± 0.00003	0.44200 ± 0.00003	0.44280 ± 0.00033	0.44282 ± 0.00033	0.43730 ± 0.00003	0.43730 ± 0.00003
$F_{gas\ in}$ (mmol/h)	2678.6 ± 26.8	2718.0 ± 24.7	2678.6 ± 26.8	2673.2 ± 26.3	2678.6 ± 26.8	2708.5 ± 26.1
$F_{gas\ out}$ (mmol/h)	2673.6 ± 26.7	2718.7 ± 24.7	2688.6 ± 26.9	2685.6 ± 26.4	2675.6 ± 26.8	2710.9 ± 26.1
O_{2out} (%)	19.465 ± 0.020	19.427 ± 0.017	19.524 ± 0.018	19.564 ± 0.012	20.010 ± 0.018	20.133 ± 0.008
CO_{2in} (%)	0.032 ± 0.000	0.032 ± 0.000	0.035 ± 0.000	0.035 ± 0.000	0.033 ± 0.000	0.033 ± 0.000
CO_{2out} (%)	-	1.576 ± 0.017	1.757 ± 0.018	1.783 ± 0.014	0.885 ± 0.009	0.921 ± 0.008
O_{2in} (%)	20.950 ± 0.000	20.950 ± 0.000	20.950 ± 0.000	20.950 ± 0.000	20.950 ± 0.000	20.950 ± 0.000
$C_{glucose\ in}$ (mmol/L)	38.000 ± 0.038	37.986 ± 0.038	19.000 ± 0.019	19.001 ± 0.019	19.000 ± 0.019	18.997 ± 0.019
C_{lysis} (mCmol/L)	11.327 ± 0.514	11.754 ± 0.502	-	9.966 ± 0.511	-	6.359 ± 0.502
$C_{glucose\ out}$ (mmol/L)	0.286 ± 0.079	0.345 ± 0.077	0.175 ± 0.063	0.161 ± 0.063	0.141 ± 0.023	0.146 ± 0.023
$C_{biomass}$ (g/L)	3.193 ± 0.046	3.316 ± 0.033	2.855 ± 0.033	2.831 ± 0.032	1.604 ± 0.057	1.780 ± 0.029
Mw biomass (g/Cmol)	27.930 ± 0.060	27.905 ± 0.060	27.930 ± 0.060	27.938 ± 0.060	27.930 ± 0.060	27.917 ± 0.060
$C_{citric\ acid\ out}$ (mmol/L)	0.000 ± 0.000	0.000 ± 0.000	2.429 ± 0.916	1.383 ± 0.315	15.378 ± 0.135	15.683 ± 0.127
$C_{citric\ acid\ in}$ (mmol/L)	0.000 ± 0.000	0.000 ± 0.000	19.000 ± 0.019	19.000 ± 0.019	19.000 ± 0.019	18.994 ± 0.019
R_{CO_2} (mmol/h)	35.80 ± 10.00	41.98 ± 0.51	46.31 ± 0.67	46.95 ± 0.58	22.79 ± 0.33	24.07 ± 0.30
R_{O_2} (mmol/h)	-40.74 ± 7.67	-41.26 ± 0.52	-36.24 ± 7.70	-34.63 ± 0.46	-25.77 ± 7.77	-21.63 ± 0.31
$R_{biomass}$ (mmol/h)	50.64 ± 0.73	52.64 ± 0.52	45.35 ± 0.52	44.95 ± 0.51	25.47 ± 0.90	28.28 ± 0.45
R_{lysis} (mCmol/h)	5.02 ± 0.23	5.21 ± 0.22	4.48 ± 0.23	4.42 ± 0.23	2.52 ± 0.23	2.82 ± 0.22
$R_{citric\ acid}$ (mmol/h)	0.00 ± 0.00	0.00 ± 0.00	-8.18 ± 0.06	-7.80 ± 0.14	-1.49 ± 0.36	-1.35 ± 0.06
$R_{glucose}$ (mmol/h)	-16.67 ± 0.04	-16.64 ± 0.04	-8.34 ± 0.03	-8.34 ± 0.03	-8.25 ± 0.08	-8.24 ± 0.01
$RQ\ (R_{CO_2}/R_{O_2})$	0.88 ± 0.30	1.02 ± 0.02	1.28 ± 0.27	1.36 ± 0.02	0.88 ± 0.27	1.11 ± 0.02
$R_{O_2}/R_{glucose}$	2.44 ± 0.46	2.48 ± 0.03	4.35 ± 0.92	4.15 ± 0.06	3.13 ± 0.94	2.62 ± 0.04
Carbon recovery (%)	91 ± 1	-	98 ± 1	-	91 ± 2	-
Redox recovery (%)	97 ± 5	-	103 ± 6	-	104 ± 12	-

Table S5.2. Unreconciled and reconciled measurements of experiment B
in strain *A. niger* NW185 in presence of itaconic acid.

Exp B						
	38mM Glucose pH 2.5		19mM Glucose + 22.8mM itaconic acid pH 2.5		19mM Glucose + 22.8mM itaconic acid pH 5.5	
	Unreconciled	Reconciled	Unreconciled	Reconciled	Unreconciled	Reconciled
F_{out} (L/h)	0.42880 ± 0.00080	0.42880 ± 0.00080	0.45670 ± 0.00017	0.45670 ± 0.00017	0.42810 ± 0.00004	0.42810 ± 0.00004
F_{in} (L/h)	0.42872 ± 0.00080	0.42872 ± 0.00080	0.45630 ± 0.00017	0.45630 ± 0.00017	0.42340 ± 0.00004	0.42340 ± 0.00004
$F_{gas\ in}$ (mmol/h)	2678.6 ± 26.8	2691.7 ± 23.3	2678.6 ± 26.8	2695.8 ± 26.2	2678.6 ± 26.8	2672.5 ± 26.3
$F_{gas\ out}$ (mmol/h)	2674.9 ± 26.7	2692.4 ± 23.3	2676.1 ± 26.8	2697.1 ± 26.2	2675.5 ± 26.8	2673.6 ± 26.3
O_{2out} (%)	19.466 ± 0.026	19.562 ± 0.011	20.127 ± 0.010	20.194 ± 0.006	20.115 ± 0.016	20.217 ± 0.007
CO_{2in} (%)	0.029 ± 0.000	0.029 ± 0.000	0.028 ± 0.000	0.028 ± 0.000	0.028 ± 0.000	0.028 ± 0.000
CO_{2out} (%)	1.404 ± 0.014	1.438 ± 0.011	0.777 ± 0.008	0.822 ± 0.006	0.772 ± 0.008	0.794 ± 0.007
O_{2in} (%)	20.950 ± 0.000	20.950 ± 0.000	20.950 ± 0.000	20.950 ± 0.000	20.950 ± 0.000	20.950 ± 0.000
$C_{glucose\ in}$ (mmol/L)	38.000 ± 0.038	37.995 ± 0.038	19.000 ± 0.019	18.998 ± 0.019	19.000 ± 0.019	19.002 ± 0.019
C_{lysis} (mCmol/L)	12.634 ± 0.301	14.360 ± 0.297	-	7.471 ± 0.299	-	8.052 ± 0.299
$C_{glucose\ out}$ (mmol/L)	0.126 ± 0.023	0.128 ± 0.023	0.128 ± 0.023	0.131 ± 0.023	0.185 ± 0.034	0.180 ± 0.034
$C_{biomass}$ (g/L)	3.448 ± 0.035	3.470 ± 0.025	1.869 ± 0.056	1.946 ± 0.027	1.932 ± 0.061	1.822 ± 0.029
Mw biomass (g/Cmol)	27.930 ± 0.060	27.922 ± 0.059	27.930 ± 0.060	27.924 ± 0.060	27.930 ± 0.060	27.937 ± 0.060
$C_{itaconic\ acid\ out}$ (mmol/L)	0.000 ± 0.000	0.000 ± 0.000	18.940 ± 0.172	19.198 ± 0.160	19.470 ± 0.178	19.432 ± 0.166
$C_{itaconic\ acid\ in}$ (mmol/L)	0.000 ± 0.000	0.000 ± 0.000	22.800 ± 0.023	22.795 ± 0.023	22.800 ± 0.023	22.801 ± 0.023
R_{CO_2} (mmol/h)	36.78 ± 0.53	37.95 ± 0.38	20.05 ± 0.29	21.43 ± 0.26	19.91 ± 0.29	20.46 ± 0.27
R_{O_2} (mmol/h)	-40.46 ± 7.69	-37.21 ± 0.38	-22.54 ± 7.78	-20.13 ± 0.26	-22.99 ± 7.79	-19.37 ± 0.27
$R_{biomass}$ (mmol/h)	52.94 ± 0.55	53.30 ± 0.38	30.55 ± 0.91	31.83 ± 0.43	29.61 ± 0.94	27.92 ± 0.44
R_{lysis} (mCmol/h)	4.42 ± 0.13	5.46 ± 0.13	3.33 ± 0.14	3.41 ± 0.14	3.44 ± 0.13	3.45 ± 0.13
$R_{itaconic\ acid}$ (mmol/h)	0.00 ± 0.00	0.00 ± 0.00	-1.75 ± 0.40	-1.63 ± 0.07	-1.32 ± 0.38	-1.33 ± 0.07
$R_{glucose}$ (mmol/h)	-16.24 ± 0.04	-16.23 ± 0.02	-8.61 ± 0.08	-8.61 ± 0.01	-7.97 ± 0.10	-7.97 ± 0.02
$RQ\ (R_{CO_2}/R_{O_2})$	0.91 ± 0.17	1.02 ± 0.01	0.89 ± 0.31	1.06 ± 0.02	0.87 ± 0.29	1.06 ± 0.02
$R_{O_2}/R_{glucose}$	2.49 ± 0.47	2.29 ± 0.02	2.62 ± 0.90	2.34 ± 0.03	2.89 ± 0.98	2.43 ± 0.03
Carbon recovery (%)	98 ± 1	-	95 ± 2	-	102 ± 2	-
Redox recovery (%)	108 ± 6	-	104 ± 10	-	121 ± 13	-

Table S5.3. Unreconciled and reconciled measurements of experiment C with itaconic acid in strain *A. niger* NW185.

Exp C						
	45.6mM Xylose pH 2.5		45.6mM Xylose + 100mM itaconic acid pH 2.5		45.6mM Xylose + 200mM itaconic acid pH 2.5	
	Unreconciled	Reconciled	Unreconciled	Reconciled	Unreconciled	Reconciled
F_{out} (L/h)	0.414 ± 0.001	0.414 ± 0.001	0.546 ± 0.004	0.546 ± 0.003	0.532 ± 0.0002	
F_{in} (L/h)	0.411 ± 0.001	0.411 ± 0.001	0.539 ± 0.004	0.540 ± 0.003	0.524 ± 0.0002	
$F_{gas\ in}$ (mmol/h)	2678.6 ± 26.8	2655.5 ± 26.2	2678.6 ± 26.8	2678.0 ± 26.8	2678.6 ± 26.8	
$F_{gas\ out}$ (mmol/h)	2677.4 ± 26.8	2655.8 ± 26.2	2679.8 ± 26.8	2678.9 ± 26.8	2678.0 ± 26.8	
O_{2out} (%)	19.224 ± 0.048	19.253 ± 0.033	19.622 ± 0.096	19.614 ± 0.042	20.654 ± 0.022	
CO_{2in} (%)	0.046 ± 0.000	0.046 ± 0.000	0.047 ± 0.000	0.047 ± 0.000	0.045 ± 0.000	
CO_{2out} (%)	1.697 ± 0.017	1.686 ± 0.016	1.415 ± 0.014	1.414 ± 0.014	0.313 ± 0.003	
O_{2in} (%)	20.910 ± 0.044	20.886 ± 0.033	20.954 ± 0.043	20.955 ± 0.039	20.940 ± 0.013	
$C_{xylose\ in}$ (mmol/L)	45.600 ± 0.046	45.608 ± 0.046	45.600 ± 0.046	45.600 ± 0.046	45.600 ± 0.046	
C_{lysis} (mCmol/L)	22.154 ± 4.608	4.904 ± 2.147	-	15.034 ± 4.459	-	
$C_{xylose\ out}$ (mmol/L)	0.289 ± 0.036	0.284 ± 0.036	8.772 ± 2.218	8.023 ± 1.765	24.060 ± 3.776	
$C_{biomass}$ (g/L)	3.278 ± 0.046	3.215 ± 0.044	2.973 ± 0.069	2.968 ± 0.068	0.757 ± 0.065	
MW _{biomass} (g/Cmol)	27.800 ± 0.190	27.921 ± 0.188	27.800 ± 0.190	27.804 ± 0.190	27.800 ± 0.190	
$C_{itaconic\ acid\ out}$ (mmol/L)	0.000 ± 0.000	0.000 ± 0.000	97.904 ± 2.453	96.951 ± 1.827	197.751 ± 5.904	
$C_{itaconic\ acid\ in}$ (mmol/L)	0.000 ± 0.000	0.000 ± 0.000	100.000 ± 0.100	100.002 ± 0.100	200.000 ± 0.200	
R_{CO_2} (mmol/h)	44.21 ± 0.64	43.55 ± 0.59	36.66 ± 0.54	36.63 ± 0.52		
R_{O_2} (mmol/h)	-45.39 ± 7.80	-43.30 ± 0.60	-35.45 ± 8.19	-35.74 ± 0.68		
$R_{biomass}$ (mmol/h)	48.81 ± 0.70	47.65 ± 0.72	58.39 ± 1.40	58.23 ± 1.43		
R_{lysis} (mCmol/h)	9.17 ± 1.91	2.03 ± 0.89	8.32 ± 2.52	8.21 ± 2.43		
$R_{itaconic\ acid}$ (mmol/h)	0.00 ± 0.00	0.00 ± 0.00	-0.46 ± 1.43	-1.08 ± 0.95		
R_{xylose} (mmol/h)	-18.63 ± 0.04	-18.65 ± 0.04	-19.80 ± 1.22	-20.24 ± 0.94		
RQ (R_{CO_2}/R_{O_2})	0.97 ± 0.17	1.01 ± 0.02	1.03 ± 0.24	1.02 ± 0.02		
R_{O_2}/R_{xylose}	2.44 ± 0.42	2.32 ± 0.03	1.79 ± 0.43	1.77 ± 0.09		
Carbon recovery (%)	110 ± 2	-	106 ± 10	-		
Redox recovery (%)	125 ± 8	-	110 ± 11	-		

Table S5.4. Unreconciled and reconciled measurements of experiment D with itaconic acid in strain *A. niger* C3.

Exp D								
	45.6mM Xylose pH 2.5		45.6mM Xylose + 100mM itaconic acid pH 2.5		45.6mM Xylose + 200mM itaconic acid pH 2.5		45.6mM Xylose + 300mM itaconic acid pH 2.5	
	Unreconciled	Reconciled	Unreconciled	Reconciled	Unreconciled	Reconciled	Unreconciled	Reconciled
F_{out} (L/h)	0.473 ± 0.0001	0.473 ± 0.0001	0.459 ± 0.0001	0.459 ± 0.0001	0.473 ± 0.0006	0.473 ± 0.0006	0.473 ± 0.0001	0.473 ± 0.0001
F_{in} (L/h)	0.471 ± 0.0001	0.471 ± 0.0001	0.451 ± 0.0001	0.451 ± 0.0001	0.461 ± 0.0006	0.462 ± 0.0006	0.456 ± 0.0001	0.456 ± 0.0001
$F_{gas\ in}$ (mmol/h)	2678.6 ± 26.8	2632.6 ± 26.4	2678.6 ± 26.8	2673.8 ± 26.6	2678.6 ± 26.8	2658.5 ± 26.5	2678.6 ± 26.8	2670.3 ± 26.7
$F_{gas\ out}$ (mmol/h)	2675.0 ± 26.7	2630.2 ± 26.4	2675.6 ± 26.8	2673.6 ± 26.6	2676.9 ± 26.8	2658.5 ± 26.5	2676.2 ± 26.8	2668.6 ± 26.7
O_{2out} (%)	19.069 ± 0.003	19.071 ± 0.003	19.185 ± 0.001	19.185 ± 0.001	19.093 ± 0.002	19.094 ± 0.002	19.977 ± 0.001	19.978 ± 0.001
CO_{2in} (%)	0.032 ± 0.000	0.032 ± 0.000	0.035 ± 0.000	0.035 ± 0.000	0.034 ± 0.000	0.034 ± 0.000	0.033 ± 0.000	0.033 ± 0.000
CO_{2out} (%)	1.688 ± 0.017	1.722 ± 0.006	1.544 ± 0.015	1.623 ± 0.005	1.691 ± 0.017	1.740 ± 0.005	0.687 ± 0.007	0.706 ± 0.006
O_{2in} (%)	20.832 ± 0.002	20.832 ± 0.002	20.781 ± 0.001	20.781 ± 0.001	20.801 ± 0.000	20.801 ± 0.000	20.702 ± 0.001	20.702 ± 0.001
$C_{xylose\ in}$ (mmol/L)	45.600 ± 0.046	45.617 ± 0.046	45.600 ± 0.046	45.602 ± 0.046	45.600 ± 0.046	45.608 ± 0.046	45.600 ± 0.046	45.603 ± 0.046
C_{lysis} (mCmol/L)	12.31 ± 3.68	10.08 ± 3.03	-	14.29 ± 3.35	-	5.19 ± 3.03	-	5.68 ± 3.42
$C_{xylose\ out}$ (mmol/L)	3.750 ± 0.512	1.602 ± 0.472	0.109 ± 0.014	0.108 ± 0.014	1.497 ± 0.226	1.299 ± 0.223	17.928 ± 1.542	14.891 ± 1.037
$C_{biomass}$ (g/L)	2.373 ± 0.038	2.288 ± 0.037	3.308 ± 0.198	3.048 ± 0.120	3.388 ± 0.093	3.146 ± 0.080	1.755 ± 0.101	1.651 ± 0.094
MW _{biomass} (g/Cmol)	27.800 ± 0.190	27.974 ± 0.189	27.800 ± 0.190	27.826 ± 0.189	27.800 ± 0.190	27.915 ± 0.189	27.800 ± 0.190	27.822 ± 0.190
$C_{itaconic\ acid\ out}$ (mmol/L)	17.915 ± 1.041	10.681 ± 0.704	99.623 ± 0.876	100.773 ± 0.739	197.962 ± 0.771	196.580 ± 0.635	283.530 ± 2.867	296.932 ± 0.895
$C_{itaconic\ acid\ in}$ (mmol/L)	0.000 ± 0.000	0.000 ± 0.000	100.000 ± 0.100	99.985 ± 0.100	200.000 ± 0.200	200.091 ± 0.198	300.000 ± 0.300	299.859 ± 0.299
R_{CO_2} (mmol/h)	44.29 ± 0.64	44.45 ± 0.51	40.38 ± 0.58	42.45 ± 0.45	44.35 ± 0.64	45.37 ± 0.48	17.50 ± 0.26	17.96 ± 0.25
R_{O_2} (mmol/h)	-47.92 ± 7.56	-46.80 ± 0.47	-43.33 ± 7.57	-42.72 ± 0.43	-46.06 ± 7.56	-45.38 ± 0.45	-19.90 ± 7.70	-19.67 ± 0.21
$R_{biomass}$ (mmol/h)	40.41 ± 0.64	38.72 ± 0.67	54.56 ± 3.27	50.22 ± 1.96	57.69 ± 1.58	53.30 ± 1.37	29.88 ± 1.72	28.09 ± 1.61
R_{lysis} (mCmol/h)	5.83 ± 1.74	4.77 ± 1.44	8.12 ± 1.69	6.55 ± 1.54	8.31 ± 1.74	2.45 ± 1.43	4.30 ± 1.74	2.69 ± 1.62
$R_{itaconic\ acid}$ (mmol/h)	8.48 ± 0.49	5.06 ± 0.33	-0.56 ± 0.40	-1.09 ± 0.34	-1.44 ± 0.41	-0.56 ± 0.31	-2.67 ± 1.37	-3.75 ± 0.40
R_{xylose} (mmol/h)	-19.71 ± 0.24	-20.74 ± 0.22	-20.52 ± 0.02	-20.53 ± 0.02	-20.33 ± 0.11	-20.45 ± 0.11	-12.32 ± 0.73	-13.76 ± 0.49
RQ (R_{CO_2}/R_{O_2})	0.92 ± 0.15	0.95 ± 0.01	0.93 ± 0.16	0.99 ± 0.01	0.96 ± 0.16	1.00 ± 0.01	0.88 ± 0.34	0.91 ± 0.02
R_{O_2}/R_{xylose}	2.43 ± 0.38	2.26 ± 0.03	2.11 ± 0.37	2.08 ± 0.02	2.27 ± 0.37	2.22 ± 0.03	1.62 ± 0.63	1.43 ± 0.05
Carbon recovery (%)	135 ± 4	-	101 ± 4	-	114 ± 4	-	71 ± 8	-
Redox recovery (%)	169 ± 10	-	100 ± 8	-	106 ± 7	-	117 ± 16	-

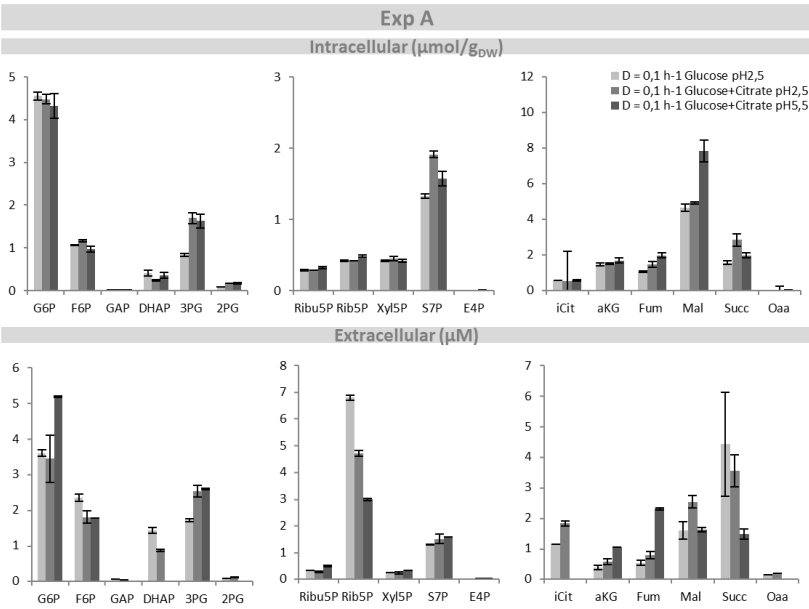


Fig. S5.3. Intracellular (upper panel) and extracellular (lower panel) amounts of glycolytic, PPP and TCA metabolites in $\mu\text{mol}/g_{\text{DW}}$ in experiment A.

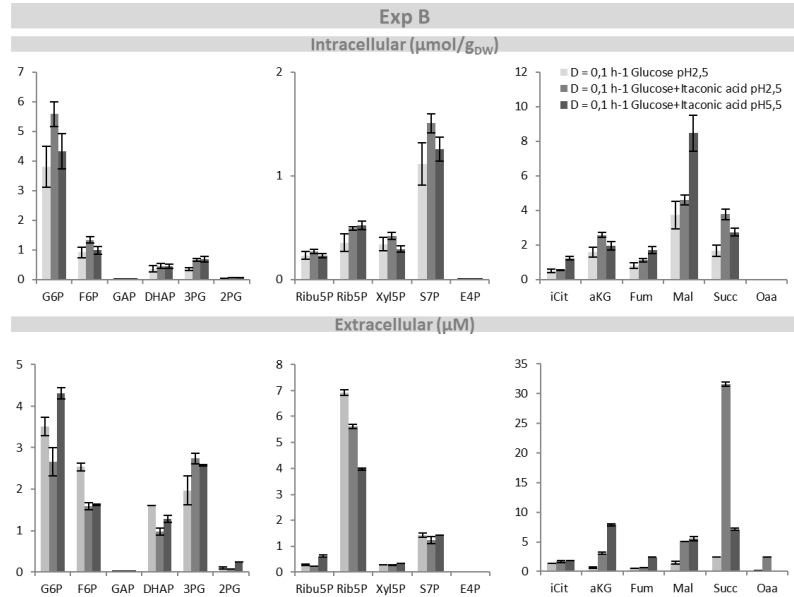


Fig. S5.4. Intracellular (upper panel) and extracellular (lower panel) amounts of glycolytic, PPP and TCA metabolites in $\mu\text{mol}/g_{\text{DW}}$ in experiment B.

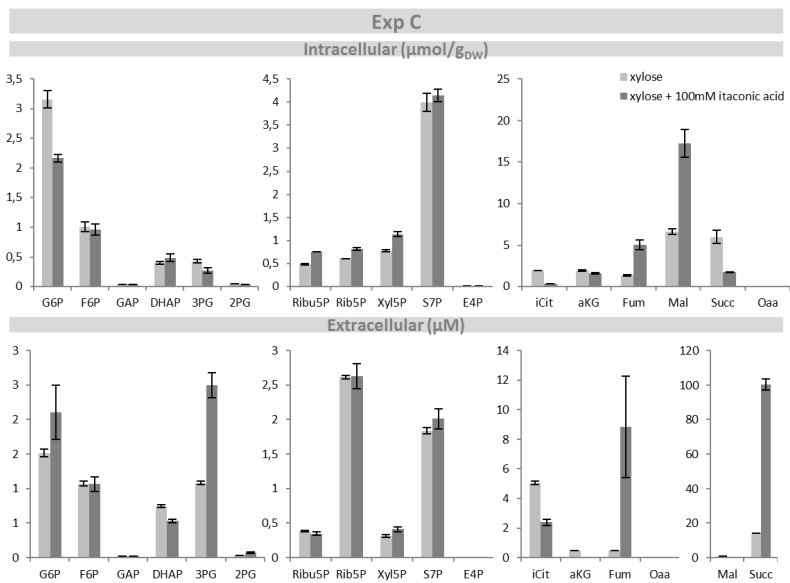


Fig. S5.5. Intracellular (upper panel) and extracellular (lower panel) amounts of glycolytic, PPP and TCA metabolites in $\mu\text{mol/g}_{\text{DW}}$ in experiment C.

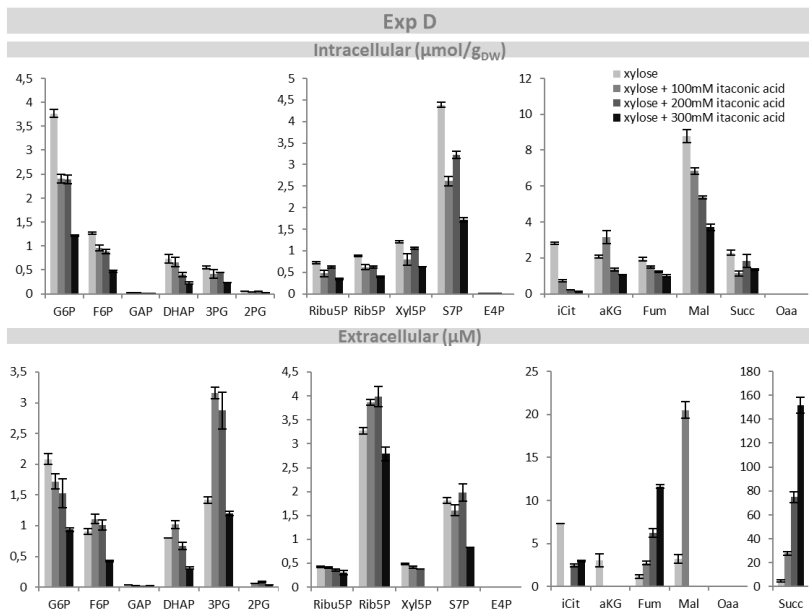


Fig. S5.6. Intracellular (upper panel) and extracellular (lower panel) amounts of glycolytic, PPP and TCA metabolites in $\mu\text{mol/g}_{\text{DW}}$ in experiment D.

Analysis of Figures S5.3 through S5.6:

In general, it was observed that the PPP metabolite levels are higher when xylose was the carbon source (experiments C and D) when compared to glucose as a carbon source (experiments A and B). This was expected because of the different metabolic pathways involved in the uptake of these two carbon sources.

Regarding intracellular metabolites, in experiment A (Fig. S5.3), higher levels of 3PG/2PG when citric acid is consumed agrees with the lower glycolytic flux ($1/2q_{\text{glucose}}$ when compared to the first steady state). In the PPP metabolites no major changes found, but expected higher citric acid cycle intermediates concentration are found intracellularly due to its metabolism.

In experiment B (Fig. S5.4), the glucose uptake rate is nearly the same and therefore no change in the glycolytic and PPP metabolites, however there is a change on the TCA metabolites due to a pH effect (higher pH on the third steady state).

In experiment C (Fig. S5.5), the inhibition effect on xylose uptake rate is reflected in the lower glycolytic intermediates.

In experiment D (Fig. S5.6), there is much more dicarboxylic acid secreted.

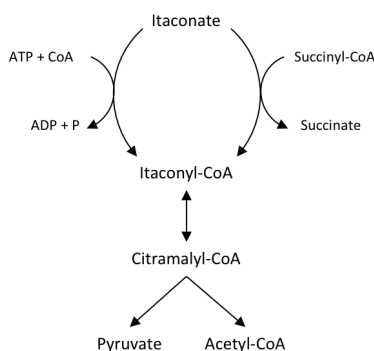


Fig. S5.7. Itaconate degradation pathway in *Pseudomonas* sp. (Cooper and Kornberg, 1964).

In absence of metabolism, the itaconic acid which passes the membrane accumulates in the cell and is balanced by cell growth:

$$q_{\text{itaconic acid}} = \mu Y_{\text{itaconic acid}} = k a C_{\text{out}}$$

From Table 5.6 these follows:

Exp	pH	C _{out} (mM)	Y _{itaconic acid} (mmo/mol _s)	q _{itaconic acid} (mmol/h/mol _s)	k (m/s)	C _{HA-}
B	2.5	19.2	0.94	0.094	9x10 ⁻¹²	0.82
	5.5	19.4	0.48	0.048	-	1.59
C	2.5	97	14.7	1.47	29x10 ⁻¹²	4.3
	5.5	200	23.9	2.54	24x10 ⁻¹²	16.4

The average value for the permeability coefficient equals $k = 21 \times 10^{-12}$ m/s

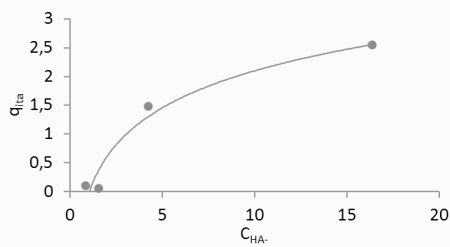


Fig. S5.8. Calculation of itaconic acid uptake rate and permeability coefficient in absence of itaconic acid metabolism.

Appendix Chapter 6

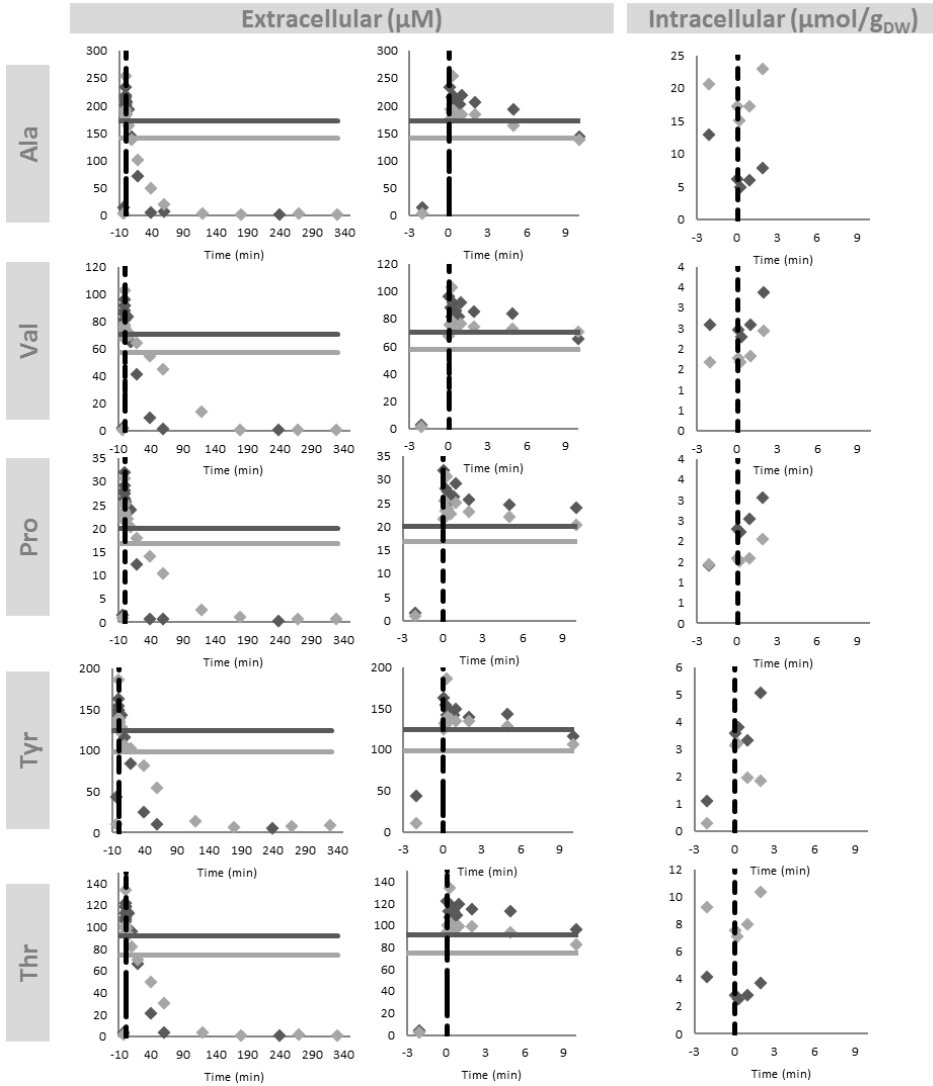


Fig. S6.1. Short-term dynamic profiles of extracellular (long and short time scale) and intracellular levels of amino acids in *A. niger* cell extracts followed an amino acid pulse in experiment B. Legends are included within each panel. *A. niger* 872.11 + empty plasmid (dark grey) and transformant 2 (light grey). Dashed line represents the beginning of the pulse (cont. 1/4).

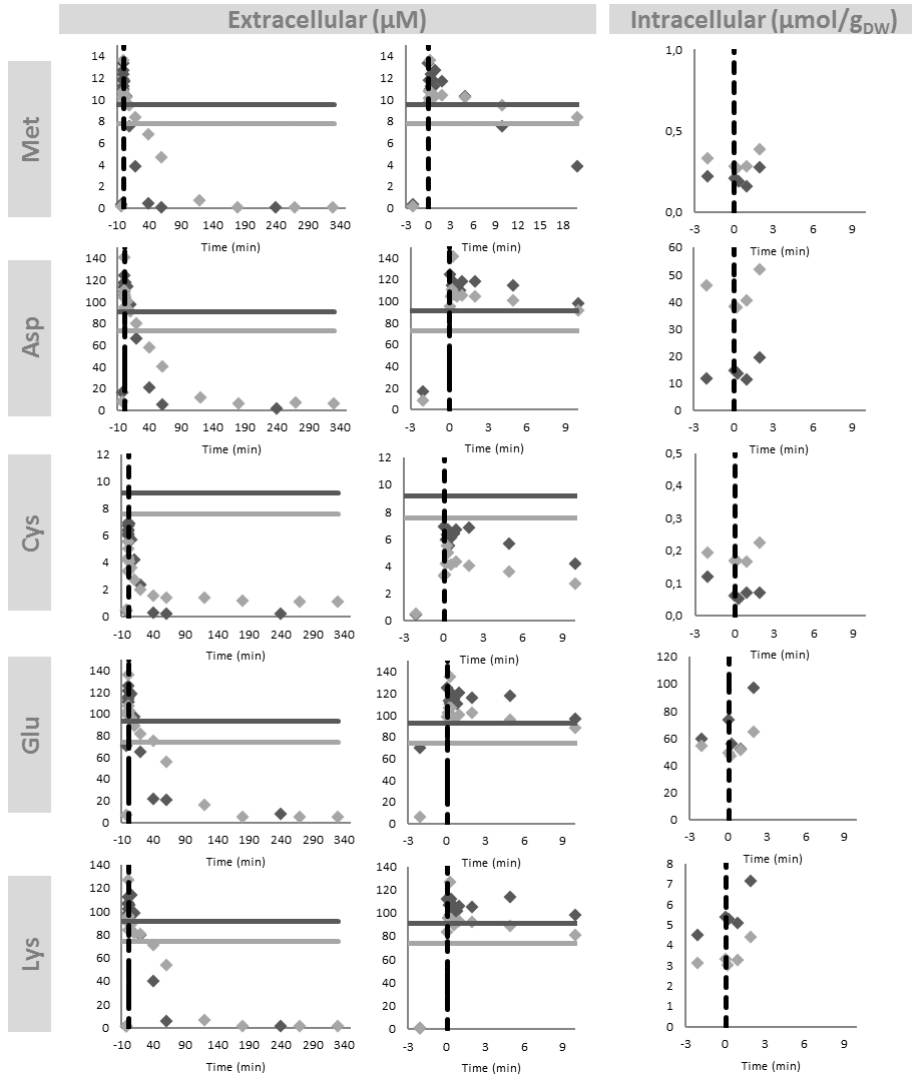


Fig. S6.1. Short-term dynamic profiles of extracellular (long and short time scale) and intracellular levels of amino acids in *A. niger* cell extracts followed an amino acid pulse in experiment B. Legends are included within each panel. *A. niger* 872.11 + empty plasmid (dark grey) and transformant 2 (light grey). Dashed line represents the beginning of the pulse (cont. 2/4).

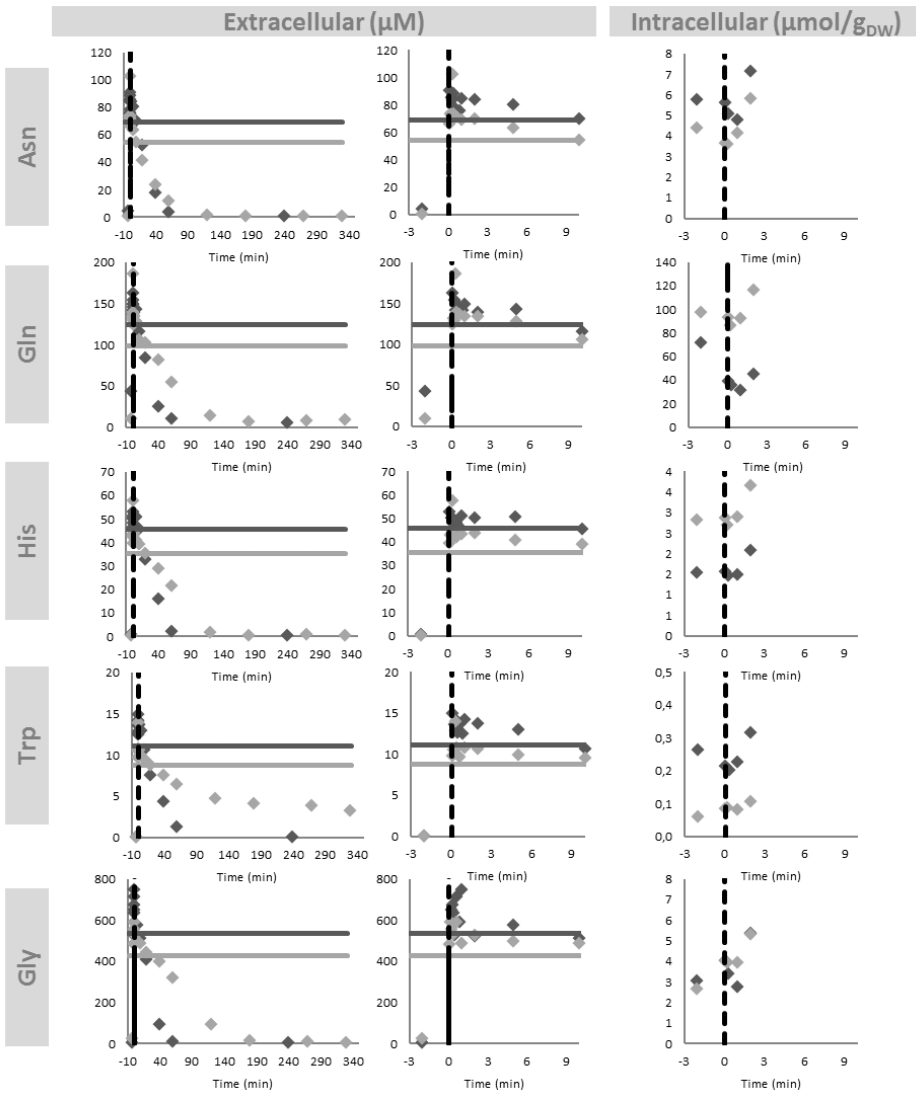


Fig. S6.1. Short-term dynamic profiles of extracellular (long and short time scale) and intracellular levels of amino acids in *A. niger* cell extracts followed an amino acid pulse in experiment B. Legends are included within each panel. *A. niger* 872.11 + empty plasmid (dark grey) and transformant 2 (light grey). Dashed line represents the beginning of the pulse (cont. 3/4).

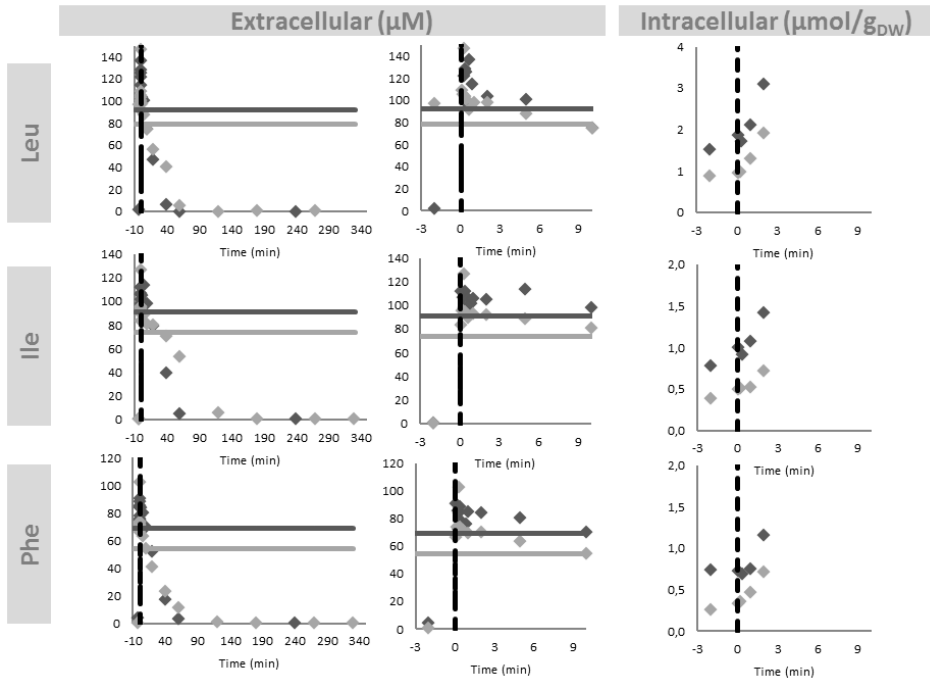
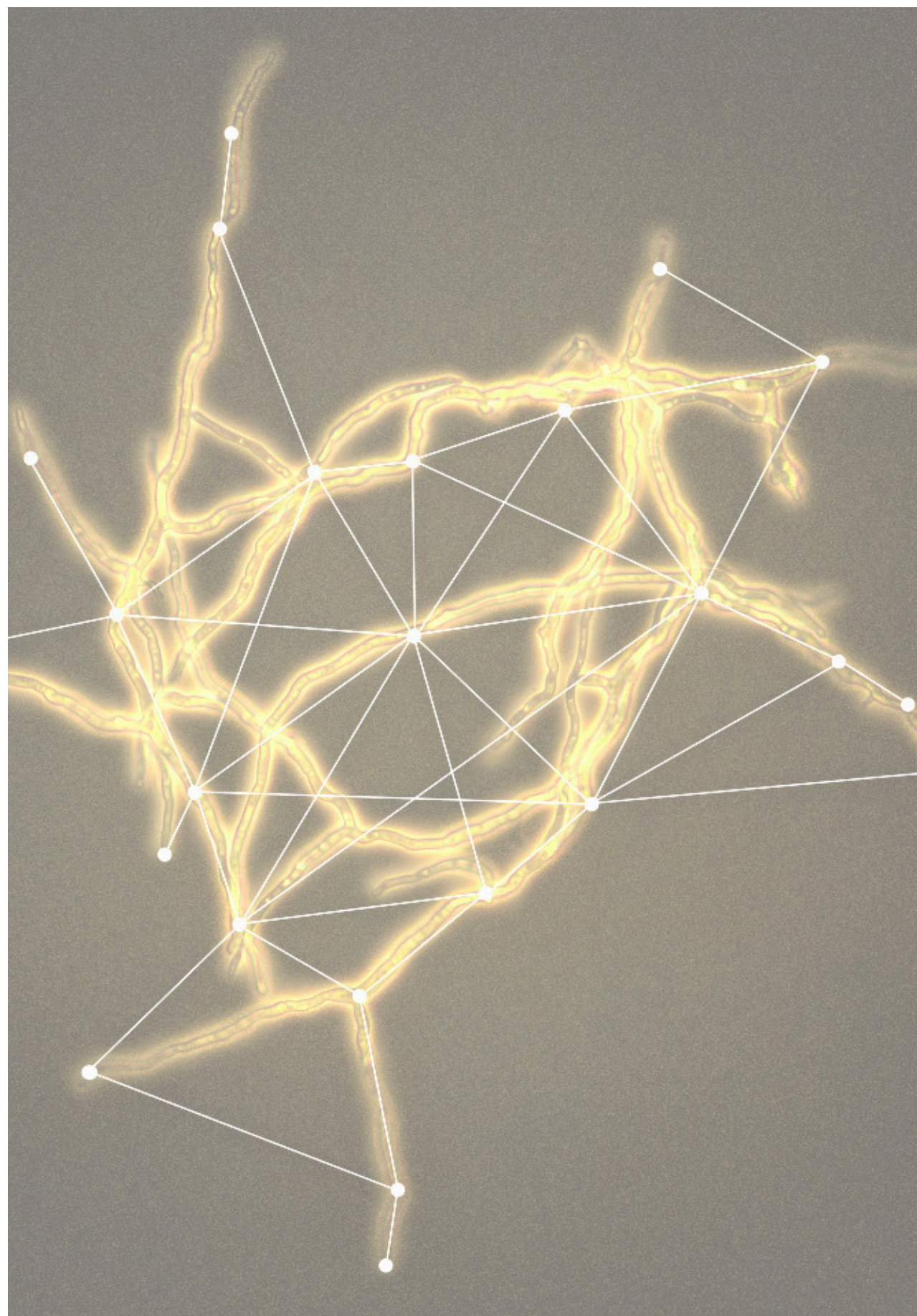


Fig. S6.1. Short-term dynamic profiles of extracellular (long and short time scale) and intracellular levels of amino acids in *A. niger* cell extracts followed an amino acid pulse in experiment B. Legends are included within each panel. *A. niger* 872.11 + empty plasmid (dark grey) and transformant 2 (light grey). Dashed line represents the beginning of the pulse (cont. 4/4).



References



Altschuler, S.J., Wu, L.F., 2010. Cellular heterogeneity: do differences make a difference? *Cell* 141, 559-563.

Andersen, M.R., Nielsen, M.L. and Nielsen, J., 2008. Metabolic model integration of the bibliome, genome, metabolome and reactome of *Aspergillus niger*. *Molecular systems biology* 4, 178.

Andersen, M.R., Salazar, M.P., Schaap, P.J., Van De Vondervoort, P. J.I., Culley, D., Thykaer, J., Frisvad, J.C., Nielsen, K.F., Albang, R., Albermann, K., Berka, R.M., Braus, G.H., Braus-Stromeier, S.A., Corrochano, L.M., Dai, Z., Van Dijck, P.W.M., Hofmann, G., Lasure, L.L., Magnuson, J.K., Menke, H., Meijer, M., Meijer, S.L., Nielsen, J.B., Nielsen, M.L., Van Ooyen, A.J.J., Pel, H.J., Poulsen, L., Samson, R.A., Stam, H., Tsang, A., Van Den Brink, J.M., Atkins, A., Aerts, A., Shapiro, H., Pangilinan, J., Salamov, A., Lou, Y., Lindquist, E., Lucas, S., Grimwood, J., Grigoriev, I.V., Kubicek, C.P., Martinez, D., Van Peij, N.N.M.E., Roubos, J.A., Nielsen, J. and Baker, S.E., 2011. Comparative genomics of citric-acid-producing *Aspergillus niger* ATCC 1015 versus enzyme-producing CBS 513.88. *Genome Research* 21, 885-897.

Andre, B., 1995. An overview of membrane transport proteins in *Saccharomyces cerevisiae*. *Yeast* 11, 1575-1611.

Burgstaller, W., 2006. Thermodynamic boundary conditions suggest that a passive transport step suffices for citrate excretion in *Aspergillus* and *Penicillium*. *Microbiology* 152, 887-893.

Canelas, A.B., Ras, C., Pierick, A., Dam, J.C., Heijnen, J.J., Gulik, W.M., 2008. Leakage-free rapid quenching technique for yeast metabolomics. *Metabolomics* 4, 226-239.

Canelas, A.B., ten Pierick, A., Ras, C., van Dam, J.C., van Gulik, W.M., Heijnen, J.J., 2009. Quantitative evaluation of intracellular metabolite extraction techniques for yeast metabolomics. *Analytical Chemistry* 81, 7379-7389.

Carnicer, M., Canelas, A.B., Ten Pierick, A., Zeng, Z., van Dam, J., Albiol, J., Ferrer, P., Heijnen, J.J., van Gulik, W., 2012. Development of quantitative metabolomics for *Pichia pastoris*. *Metabolomics* 8, 284-298.

Cipollina, C., ten Pierick, A., Canelas, A.B., Seifar, R.M., van Maris, A.J. a, van Dam, J.C., Heijnen, J.J., 2009. A comprehensive method for the quantification of the non-oxidative pentose phosphate pathway intermediates in *Saccharomyces cerevisiae* by GC-IDMS. *Journal of Chromatography B* 877, 323-6.

- Coelho, M.A., Gonçalves, C., Sampaio, J.P., Gonçalves, P., 2013.** Extensive Intra-Kingdom Horizontal Gene Transfer Converging on a Fungal Fructose Transporter Gene. *PLoS Genetics* 9.
- Colabardini, A.C., Ries, L.N.A., Brown, N.A., dos Reis, T.F., Savoldi, M., Goldman, M.H.S., Menino, J.F., Rodrigues, F., Goldman, G.H., 2014.** Functional characterization of a xylose transporter in *Aspergillus nidulans*. *Biotechnology for Biofuels* 7, 46.
- Cooper, R.A. and Kornberg, H.L., 1964.** The utilization of itaconate by *Pseudomonas* sp., *The Biochemical Journal* 91, 82-91.
- Cruz, A.L.B., Verbon, A.J., Geurink, L.J., Verheijen, P.J.T., Heijnen, J.J., van Gulik, W.M., 2012.** Use of sequential-batch fermentations to characterize the impact of mild hypothermic temperatures on the anaerobic stoichiometry and kinetics of *Saccharomyces cerevisiae*. *Biotechnology and Bioengineering* 109, 1735-1744.
- David, H., Åkesson, M., Nielsen, J., 2003.** Reconstruction of the central carbon metabolism of *Aspergillus niger*. *European Journal of Biochemistry* 270, 4243-4253.
- de Groot, M.J.L., Prathumpai, W., Visser, J. and Ruijter, G. J. G., 2005.** Metabolic control analysis of *Aspergillus niger* L-arabinose catabolism. *Biotechnology progress* 21, 1610-1616.
- de Groot, M.J.L., van de Vondervoort, P.J.I., de Vries, R.P., vanKuyk, P.A., Ruijter, G.J.G. and Visser, J., 2003.** Isolation and characterization of two specific regulatory *Aspergillus niger* mutants shows antagonistic regulation of arabinan and xylan metabolism. *Microbiology* 149, 1183-1191.
- de Jonge, L.P., Buijs, N.A.A., ten Pierick, A., Deshmukh, A., Zhao, Z., Kiel, J.A.K.W., Heijnen, J.J., van Gulik, W.M., 2011.** Scale-down of penicillin production in *Penicillium chrysogenum*. *Biotechnology Journal* 6, 944-958.
- de Jonge, L.P., Douma, R.D., Heijnen, J.J., van Gulik, W.M., 2012.** Optimization of cold methanol quenching for quantitative metabolomics of *Penicillium chrysogenum*. *Metabolomics* 8, 727-735.
- de Koning, W., van Dam, K., 1992.** A method for the determination of changes of glycolytic metabolites in yeast on a subsecond time scale using extraction at neutral pH. *Analytical Biochemistry* 204, 118-123.
- de Souza, W.R., de Gouvea, P.F., Savoldi, M., Malavazi, I., de Souza Bernardes, L. a, Goldman, M.H.S., de Vries, R.P., de Castro Oliveira, J. V, Goldman, G.H., 2011.**

Transcriptome analysis of *Aspergillus niger* grown on sugarcane bagasse. *Biotechnology for Biofuels* 4, 1-16.

de Vries, R.P., Visser, J., Ronald, P., de Vries, R., P., 2001. *Aspergillus* Enzymes Involved in Degradation of Plant Cell Wall Polysaccharides. *Microbiology and Molecular Biology Reviews* 65, 497-522.

dos Reis, T.F., de Lima, P.B.A., Parachin, N.S., Mingossi, F.B., de Castro Oliveira, J.V., Ries, L.N.A., Goldman, G.H., 2013. Identification and characterization of putative xylose and cellobiose transporters in *Aspergillus nidulans*. *Biotechnology for Biofuels* 9, 204.

Douma, R.D., de Jonge, L.P., Jonker, C.T.H., Seifar, R.M., Heijnen, J.J., van Gulik, W.M., 2010. Intracellular metabolite determination in the presence of extracellular abundance: Application to the penicillin biosynthesis pathway in *Penicillium chrysogenum*. *Biotechnology and Bioengineering* 107, 105-115.

EIA, US Energy Information Administration, 2016. Retrieved from <https://www.eia.gov/todayinenergy/detail.php?id=26912>.

Escher, B.I., Berger, C., Bramaz, N., Kwon, J., Richter, M., Tsinman, O., Avdeef, A., 2008. Membrane-water partitioning, membrane permeability, and baseline toxicity of the parasiticides, ivermectin, albendazole, and morantel. *Environmental Toxicology and Chemistry* 27, 909-918.

Flagfeldt, D.B., Siewers, V., Huang, L., Nielsen, J., 2009. Characterization of chromosomal integration sites for heterologous gene expression in *Saccharomyces cerevisiae*. *Yeast* 26, 545-551.

Flippi, M., Van de Vondervoort, P.J.I., Ruijter, G.J.G., Visser, J., Arst, H. N., Felenbok, B., 2003. Onset of carbon catabolite repression in *Aspergillus nidulans*: Parallel involvement of hexokinase and glucokinase in sugar signaling. *The Journal OF biological Chemistry* 278, 11849-11857.

Fries, N., Kallstromer, L., 1965. A requirement for Biotin in *Aspergillus niger* when grown on a rhamnose medium at high temperature. *Physiologia Plantarum* 18, 191-200.

Geitmann, A., Emons, A.M.C., 2000. The cytoskeleton in plant and fungal cell tip growth. *Journal of Microscopy* 198, 218-245.

Goldberg, I., Rokem, J.S., Pines, O., 2006. Organic acids: old metabolites, new themes. *Journal of Chemical Technology and Biotechnology* 81, 1601-1611.

Gouka, R.J., Punt, P.J., Van Den Hondel, C.A., 1997. Efficient production of secreted proteins by *Aspergillus*: progress, limitations and prospects. *Applied Microbiology and Biotechnology* 47, 1-11.

Gruben, B.S., Zhou, M., Wiebenga, A., Ballering, J., Overkamp, K.M., Punt, P.J. and de Vries, R.P., 2014. *Aspergillus niger* RhaR, a regulator involved in L-rhamnose release and catabolism. *Applied microbiology and biotechnology* 98, 5531-5540.

Herbert, D., Elsworth, R., Telling, R.C., 1956. The continuous culture of bacteria; a theoretical and experimental study. *Journal of general microbiology* 14, 601-622.

Hesse, S.J.A., Ruijter, G.J.G., Dijkema, C., Visser, J., 2002. Intracellular pH homeostasis in the filamentous fungus *Aspergillus niger*. *European Journal of Biochemistry* 269, 3485-3494.

IEA International Energy Agency, 2015. Retrieved from: <https://www.iea.org/publications/freepublications/publication/KeyWorld2017.pdf>.

Ilyes, H., Fekete, E., Karaffa, L., Fekete, E., Sandor, E., Szentirmai, A., Kubicek, C.P., 2004. CreA-mediated carbon catabolite repression of beta-galactosidase formation in *Aspergillus nidulans* in growth rate dependent. *FEMS Microbiology Letters* 235, 147-151.

INCHEM, 2017. Citric acid. Retrieved from <http://www.inchem.org/documents/icsc/icsc/eics0855.htm>.

Jamalzadeh, E., 2013. Transport of Dicarboxylic Acids in *Saccharomyces cerevisiae*. PhD thesis. Delft University of Technology, Delft.

Jernejc, K., 2004. Comparison of different methods for metabolite extraction from *Aspergillus niger* mycelium. *Acta Chimica Slovenica* 51, 567-578.

Jørgensen, T.R., Nielsen, K.F., Arentshorst, M., Park, J., van den Hondel, C. a, Frisvad, J.C., Ram, A.F., 2011. Submerged conidiation and product formation by *Aspergillus niger* at low specific growth rates are affected in aerial developmental mutants. *Applied and Environmental Microbiology* 77, 5270-5277.

Jørgensen, T.R., vanKuyk, P. a, Poulsen, B.R., Ruijter, G.J.G., Visser, J., Iversen, J.J.L., 2007. Glucose uptake and growth of glucose-limited chemostat cultures of *Aspergillus niger* and a disruptant lacking MstA, a high-affinity glucose transporter. *Microbiology* 153, 1963-1973.

- Karaffa, L., Kubicek, C.P., 2003.** *Aspergillus niger* citric acid accumulation: do we understand this well working black box? *Applied Microbiology and Biotechnology* 61, 189-196.
- Kfivnkovi, I., Mareiinov, M., Sohnel, O., 1992.** Solubility of Itaconic and Kojic Acids Equilibrium Diagram of the Ternary System Water-Malic Acid-Tributyl Phosphate and the Influence of Temperature. *Journal of Chemical and Engineering Data* 37, 23-24.
- Kluyver, A.J., Perkin, L.H.C., 1932.** Zur Methodik der Schimmelfeststoffwechseluntersuchung. *Biochem Z*, 266, 68-81.
- Kopylova, E., Noé, L., Touzet, H., 2012.** SortMeRNA: fast and accurate filtering of ribosomal RNAs in metatranscriptomic data. *Bioinformatics* 28, 3211-3217.
- Kromer, J.O., Nielsen, L.K. and Blank, L.M., 2014.** *Metabolic Flux Analysis*. Hatfield. Human Press.
- Krull, R., Cordes, C., Horn, H., Kampen, I., Kwade, A., Neu, T.R., No, B., 2010.** Morphology of Filamentous Fungi: Linking Cellular Biology to Process Engineering Using *Aspergillus niger*. *Advances in Biochemical Engineering and Biotechnology* 121, 1-21.
- Kubicek, C.P., Punt, P., Visser, J., 2010.** *Production of Organic Acids by Filamentous Fungi, Industrial Applications*. 2nd edition. Heidelberg. Springer-Verlag.
- Lameiras, F., Heijnen, J.J., van Gulik, W.M., 2015.** Development of tools for quantitative intracellular metabolomics of *Aspergillus niger* chemostat cultures. *Metabolomics* 11, 1253-1264.
- Lameiras, F., Ras, C., ten Pierick, A., Heijnen, J.J., van Gulik, W.M., 2017.** Stoichiometry and kinetics of single and mixed substrate uptake in *Aspergillus niger*. *Bioprocess and Biosystems Engineering* 41, 157-170.
- Lange, H.C., Eman, M., van Zuijlen, G., Visser, D., van Dam, J.C., Frank, J., de Mattos, M.J., Heijnen, J.J., 2001.** Improved rapid sampling for in vivo kinetics of intracellular metabolites in *Saccharomyces cerevisiae*. *Biotechnology and Bioengineering* 75, 406-415.
- Langmead, B., Salzberg, S.L., 2012.** Fast gapped-read alignment with Bowtie 2. *Nature Methods* 9, 357-359.

- Larsen, B., Rask Poulsen, B., Eriksen, N.T., Lønsmann Iversen, J.J., 2004.** Homogeneous batch cultures of *Aspergillus oryzae* by elimination of wall growth in the Variomixing bioreactor. *Applied Microbiology and Biotechnology* 64, 192-198.
- Larsson, G., Törnkvist, M., 1996.** Rapid sampling, cell inactivation and evaluation of low extracellular glucose concentrations during fed-batch cultivation. *Journal of Biotechnology* 49, 69-82.
- Leandro, M.J., Fonseca, C., Goncalves, P., 2009.** Hexose and pentose transport in ascomycetous yeasts: An overview. *FEMS Yeast Research* 9, 511-525.
- Lendenmann, U., Snozzi, M., Egli, T., Egli, T., 1996.** Kinetics of the simultaneous utilization of sugar mixtures by *Escherichia coli* in continuous culture. *Applied and Environmental Microbiology* 62, 1493-1499.
- Liaud, N., Giniés, C., Navarro, D., Fabre, N., Crapart, S., Gimbert, I.H., Levasseur, A., Raouche, S., Sigoillot, J.C., 2014.** Exploring fungal biodiversity: organic acid production by 66 strains of filamentous fungi. *Fungal Biology and Biotechnology* 1, 1-10.
- Lin, Y., Tanaka, S., 2006.** Ethanol fermentation from biomass resources: Current state and prospects. *Applied Microbiology and Biotechnology* 69, 627-642.
- Lorraine, B.L., Thomas, K.N., 1989.** Fermentation Processes for carboxylic acids. Patent number 4877731.
- Magnuson, J.K., Lasure, L.L., 2004.** Organic Acid Production by Filamentous Fungi. *Advances in Fungal Biotechnology for Industry, Agriculture and Medicine*. Richland. Kluwer Academic/Plenum Publishers.
- Martens-Uzunova, E.S., Schaap, P.J., 2008.** An evolutionary conserved d-galacturonic acid metabolic pathway operates across filamentous fungi capable of pectin degradation. *Fungal Genetics and Biology* 45, 1449-1457.
- Martin, M., 2011.** Cutadapt removes adapter sequences from high-throughput sequencing reads. *The European Molecular Biology Network Journal* 17, 10-12.
- Mashego, M.R., Gulik, W.M. Van, Vinke, J.L., Heijnen, J.J., 2003.** Critical Evaluation of Sampling Techniques for Residual Glucose Determination in Carbon-Limited Chemostat Culture of *Saccharomyces cerevisiae*. *Biotechnology and Bioengineering* 83, 395-399.
- Mashego, M.R., Wu, L., Van Dam, J.C., Ras, C., Vinke, J.L., Van Winden, W. a, Van Gulik, W.M., Heijnen, J.J., 2004.** MIRACLE: mass isotopomer ratio analysis of U-13C-labeled

extracts. A new method for accurate quantification of changes in concentrations of intracellular metabolites. *Biotechnology and Bioengineering* 85, 620-628.

Max, B., Salgado, J. M., Rodriguez, N., Cortes, S., Converti, A. and Dominguez, J. M., **2010**. Biotechnology production of citric acid. *Brazilian Journal of Microbiology* 41, 862-875.

Mojzita, D., Penttilä, M. and Richard, P., **2010**. Identification of an L-arabinose reductase gene in *Aspergillus niger* and its role in L-arabinose catabolism. *The Journal of biological chemistry* 285, 23622-23628.

Moses, V., Prevost, C., **1966**. Catabolite repression of B-galactosidase synthesis in *Escherichia coli*. *Biochemical Journal* 100, 336-352.

Mullin, J.W., **2001**. Crystallization. *Kirk-Othmer Encyclopedia of Chemical Technology*. Fourth edition. Oxford. Butterworth Heinemann Publishers.

Nasution, U., **2007**. A Dynamic and Steady State Metabolome Study of Central Metabolism and Its Relation with the Penicillin Biosynthesis Pathway in *Penicillium chrysogenum*. PhD thesis. Delft University of Technology, Delft.

Nasution, U., Gulik, W.M. Van, Kleijn, R.J., Winden, W.A. Van, **2006**. Measurement of Intracellular Metabolites of Primary Metabolism and Adenine Nucleotides in Chemostat Cultivated *Penicillium chrysogenum*. *Biotechnology Advances* 94, 159-166.

Niedenführ, S., ten Pierick, A., van Dam, P.T.N., Suarez-Mendez, C.A., Nöh, K., Wahl, S.A., **2016**. Natural isotope correction of MS/MS measurements for metabolomics and ¹³C fluxomics. *Biotechnology and Bioengineering* 113, 1137-1147.

Odoni, D.I., Tamayo-Ramos, J.A., Sloothak, J., van Heck, R.G.A., Martins dos Santos, V.A.P., de Graaff, L.H., Suarez-Diez, M., Schaap, P.J., **2017**. Comparative proteomics of *Rhizopus delemar* ATCC 20344 unravels the role of amino acid catabolism in fumarate accumulation. *PeerJ* 5, 1-18.

Okabe, M., Lies, D., Kanamasa, S., Park, E.Y., **2009**. Biotechnological production of itaconic acid and its biosynthesis in *Aspergillus terreus*. *Applied Microbiology and Biotechnology* 84, 597-606.

Panneman, H., Ruijter, G.J., van den Broeck, H.C. and Visser, J., **1998**. Cloning and biochemical characterisation of *Aspergillus niger* hexokinase: the enzyme is strongly inhibited by physiological concentrations of trehalose 6-phosphate. *European journal of biochemistry* 258, 223-232.

- Papagianni, M., 2007.** Advances in citric acid fermentation by *Aspergillus niger*: Biochemical aspects, membrane transport and modeling, *Biotechnology Advances*. 25, 244-263.
- Pedersen, H., Beyer, M., Nielsen, J., 2000.** Glucoamylase production in batch, chemostat and fed-batch cultivations by an industrial strain of *Aspergillus niger*. *Applied Microbiology and Biotechnology* 53, 272-277.
- Pel, H.J., de Winde, J.H., Archer, D.B., Dyer, P.S., Hofmann, G., Schaap, P.J., Turner, G., de Vries, R.P., Albang, R., Albermann, K., Andersen, M.R., Bendtsen, J.D., Benen, J. a E., van den Berg, M., Breestraat, S., Caddick, M.X., Contreras, R., Cornell, M., Coutinho, P.M., Danchin, E.G.J., Debets, A.J.M., Dekker, P., van Dijck, P.W.M., van Dijk, A., Dijkhuizen, L., Driessen, A.J.M., d'Enfert, C., Geysens, S., Goosen, C., Groot, G.S.P., de Groot, P.W.J., Guillemette, T., Henrissat, B., Herweijer, M., van den Hombergh, J.P.T.W., van den Hondel, C. a M.J.J., van der Heijden, R.T.J.M., van der Kaaij, R.M., Klis, F.M., Kools, H.J., Kubicek, C.P., van Kuyk, P. a, Lauber, J., Lu, X., van der Maarel, M.J.E.C., Meulenberg, R., Menke, H., Mortimer, M. a, Nielsen, J., Oliver, S.G., Olsthoorn, M., Pal, K., van Peij, N.N.M.E., Ram, A.F.J., Rinas, U., Roubos, J. a, Sagt, C.M.J., Schmoll, M., Sun, J., Ussery, D., Varga, J., Vervecken, W., van de Vondervoort, P.J.J., Wedler, H., Wösten, H. a B., Zeng, A.-P., van Ooyen, A.J.J., Visser, J., Stam, H., 2007.** Genome sequencing and analysis of the versatile cell factory *Aspergillus niger* CBS 513.88. *Nature Biotechnology* 25, 221-231.
- Peng, Y., Leung, H.C.M., Yiu, S.M., Chin, F.Y.L., 2012.** IDBA-UD: a de novo assembler for single-cell and metagenomic sequencing data with highly uneven depth. *Bioinformatics* 28, 1420-1428.
- Portnoy, T., Margeot, A., Linke, R., Atanasova, L., Fekete, E., Sandor, E., Harti, L., Karaffa, L., Druzhinina, I.S., Seiboth, B., Le Crom, S., Kubicek, C.P., 2011.** The CRE1 carbon catabolite repressor of the fungus *Trichoderma reesei*: a master regulator of carbon assimilation. *BMC Genomics* 12, 269.
- Punt, P.J., Van Biezen, N., Conesa, A., Albers, A., Mangnus, J., Van Den Hondel, C., 2002.** Filamentous fungi as cell factories for heterologous protein production. *Trends in Biotechnology* 20, 200-206.
- Quinlan, A.R., Hall, I.M., 2010.** BEDTools: a flexible suite of utilities for comparing genomic features. *Bioinformatics* 26, 841-842.
- Ramos, J., Sychrová, H., Kschischo, M., 2016.** Yeast Membrane Transporter. Heidelberg. Springer.

Roels, J.A., 1983. Energetics and Kinetics in Biotechnology. Amsterdam. Elsevier Biomedical Press BV.

Ronne, H., 1995. Glucose repression in fungi. Trends in genetics 11, 12-17.

Ruijter, G. J. G. and Visser, J., 1996. Determination of intermediary metabolites in *Aspergillus niger*, Journal of Microbiological Methods 25, 295-302.

Ruijter, G. J., van de Vondervoort, P.J., Visser, J., 1999. Oxalic acid production by *Aspergillus niger*: an oxalate-non-producing mutant produces citric acid at pH 5 and in the presence of manganese. Microbiology 145, 2569-2576.

Rumbold, K., van Buijsen, H.J.J., Overkamp, K.M., van Groenestijn, J.W., Punt, P.J., van der Werf, M.J., 2009. Microbial production host selection for converting second-generation feedstocks into bioproducts. Microbial cell Factories 8, 1-11.

Sauer, M., Porro, D., Mattanovich, D., Branduardi, P., 2008. Microbial production of organic acids: expanding the markets. Trends in Biotechnology 26, 100-108.

Schädel, F., Franco-Lara, E., 2009. Rapid sampling devices for metabolic engineering applications. Applied Microbiology and Biotechnology 83, 199-208.

Schäuble, S., Stavrum, A.K., Puntervoll, P., Schuster, S., Heiland, I., 2013. Effect of substrate competition in kinetic models of metabolic networks. FEBS Letters 587, 2818-2824.

Schmieder, R., Edwards, R., 2011. Quality control and preprocessing of metagenomic datasets. Bioinformatics 27, 863-864.

Schneider, R.P., Wiley, W.R., 1971. Regulation of sugar transport in *Neurospora crassa*. Journal of Bacteriology 106, 487-492.

Schrickx, J.M., Krave, A.S., Verdoes, J.C., van den Hondel, C. a, Stouthamer, A.H., van Verseveld, H.W., 1993. Growth and product formation in chemostat and recycling cultures by *Aspergillus niger* N402 and a glucoamylase overproducing transformant, provided with multiple copies of the *glaA* gene. Journal of general Microbiology 139, 2801-2810.

Schuster, E., Dunn-Coleman, N., Frisvad, J.C., Van Dijck, P.W.M., 2002. On the safety of *Aspergillus niger* - a review. Applied Microbiology and Biotechnology 59, 426-435.

Sengupta, D., 2010. Integrating Bioprocesses into Industrial Complexes for sustainable development. PhD thesis, Louisiana State University and Agricultural and Mechanical College, Louisiana.

Shah, M. V., van Mastrigt, O., Heijnen, J.J., van Gulik, W.M., 2016. Transport and metabolism of fumaric acid in *Saccharomyces cerevisiae* in aerobic glucose-limited chemostat culture. *Yeast* 33(4), 145-161.

Sivakumar, A., 1994. Extended monod kinetics for substrate inhibited systems. *Bioprocess* 11, 11-14.

Sloothaak, J., Odoni, D.I., de Graaff, L.H., Martins dos Santos, V. a. P., Schaap, P.J., Tamayo-Ramos, J.A., 2015. *Aspergillus niger* membrane-associated proteome analysis for the identification of glucose transporters. *Biotechnology for Biofuels* 8, 1-15.

Sloothaak, J., Odoni, D.I., Martins dos Santos, V.A.P., Schaap, P.J., Tamayo-Ramos, J.A., 2016a. Identification of a novel L-rhamnose uptake transporter in the filamentous fungus *Aspergillus niger*. *PLOS genetics* 12, 1-27.

Sloothaak, J., Schilders, M., Schaap, P.J., de Graaff, L.H., 2014. Overexpression of the *Aspergillus niger* GatA transporter leads to preferential use of D-galacturonic acid over D-xylose. *AMB Express* 4, 1-9.

Sloothaak, J., Tamayo-Ramos, J.A., Odoni, D.I., Laothanachareon, T., Derntl, C., Mach-Aigner, A.R., Martins dos Santos, V.A.P., Schaap, P.J., 2016b. Identification and functional characterization of novel xylose transporters from the cell factories *Aspergillus niger* and *Trichoderma reesei*. *Biotechnology for Biofuels* 9, 1-15.

Straathof, A.J.J., 2014. Transformation of biomass into commodity chemicals using enzymes or cells. *Chemical Reviews* 114, 1871-1908.

Swift, R.J., Wiebe, M.G., Robson, G.D., Trinci, A.P., 1998. Recombinant glucoamylase production by *Aspergillus niger* B1 in chemostat and pH auxostat cultures. *Fungal Genetics and Biology* 25, 100-109.

Tamayo-Ramos, J. a, Flipphi, M., Pardo, E., Manzanares, P., Orejas, M., 2012. L-rhamnose induction of *Aspergillus nidulans* α -L-rhamnosidase genes is glucose repressed via a CreA-independent mechanism acting at the level of inducer uptake. *Microbial cell Factories* 11, 1-17.

Taymaz-Nikerel, H., de Mey, M., Ras, C., ten Pierick, A., Seifar, R.M., van Dam, J.C., Heijnen, J.J., van Gulik, W.M., 2009. Development and application of a differential

method for reliable metabolome analysis in *Escherichia coli*. *Analytical Biochemistry* 386, 9-19.

TCBD.org, 2016. The Dicarboxylate/Amino Acid:Cation (Na⁺ or H⁺) Symporter (DAACS) Family. Retrieved from <http://tcdb.org/search/result.php?tc=2.A.23>.

van Dam, J.C., Eman, M.R., Frank, J., Lange, H.C., van Dedem, G.W., Heijnen, S.J., 2002. Analysis of glycolytic intermediates in *Saccharomyces cerevisiae* using anion exchange chromatography and electrospray ionization with tandem mass spectrometric detection. *Analytical Chimica Acta* 460, 209-218.

Van der Heijden, R.T.J.M., Heijnen, J.J., Hellinga, C., Romein, B., Luyben, K.C.A.M., 1994a. Linear constraint relations in biochemical reaction systems: I. Classification of the calculability and the balanceability of conversion rates. *Biotechnology and Bioengineering* 43, 3-10.

Van der Heijden, R.T.J.M., Heijnen, J.J., Hellinga, C., Romein, B., Luyben, K.C.A.M., 1994b. Linear constraint relations in biochemical reaction systems: II. Diagnosis and estimation of gross errors. *Biotechnology and Bioengineering* 43, 3-10.

van der Straat, L., de Graaff, L.H., 2016. Optimization Strategies for Microbial Itaconic Acid Biosynthesis. *Current Biotechnology* 5, 1-8.

van der Straat, L., Tamayo-Ramos, J. a, Schonewille, T., de Graaff, L.H., 2013. Overexpression of a modified 6-phosphofructo-1-kinase results in an increased itaconic acid productivity in *Aspergillus niger*. *AMB Express* 3, 1-9.

van der Straat, L., Vernooij, M., Lammers, M., van den Berg, W., Schonewille, T., Cordewener, J., van der Meer, I., Koops, A., de Graaff, L.H., 2014. Expression of the *Aspergillus terreus* itaconic acid biosynthesis cluster in *Aspergillus niger*. *Microbial cell Factories* 13, 1-9.

van Gulik, W.M., de Laat, W.T., Vinke, J.L., Heijnen, J.J., 2000. Application of metabolic flux analysis for the identification of metabolic bottlenecks in the biosynthesis of penicillin-G. *Biotechnology and Bioengineering* 68, 602-618.

van Kuyk, P. a, Diderich, J. a, MacCabe, A.P., Hererro, O., Ruijter, G.J.G., Visser, J., 2004. *Aspergillus niger* mstA encodes a high-affinity sugar/H⁺ symporter which is regulated in response to extracellular pH. *The Biochemical Journal* 379, 375-383.

van Kuyk, P.A., de Groot, M.J.L., Ruijter, G.J.G., de Vries, R. P. and Visser, J., 2001. The *Aspergillus niger* D-xylulose kinase gene is co-expressed with genes encoding arabinan

degrading enzymes, and is essential for growth on D-xylose and L-arabinose. *European Journal of Biochemistry* 268, 5414-5423.

van Maris, A.J., Winkler, A., Porro, D., Dijken, Johannes van, Pronk, J., 2004. Homofermentative Lactate Production Cannot sustain anaerobic growth of engineered *saccharomyces cerevisiae*: possible consequences of energy dependent lactate export. *Applied and Environmental Microbiology* 70, 2898-2905.

van Maris, A.J.A., Abbott, D.A., Bellissimi, E., van den Brink, J., Kuiper, M., Luttik, M.A.H., Wisselink, H.W., Scheffers, W.A., van Dijken, J.P., Pronk, J.T., 2006. Alcoholic fermentation of carbon sources in biomass hydrolysates by *Saccharomyces cerevisiae*: Current status. *Antonie van Leeuwenhoek, International Journal of General and Molecular Microbiology* 90, 391-418.

Verheijen, P.J.T., 2010. Data Reconciliation and Error Detection. Balances and Reaction Models. In: Smolke, C. D., (Ed.), *The metabolic pathway engineering handbook*. CRC Press, Boca Raton

Verviers, M. C. A., 2012. Extraction as improved recovery for itaconic acid. Master thesis. Delft University of Technology, Delft.

Vishniac, W., Santer, M., 1957. The thiobacilli. *Microbiology and Molecular Biology Reviews* 21, 195-213.

Wei, H., Vienken, K., Weber, R., Bunting, S., Requena, N., Fischer, R., 2004. A putative high affinity hexose transporter, *hxtA*, of *Aspergillus nidulans* is induced in vegetative hyphae upon starvation and in ascogenous hyphae during cleistothecium formation. *Fungal Genetics and Biology* 41, 148-156.

Werpy, T., Petersen, G., Aden, A., Bozell, J., 2004. Top Value Added Chemicals from Biomass. Volume 1 - Results of Screening for Potential Candidates from Sugars and Synthesis Gas. U.S. Dep. Energy.

Willke, T., Vorlop, K.D., 2001. Biotechnological production of itaconic acid. *Applied Microbiology and Biotechnology* 56, 289-295.

Witteveen, C.F.B., Busink, R., van de Vondervoort, P., Dijkema, C., Swart, K. and Visser, J., 1989. L-Arabinose and D-Xylose Catabolism in *Aspergillus niger*. *Journal of general microbiology* 135, 2163-2171.

Witteveen, C.F.B., 1993. Gluconate formation and polyol metabolism in *Aspergillus niger*. PhD thesis. Wageningen University, Wageningen.

Wösten, H.A., Moukha, A.S.M., Sietsma, J.H., Wessels, J.G., **1991**. Localization of growth and secretion of proteins in *Aspergillus niger*. *Journal of general Microbiology* 137, 2017-2023.

Wu, L., Mashego, M.R., van Dam, J.C., Proell, A.M., Vinke, J.L., Ras, C., van Winden, W. a, van Gulik, W.M., Heijnen, J.J., **2005**. Quantitative analysis of the microbial metabolome by isotope dilution mass spectrometry using uniformly ¹³C-labeled cell extracts as internal standards. *Analytical Biochemistry* 336, 164-171.

Young, E., Poucher, A., Comer, A., Bailey, A., Alper, H., **2011**. Functional survey for heterologous sugar transport proteins using *Saccharomyces cerevisiae* as a host. *Applied and Environmental Microbiology* 77, 10.

Zhou, Y., Du, J., Tsao, G.T., **2000**. Mycelial pellet formation by *Rhizopus oryzae* ATCC 20344. *Applied Biochemistry and Biotechnology* 84, 779-789.

Acknowledgements

Sef, thank you for the opportunity to work with you. I admire your capacity to be so precise and professional. You really have a gift for teaching and challenging your students. And it always amazes me how thermodynamics is simple and fun for you!

Walter, you were more than a supervisor. I was very lucky to have you by my side during these four years. I thank you for all the times you came down to the lab and showed me around; all the times you checked my calculations; and all the times you made corrections to my reports and manuscripts. I admire your perfectionism. Thank you! ☺

Jenifer, you are so fun! Somehow in every group dinner we sat together and had a blast. Thank you for your efficiency with bureaucratic issues, but most importantly thank you for your confidence.

Peter, I always (in one way or another) enjoyed our meetings... thank you for the stories you have shared, for all the MATLAB help, for all the advices, and for caring so much. You made your best to push me to the finish line, but above all you were my conscience.

Sybe, Leo, Peter, Juanan, Dorett, Jasper, Laura and Kiira: the BE-Basic project brought us together and I learnt so much with all of you. The contact between us was not so frequent as we would like it to be, but I think we made the best out of it.

Angie, Cor, Johan, Patricia and Reza, even though many times you are in the backstage, you make sure the quality of our data is excellent. A big thank you to all of you.

Song, there's not enough *thank you's* to show you how grateful I am for all your help and manpower while carrying the 50 kg vessels and fermentors. Dirk and Rob, who baptized me in my first year as the *fungi girl*, thank you for all the troubleshooting you did for me, even off hours.


Apilena, Astrid and Jannie, thank you for sterilizing my fermentors at least 62 times (yes, I did some calculations), and for being so friendly.

Arno, Ruud and Marcel, I have to thank you for all the times you had to fix valves or loose bearings in my fermentation setup. More than that, you built three sampling devices from scratch for me, which were the working horses of this project.

Kiki, Elli and Stefan, you were my students but I also learned great lessons with all of you.

Jinrui, Sushil, Karel, Aljoscha, Leonor, Robin, Eleni, Yaya, Alex, Lucas and Florence, thank you for the nice moments together as a group. Everyone is so different and has a special role here. That is what makes CSE a cool group! A special thanks goes to Mihir, Anisha and Marianita. Camilo, Cristina, Angel and Manuel, you adopted me when I arrived in Delft. Thank you for the warm Latin moments in the cold days...

Katelijne and Luisa we did not have a lot of contact as you left when I arrived in the group, but you were both crucial. Luisa you were the person who influenced me to take this position, and Katelijne you taught me everything about fermentors! It was very nice to hang out again with you girls in Japan.

Hugo, my favorite Mexican drama queen, thank you for going along with my craziness about cows. A last one for you: ! Thank you for teaching me so much and make sure I finish this PhD. You were there at the right moment.

Emma and Monica, you are my family here! Thank you for your shoulders, all the coffee breaks, meals, gossips, sports, travels, and friendship! You made my stay in Delft very complete.

Ritinha, Cata, Rafa and Joana, thank you for your support and kindness, and for so many advices during the common PhD life!

Kris, Ronan and Cris, you guys make us (Julien and I) want to come back to Delft! Thank you for so many nice evenings!

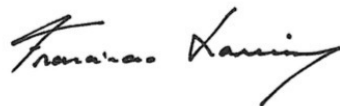
Thank you Pedro, living away from your friends is not easy, but true friendships always survive! Le, Mikas, Ritinha, Claudinha and Pisto, much of what I know today, we learnt it together!

Thank you to all the friends back home: Ritz, Ni, Ritinha, Rakas, Cris, Fla, Rita R., Xavi, Jo, Sergio, Nuno, Peruzzi and particularly to my dear Rafa, with whom I spent hours on skype sharing thoughts and confidences. Even though we belong to completely different fields, you have been such a great example of professionalism and efficiency to me! I am very proud of you.

In the end, it all comes down to family. I thank my brother, who has always been my idol, and who constantly and very rationally supported me in the worst moments. And thank you Rita, because next to a great man, there's always a great woman! I thank my parents too: I owe them everything. I would never have reached this place without their unconditional love, support and enthusiasm. They all believe in me, better than I do.

Finally, I thank my Julien. Thank you for sharing the same "PhD feelings" with me, for the many hours of conversation and confidence, for your eternal good mood, for all our travels, food experiments, holiday escapes and countless good moments. Thank you for making me a better and happier person.

Obrigada,

A handwritten signature in black ink, appearing to read "Francisco Xavier". The signature is fluid and cursive, with a long horizontal stroke at the end.

Delft, January 2017

Curriculum vitae

Francisca da Fonte Lameiras was born on the 17th January 1989 in Guimarães, Portugal.

She enrolled in the Biological Engineering study program in Minho University (Braga), following the food and chemical technology track, in September 2007.



Her early interest in research started during her Bachelor studies when she obtained a research grant from FCT (*Fundação para a Ciência e a Tecnologia*) on the topic “Modification of bacterial cellulose for biomedical applications” in 2009.

During the last year of her studies she moved to Sweden to work on her Master thesis entitled “Biobutanol production with lactic acid bacteria”, at Prof. Jens Nielsen’s Sys²bio group in Chalmers University of Technology, Gothenburg, where she obtained the classification 19/20.

In January 2013, Francisca moved to The Netherlands and started her PhD at Delft University of Technology, under supervision of Dr. Walter van Gulik and Prof. ir. J.J. Heijnen at the Cell Systems Engineering research group.

Currently, Francisca has a position at iCellate Medical AB as Head of Laboratory, and lives in Stockholm, Sweden.

List of Publications

✓ Published papers

Ghiaci, P., **Lameiras, F.**, Norbeck, J., Larsson, C., **2014**. Production of 2-butanol through meso-2,3-butanediol consumption in lactic acid bacteria. *FEMS Microbiology Letters* 360, 70–5.

Lameiras, F., Heijnen, J.J., van Gulik, W.M., **2015**. Development of tools for quantitative intracellular metabolomics of *Aspergillus niger* chemostat cultures. *Metabolomics* 11, 1253–1264.

Lameiras, F., Ras, C., ten Pierick, A., Heijnen, J.J., van Gulik, W.M., **2017**. Stoichiometry and kinetics of single and mixed substrate uptake in *Aspergillus niger*. *Bioprocess and Biosystems Engineering* 41, 157-170.

Lameiras, F., Ras, C., Heijnen, J.J., van Gulik, W.M., **2018**. Metabolic network analysis and transport mechanism of lignocellulosic substrates in *Aspergillus niger*. (manuscript under preparation).

Lameiras, F., Heijnen, J.J., van Gulik, W.M., **2018**. Transport insights on citric and itaconic acid in *Aspergillus niger*. (manuscript under preparation).

✓ Oral Presentations

Lameiras, F., Heijnen, J.J., van Gulik, W.M., **2014**. Development of tools for quantitative metabolomics in *Aspergillus niger*. BE-BASIC symposium. Noordwijkerhout, The Netherlands.

Lameiras, F., Heijnen, J.J., van Gulik, W.M., **2015**. Sugar uptake in *Aspergillus niger*. 3rd Delft Process Technology Institute annual event. Kijkduin, The Netherlands.

✓ **Poster Presentations**

Lameiras, F., Heijnen, J.J., van Gulik, W.M., **2013.** Transport processes in the production of organic acids by *Aspergillus niger*. 1st Delft Process Technology Institute annual event. Kijkduin, The Netherlands.

Lameiras, F., Heijnen, J.J., van Gulik, W.M., **2014.** Development of tools for quantitative metabolomics in *Aspergillus niger*. 12th European Conference on Fungal Genetics. Seville, Spain.

Lameiras, F., Heijnen, J.J., van Gulik, W.M., **2014.** Transport processes in the production of organic acids by *Aspergillus niger*. 2nd Delft Process Technology Institute annual event. Rotterdam, The Netherlands.

Lameiras, F., Heijnen, J.J., van Gulik, W.M., **2014.** Development of tools for quantitative metabolomics in *Aspergillus niger*. BIOPRO World Talent Campus. Sorø, Denmark.

Lameiras, F., Heijnen, J.J., van Gulik, W.M., **2015.** Sugar uptake in *Aspergillus niger*. BE-BASIC symposium. Noordwijkerhout, The Netherlands.

Lameiras, F., Heijnen, J.J., van Gulik, W.M., **2016.** Stoichiometry and kinetics of single and mixed substrate uptake in *Aspergillus niger*. 11th Metabolic Engineering conference. Awaji, Japan.

Copyright © 2018 by Francisca Lameiras

ISBN: 978-94-6299-902-2